NANYANG TECHNOLOGICAL UNIVERSITY

LC-MS/MS ANALYSIS OF THE PROTEIN PROFILES OF ESCHERICHIA COLI IN RESPONSE TO THE CHALLENGE OF ANTIBACTERIAL PEPTIDES

ZHOU YUSI

SCHOOL OF CHEMICAL AND BIOMEDICAL ENGINEERING

2012

LC-MS/MS ANALYSIS OF THE PROTEIN PROFILES OF ESCHERICHIA COLI IN ZHOU YUSI 2012

LC-MS/MS ANALYSIS OF THE PROTEIN PROFILES OF ESCHERICHIA COLI IN RESPONSE TO THE CHALLENGE OF ANTIBACTERIAL PEPTIDES

ZHOU YUSI

School of Chemical and Biomedical Engineering

A thesis submitted to the Nanyang Technological University
in fulfillment of the requirement for the degree of
Doctor of Philosophy

2012

Summary

Novel antibacterial drugs are in urgent need to overcome the continuous growth in the emergence of bacterial resistance to current antibiotics. Antibacterial peptides (ABPs), especially non-membrane-permeabilizing ABPs which kill bacteria by specific mechanisms other than direct membrane disruption, are excellent candidates for development as novel antibacterial drugs. Systematic and comprehensive understanding their mechanisms of action was thus urgently required.

In this study, liquid chromatography-tandem mass spectrometry (LC-MS/MS) technique was utilized to analyze the protein profiles of *Escherichia coli* (*E. coli)* in response to the challenge of two representatives of non-membrane-permeabilizing ABPs, apidaecin IB and human neutrophil peptides 1 (HNP-1).

A number of proteins which take essential roles in cellular protein quality control were found to be significantly changed. Levels of 60 kDa charperonin (GroEL) and 10 kDa charperonin (GroES), which together form the only essential chaperon system in *E. coli* cytoplasm under all growth conditions, were decreased; in contrast, levels of ATP-dependent protease ClpX and FtsH, which located in cytoplasm and inner membrane respectively, were increased. The increase in the proteases was probably

involved in a compensatory response to the suppression effect. However, the overproduction of FtsH further intensified the degrading of UDP-3-O-acyl-N-acetylglucosamine deacetylase (LpxC), an enzyme catalyzing the first committed step in the biosynthesis of the lipid A moiety of lipopolysaccharide (LPS). As the same reaction precursor (R-3-hydroxymyristoyl-ACP) is used by LpxC for the biosynthesis of the lipid A moiety of LPS and by (3R)-hydroxymyristoyl-[acyl-carrier-protein] dehydratase (FabZ) for the synthesis of fatty acid, the reduction in LpxC led to further unbalanced synthesis of LPS and phospholipids and the loss of membrane lipid homeostasis.

However, in response to HNP-1 challenge, levels of a number of enzymes in glycolysis were decreased, including 6-phosphofructokinase isozyme 1, glyceraldehyde-3-phosphate dehydrogenase A, phosphoglycerate kinase, enolase, and pyruvate kinase; in contrast, levels of enzymes (dehydrogenase and aconitate hydratase 2) which regulate the conversion of pyruvate into isocitrate were increased. In concert with the decreasing in cellular ATP and the slowing down in the growth of *E. coli* culture, central metabolism was suggested to be involved in the *E. coli* response to HNP-1 challenge.

Our findings provide new insights into the antibacterial mechanism of action of apidaecin IB and HNP-1. The LC-MS/MS-based proteomic

analysis platform established here may be expanded into the mechanistic studies of all other non-membrane-permeabilizing ABPs and perhaps, by extension, all other candidates of novel antibacterial drugs. The identified altered proteins may well be novel targets for more effective antibacterial intervention.

Acknowledgements

I would first like to express great appreciation to my supervisor Prof. Chen Wei Ning, William for giving me their continuous guidance, encouragement and precious suggestion for this project.

I would also like to express appreciation to Prof. Mary Chan and my co-supervisor Asst. Prof. Matthew Chang for their support.

I want to extend my appreciation to Menicon for their funding support.

Many thanks also go to group members in Prof. Chen's lab, Dr. Sui Jianjun, Dr. Zhang Jianhua, Dr. Feng Huixing, Dr. Niu Dandan, Dr. Bai Jing, Mr. Wang Mingxuan, Ms. Laleh Sadrolodabaee, Ms. Chen Liwei, Ms. Tang Xiaoling, Mr. Lee Jia Hong, Mr. Tan Kee Yang, Ms. Shi Jiahua and Ms. Li Xiang, for their support and helping me forget about research when it was most needed.

Finally and the most importantly, I would like to thank the dearest people in my life, my parents and my husband. They always support me in whatever I wanted to do and offer me encouragement, advice and blessings. It is to them I dedicate this thesis.

Table of Contents

List of Figures

List of Tables

List of Abbreviations

2D	two-dimensional
ABPs	antibacterial peptides
AceE	pyruvate dehydrogenase
AcnB	aconitate hydratase 2
CFUs	colony-forming units
CID	collision induced dissociation
Cra	catabolite repressor/activator
E. coli	*Escherichia coli*
EF	error factor
ESI	electrospray ionization
Eno	enolase
FabZ	(3R)-hydroxymyristoyl-[acyl-carrier-protein] dehydratase
FT-ICR	Fourier transform-ion cyclotron resonance
FtsH	cell division protease
GapA	glyceraldehyde-3-phosphate dehydrogenase A
GroEL	60 kDa charperonin
GroES	10 kDa charperonin
HNP-1	human neutrophil peptide 1
ICATs	isotope-coded affinity tags
IM	inner membrane
iTRAQ	isobaric tags for relative and absolute quantification
KDO	2-keto-3-deoxyheptonic acid
LC-MS/MS	liquid chromatography-tandem mass spectrometry
LPS	lipopolysaccharide
LpxC	UDP-3-O-acyl-N-acetylglucosamine deacetylase
MALDI	matrix-assisted laser desorption/ionization
MH	Mueller-Hinton

MIC	minimal inhibitory concentration
m/z	mass-to-charge ratio
OD_{600}	optical density at 600nm
OM	outer membrane
RF	reverse-phase
RpoA	DNA-directed RNA polymerase subunit alpha
SCX	strong-cation exchange
SDS	sodium dodecyl sulphate
SILAC	stable isotope labeling by amino acids in cell culture
SIM	selected ion dissociation
TOF	time-of-fight
PAGE	polyacrylamide gel electrophoresis
PfkA	6-phosphofructokinase isozyme 1
Pgk	phosphoglycerate kinase
PVDF	polyvinylidine fluoride
PykF	pyruvate kinase I

List of Publications

(** for corresponding author and # for co-first author*)

- **Zhou, YS** and Chen W*. (2011) iTRAQ-coupled 2-D LC-MS/MS Analysis of Cytoplasmic Protein Profile in *Escherichia coli* Incubated with Apidaecin IB. J. Proteomics. 75(2): 511-6.
- **Zhou, YS** and Chen W*. (2011) iTRAQ-Coupled 2-D LC-MS/MS Analysis of Membrane Protein Profile in *Escherichia coli* Incubated with Apidaecin IB. PLoS One. 6(6): e20442.
- Lee JH#, **Zhou YS#**, Wang MX and Chen W*. (2011) Inhibitory effect of Bovine lactoferrin on human hepatitis B virus expression in HepG2.2.15 cell line. BIO. 1: 64-6.
- **Zhou YS**, Leong SS, Chan-Park MB, Chang MW, Mouad L and Chen W*. (2010) iTRAQ-coupled 2-D LC-MS/MS analysis on protein profile in *Escherichia coli* cells incubated with human neutrophil peptide 1. Rapid Commun. Mass Spec. 24(18): 2787-90.

Chapter 1: Introduction

Few developments in the history of medicine have had such a profound effect on human life and society as the development of the power to control infections by bacteria. In the fight against infectious disease, antibacterial drugs play a remarkable role. The majority of antibacterial drugs were discovered in the 1940-1960s. Owing to the improved hygiene measures and the success story of treatment of bacterial pathogens by antibacterial drugs, in 1969 the Surgeon General of the United States stated that it was time “to close the book of infectious diseases” [1]. Unfortunately, since the heady optimism of the 1960s we have learned to our cost that bacterial pathogens still have the capacity to spring unpleasant surprises on the world. The problem of acquired bacterial resistance to antibiotics, recognized since the very beginning of antibacterial therapy, has become ever more threatening.

Antibacterial drugs act by impairing cellular functions and structures essential for bacterial growth and survival. However, bacteria are extremely adaptable. Their lifestyles require the swift phenotypic adaptation to a variety of changing environmental factors. Even genetic adaptation is comparably fast due to a concurrence of short generation times, haploid genomes, and various routes of transfer of genetic material. In most cases, only a few genes or a single gene is sufficient to render a bacterium resistant to a particular antibacterial drug. Such genes can encode efflux

pumps, antibacterial-drug degrading or modifying enzymes, or a mutated target resistant to the action of antibacterial drugs. As these resistance genes become essential for survival under drug selection pressure, carriers might be the only survivors. Once presenting within the gene pool of pathogenic bacteria, resistance traits may be disseminated within and between species [2]. Resistance to one antibacterial drug would not pose a major threat, as a variety of antibacterial drugs are available to us. However, frequently resistance traits accumulate and multidrug-resistant pathogens cause major problems especially in places with high antibacterial-drug use [3]. During the past decade, multidrug-resistant pathogens have also taken hold in the community so that a fair number of deaths are now caused by community-acquired multidrug-resistant strains [4]. To combat multidrug-resistant pathogens, novel antibacterial drugs are in urgent need.

Antibacterial peptides (ABPs) are a group of relatively short (less than 100 amino acid residues), positively charged and amphiphilic peptides produced by a wide range of organisms as part of their first line of defense [5-7]. They exhibit activities against both Gram-positive and Gram-negative bacteria [8-10]. Most of them even have activities against fungi [8, 11, 12], protozoa [8, 13, 14] and viruses [15-17]. The modes of action of ABPs can be generally classified as either membrane-permeabilizing or non-membrane-permeabilizing [18]. Membrane-permeabilizing peptides can disrupt the membrane by forming transmembrane pores, micellarizing or dissolving the membrane. In contrast, non-membrane-permeabilizing peptides can translocate across the membrane and accumulate in the cytoplasm, where they kill bacteria by targeting different essential cellular

processes.

Non-membrane-permeabilizing ABPs generally exhibit a broad range of activity, act by specific mechanisms other than direct membrane disrupting, do not easily induce antibacterial-drug resistance, are bactericidal as opposite to bacteriostatic, and require a short time to induce cell killing [19-21]. All these features make them excellent candidates for development as novel antibacterial drugs. Systematic and comprehensive understanding of their antibacterial mechanism of action is thus urgently required.

Two representatives of non-membrane-permeabilizing ABPs are apidaecin IB and human neutrophil peptide 1 (HNP-1). Apidaecin IB is a 20 amino-acid, proline-rich ABP found in insects [22]. It is predominantly active against Gram-negative bacteria [23-25]. Previous studies showed that the antibacterial mechanism of apidaecin IB was based on its ability to bind the chaperone DnaK and inhibit the function of DnaK in assisting the folding of polypeptides [21]. However, it is possible that apidaecin IB kill bacteria by other mechanisms not yet explored. HNP-1 is a 30 amino-acid, β-sheet ABP found in human neutrophils [26, 27]. HNP-1 has a wide spectrum activity against bacteria (both Gram-positive and Gram-negative) [28], yeast [29, 30] and enveloped viruses [31]. It was originally proposed that permeabilization of the target cell membrane was the mechanism of action of this type of peptides [32]. However, there is an increasing body of evidence indicating that the targeting of essential cellular processes, such as inhibition of nucleic acid synthesis, plays more important roles in mediating cell death.

Proteomics is a new discipline that originated in the mid-1990s and has grown rapidly in a very short time. The best current definition of proteomics is “any large-scale protein-based systematic analysis of the proteome or defined sub-proteome from a cell, tissue, or entire organism” [33-35]. Quantitative protein profiling, which attempts to quantitatively compare changes in the level of proteins between two or more experimental conditions, is the most common type of proteomic study [36]. Antibacterial agents act by interfering with essential cellular functions or structures of bacteria. The bacterial proteome is dynamic in nature and quickly adjusts in response to an antibacterial-agent challenge to physiological homeostasis. Therefore, quantitatively comparing changes in the level of proteins between control and antibacterial-agent-treated conditions may aid mechanistic studies of antibacterial agents such as ABPs.

The overall objective of this Ph.D. research project is to investigate changes in the proteome of *Escherichia coli* (*E. coli*) in response to the challenge of apidaecin IB and HNP-1, two representatives of non-membrane-permeabilizing ABPs, using quantitative protein profiling technique and thus infer the possible antibacterial mechanisms involved. Experimentally, Isobaric tag for relative and absolute quantitation (iTRAQ)-coupled two dimensional (2D) liquid chromatography–tandem mass spectrometry (LC-MS/MS) was applied. Working on this sophisticated approach, we hope our results can shed new lights and thereby provide better understandings of the mechanism of action of these two ABPs. We also hope the platform developed in this study can be expanded into the mechanistic studies of all other non-membrane-permeabilizing ABPs and

perhaps, by extension, all other candidate novel antibacterial drugs; and the identified altered proteins can be used as the novel targets for more effective antibacterial intervention.

The work presented in this dissertation is organized as follows.

In chapter 2, a brief review of the available literature concerning ABPs and proteomics is presented. The purpose of this chapter is to elucidate the context and address the importance of the present work.

In chapters 3 and 4, alterations in the level of cytoplasmic and membrane proteins in *E. coli* in response to apidaecin IB challenge were analyzed by utilizing an iTARQ-coupled 2D LC-MS/MS technique. New targets of apidaecin IB were identified, and the underling molecular mechanisms were explored.

In chapter 5, cytoplasmic protein profile of *E. coli* in response to HNP-1 challenge was investigated by utilizing the LC-MS/MS-based quantitative protein profiling platform established in chapter 3. Altered proteins, which may be novel targets of HNP-1, were identified.

In chapter 6, conclusions of the overall research achieved from this project are summarized, and limitations lying in the study are also discussed.

In chapter 7, the potential avenues for future work are presented.

Chapter 2: Literature Review

2.1 Overview of ABPs

ABPs are a group of relatively short (less than 100 amino acid residues), positively charged (net charge of +2 to +9) and amphiphilic peptides isolated from single-celled microorganisms, insects and other invertebrates, plants, amphibians, birds, fish, and mammals, including humans [5-7]. They form part of the ancient, nonspecific innate immune system, which is the principal defense system for the majority of living organisms. They process activities against both Gram-positive and Gram-negative bacteria [8-10]. Most of them even have activities against fungi [8, 11, 12], protozoa [8, 13, 14] and viruses [15-17]. In many cases, their primary role is in the killing of invading pathogenic organisms; however, it is increasingly recognized that they may also function as modulators of the innate immune response in higher organisms [37-40]. ABPs may be expressed constitutively in some cases or may be inducibly expressed in response to pathogenic challenge. In multicellular animals, they may be expressed systemically (for example, in insect hemolymph or vertebrate immune cells) and/or localized to specific cell or tissue types in the body most susceptible to infection, such as mucosal epithelia and the skin. To date, hundreds of such ABPs have been identified. Besides these naturally occurring ABPs,

numerous synthetic analogues have also been produced [41].

2.1.1 Structure

ABPs can be categorized into three subgroups on the basis of their amino-acid composition and structure: *(i)* α-helical peptides; *(ii)* cysteine stabilized β-sheet peptides; and *(iii)* those rich in specific amino acid residues, but variable in conformation. The first two subgroups are the most common in nature [42-44]. Representative structures from each of these subgroups are presented in Figure 2.1 [45].

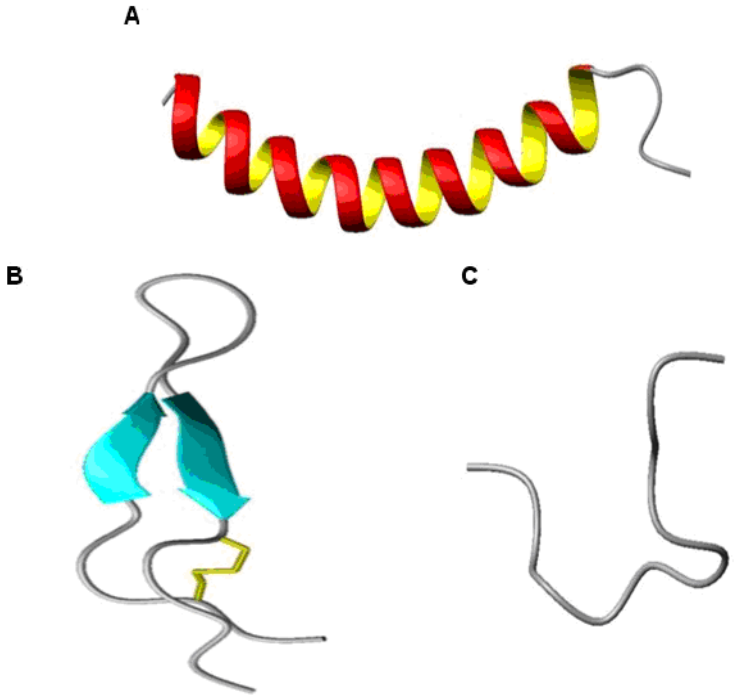

Figure 2.1 Structural classes of ABPs [45]. (A) α-helical, LL-37; (B) cysteine stabilized β-sheet, tachyplesin I; and (C) specific amino acid-rich, indolicidin (rich in tryptophan and proline). Disulfide bonds are in yellow.

Peptides from the first subgroup are short (less than 40 amino acids), lack cysteine residues, and sometimes have a hinge in the middle [46]. In aqueous solutions, many of these peptides are disordered; however, in the presence of trifluoroethanol, sodium dodecyl sulphate (SDS) micelles, phospholipid vesicles or lipid A, all or part of the molecule is converted into an α-helix [46]. LL-37, the only cathelicidin family of ABPs in human, is a representative of this group of peptides. In water, it exhibits a circular dichroism spectrum that is consistent with a disordered structure [47]. However, in 15 mM HCO_3^-, SO_4^{2-}or $CF_3CO_2^-$, the peptide forms a helical structure (Figure 2.1 A) [47].

The cysteine stabilized β-sheet peptides are characterized by the presence of at least one antiparallel β-sheet stabilized by disulfide bonds between cysteine residues. The tachyplesins isolated from the haemocytes of the Japanese horseshoe crab *Tachypleus tridentatus*, are representative of this class [9]. NMR studies of tachyplesin I showed the presence of an antiparallel β-sheet stabilized by two disulfide bridges formed between residues 3 and 16 and residues 7 and 12 (Figure 2.1 B) [48].

Peptides in the third subgroup are rich in certain amino acids. For example, apidaecins isolated from insects are rich in proline, and the indolicidin isolated from the cytoplasmic granules of bovine neutrophils is rich in tryptophan and proline (Figure 2.1 C) [10]. This subgroup of ABPs lack

cysteine residues and are linear, though some can form extended coils.

2.1.2 Physicochemical Features

2.1.2.1 Cationicity

ABPs generally display a net positive charge of +2 to +9 owing to an excess of basic amino acids (arginine, lysine and histidine) over acidic amino acids [49]. Cationicity is critical for the initial electrostatic attraction of ABPs to the surface of the bacterial cell, which is rich in negatively charged components including the acidic phospholipids (in the cytoplasmic membrane), the lipopolysaccharides (LPS, in the outer membrane of Gram-negative bacteria), and the teichoic or teichuronic acids (in the peptidoglycan of Gram-positive bacteria) [50].

2.1.2.2 Amphipathicity

Almost all ABPs form amphipathic structures upon interaction with target membranes [51]. Amphipathicity is an essential feature for ABPs-membrane interaction. It allows ABPs to partition into the membrane lipid bilayer [52].

2.1.3 Cell Selectivity

Cell selectivity describes the ability of ABPs to preferentially interact with the bacterial cells. This feature enables ABPs to kill bacteria without being significantly toxic to mammalian cells. The cationic property of ABPs mainly contributes to this cell selectivity. The bacterial cell membrane is rich in acidic phospholipids, such as phosphatidylglycerol and cardiolipin. Therefore, the outer leaflet of the bilayer of the bacterial membrane is negatively charged. Moreover, LPS in the outer membrane of Gram-negative bacteria and the teichoic or teichuronic acids present in the peptidoglycan of Gram-positive bacteria impart additional negative charges to the surface of these cells. By contrast, in the case of mammalian cells, acidic phospholipids are usually located in the inner leaflet of the membrane; the outer leaflet is mainly composed of zwitterionic phosphatidylcholine, and sphingomyelin. As a result, the surface of bacterial cells is more negatively charged than that of mammalian cells, and thus more attractive to cationic ABPs (Figure 2.2). Other factors also contribute to cell selectivity such as higher transmembrane potential of bacterial cells and the existence of membrane-stabilizing cholesterol in mammalian cells [53]. However, ABPs with strong membrane-disrupting activities can also damage mammalian cell membranes, and thus are toxic to these cells.

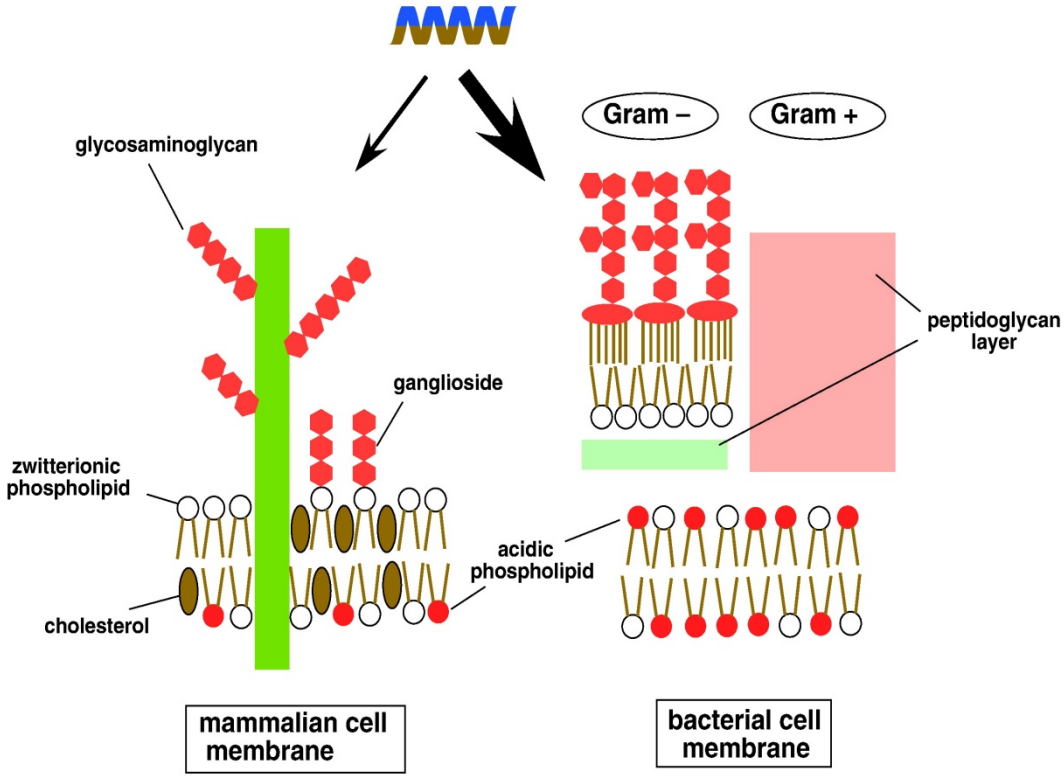

Figure 2.2 Molecular basis of cell selectivity of ABPs [53]. ABPs form amphipathic structures with a postiively charged face (blue) and a hydrophobic face (brown).

2.1.4 Mode of Action

Regardless their specific antibacterial mechanisms, the activities of ABPs are almost universally dependent on the interaction with the bacterial cell membrane [54]. The first step of this interaction is the initial attraction between the peptides and the target cell, which is thought to achieve by electrostatic bonding between cationic peptides and negatively charged components present on the bacterial cell surface, such as phosphate groups within the LPS of Gram-negative bacteria, or the teichoic acids on the surface of Gram-positive bacteria [43, 55]. Once close to the bacterial surface, ABPs are inserted into the outer membrane in a process driven by

hydrophobic interactions in the case of Gram-negative bacteria. Alternatively, ABPs traverse capsular polysaccharides, teichoic acids and lipoteichoic acids in the case of Gram-positive bacteria before they can interact with the cytoplasmic membrane [54]. Once ABPs have gained access to the cytoplasmic membrane, they can associate with the lipid bilayer through electrostatic and hydrophobic interactions. The events that occur at the cytoplasmic membrane surface are the subject of extensive debate, and several models (called “aggregate”, “toroidal-pore”, “barrel-stave” and “carpet” models) have been proposed. Each of these models describes different forms of intermediates which can lead to one of three kinds of events: formation of a transient channel, micellarization or dissolution of the membrane, or translocation across the membrane. Consequently, peptides can permeabilize the membrane, and/or translocate across the membrane and into the cytoplasm without causing significant membrane disruption. For this reason, the mode of action of ABPs can be broadly classified as either membrane permeabilizing or non-membrane permeabilizing.

2.1.4.1 Membrane-permeabilizing ABPs

Four different models have been proposed to explain how, following initial attachment, ABPs insert into the bacterial membrane to form transmembrane pores, which result in membrane permeabilization. The

amphipathic feature of ABPs mainly contributes to this process, as hydrophobic regions are necessary to interact directly with the lipid components of the membrane, while the hydrophilic regions either interact with the head groups of the phospholipid or face the lumen of the pore. Once arriving at the cytoplasmic membrane, membrane-permeabilizing ABPs first interact with the negatively-charged group of lipids at the membrane surface, adopting an orientation parallel to the membrane [18, 51]. It is at this point that the “aggregate”, the “toroidal-pore”, the “barrel-stave”, and the “carpet” models separate. In the “aggregate” model, ABPs reorient to span the membrane as micelle-like complexes of peptides and lipids (the peptides adopt no particular orientation) (Figure 2.3 A). Lacking of a formal channel structure makes the peptide have the capacity to translocate across the lipid bilayer as the aggregates collapse. This model can explain both membrane permeabilization, whereby informal channels with a variety of sizes and lifetimes form, and translocation across the bilayer [18]. In the “toroidal-pore” model, peptides insert perpendicularly into the membrane and induce the lipid monolayer to bend continuously along the pore so that the water core is lined by both the inserted peptides and lipid head groups (Figure 2.3 B) [56-59]. In the “barrel stave” model, peptides reorient and insert perpendicularly into the membrane and align (like the staves in a barrel) in a manner in which the hydrophobic surface interacts with the lipid core of the membrane while the

hydrophilic surface points inward to form transmembrane pores; this is a true protein-pore model (Figure 2.3 C) [60-63]. In the mechanism known as the “carpet” model, peptides align parallel to the phospholipids bilayer (like a carpet), remaining in contact with the phospholipids head groups (Figure 2.3 D) [64-66]. Once a threshold concentration of peptides is reached, this orientation results in a detergent-like effect which causes formation of micelles and membrane pores [64-66]. The α-helical subgroup of ABPs generally exhibits their antibacterial action through this membrane-permeabilizing mode.

2.1.4.2 Non-membrane-permeabilizing ABPs

However, a growing number of ABPs have been shown to translocate across the membrane and accumulate in the cytoplasm, where they target various essential cellular processes to mediate cell death. Mechanisms of action which have been demonstrated include inhibiting actual nuclear acid synthesis (Figure 2.3 E), protein synthesis and folding (Figure 2.3 F and D) enzyme activity (Figure 2.3 H) and cell wall synthesis (Figure 2.3 I). The frog ABP buforin II translocates across the bacterial membrane without causing permeabilization and binds to both DNA and RNA within the cytoplasm of *E. coli* [67]. Similarly, peptides such as derivatives of pleurocidin, a fish-derived ABP, and dermaseptin, isolated from frog skin, cause inhibition of DNA and RNA synthesis at their MICs without

destabilizing the membrane of *E. coli* cells [68]. Inhibition of nucleic acid synthesis has also been demonstrated for ABPs from different structural classes, such as the β-sheet human defensin, HNP-1 [32], and the extended-structure bovine peptide indolicidin [69]. Additionally, some of these peptides have been shown to interfere with protein synthesis. Pleurocidin and dermaseptin can block tritiated leucine uptake in *E. coli*, and PR-39- and indolicidin-treated cells also exhibit reduced rates of protein synthesis [68-71]. Inhibition of cellular enzymatic activity by proline-rich insect ABPs has also been observed. Pyrrhocidin enters the target cell and binds to DnaK, a heat shock protein that is involved in chaperone-assisted protein folding. Specifically, the peptide inhibits the ATPase activity of DnaK, preventing protein folding, which results in the accumulation of misfolded proteins and cell death [72, 73]. ABPs can also target the formation of structural components, such as the cell wall. The bacterially produced lantibiotic mersacidin interferes with transglycosylation of lipid II, a necessary step in the synthesis of peptidoglycan [74]. Nisin, another lantibiotic, can also bind to lipid II, thus inhibiting cell wall synthesis in addition to its pore-forming activity [75]. Interestingly, this is the same biosynthetic process that is targeted by the antibiotic vancomycin; however, mersacidin and nisin are thought to act by interacting with distinct molecular moieties within lipid II, explaining why these peptides are still active against vancomycin-resistant bacteria [75,

76].

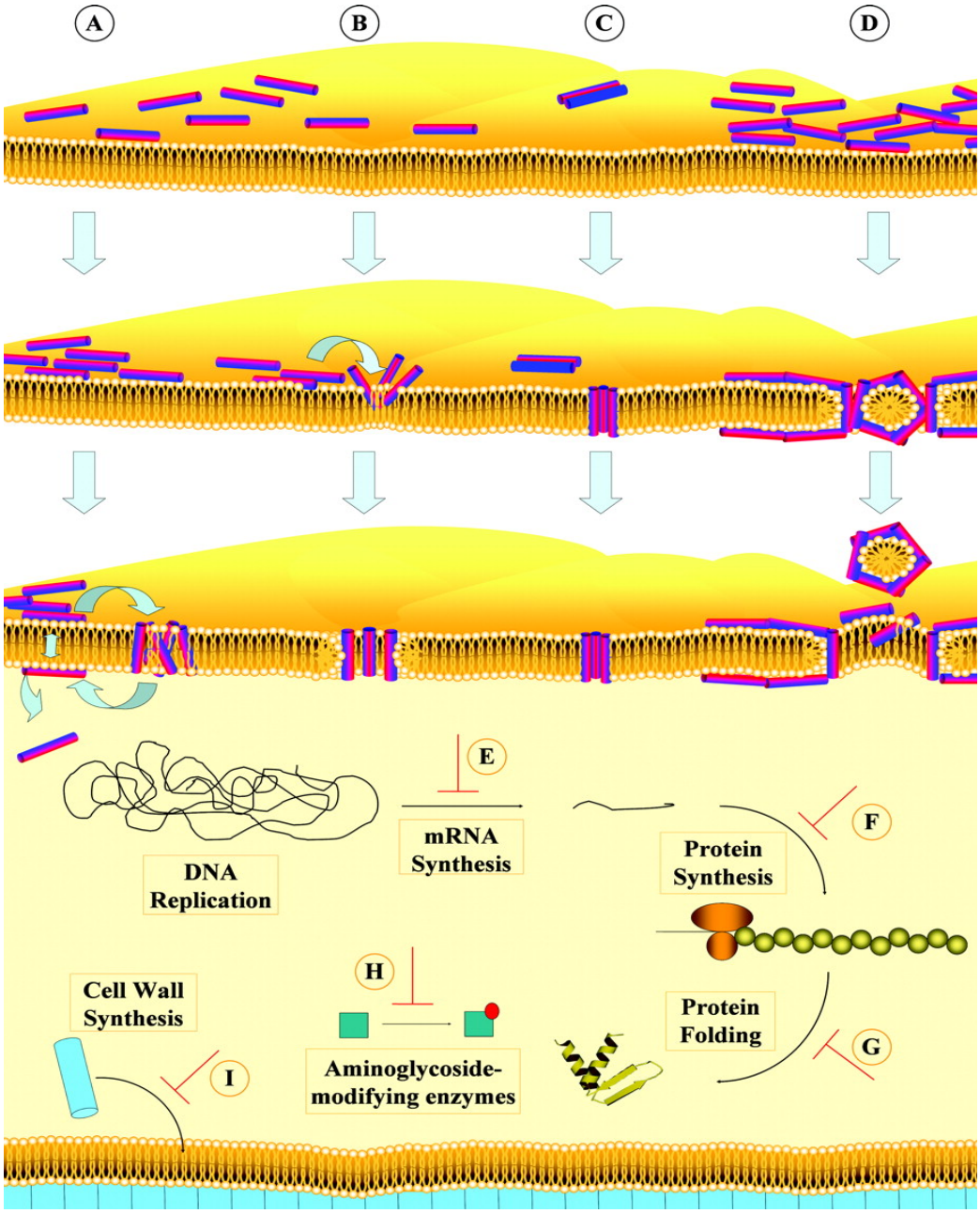

Figure 2.3 Mechanisms of action of ABPs [18]. The bacterial membrane is yellow lipid bilayer with the peptides shown as cylinders, where the hydrophilic regions are red and the hydrophobic regions are blue. Cell wall-associated peptidoglycan molecules are depicted as purple cylinders. (A) the "aggregate" model; (B) the "toroidal pore" model; (C) the "barrel-stave" model; (D) the "carpet" model; (E) nuclear acid synthesis inhibition; (F) and (G) protein synthesis and folding inhibition; (H) enzyme activity inhibition; and (I) cell wall synthesis inhibition.

2.1.5 Candidates for Development as Novel Antibacterial Drugs

Non-membrane-permeabilizing ABPs generally exhibit a broad range of activity, act by specific mechanisms other than direct membrane disruption, do not easily induce antibacterial-drug resistance, are bacteriocidal as opposite to bacteriostatic, and require a short time to induce killing [19-21]. All these features make non-membrane-permeabilizing ABPs excellent candidates for development as novel antibacterial drugs. Systematic and comprehensive understanding of the underlying mechanisms of action of such ABPs is thus urgently required.

2.2 Apidaecin IB and HNP-1

Apidaecin IB and HNP-1 are two representatives of non-membrane-permeabilizing ABPs. Apidaecin IB is a 20 amino-acid, proline-rich peptide found in insects [22]. It is predominantly active against Gram-negative bacteria [23-25]. HNP-1 is a 30 amino-acid, β-sheet defensin found in human neutrophils [26, 27]. It has wide-spectrum activity against bacteria (Gram-positive and Gram-negative) [28], yeast [29, 30] and enveloped viruses [31].

2.2.1 Apidaecin IB

Short proline-rich ABPs (less than 21 amino acid residues) refer to a group of linear peptides produced by insects [22, 77, 78]. They include apidaecins isolated from several hymenopteran species, drosocin from *Drosophila melanogaster*, pyrrhocoricin from the hemypteran species *Pyrrhocoris apterus*, formaecins from the bulldog ant *Myrmecia gulosa*, and metalnikowins from the bug *Palomena prasina* [77]. The sequences of this type of peptides are shown in Figure 2.4. Members of this group of ABPs are predominantly active against Gram-negative bacteria, which they kill without bacterial membrane permerbilization [20, 77].

Apidaecin Ia (honey bee)	+GNNRPVYIPQPRPPHPRI-
Apidaecin Ib (honey bee)	+GNNRPVYIPQPRPPHPRL-
Apidaecin II (honey bee)	+GNNRPIYIPQPRPPHPRL-
Apidaecin (European bumblbee)	+GN RPVYIPPPRPPHPRL-
Drosocin (fruit fly)	+GKPRPYSPRPTSHPRPIRV-
Formaecin 1 (red bulldog ant)	+GRPNPVNNKPTPHPRL-
Formaecin 2 (red bulldog ant)	+GRPNPVNTKPTPYPRL-
Pyrrhocoricin (firebug)	+VDKGSYLPRPTPPRPIYNRN-
Metalnikowin I (green shield bug)	+VDKPDYRPRPRPPNM-
Metalnikowin IIA (green shield bug)	+VDKPDYRPRPWPRPN-
Metalnikowin IIB (green shield bug)	+VDKPDYRPRPWPRNMI-
Metalnikowin III (green shield bug)	+VDKPDYRPRPWPRPNM-

Figure 2.4 Amino acid sequences of short proline-rich ABPs [78].

The ability of short proline-rich ABPs to penetrate into the cytoplasmic membrane is closely associated with their high content of proline resides. Proline is an unusual amino acid, whose amino nitrogen is cyclized with the side chain terminal carbon. This leads to three consequences: the backbone conformation of proline itself is severely restricted; the conformation of the residue preceding proline is also restricted because of the bulkiness of the N-CH_2 group; and proline is unable to act as a hydrogen bond donor because of the amide proton is replaced by a CH_2 group [79]. A sequence of four or more proline residues in a row adapts to a single confirmation known as the polyproline II helix, which is an extended structure with three residues per turn [79]. Previous studies showed that short proline-rich ABPs form the polyproline II helix and this structural module promote penetration of these peptides into the membrane [80]

Apidaecins are the largest group of short-proline-rich ABPs known up to now [22]. They generally have 18 to 20 amino acid residues with proline content of 33% or more [23, 25]. Till now, a total of eighteen isoforms of apidaecins were isolated from six different insects including the honey bee *Apis mellifera*, the bumblebee *Bombus terrestris*, the cicada killer *Sphecius speciosus*, the baldfaced hornet *Dolichovespula maculate*, the yellowjacket *Vespula maculitrons*, the german wasps *Paravespula germanica* and the

parasitic wasps *Coccygomimus disparis* (Table 2.1) [24, 81]. Among them, apidaecin IB shows the strongest activity.

Table 2.1 Sequence alignment of apidaecins [24].

Resources	Isoforms	Peptides sequences
Honey bee	HbIa	GNN**RP**VYIPQ**PRPPHPR**I
	HbIb	GNN**RP**VYIPQ**PRPPHPR**L
	HbII	GNN**RP**IYIPQ**PRPPHPR**L
	HbIII	GNN**RP**IYISQ**PRPPHPR**L
		***** ** ********
Bumble bee	Bb + A	AN**RP**VYIPP**PRPPHPR**L
	Bb − A	-N**RP**VYIPP**PRPPHPR**L
		**********
Cicada killer	Ck P	N**RP**TYVPP**PRPPHPR**L
	Ck A	N**RP**TYVPA**PRPPHPR**L
		******* ********
Bald-faced hornet	Ho+	GKP**RP**QQVP-**PRPPHPR**L
	Ho−	---**RP**QQVP-**PRPPHPR**L
		****** ********
Yellow jackets and German wasps	Yj + S	SNKP**RP**QQVP-**PRPPHPR**L
	Yj − S	-NKP**RP**QQVP-**PRPPHPR**L
		********* ********
C. disparis	Cd1+	GKPNRP**RP**APIQ-**PRPPHPR**L
	Cd1−	---NRP**RP**APIQ-**PRPPHPR**L
	Cd2+	GKPNKP**RP**APIK-**PRPPHPR**L
	Cd2−	---NKP**RP**APIK-**PRPPHPR**L
	Cd3+	GKPSKP**RP**APIK-**PRPPHPR**L
	Cd3−	---SKP**RP**APIK-**PRPPHPR**L
		****** ********
Conserved sequence of all the isoforms		**RP** **PRPPHPR**

Previous studies proposed a five-step mechanism by which apidaecins and some other short proline-rich ABPs exert their activity against *E. coli* and other Gram-negative bacteria: *i)* binding to negatively charged components (most probably LPS) of the outer membrane (OM) in a non-specific manner; *ii)* self-promoted invading into the periplasmic space; *iii)* irreversible interaction with a hypothetical docking molecule/receptor molecule on the inner membrane (IM); *iv)* translocation across the membrane and into the cytoplasm of the cell; *v)* Binding its target most probably DnaK protein to

mediate cell death (Figure 2.5) [21, 24, 72, 82-84]. However, it is possible that these peptides kill bacteria by other mechanisms not yet identified.

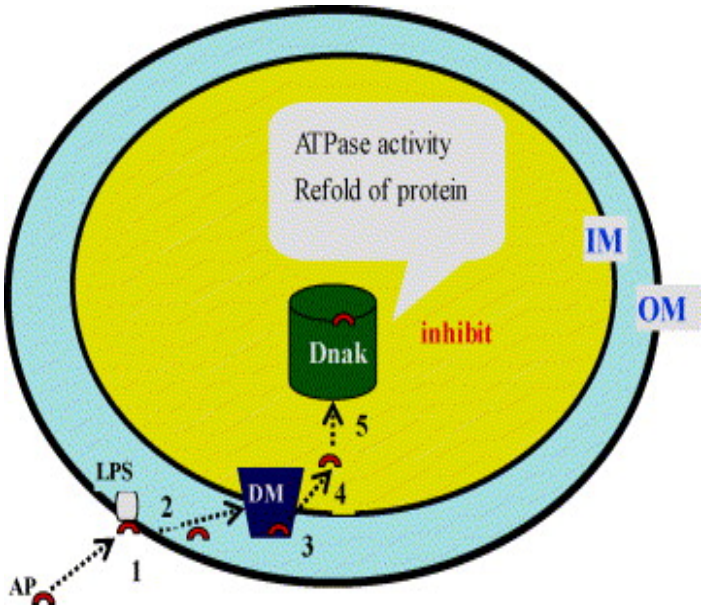

Figure 2.5 Mechanisms of action of apidaecins [24]. AP, apidaecin; LPS, lipopolysaccharides; DM, docking molecule or a receptor; OM, outer membrane; and IM, inner membrane. (1) binding to negatively charged components (most probably LPS) of the OM in a non-specific manner; (2) self-promoted invading into the periplasmic space; (3) irreversible interaction with a hypothetical docking molecule/receptor molecule on the IM; (4) translocation across the membrane and into the cytoplasm of the cell; (5) binds its ultimate target most probably DnaK protein.

2.2.1 HNP-1

Defensins are a family of evolutionarily related vertebrate ABPs with a characteristic triple-stranded antipatallel β-sheet stabilized by three intramolecular disulfide bonds between six cysteines. Typical defensins have been found in all mammals, as well as in chickens and turkeys [30, 85]. The two main defensin subfamilies, α- and β-defensins, differ in the length and the pairing of the cysteine residues. α-defensins contain about

30 amino acids, and their three disulfide bonds connect cysteines 1 and 6, 2 and 4, and 3 and 5 [85, 86]. By contrast, β-defensins are somewhat larger, and their three disulfide bonds are between cysteines 1 and 5, 2 and 4, and 3 and 6. Representative structures from each of these subfamilies are presented in Figure 2.6.

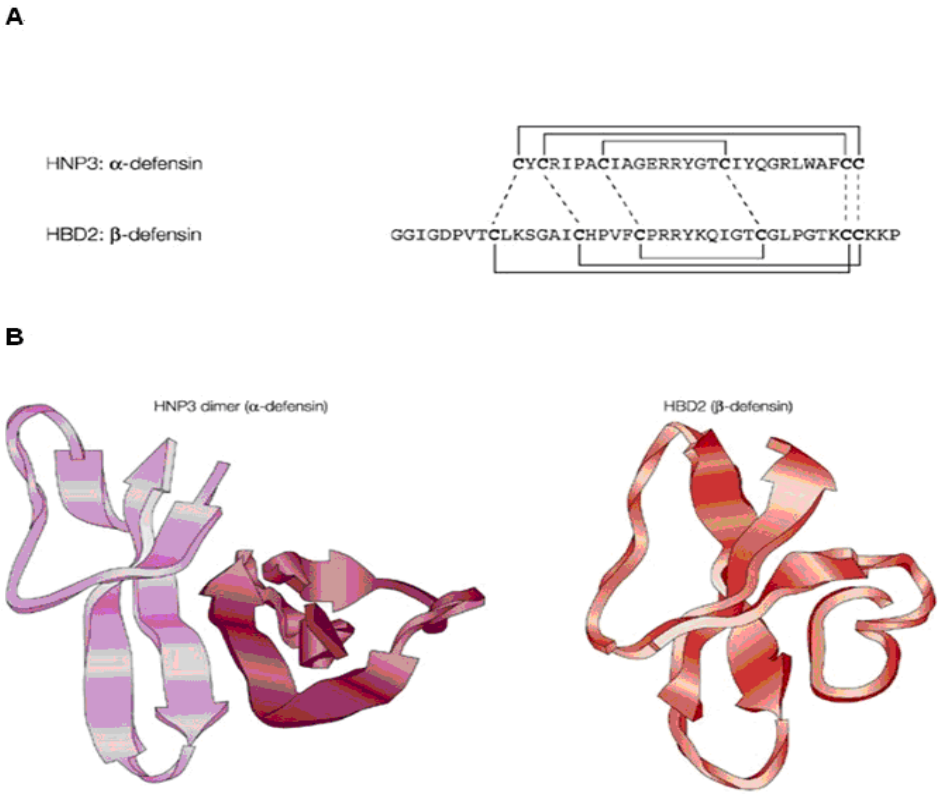

Figure 2.6 Structure of α- and β-defensins [85]. (A) The corresponding cysteines in α- and β-defensins are indicated by dotted lines, disulphide bonds by solid lines. Whereas in α-defensins the six cysteines are linked in the 1–6, 2–4, 3–5 pattern, in β-defensins the pattern is 1–5, 2–4, 3–6. (B) β-sheet structures are indicated by flat ribbons and arrows.

HNP-1 is the most active α-defensin, which includes four human neutrophil peptides (HNP-1 to HNP-4) exclusively present in neutrophil granulocytes, and two enteric defensins (HD-5 and HD-6) found in the granules of Paneth cells (Figure 2.7). It has activities against bacteria (Gram-positive and Gram-negative), yeast, and enveloped viruses. It was originally proposed that permeabilization of the target cell membrane was the mechanism of action of HNP-1 [32]. However, there is an increasing body of evidence indicating that targeting the essential cellular processes, such as inhibition of nucleic acid synthesis, plays a more important role in mediating cell death. Further investigations on different aspects of its mechanisms of action are still required.

Figure 2.7 Amino acid sequences of human α-defensins. Cysteine residues in the defensins are underlined.

2.3 Overview of Proteomic Analysis

Proteomics is a new discipline that originated in the mid-1990s and has grown rapidly in a very short time. The best current definition of proteomics is “any large-scale protein-based systematic analysis of the proteome or defined sub-proteome from a cell, tissue, or entire organism” [33-35]. Most proteomic studies fall into one of the three types: *i)* quantitative protein profiling, *ii)* protein composition analysis, and *iii)* protein-protein interaction analysis [36].

Quantitative protein profiling attempts to quantitatively compare changes in the level of proteins between two or more experimental conditions such as normal versus infected cells, time courses after drug treatment, or responses to stimuli or stresses [36]. It can provide highly informative insights into biological processes and diseases.

Protein composition analysis attempts to identify the total protein complement of a proteome such as that of *E. coli*, or all the proteins present in a cellular fraction or compartment such as outer membrane [36]. The difference relative to quantitative protein profiling is that in protein composition studies, the quantitation of protein levels is not involved. The favored analysis methods for this study are various related multidimensional chromatographic methods coupled to tandem mass

spectrometry, an approach that has been referred to as multidimensional protein identification technology [87].

The third type of proteomic studies is systematic analysis of protein-protein interactions [36]. Most cellular processes are mediated by multi-protein complexes or pathways comprising interacting proteins. For this reason, systematic identification of protein-protein interactions is expected to provide new insights into cellular pathways and networks. In the same way, identification of which proteins of known function associate with a protein of unknown function can provide insights into the role of the latter and the underlying molecular mechanisms involved. Hence, protein-protein interaction maps for a number of model organisms are being constructed [88]. The most direct approach for identification of interacting proteins is isolating a macromolecular complex, followed by identification of all components using MS methods [89, 90].

2.4 LC-MS-Based Quantitative Protein Profiling

LC-MS has become a powerful molecular biology tool, and multiple strategies for peptide and protein quantitation by LC-MS have been developed and applied to address a wide range of biological questions. It is being used more and more to quantitatively compare changes in the level of proteins between two or more experimental conditions.

2.4.1 Protein Identification

LC-MS-based protein identification starts with a purified protein complex, a subcellular protein fraction, or a whole cell lysate. The complex mixture of proteins in solution is first denatured and reduced. The mixture of proteins is then cleaved either enzymatically (*i.e.*, digestion) or chemically to generate a mixture of peptide fragments. The complex peptide mixture is fractionated and analyzed by multidimensional LC coupled with electrospray ionization (ESI) and automated tandem MS. The acquired tandem mass spectra are computationally compared to protein sequences in either protein or translated nucleic acid databases. The list of peptides significantly matching sequences in the databases are used to generate a list of proteins in the original protein complex, subcellular compartment, or whole cell lysate. The workflow of LC-MS/MS-based protein identification is shown in Figure 2.8.

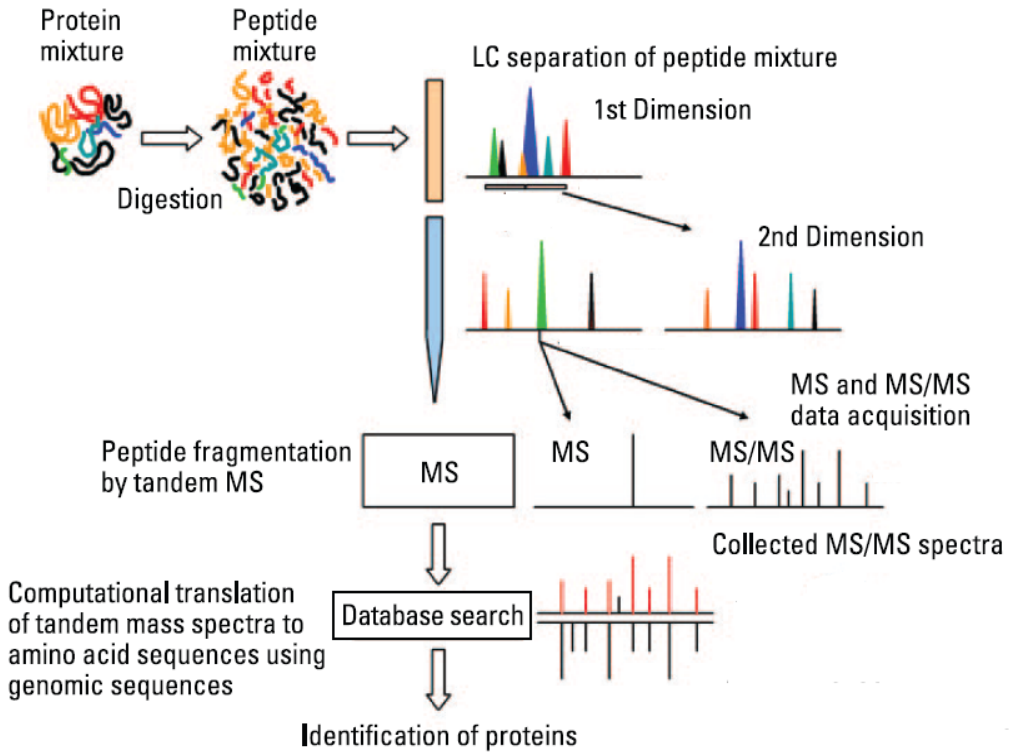

Figure 2.8 Workflow of LC-MS/MS-based protein identification [91].

2.4.1.1 LC Separation

Analyte molecules must be ionized before MS analysis. The method of producing the ions is termed the ionization technique. The two major types of ionization for proteomic analysis are ESI [92] and matrix-assisted laser desorption/ionization (MALDI) [93]. One of the fundamental differences between the two methods is that MALDI is employed on samples in a solid state, whereas ESI is employed on samples in a liquid state. Hence, interfacing LC with ESI is relatively straightforward, whereas LC–MALDI analysis is an offline process, where fractions are collected and then analyzed by MALDI at a later stage. Partly as a result of this, ESI is the dominant ionization process for analysis of samples separated by LC, and

will be the emphasis of discussion from hereon.

The process of ESI converts a solution into a mist of charged droplets. These droplets shrink as the solvent is evaporated and when the charge density in the droplet reaches a critical level, coulombic repulsion causes desorption of charged gaseous ions from the droplet [94, 95]. This process continues; as solvent continues to evaporate, droplets get smaller and more ions are ejected into the gaseous phase. Unsurprisingly, this conversion of liquid sample into gaseous ions is more efficient when less solvent is present. Hence, electrospray is referred to as a concentration-sensitive process. This means that the smaller the volume of sample introduced, the better the efficiency and sensitivity of the process. Increasing sample concentration can be achieved in two ways using LC. First, use of a narrower column and lower flow rate will cause elution in smaller volumes. Second, by improving the resolution of separation, the same amount of sample will elute in a narrower profile, giving a higher concentration at the maxima of peak elution.

Nanospray is more sensitive than ESI approaches at higher flow rates [96]; so sub-microliter flow rates are typically used for proteomic analyses. Many chromatographic systems cannot natively produce reliable gradients at these low flow rates due to the presence of solvent-mixing chambers in the plumbing that have too large volumes in comparison to the solvent flow rate,

leading to inconsistent solvent mixing and irreproducible gradients. Hence, pressure-based flow-splitting systems are commonly employed and built into the chromatography system. Generally, a split in the range of 1:100 to 1:1,000 is used post-pump but prior to the separation column, allowing efficient mixing of solvents prior to chromatography to produce consistent separations, albeit with large amounts of solvent waste. Recently, some systems have been developed that use air pressure as the pumping mechanism and allow splitless delivery of reproducible nanoliter per minute flow rates.

Different stationary phases in chromatography columns provide variable levels of resolution. Reverse-phase (RF) chromatography is highly compatible with subsequent mass spectrometric analysis due to the lack of salts in the buffers and provides relatively high-resolution separation, so is widely used for proteomic analysis. With the growing need for more powerful and highly resolving separation methods, the use of multidimensional LC in proteomics has thrived. Multidimensional LC combines two or more forms of LC to increase the peak capacity, and thus the resolving power, of separations to better fractionate peptides prior to entering the mass spectrometer [87].

2.4.1.2 Mass Analysis

Mass spectrometer is an analytical technique that measures the mass-to-charge ratio (m/z) of ions based upon their motion in an electric or a magnetic field. Sample molecules are converted into ions in the gas phase and separated according to their m/z; positively and negatively charged ions can be formed. Mass spectrometer typically consists of three components: ionization source, analyzer and detector. Ionization source is the region where the gas phase ions are produced from sample molecules. ESI and MALDI are the two major types of ionization techniques for proteomic analysis, and this has been discussed in above section. Mass analyzer is the component that separates the ions according to their m/z. Detector is the final component which records the signal produced by ions. Although in theory any type of mass analyzer could be used for LC-MS, four types including quadrupole, time-of-flight (TOF), ion trap, Fourier transform-ion cyclotron resonance (FT-ICR) are used most often.

Quadrupole

A quadrupole mass analyzer (Figure 2.9) consists of four parallel rods arranged in a square. The analyte ions are directed down the center of the square. Voltages applied to the rods generate electromagnetic fields. These fields determine which m/z of ions can pass through the filter at a given time.

Quadrupoles tend to be the simplest and least expensive mass analyzers. They can operate in two modes: scan mode and selected ion monitoring (SIM) mode (Figure 2.9). In scan mode, the mass analyzer monitors a range of m/z. In SIM mode, the mass analyzer monitors only a few m/z. SIM mode is significantly more sensitive than scan mode but provides information about fewer ions. Scan mode is typically used for qualitative analyses or for quantitation when all analyte masses are not known in advance. SIM mode is used for quantitation and monitoring of target compounds.

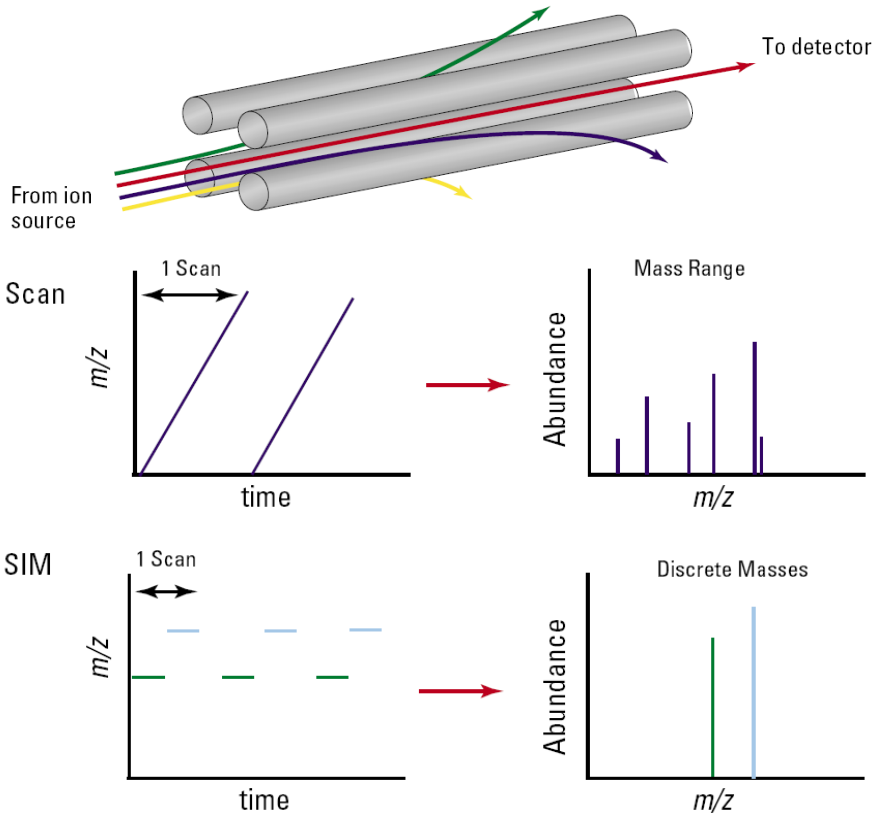

Figure 2.9 Quadrupole mass analyzer. The quadrupole mass analyzer can scan over a range of m/z or alternate between just a few.

TOF

In a TOF mass analyzer (Figure 2.10), a uniform electromagnetic force is applied to all ions at the same time, causing them to accelerate down a flight tube. Lighter ions travel faster and arrive at the detector first, so the m/z of the ions is determined by their arrival times. TOF mass analyzers have a wide mass range and can be very accurate in their mass measurements.

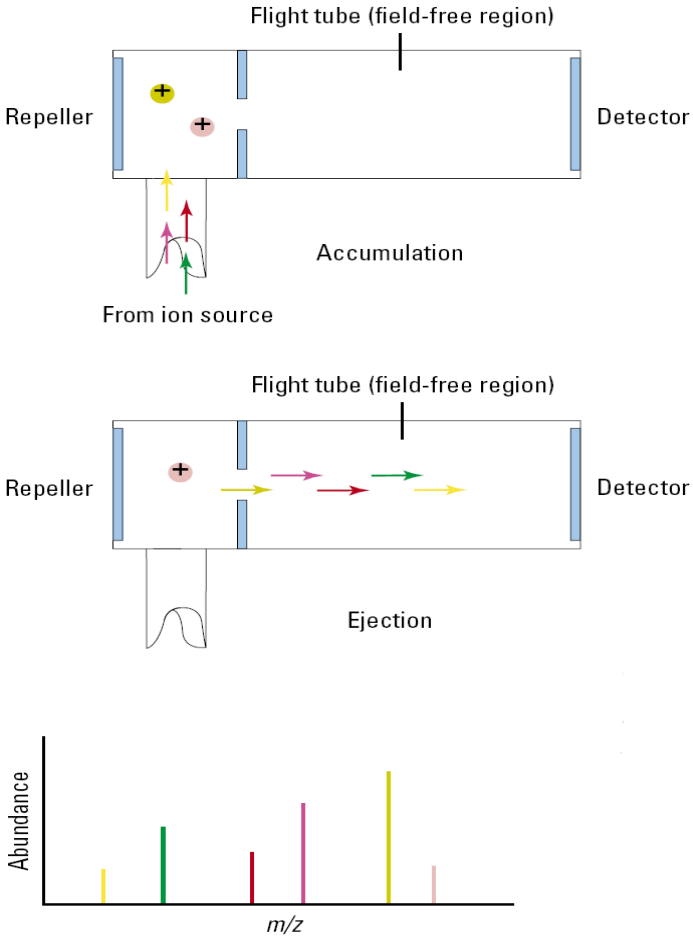

Figure 2.10 TOF mass analyzer.

Ion Trap

An ion trap mass analyzer (Figure 2.11) consists of a circular ring electrode plus two end caps that together form a chamber. Ions entering the chamber are “trapped” there by electromagnetic fields. Another field can be applied to selectively eject ions from the trap. Ion traps have the advantage of being able to perform multiple stages of MS without additional mass analyzers.

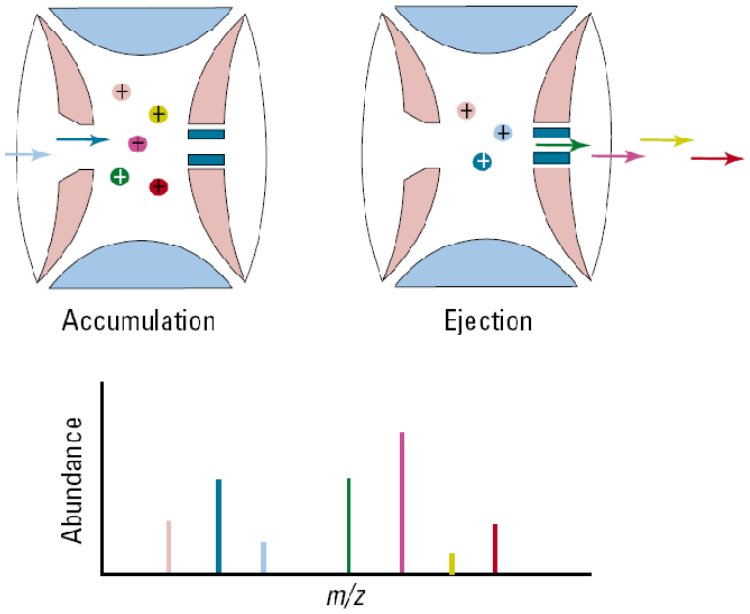

Figure 2.11 Ion trap mass analyzer.

FT-ICR

An FT-ICR mass analyzer (also called FT-MS, Figure 2.12) is another type of trapping analyzer. Ions entering a chamber are trapped in circular orbits by powerful electrical and magnetic fields. When excited by a

radio-frequency electrical field, the ions generate a time-dependent current. This current is converted by Fourier transform into orbital frequencies of the ions which correspond to their m/z. Like ion traps, FT-ICR mass analyzers can perform multiple stages of MS without additional mass analyzers. They also have a wide mass range and excellent mass resolution. They are, however, the most expensive of the mass analyzers.

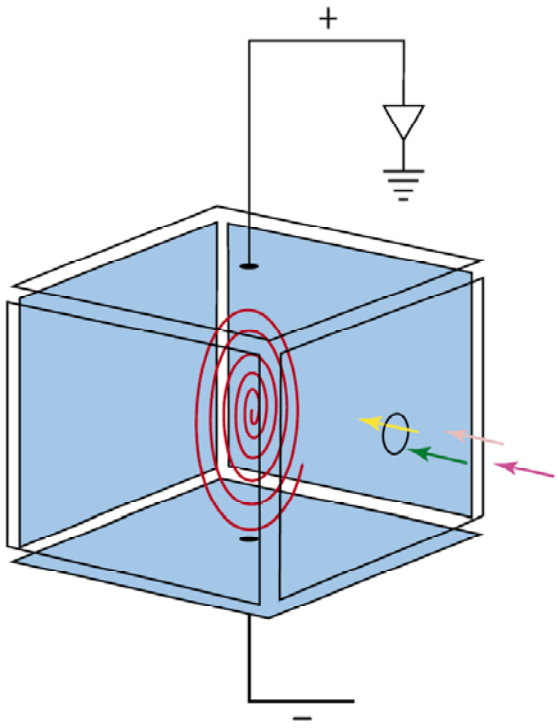

Figure 2.12 FT-ICR mass analyzer.

2.4.1.3 Tandem MS

For identification of peptides in complex mixtures, measurement of peptide mass alone is not sufficiently informative. While the combination of accurate mass and retention time can be employed for identification in well-defined

samples [97], the most flexible and generally applicable approach involves fragmentation analysis of components. In an initial scan, the masses of intact components are measured, and then in a subsequent scan/s, individual components are isolated in the mass spectrometer and then fragmented.

Generally, these experiments are performed successfully on two types of instruments: those where analyzers are in series (tandem in space) such as the triple quadrupole and hybrid quadrupole-TOF configurations; and secondly those instruments which employ ion trapping mechanisms such as the quadrupole ion trap and FT-ICR analyzer (tandem in time). In triple-quadrupole or hybrid quadrupole-TOF instruments (Figure 2.13), the first quadrupole is used to select the precursor ion. Fragmentation takes place in the second stage (quadrupole or octopole), which is called the collision cell. The third stage (quadrupole or TOF) then generates a spectrum of the resulting product ions. It can also perform SIM of only a few product ions when quantitating target compounds. However, in ion trap and FT-ICR MS, all ions except the desired precursor ion are ejected from the trap. The precursor ion is then energized and collided to generate product ions. The product ions can be ejected to generate a mass spectrum, or a particular product ion can be retained and collided to obtain another set of product ions (Figure 2.14). This process can be sequentially automated so

that the most abundant ion(s) from each stage of MS are retained and collided.

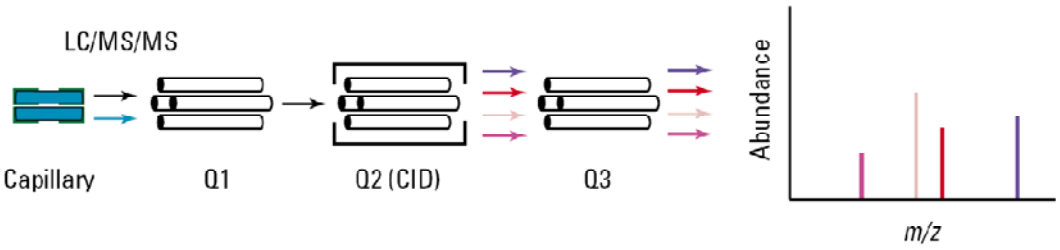

Figure 2.13 MS/MS in a triple-quadrupole mass spectrometer.

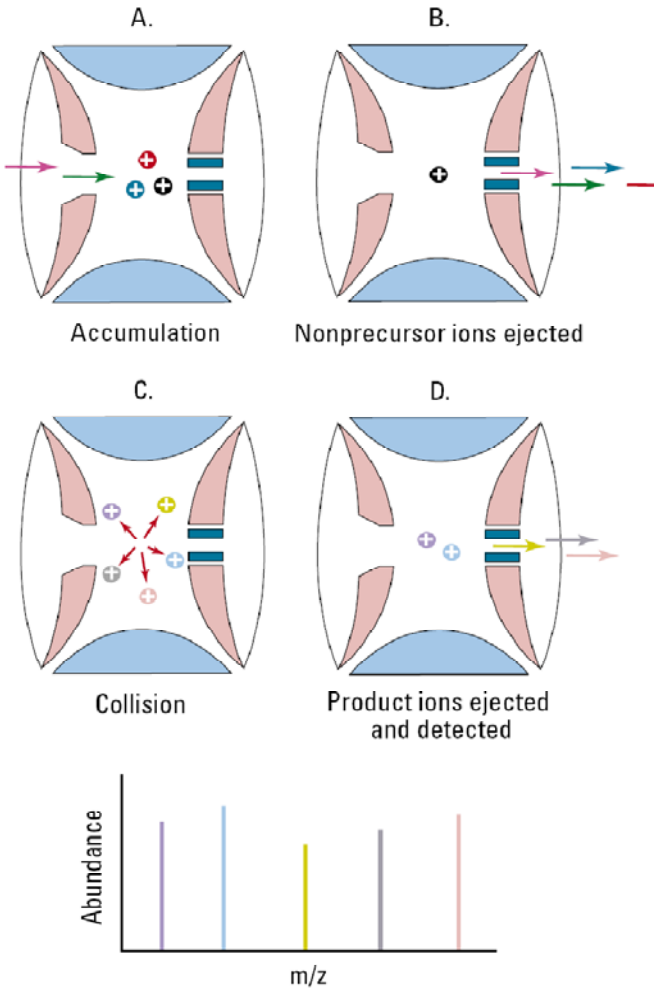

Figure 2.14 MS/MS in an ion trap mass spectrometer.

Collision induced dissociation (CID) is the major fragmentation approach. Peptide molecular ions are allowed to collide with neutral gas molecules (helium, nitrogen or argon) within a cell in the mass spectrometer. As a result of the collision, some of the kinetic energy possessed by the molecular ion is converted into internal energy which results in bond breakage and the fragmentation of the molecular ion into smaller fragments. Fragmentation within triple quadrupole, quadrupole ion trap and hybrid quadrupole TOF analyzers occurs at collisional energies in the order of 10–100 eV range, whilst fragmentation within FT-ICR analyzer occurs at collisional energies at least an order of magnitude higher in the keV range. The former is described as low-energy CID whilst the latter is described as high-energy CID. As a result of the low-energy collisional fragmentation, the peptide precursor ion fragments predictably at each peptide amide bond along the peptide backbone yielding a distribution of product ions in two complementary ion series forming a ladder which is indicative of the peptide sequence. This fragmentation nomenclature was described by Roepstorff and Fohlman [98] (Figure 2.15). The two complementary ion series are: N-terminal ion series, or b-ion series. The ions of the n-terminal ion series will contain the N-terminal amino acid and extensions from this residue. At higher collisional energies, the peptide is additionally fragmented at the amino acid side-chains [99], the subsequent fragmentation pattern can be used to differentiate the isobaric reisudes, leucine and isoleucine.

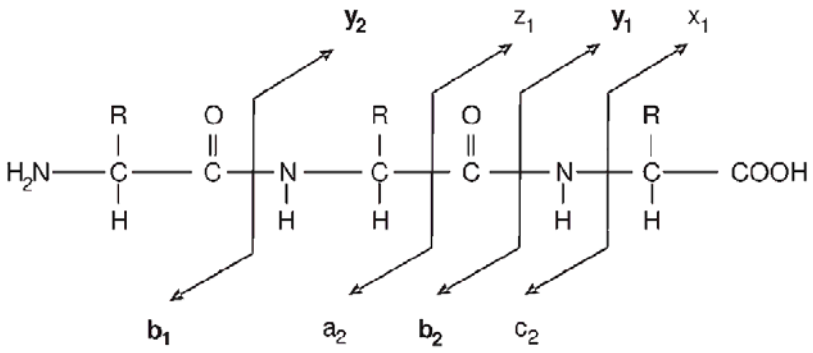

Figure 2.15 Fragmentation nomenclature according to Roepstorff and Fohlmann [98].

2.4.2 Protein Quantification

LC-MS protein quantification strategies generally involve protein/peptide labeling (known as differential mass tagging or isotopic labeling). Labeling strategies permit the mixing of samples prior to LC-MS, and in some cases upstream of any fractionation. Thus, multiple specimens can be run simultaneously with the same peptides (or proteins) being identically separated and co-eluted into the mass spectrometer with ion intensities being directly compared in the same MS or MS/MS scans. The labeling strategies thus improve throughput and quantitative accuracy.

Differential labeling approaches for quantitative LC-MS in proteomics fall into two main categories: those which use chemical derivatization or enzymatic modification of proteins or peptides after sample collection, and those which use incorporation of isotope-labeled amino acids in vivo. The chemical labeling approaches make use of tags with the same (isobaric labeling) or different masses (isotopic labeling). Isobaric labeling,

exemplified by iTRAQ [100], consists of peptide tags which generate specific fragment ions by MS/MS. Samples are differentially labeled and then combined and concurrently analyzed by LC-MS/MS, with relative quantitation performed by comparison of intensities of the 'reporter' fragments in the MS/MS spectra. In contrast, isotopic labeling methods, such as isotope-coded affinity tags (ICATs) [101] or proteolytic ^{18}O labeling [102], generate pairs (or more) of peptides with a mass difference introduced by the label. The ion intensities of the isotopic forms of the labeled peptides which should have identical LC elution profiles are then compared to give a peptide ratio of the 'heavy'-labeled versus 'light'-labeled peptide. In a similar manner, differential isotopic labeling in vivo allows quantification of peptides following incorporation of 'light' (^{12}C, ^{14}N, ^{1}H) and 'heavy' stable isotope-labeled (^{13}C, ^{15}N, ^{2}H) amino acids and is exemplified by the stable isotope labeling of amino acids in culture (SILAC) strategy [103]. In all of these methods, the ratios of detected 'reporter' fragments or isotopically labeled peptides are computed and integrated into protein ratios which can then be evaluated statistically. Multiple software solutions for the analysis of quantitative information using these labeling strategies are available. Although many of these solutions are instrument, data or tag dependent, they all work on the same principle whereby isotopically labeled peptide pairs (or reporter ions) are extracted on the basis of their characteristic mass differences and successful MS/MS

peptide assignments. Ratios of the extracted isotopic pairs are then computed and statistical evaluation performed. It is important to note that the smaller the mass difference of the tags is, then the more difficult it becomes to interpret the data and perform accurate quantification, since the isotope envelopes of the differentially labeled peptides may overlap. When using any labeling approach for LC-MS, the labels are best introduced at the earliest point in the workflow to minimize differences introduced into the samples by handling or quantitative differences between LC-MS runs. In this sense, the in vivo labeling strategies outperform the chemical and enzymatic labeling strategies in terms of accuracy of quantitation; however, as will be discussed below, multiplexing using in vivo labeling is presently more limited than chemical labeling, where 12-plex strategies have been reported [104]. Another important difference in these tagging strategies is in the analysis of primary tissues and clinical samples such as tissues, body fluids and urine, which are only amenable to the in vitro labeling approaches.

2.4.2.1 ICAT

Although stable isotope labeling for protein quantitation had been previously reported, ICAT was the first robust and universal differential labeling strategy to be developed for quantitative LC-MS and is based on cysteine thiol group modification using iodoacetamide tags. In the first

report, ICAT was used to examine the expression profiles of yeast growing on either galactose or ethanol in a single analysis [101]. Stable isotopes were incorporated into intact proteins after lysis by selective alkylation of cysteines with either a heavy (deuterium D_8) or a light (deuterium D_0) reagent bearing a biotin tag. Prior to LC-ESI-MS/MS analysis, the protein mixture was digested with trypsin and the ICAT labeled (cysteine-containing) peptides enriched on monomeric avidin–agarose. This had the advantage of simplifying the peptide mixture for downstream LC-MS/MS-based identification. Outline of a protocol for ICAT-based quantification of proteins in two biological samples is shown in Figure 2.16.

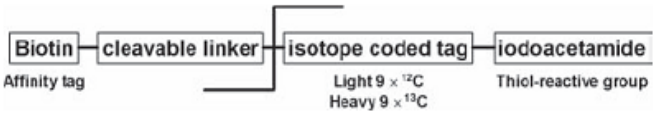

Structure of cleavable isotope-coded affinity tag (ICAT) reagent

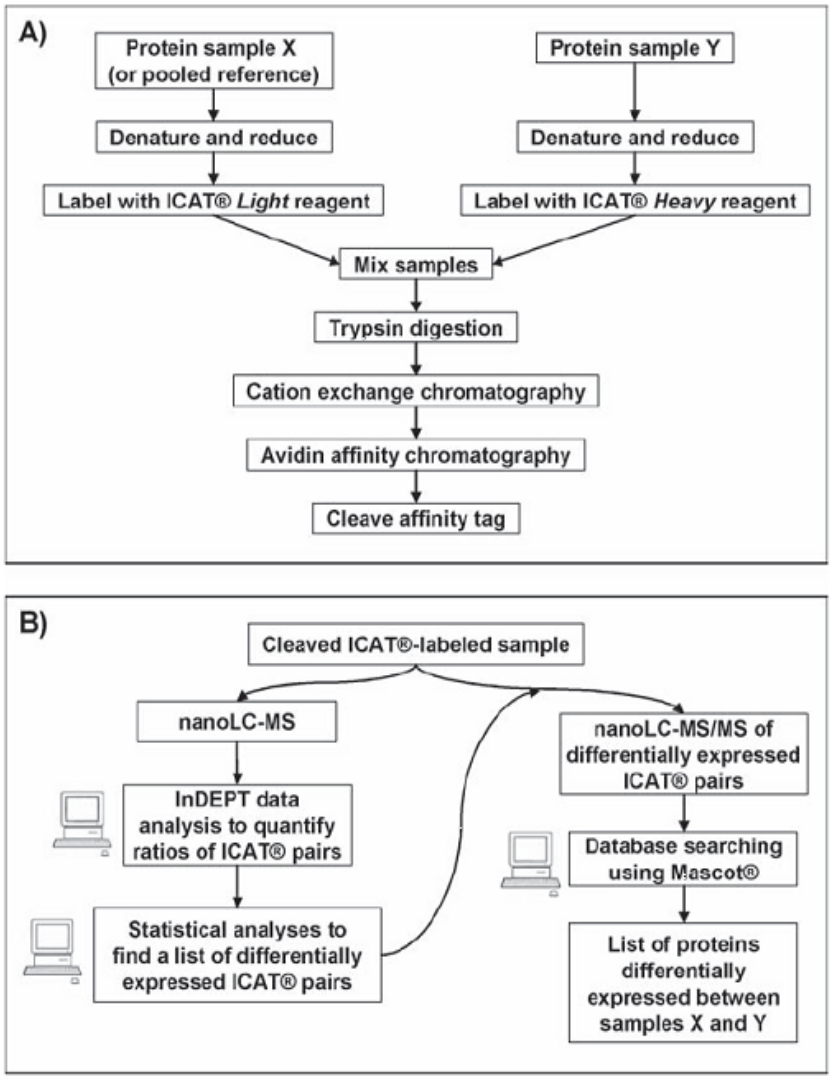

Figure 2.16 Outline of a protocol for ICAT-based quantification of proteins in two biological samples [105]. (A) Steps involved in ICAT labeling and purification. One of the samples may be a pooled reference if more than two samples are compared. (B) Targeted MS analysis of ICAT samples for quantification and identification of differentially expressed proteins. Steps involving computerized data analysis are indicated with a computer icon.

Several technical problems were reported with the original deuterated ICAT reagents. Prominent of these was the differential elution of ICAT-labeled peptide pairs in RP-LC leading to errors in the quantification [106, 107]. A further problem was the relatively low efficiencies of labeled peptide CID, which was speculated to be due to the relatively large size of the ICAT moiety [108]. Poor recovery of tagged peptides from avidin may also contribute to reduced proteomic coverage. To improve these issues, a new generation of ICAT reagents were developed where the deuterium atoms were substituted for nine ^{12}C (light) or ^{13}C (heavy) atoms and an acid-cleavable linker added. These new generation cleavable ICAT reagents gave more precise co-migration of the light- and heavy-tagged peptides in RP-LC, whilst the cleavage strategy eliminated undesired residual fragmentation of biotinylated peptides and improved recovery [109]. However, an additional clean-up step was required for removal of the cleaved biotin moiety prior to LC-MS analysis.

2.4.2.2 Differential Proteolytic $^{16}O/^{18}O$ Labeling

Differential stable isotopic labeling can also be achieved enzymatically. The major method relies on the oxygen atom exchange that takes place at the C-terminal carboxyl group of peptides during proteolytic digestion. Here, one or two ^{16}O atoms are replaced by one or two ^{18}O atoms through enzyme-catalyzed exchange in the presence of $H_2{}^{18}O$. The method was

first suggested as a protein quantification tool when ^{18}O-labelled internal standards were generated for absolute quantification by MALDI–MS [110]. This was followed by the reporting of conditions for protein labeling [111] and then the first proteomic application of the method, where trypsin was used to incorporate two ^{18}O atoms into the C termini of all tryptic peptides and was applied to compare proteins from two serotypes of adenovirus [102]. Subsequent work by the same group showed that Glu-C could also be used for labeling, that ^{18}O-labelled and unlabelled (^{16}O) peptide pairs co-eluted in RP-LC and measurements of isotope ratios by LC-MS were accurate and precise [112]. Schematic representation of the enzyme-catalyzed ^{18}O-labeling strategy is shown in Figure 2.17.

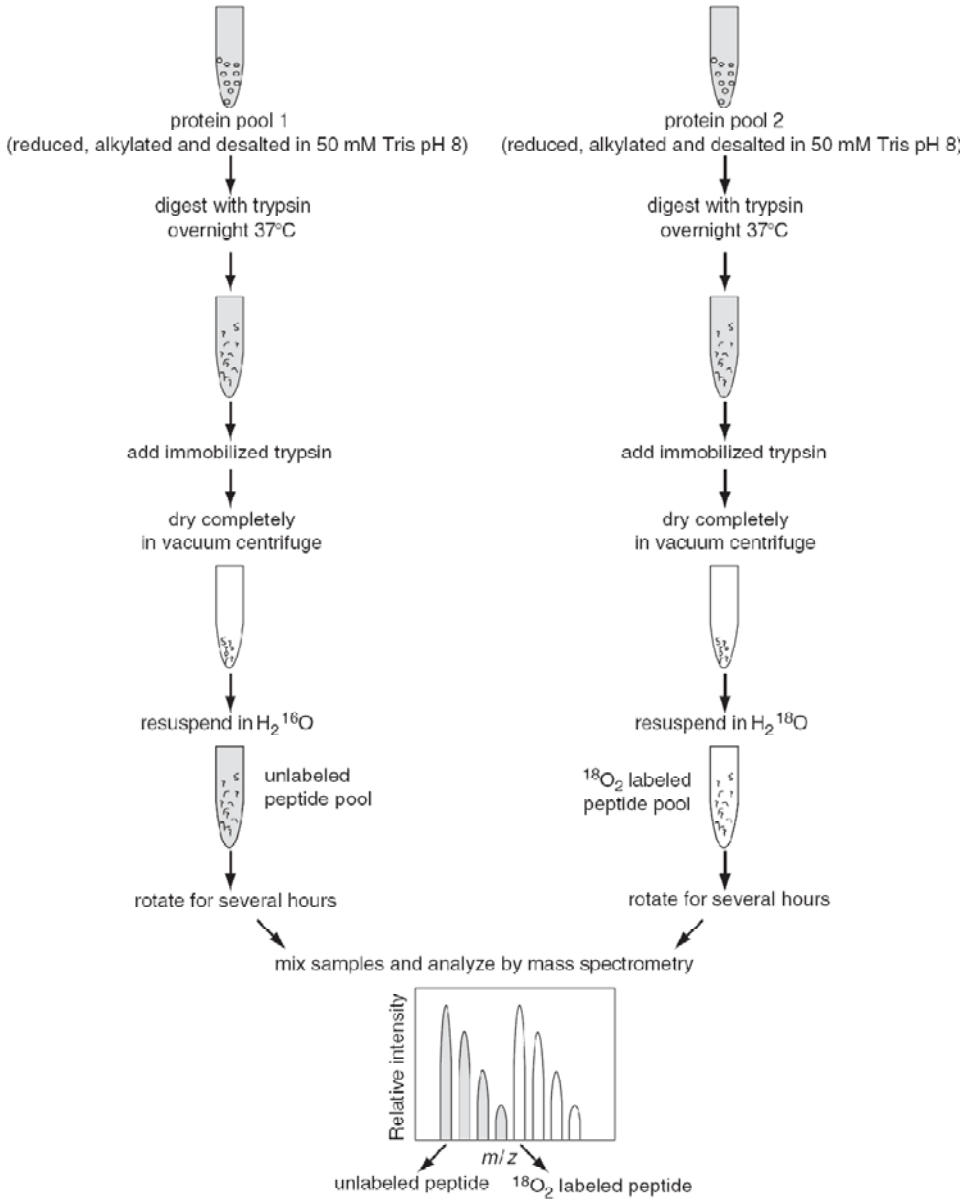

Figure 2.17 Schematic representation of the enzyme-catalyzed 18O-labeling strategy for comparative proteomics with digestion and labeling steps decoupled [113].

Several drawbacks of the proteolytic labeling strategy are apparent. Only two samples can be compared simultaneously, C-terminal peptides of proteins cannot be quantified and variable incorporation of ^{18}O into peptides can occur [114]. There is also a lack of computational tools for accurate quantification of peptide differences and this is exacerbated by

the overlap of isotopic envelopes for ^{16}O- and $^{18}O_1$- and $^{18}O_2$-labelled peptides.

2.4.2.3 iTRAQ

Isobaric tagging is a multiplex peptide labeling method that relies on the introduction of stable isotope tags that are chemically identical but distinguishable by MS/MS due to their fragmentation into reporter ions of different masses. The most commonly used method of this type has been the 4-plex iTRAQ reagents, which are N-hydroxysuccinimidyl esters for the labeling of primary amino groups. A specific reporter group in each tag based on N-methylpiperazine generates ions of 114, 115, 116 and 117 m/z upon CID fragmentation (Figure 2.18 A). These appear in an ion-sparse region of MS/MS spectra and their relative intensities provide the relative abundance of labeled peptides between the samples. The reporter groups in each tag are mass-balanced with a linker group making the tags isobaric. The major advantage of this MS/MS-dependent strategy is that the multiplex labeling does not increase the mass complexity of the samples and only peptides subjected to CID fragmentation are quantified. In addition, higher signal-to-noise ratios can be achieved with MS/MS-based detection versus MS-mode measurements. In the first reported use of iTRAQ, Ross et al. [100] compared global protein expression of wild-type and mutant yeast strains defective in the nonsense-mediated and 5’ to 3’

mRNA decay pathways using 2D-LC linked to MALDI- and ESI-MS/MS. Under optimized labeling conditions, there was an estimated 97% labeling of N termini and lysine-amino groups, with a minimal degree of unlabelled or tyrosine-labeled peptides. Lysinederivatised peptides were more frequently identified, possibly due to their higher ionization efficiency versus arginine-terminated peptides. Peptide ratios were averaged for each protein and 685 proteins were quantified in all three yeast strains using two or more significant scoring peptides. A high degree of reproducibility for individual peptides contributing to any given protein was reported. This study also determined the absolute levels of a target protein after spiking with a synthetic peptide standard labeled with one of the isobaric tags. An 8-plex version of iTRAQ has also been commercialized, generating a spectrum of eight unique reporter ions at 113, 114, 115, 116, 117, 118, 119 and 121 m/z increasing sample throughput for complex differential analyses [115-117]. An overview of an iTRAQ workflow is shown in Figure 2.18 B.

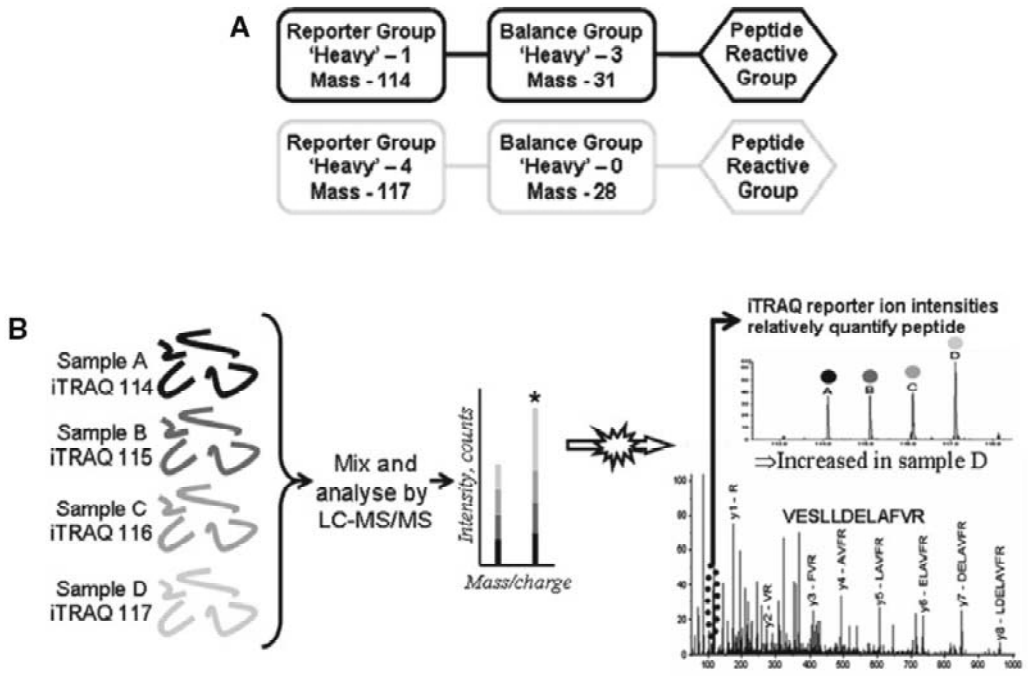

Figure 2.18 A generic iTRAQ experiment [118]. (A) A schematic of two iTRAQ tags, showing three distinct groups, a peptidereactive group, the reporter group, which allows relative quantification upon MS/MS, and a balance group, which maintains the isobaric nature of the tags. (B) An overview of an iTRAQ workflow. Peptides from multiple samples are labeled with iTRAQ tags. These samples are pooled, generating a single ion for each peptide. One putative peptide ion (marked with a ∗ in the figure) is then selected and fragmented. A typical MS/MS spectrum is shown, demonstrating sequence identification, with the reporter ion region expanded to demonstrate how peptide-relative quantification is determined.

There are several drawbacks to the isobaric tagging methods when compared to other labeling strategies. The iTRAQ reagents are expensive, difficult to synthesize and show signals only when peptides are subjected to fragmentation. Thus, the strategy misses peptides not selected for MS/MS, thus lowering proteomic coverage. Dedicated software must also be used for data analysis, although as well as commercially available software (Mascot, Proteome Discoverer, Protein Pilot), free computational tools for iTRAQ quantification and protein identification with details of

statistical considerations when analyzing iTRAQ data have been reported [119-127]. It is also evident that the low collision energies used in ion traps and some Q-TOF platforms can result in low iTRAQ reporter ion abundances and hence less accurate quantification data. Thus, higher energy CID methods have been employed, such as pulsed Q dissociation available on the popular LTQ linear ion-trap instruments or 'higher energy CID' available on the LTQ-Orbitrap. However, it is apparent that careful tuning is required for optimal fragmentation [128-130]. Finally, isotope purity correction in measured peak areas needs to be applied for each batch of reagents used and there is reported evidence of the compression of the dynamic range of ratios determined by the iTRAQ technique [131].

2.4.2.4 SILAC

As mentioned previously, SILAC is an in vivo stable isotope labeling method which uses heavy and light versions of essential amino acids that are added to the growth media of metabolically active cells. The idea behind the strategy originates from comparative proteomic experiments of simple model organisms [132-135] and plants [135] which can be grown in either medium containing ^{14}N at natural abundance (99.6%) or the same medium enriched in ^{15}N. The method was adapted for the analysis of mammalian cell culture systems where deuterated leucine ([D3]Leu) was supplemented into the growth media of cells in one state for comparison with unlabelled

cells in another state [103]. Cells were harvested and equal amounts of cells or protein lysate mixed prior to fractionation and LC-MS. As mentioned above, this has the benefit of reducing technical variability since the samples for comparison are mixed at the earliest possible stage in the workflow and are thus treated as one sample and subjected to the same downstream manipulations. The intensities of all peptides ions containing the label can be compared with their unlabelled counterparts for relative quantification.

The method was improved with the introduction of [$^{13}C_6$]Lys and [$^{13}C_6$]Arg, providing a larger mass difference between light and heavy peptides, giving predominantly C-terminal tagging of tryptic peptides and improving co-elution of heavy and light peptides by RP–LC. Various labels have subsequently been combined for 3-, 4- and 5-plex comparisons ([$^{13}C_6$]Lys (+6 Da); [$^{13}C_6$]Arg (+6 Da); [$^{15}N_4$]Arg (+4 Da); [D_4]Lys (+4 Da); [$^{13}C_6$,$^{15}N_2$]Lys (+8 Da); [$^{13}C_6$,$^{15}N_4$]Arg (+10 Da); [$^{13}C_6$,$^{15}N_2$,D_9]Lys (+17 Da); [$^{13}C_6$,$^{15}N_4$,D_7]Arg (+17 Da)], with the method shown to give reproducible quantitative information [136-138]. Software platforms for SILAC-based quantification have also been described, including MaxQuant for LTQOrbitrap- acquired data [139]. Example of Arg6-SILAC labeling and assessment of proline conversion is shown in Figure 2.19.

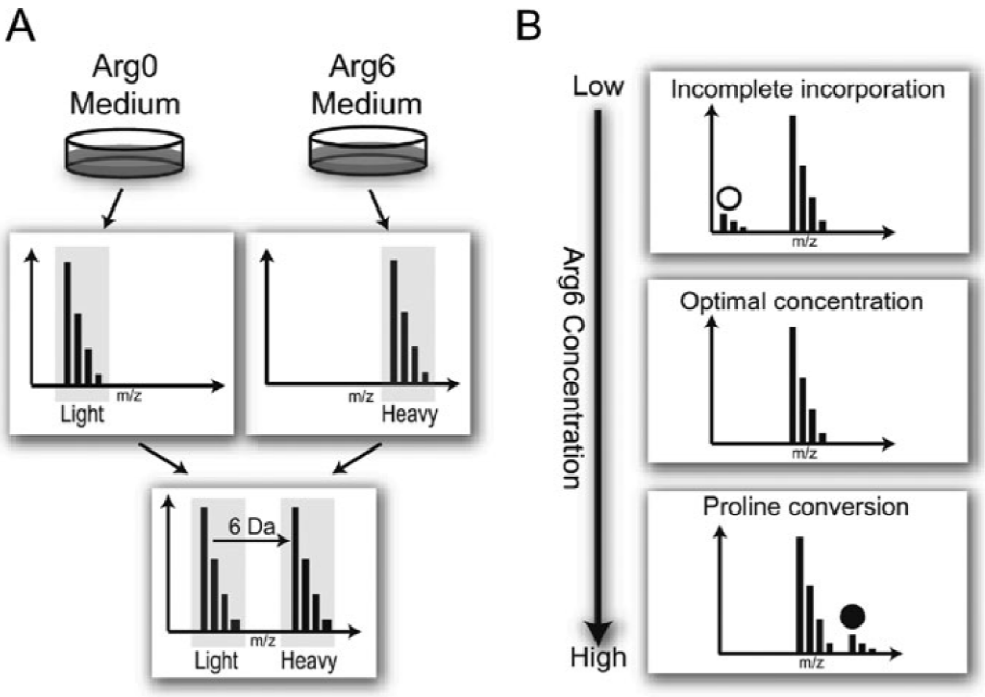

Figure 2.19 Example of Arg6-SILAC labeling and assessment of proline conversion [140]. (A) Peptides from cells passaged in either Arg0- or Arg6-containing medium can be distinguished by MS because they are separated in mass by 6 Da as a consequence of the different isotopic labeling. (B) Too low concentrations of arginine in the labeling media cause incomplete incorporation (top panel, unfilled circle) while too high concentrations can lead to proline conversion (bottom panel, filled circle). In between a range of optimal arginine concentrations can be established where the incorporation is complete and the degree of proline conversion is negligible (middle panel).

The major drawback of the SILAC method is that it can be used only for samples where in vivo labelling is possible. This has restricted its use to simple organisms or cultured cell models, and so the quantitative comparison of proteins derived from tissues or body fluids is not possible. An additional drawback of the SILAC method is the cellular conversion of isotopelabelled arginine to proline, resulting in dilution of heavy peptide ion signals and hence inaccuracies in quantification. This is of particular concern as it can effect up to half of all peptides in a proteomic experiment.

The problem can however be alleviated by reducing the L-arginine concentration [141], by supplementing L-proline into the SILAC media [142] or by mathematical correction.

2.4.3 Role in Mechanistic Studies of ABPs

Antibacterial agents act by interfering with essential cellular functions or structures of bacteria. The bacterial proteome is dynamic in nature and quickly adjusts in response to antibacterial-agent attacks on physiological homeostasis. The cellular responses are highly specific for the physiological impairment encountered and usually directed at either compensating for the loss of a particular function or counteracting the inflicted damage. The cellular response to antibacterial-agent treatment therefore virtually mirrors the antibacterial mechanism of action. As a result, quantitatively comparing changes in the level of proteins between control and antibacterial-agent-treated conditions may aid mechanistic studies of antibacterial agents such as ABPs.

Chapter 3: LC-MS/MS Analysis of Cytoplasmic Protein Profile of *E. coli* in Response to Apidaecin IB Challenge

(Part of this section was from our paper published in J Proteomics. 75(2): p. 511-6. Permission to use the article in this dissertation was obtained from publisher.)

3.1 Introduction

Apidaecins, 18- to 20-residue peptides produced by insects, are the largest group of proline-rich ABPs known to date. They are predominantly active against Gram-negative bacteria including a wide range of plant-associated bacteria and some human pathogens [22]. Previous studies suggested that the antibacterial mechanism of apidaecins was based on their ability to bind the chaperone DnaK and inhibit its function of assisting the polypeptides folding. However, it is possible that these peptides inactivate bacteria by other mechanisms not yet identified. Therefore, identifying new targets, exploring the underling molecular mechanisms involved, and thus improving the understanding of the mechanisms of action of these peptides are needed.

In this chapter, an iTRAQ-coupled 2D LC-MS/MS technique was utilized to identify cytoplasmic proteins of *E. coli* altered in response to apidaecin IB

challenge. Levels of 60 kDa charperonin (GroEL) and 10 kDa charperonin (GroES), which together form the only essential chaperone system in *E. coli* cytoplasm under all growth conditions, were decreased in cells incubated with apidaecin IB. The reduction in the amount of the GroEL/GroES chaperon team was further found to be involved in a new antibacterial mechanism of these peptides.

3.2 Materials and Methods

3.2.1 Bacterial Strain and Culture

The bacterial strain used in this work was *E. coli* ATCC 25922 obtained from the American Type Culture Collection (Rockville, MD). Frozen *E. coli* stock was streaked onto Mueller-Hinton (MH) agar plates and grown at 37 °C. Cells from a single colony were inoculated into MH broth and cultured overnight at 37 °C with shaking at 225 rpm for subsequent experiments.

3.2.2 Minimal Inhibitory Concentration (MIC) Assay

The MIC of apidaecin IB was determined as described previously [143]. An aliquot of fresh overnight culture was inoculated into MH broth and incubated at 37 °C with shaking at 225 rpm until the optical density at

600nm (OD_{600}) of the undiluted culture was between 0.2 and 0.4. Cell suspension was diluted to obtain a concentration of 5×10^5 colony-forming units (CFUs)/ml. Apidaecin IB (AnaSpec, Inc., USA) was diluted in 0.01% acetic acid buffer to obtain a concentration of 1280 μg/ml. The diluted cell suspension (100 μl) and the serial two-fold dilution of the peptide solution (11 μl) were distributed in each well of round-bottomed, 96-well microtiter plate. Growth of cells in the plate was determined by visual inspection after 16–20 hr incubation at 37 °C. The MIC was defined as the lowest concentration that inhibited visible growth of the tested isolate.

3.2.3 Growth Kinetics of *E. coli* Incubated with Apidaecin IB

An aliquot of fresh overnight culture was inoculated into MH broth and incubated at 37 °C with shaking at 225 rpm until OD_{600} of the undiluted culture was between 0.2 and 0.4. Cell suspension was diluted to obtain a concentration of 5×10^5 CFUs/ml and then incubated without and with $^1/_{10}$ MIC of apidaecin IB. Cell growth was checked by measuring OD_{600} at 0, 0.5, 1, 1.5, 2, 2.5, 3, 3.5 and 4 hr.

3.2.4 Cytoplasmic Protein Isolation

E. coli cells (5×10^5 CFUs/ml) were incubated with $^1/_{10}$ MIC of apidaecin IB for 1 and 2 hr. Cells were then harvested by centrifugation at 3000 × g for

10 min at 4 °C and lysed in lysis buffer (50 mM NaCl, 5 mM DTT, 1 mM PMSF and 50 mM Tris·Cl, pH 8.0) by intermittent sonication. Unbroken cells were removed by centrifugation at 3000 × g for 10 min at 4 °C. The supernatants containing the cytoplasmic proteins were collected by centrifugation at 15,000 × g for 30 min at 4 °C. The concentration of the proteins was determined by Bradford assay (Bio-Rad Laboratories, Inc., USA). Standard curves were made using γ-globulin as a control.

3.2.5 iTRAQ Labeling

Proteins from each sample (100 μg) were precipitated by the addition of four volumes of cold acetone at -20 °C for 2 hr. After centrifugation at 15,000 × g for 30 min at 4 °C, the precipitated pellets were reduced, denatured, cysteine blocked, digested and labeled with respective isobaric tags using iTRAQ reagent Multiplex kit (Applied Biosystems Inc., CA, USA) according to manufacturer's protocol. Briefly, each sample was dissolved in 20 μl dissolution buffer and denatured by adding 1 μl of Denaturant in the kit. After being completely dissolved, the sample was reduced by adding 2 μl of Reducing Reagent and incubated at 60 °C for 1 hr. The cysteine residues of each sample were blocked by incubation with 1 μl of Cysteine-Blocking Reagent at room temperature for 10 min. After that, proteins of the sample were digested by incubation with 20 μl of 0.25 mg/ml sequence-grade-modified trypsin solution (Promega Corp., USA) at

37 °C overnight. The sample was then labeled with iTRAQ reagents as follows: iTRAQ tags 114, Control 2 hr; iTRAQ tags 115, apidaecin IB-incubated 2 hr; iTRAQ tags 116, Control 1 hr; iTRAQ tags 117, apidaecin IB-incubated 1 hr. Samples were then pooled for LC-MS/MS analysis.

3.2.6 LC-MS/MS Analysis

The analysis was performed on a combined of an Agilent 1200 nanoflow LC system (Agilent Technologies Inc., USA) and a 6530 Q-TOF mass spectrometer (Agilent Technologies Inc., USA). Peptide mixture was separated by 2D LC, *i.e.* the combination of strong-cation exchange (SCX) with RP chromatography. The combined peptide mixture (3 µl) was loaded onto the PolySulfoethyl A SCX column (0.32 × 50 mm, 5 µm, PolyLC Inc., USA) and was eluted stepwise by injecting 10 different molar concentrations (10, 20, 30, 40, 50, 60, 80,100, 300, and 500 mM) of KCl solution. The sequentially eluted peptides from the SCX column were trapped onto the enrichment HPLC chip (Agilent Technologies Inc., USA) and further eluted with buffer A (0.1% formic acid) and buffer B (a nanoflow gradient of 5-80% acetonitrile plus 0.1% formic acid) at a flow rate of 300 nl/ min. The mass spectrometer was operated at a nanospray voltage of 2.2 kV. Data were acquired in the positive ion mode with a selected mass range of 300–1500 m/z. Up to two precursor peptides with +2 to +4

charges and 100–2000 m/z were selected for MS/MS using dynamic exclusion. The automatic rolling collision energy was used to promote fragmentation. The peak areas of the iTRAQ reporter ions reflect the relative abundance of the proteins in the sample.

3.2.7 Data Analysis

The identification and quantification of the proteins were performed using Spectrum Mill MS Proteomics Workbench (Agilent Technologies, Software Revision A.03.03.084 SR4). Each MS/MS spectrum was searched for species of *E. coli* against the UniProt_sprot_20070123 database. The searches were run using the following parameters: fixed modification of methylmethanethiosulfate-labeled cysteine and fixed iTRAQ modification of free amine in the amino terminus and lysine. Other parameters such as tryptic cleavage specificity, precursor ion mass accuracy, and fragment ion mass accuracy are built-in functions Spectrum Mill software. The protein profile results were filtered with protein score of 11 or greater in combination with peptide score of 7 or greater and **%** SPI (the percentage of the spectral peak-detected ion current explained by the search interpretation) of 60% or greater. Relative quantification of proteins in the case of iTRAQ was performed on the MS/MS scans and displayed as the ratio of the areas under the peaks at 114, 115, 116 and 117 Da, which were the masses of the tags that correspond to the iTRAQ reagents.

Sequence coverage was calculated by dividing the number of amino acids observed by the protein amino acid length. The following criteria were required to consider a protein for further statistical analysis: two or more distinct peptides had to be identified and the average ratio had to be greater than 1.2 or less than 0.8.

3.2.8 Western Blot Analysis

Western blotting was performed as described previously [144]. Briefly, equal amount of total protein (20 µg) were resolved using 7.5%- to 12%-sodium dodecyl sulfate polyacrylamide gel electrophoresis (SDS-PAGE). The resolved proteins were semi-dry electro-transferred to Polyvinylidine Fluoride (PVDF) membrane (Bio-Rad Laboratories Inc., USA). The membrane was then blocked in 1 × PBST (3.2 mM Na_2HPO_4, 0.5 mM KH_2PO_4, 1.3 mM KCl, 135 mM NaCl and 0.05% Tween 20, pH 7.4) at room temperature for 1 to 2 hr and then probed with primary antibody, either anti-groEL or anti-groES (Abcam, UK), at 4 °C overnight. Horseradish peroxidase-conjugated goat anti-rabbit or goat anti-mouse antibody (Santa Cruz Biotechnology Inc., USA) was used as the secondary antibody. The membrane was then incubated with SuperSignal West Pico Chemiluminescent Substrate (Thermo Fisher Scientific Inc., USA) for 3 to 5 min in dark, and exposed to CL-XPosure Film (Thermo Fisher Scientific Inc., USA) for a few seconds. The X-ray film was then developed

sequentially. The expression of DNA-directed RNA polymerase subunit alpha (RpoA) was used as a loading control.

3.2.9 Growth Kinetics of Gene-overexpression Strains in Response to Apidaecin IB Challenge

Plasmid that permits controlled expression of GroEL–GroES or DnaK–DnaJ–GrpE chaperone team (purchased form Takara, Japan) was transformed into *E. coli* BL21 (DE3) cells. Expression of the two chaperone teams is induced by the addition of L-arabinose (1 mg/ml) for 2 hr. Cell suspensions were then diluted to obtain a concentration of 5×10^5 CFU/ml and incubated without and with $^1/_{10}$ MIC of apidaecin IB. Cell growth was checked by measuring OD_{600} in interval of 1 hr.

3.2.10 Statistical Analysis

Unless indicated in the figure legends, all experiment were replicated three times. The statistical significance was assessed by Student's t-tests. A *p*-value of 0.05 or less was considered significant.

3.3 Results

3.3.1 MIC of Apidaecin IB

MIC is the lowest concentration of an antimicrobial that will inhibit the visible growth of a microorganism after overnight incubation. MIC is important in diagnostic laboratories to monitor the activity of new antimicrobial agents. In this study, MIC of apidaecin IB was evaluated by the broth micro-dilution assay. Apidaecin IB showed obvious antibacterial activity and its MIC was found to be 16 μg/ml.

3.3.2 Growth Kinetics of *E. coli* in Response to Apidaecin IB Challenge

In our work of monitoring the growth kinetics of *E. coli* cells in the presence of different concentrations of apidaecin IB, we found that apidaecin IB with any concentrations higher than $^{1}/_{10}$ MIC could have inhibition effects on the growth of *E. coli* although the effect was not as strong as that by using MIC of apidaecin IB. As a result, the concentration of $^{1}/_{10}$ MIC was chosen for all the following experiments.

The growth kinetics of *E. coli* incubated with $^{1}/_{10}$ MIC of apidaecin IB is shown in Figure 3.1. Apidaecin IB started to inhibit *E. coli* growth at 0.5 h

after its incubation. The inhibition in the growth of *E. coli* was probably the result of the interference in essential cellular functions or structures of cells by apidaecin IB. The bacterial proteome is dynamic in nature and quickly adjusts in response to antimicrobial attacks on physiological homeostasis. Therefore, quantitatively comparing changes in the level of proteins between control and apidaecin IB-incubated conditions when the inhibition effect occurs may aid mechanistic studies of this peptide. Two time points (1 hr and 2 hr) were thus chosen for the quantitative protein profiling analysis.

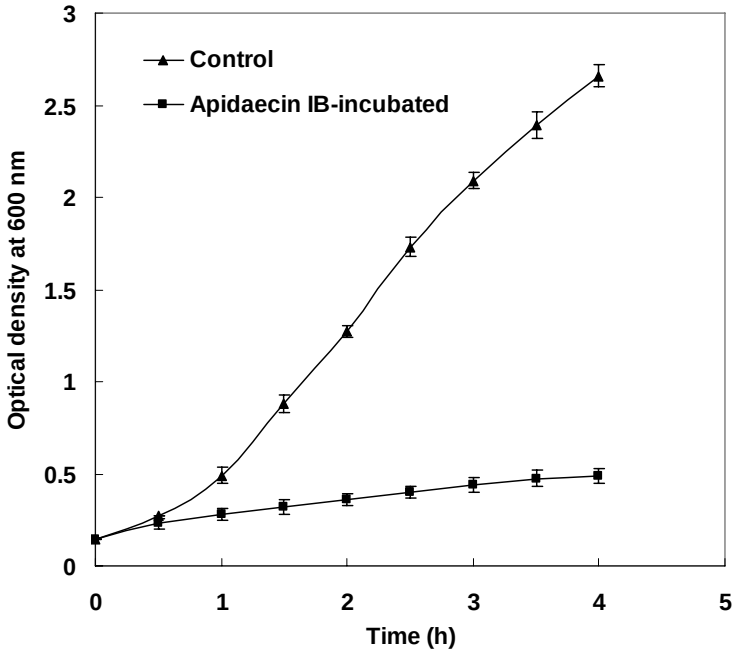

Figure 3.1 Growth kinetics of *E. coli* incubated with $^{1}/_{10}$ MIC of apidaecin IB. Each value represents the mean optical density (OD) readings from two cultures.

3.3.3 Cytoplasmic Proteins Altered in Response to Apidaecin IB Challenge

To establish the biological difference between apidaecin IB-incubated cells and control cells, the protein profiles in *E. coli* cells incubated with and without apidaecin IB were analyzed. Proteins from cells were collected, lysed, and labeled prior to 2D LC-MS/MS. Combining three independent experiments, a total of 391 distinct proteins were identified based on the following criteria: protein score of 11 or greater, peptide score of 7 or greater and **%** SPI of 60% or greater. The criteria give a confidence value of the identified protein of 99% or greater. All information about the 391 proteins was shown in Appendix 1.

Among the identified 391 proteins, 18 proteins displayed significant changes (p<0.05), and the trend of the changes in 2 hr-apidaecin IB-incubated cells was in accordance with that in 1 hr-apidaecin IB-incubated cells (Table 3.1). These proteins were subsequently categorized into seven groups based on their cellular functions: protein folding, oxidation-reduction process, tRNA processing, transcription regulation, and lipid, amino acid and carbohydrate metabolism.

Table 3.1 Cytoplasmic proteins of *E. coli* altered in response to apidaecin IB challenge

Accession Number	Protein Name	Distinct Peptides	% AA Cov	Avg A:C (±S.D.)[a] 1 hr	Avg A:C (±S.D.) 2 hr
Protein Folding					
P0A6F5	60 kDa chaperonin	25	59	0.70±0.01	0.62±0.01
P0A6H1	ATP-dependent Clp protease ATP-binding subunit ClpX	4	15	1.20±0.16	1.33±0.18
P0A6F9	10 kDa chaperonin	4	50	0.80±0.01	0.61±0.01
Lipid Metabolism					
P0A715	2-dehydro-3-deoxyphosphooctonate aldolase	4	26	0.70±0.00	0.50±0.00
P0AAI9	Malonyl CoA-acyl carrier protein transacylase	4	23	0.77±0.01	0.74±0.06
P0A6A8	Acyl carrier protein	3	33	0.70±0.00	0.57±0.00
Oxidation-reduction Process					
P13029	Catalase-peroxidase	6	15	0.70±0.00	0.62±0.00
P61949	Flavodoxin-1	2	19	0.58±0.00	0.48±0.00
Amino Acid Metabolism					
P00805	L-asparaginase 2	4	15	0.50±0.01	0.29±0.04
P00509	Aspartate aminotransferase	2	8	0.65±0.00	0.62±0.00
tRNA Processing					
P0AEI1	(Dimethylallyl)adenosine tRNA methylthiotransferase miaB	3	11	0.70±0.01	0.61±0.06
Transcription Regulation					
P0A9Y6	Cold shock-like protein CspC	3	40	0.79±0.01	0.52±0.02
Carbohydrate Metabolism					
P0A715	2-dehydro-3-deoxyphosphooctonate aldolase	4	26	0.70±0.00	0.50±0.00
P09147	UDP-glucose 4-epimerase	4	14	0.75±0.07	0.43±0.04

P0A858	Triosephosphate isomerase	3	13	0.42±0.00	0.43±0.00
P0AFG6	Dihydrolipoyllysine-residue succinyltransferase component of 2-oxoglutarate dehydrogenase complex	3	8	0.63±0.00	0.41±0.00
P0A955	KHG/KDPG aldolase	2	15	0.55±0.00	0.52±0.00
P0AC47	Fumarate reductase iron-sulfur subunit	2	11	0.68±0.00	0.38±0.00

[a] The ratio of proteins in the apidaecin IB-incubated cells relative to control cells.

3.3.4 Western Blot Analysis on GroEL and GroES

Western blot analysis was then performed to validate the changes in the level of GroEL and GroES identified by LC-MS/MS analysis. Equal amount of cell lysates from apidaecin IB-incubated cells and control cells were tested with antibodies to GroEL and GroES respectively. Results shown in Figure 3.2 indicated that levels of both GroEL and GroES were decreased in cells incubated with apidaecin IB for both 1 h and 2 h, and the reduction in the amount of both proteins was higher in 2h-apidaecin IB-incubated cells.

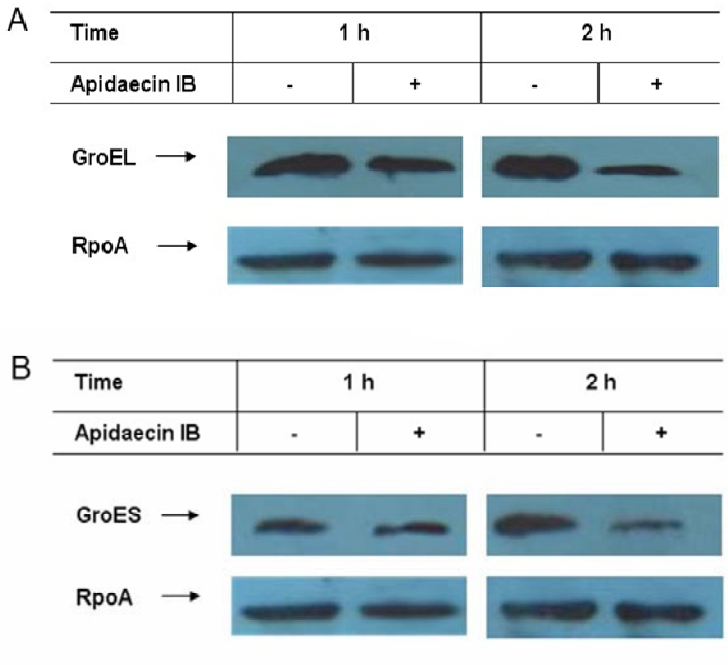

Figure 3.2 Western blot analysis of GroEL (A) and GroES (B) in *E. coli* incubated with apidaecin IB.

3.3.5 Growth Kinetics of Gene-overexpression Strains

To construct the GroEL–GroES and DnaK–DnaJ–GrpE chaperone overexpression strains, plasmid that permits controlled expression of GroEL–GroES or DnaK–DnaJ–GrpE chaperone team was transformed into *E. coli* BL21 (DE3) cells, separately. Expressions of these two chaperone teams were validated by western blot analysis on GroEL and DnaK (Figure 3.3). The growth of the cells in which GroEL-GroES or DnaK–DnaJ–GrpE chaperone team was overexpressed in response to apidaecin IB challenge was subsequently checked. The results shown in Figure 3.4 indicated that either overexpression of GroEL-GroES chaperone team or overexpression DnaK–DnaJ–GrpE chaperone team can alleviate the inhibition effect of apidaecin IB on cells; however, the alleviation effect of DnaK-DnaJ-GrpE overexpression was less than that of GroEL-GroES overexpression.

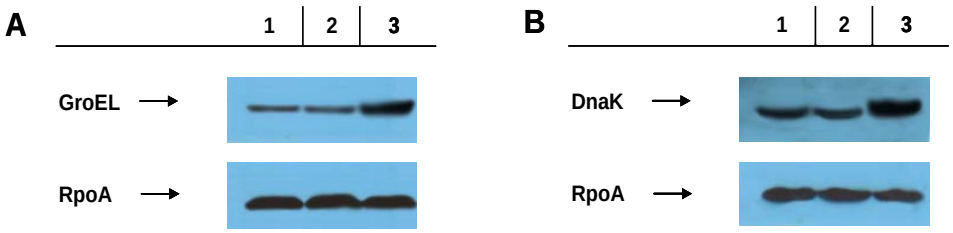

Figure 3.3 Validation the expression of GroEL (A) and DnaK (B) by western blot analysis. Lane 1, mock transformation; lane 2, transformation of empty plasmid; and lane 3, transformation of plasmid that permits controlled expression of GroEL–GroES or DnaK–DnaJ–GrpE chaperone team.

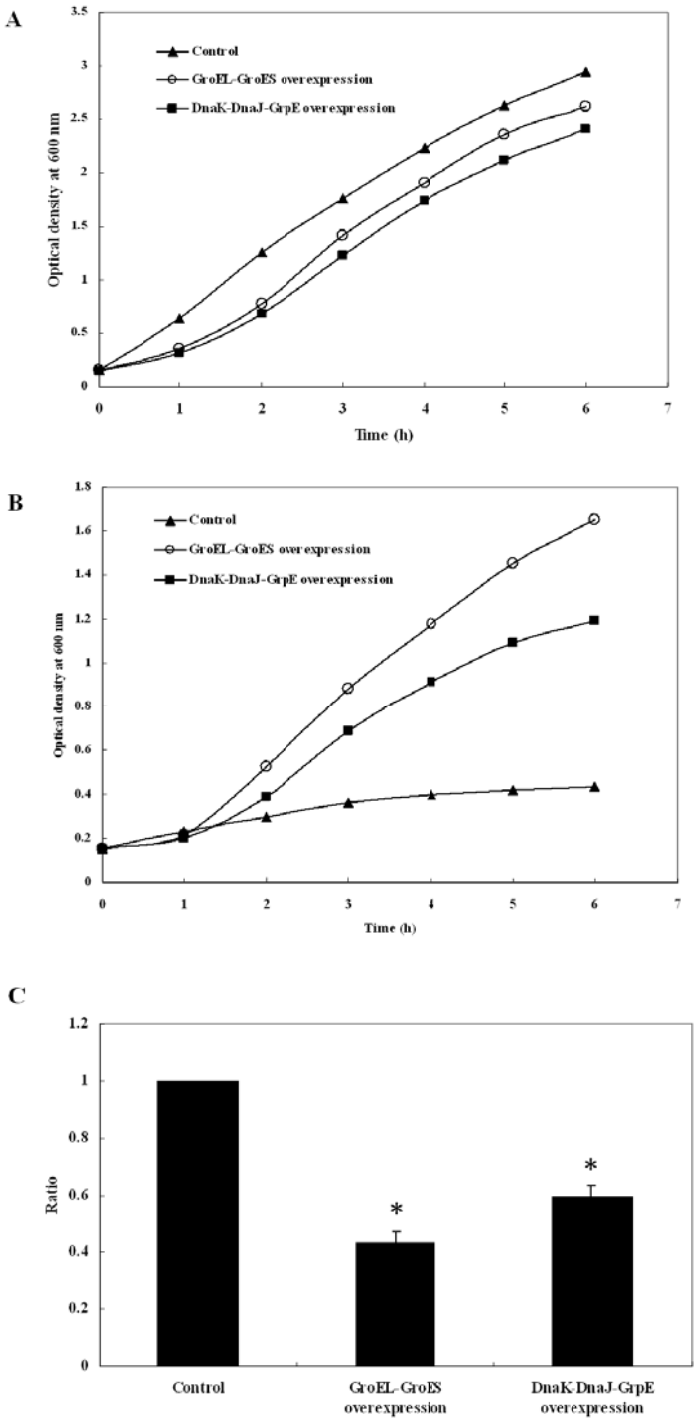

Figure 3.4 Effect of GroEL-GroES and DnaK-DnaJ-GrpE overexpression on the growth of *E. coli* incubated with apidaecin IB. (A) Growth curve of control, GroEL-GroES overexpression and DnaK-DnaJ-GrpE overexpression cells without apidaecin IB incubation. (B) Growth curve of control, GroEL-GroES overexpression and DnaK-DnaJ-GrpE overexpression cells with apidaecin IB incubation. (C) OD_{600} ratio from 6 h of culture. OD_{600} ratio of control cells was adjusted to 1 and those of cells overexpressing GroEL-GroES and DnaK-DnaJ-GrpE chaperone teams were normalized accordingly. Asterisk indicates $p<0.05$.

3.4 Discussion

Apidaecins are good representatives of non-membrane-permeabilizing ABPs which can translocate across the membrane and accumulate in the cytoplasm, where they kill bacteria by targeting different essential cellular processes. Previous studies proposed a five-step mechanism by which apidaecins exert their activity against *E. coli* and other Gram-negative bacteria: *i)* binding to negatively charged components (most probably LPS) of the OM in a non-specific manner; *ii)* self-promoted invading into the periplasmic space; *iii)* irreversible interaction with a hypothetical docking molecule/receptor molecule on the IM; *iv)* translocation across the membrane and into the cytoplasm of the cell; *v)* binding its target most probably DnaK protein to mediate cell death (Figure 2.5) [21, 24, 72, 82-84]. However, it is possible that these peptides kill bacteria by other mechanisms not yet identified.

In this study, an iTRAQ-coupled 2D LC–MS/MS approach was utilized to analyze the cytoplasmic protein profile of *E. coli* in response to apidaecin IB challenge in aim to identify target proteins whose alterations are involved in the antibacterial mechanism of action of apidaecin IB. A total of 18 proteins showed differential changes, and the trend of the changes in 2 hr-apidaecin IB-incubated cells was in accordance with that in 1 hr-apidaecin IB-incubated cells (Table 3.1). Two of the altered proteins,

GroEL and GroES, captured our attention. Levels of the two proteins were decreased in both 1 hr and 2 hr-apidaecin-incubated cells, with the decrease in the latter greater than that in the former (Table 3.1). The changes of GroEL and GroES were further validated by western blot analysis (Figure 3.2).

As we know, folding of polypeptides in the cell typically requires the assistance of a set of proteins termed molecular chaperones [145]. Chaperones are necessary for cell viability under both normal and stress conditions [146]. Chaperones can assist in the efficient folding of newly-translated proteins as these proteins are being synthesized on the ribosome and can maintain pre-existing proteins in a stable conformation [146]. Chaperones can also promote the disaggregation of preformed protein aggregates [147]. There are several chaperone systems in *E. coli* which carry out a multitude of functions all aiming towards insuring the proper folding of target proteins [148]. However, the chaperonin GroEL with its cofactor GroES form the only essential chaperone system in *E. coli* cytoplasm under all growth conditions [149]. About 300 proteins, representing 10-15% of total cytoplasmic *E. coli* proteins, utilize GroEL for de novo folding under normal growth conditions and about twice as much under stress conditions [150-152]. As a result, the decrease in the level of GroEL and GroES could be correlated with the antibacterial activity of

apidaecin IB.

The growth of the cells in which GroEL-GroES chaperone team was overexpressed in response to apidaecin IB incubation was therefore checked. The results showed that overexpression of GroEL-GroES chaperone team significantly alleviated the inhibition effect of apidaecin IB on cells (Figure 3.4). As previous studies showed that apidaecins could inhibit another chaperone-DnaK (a component of DnaK/DnaJ/GrpE chaperone system) to mediate cell death [21], the alleviation of the inhibition effect of apidaecin IB on the GroEL-GroES overexpression cells could be the result of the GroEL/GroES chaperone system partially compensating for the loss of DnaK's function, but not the result of the decrease in the level of GroEL and GroES in response to apidaecin IB. The growth of the cells in which DnaK-DnaJ-GrpE chaperone team was overexpressed in response to apidaecin IB incubation was further checked. The results showed that overexpression of DnaK-DnaJ-GrpE chaperone team can also alleviate the inhibition effect of apidaecin IB on cells; however the alleviation effect of DnaK-DnaJ-GrpE overexpression was less than that of GroEL-GroES overexpression (Figure 3.4). Thus, the alleviation of the inhibition effect of apidaecin IB on the GroEL-GroES overexpression cells could be at least partially the result of the decrease in the level of GroEL and GroES in response to apidaecin IB. Collectively, the

data suggest that, besides inhibiting DnaK's function, apidaecin IB can also cause the decrease in the level of GroEL-GroES chaperone team, which could be involved in a new antibacterial mechanism of the peptides.

Except locating in the cytoplasm of bacteria, some proteins are attached to, or associated with the inner or outer bacterial membrane. These proteins are called membrane proteins and account for about one quarter to one third of all bacterial proteins. As membrane proteins perform essential physiological functions, they may be the target of antibacterial agents. Further analysis of the membrane protein profile is required to comprehensively investigate the changes in the global proteome of *E. coli* in response to the challenge apidaecin IB and thus infer the possible mechanisms of action of these peptides.

Chapter 4: LC-MS/MS Analysis of Membrane Protein Profile of *E. coli* in Response to Apidaecin IB Challenge

(Part of this section was from our paper published in PLoS One. 6(6): e20442. Permission to use the article in this dissertation was obtained from publisher.)

4.1 Introduction

Our previous work focused on analysis of changes in the cytoplasmic proteins in response to the challenge of apidaecin IB. However, except cytoplasmic proteins, about one quarter to one third of all bacterial genes encode proteins of inner or outer bacterial membrane. These membrane proteins perform essential physiological functions, such as the import or export of metabolites, the homeostasis of metal ions, the extrusion of toxic substances, and the generation or conversion of energy. For this reason, these proteins may be targeted by antibacterial agents. It is thus necessary to analyze changes of membrane proteins in response to apidaecins challenge, with of hope of identifying new targets of these peptides.

In this chapter, the iTRAQ-coupled 2D LC-MS/MS technique was utilized to identify membrane proteins of *E. coli* altered in response to the challenge of apidaecin IB. Cell division protease ftsH (FtsH), an essential regulator in maintenance of membrane lipid homeostasis, was overproduced in cells incubated with apidaecin IB for both 1 hr and 2 hr. Its overproduction intensified the degradation of cytoplasmic protein

UDP-3-O-acyl-N-acetylglucosamine deacetylase (LpxC), which catalyzes the first committed step in the biosynthesis of the lipid A moiety of LPS, and thus led to the further unbalanced biosynthesis of LPS and phospholipids. These findings suggested a new antibacterial mechanism of apidaecins.

4.2 Materials and Methods

4.2.1 Bacterial Strain and Culture

Bacterial strain and its culture procedure was the same as described in Section 3.2.1 in Chapter 3.

4.2.2 Membrane and Cytoplasmic Protein Isolation

E. coli cells (5×10^5 CFUs/ml) were incubated with $^1/_{10}$ MIC of apidaecin IB for 1 and 2 h. The membrane proteins were isolated as described previously with a slightly modification [28]. Briefly, the cells were harvested by centrifugation at 3000 × g for 10 min at 4 °C and lysed in lysis buffer (50 mM NaCl, 5 mM DTT, 1 mM PMSF and 50 mM Tris·Cl, pH 8.0) by intermittent sonication. Unbroken cells were removed by centrifugation at 3000 × g for 10 min at 4 °C. The supernatants containing the cytoplasmic proteins were collected by centrifugation at 120,000 × g for 60 min at 4 °C. The resulting pellets were resuspended in IM solubilization buffer (1% Sarkosyl, 100 mM NaCl and 50 mM Tris·Cl, pH 8.0) and incubated at room temperature for 60 min with gentle shaking. The supernatants containing the solubilized inner membrane proteins were collected by centrifugation at 120,000 × g for 60 min at 4 °C again. The pellets were resuspended in Milli-Q water and

centrifuged for up to three times. The resulting pellets were resuspended in OM solubilization buffer (3% n-octylpolyoxyethylene, 150 mM NaCl, 50 mM EDTA, 10 mM DTT, 0.1 mg/ml lysozyme and 50 mM Tris·Cl, pH 8.0) and incubated at room temperature for 60 min with stirring. The supernatants containing the solubilized outer membrane proteins were collected by centrifugation as above. The concentration of cytoplasmic, inner and outer membrane proteins were determined by Bradford assay (Bio-Rad Laboratories, Inc., USA). Standard curves were made using γ-globulin as a control.

4.2.3 iTRAQ Labeling

iTRAQ Labeling was performed using the same procedure as described in Section 3.2.5 in Chapter 3.

4.2.4 LC-MS/MS analysis

iTRAQ-labeled peptide mixtures were analyzed by 2D nanoflow LC system (Agilent Technologies Inc., USA) interfaced with a QSTAR XL mass spectrometer (Applied Biosystems Inc., USA), as described previously [144, 153-156]. The peptide mixture was loaded into a PolySulfoethyl A SCX column (50 × 0.32 mm, 5 mm, PolyLC Inc., USA) and fractionated by ten salt steps (10, 20, 30, 40, 50, 60, 80, 100, 300, and 500 mM KCl) in the first dimension. The peptides eluted from the SCX column were concentrated and desalted in a ZORBAX 300SB C18 RP column (5 × 0.3 mm, 5 mm, Agilent Technologies Inc., USA). The second dimensional chromatographic separation was carried out with a ZORBAX 300SB C18 RP column (50 ×

0.075 mm, 3.5 mm, Agilent Technologies Inc., USA) directly into a PicoFrit nanospray tip (New Objective, USA) operating with gradient starting from 5% up to 80% of acetonitrile at a flow rate of 500 nl/min over 100 min. The mass spectrometer was operated at a nanospray voltage of 2.2 kV. Data were acquired in the positive ion mode with a selected mass range of 300–1500 m/z. Up to two precursor peptides with +2 to +4 charges and 100–2000 m/z were selected for MS/MS using dynamic exclusion. The automatic rolling collision energy was used to promote fragmentation. The peak areas of the iTRAQ reporter ions reflect the relative abundance of the proteins in the sample.

4.2.5 Data Analysis

The identification and quantification of the proteins were performed using ProteinPilot Software 3.0 (Applied Biosystems Inc., USA). The *Paragon Algorithm* in the ProteinPilot software was used for the peptide identification and further processed by *Pro Group Algorithm* where isoform-specific quantification was adopted to trace the differences between expressions of various isoforms. The defined parameters were as follows: (i) Sample Type, iTRAQ 4-plex (Peptide Labeled); (ii) Cysteine alkylation, MMTS; (iii) Digestion, Trypsin; (iv) Instrument, QSTAR ESI; (v) Special factors, None; (vi) Species, *E. coli*; (vii) Specify Processing, Quantitate, Bias correction (viii) ID Focus, Biological modifications; (ix) Database, UniProt_sprot_20070123; (x) Search effort, thorough. Protein confidence for a detected protein is measured by Unused ProtScore. It calculated from the peptide confidence for peptides from spectra that are not already completely “used” by higher

scoring winning proteins. A protein with Unused ProtScore of 2.0, which corresponds to 99% confidence, is generally true. The peptide for quantification was automatically selected by *Pro Group Algorithm*, with the criterion that the peptide was usable for quantitation, identified with good confidence, and not shared with another protein identified with higher confidence, to calculate the reporter peak area, *p*-value and error factor (EF). *p*-value is a measure of the certainty that the average ratio randomly differs from 1. The smaller the *p*-value, the more likely any differential expression is real. EF is a statistic that was expressed to reflect the true value for the average ratio that was used for the quantification of differentially expressed proteins (EF= $10^{95\% \text{ confidence interval}}$, in which 95% confidence interval= (ratio × EF) - (ratio/EF)). The average ratio is far from the actual value when the EF value is more than 2. The following criteria were required to consider a protein for further statistical analysis: the EF had to be of 2 or less and the average ratio had to be greater than 1.1 or less than 0.9.

4.2.6 Western Blot Analysis

Rabbit antisera to FtsH and LpxC were produced by Invitrogen Corp., USA. The specificity of anti-FtsH and LpxC was validated. These antisera were used as the primary antibodies. Western blotting was performed using the same procedure as described in Section 3.2.8 in Chapter 3.

4.2.7 LPS and Phospholipids Analysis

LPS was extracted by using LPS extraction kit (iNtRON Biotechnology,

Korea) according to manufacturer's protocol. Briefly, cells were lysed in 1 ml of Lysis Buffer and then mixed with 200 µl of chloroform for 5 min. After centrifuging at 4 °C, 13,000 rpm for 10 min, supernatant was transferred to a new tube and mixed with 800 µl of Purification Buffer at -20 °C for 10 min. The mixture was centrifuged again at 4 °C, 13,000 rpm for 5 min. The LPS pellet was washed with 1 ml of 70% ethanol and dissolved in 10 mM Tris·Cl, pH 8.0. The LPS was then quantified by measuring 2-keto-3-deoxyheptonic acid (KDO) as described previously [157]. Phospholipids were extracted by a method described previously with a slight modification [158]. In brief, the cell pellets were resuspended in 2 volumes of Milli-Q water and mixed with 7.5 volumes organic solvent mixture (methanol-chloroform 2:1, v/v). This suspension was incubated at room temperature for 2 hr with periodic vortexing. After centrifuging at 3000 × g for 10 min, extract from the top was removed and mixed with half volume of chloroform and Milli-Q water. After thorough vortexing, the mixture was centrifuged again. Extract from the lower chloroform phase was removed and qualified by phosphate assay as described previously [159].

4.2.8 Gene Cloning

Whole genome extraction

Whole genome of *E. coli* was purified by using DNeasy Blood & Tissue Kit (QIAGEN, Germany). Briefly, cells were harvested in a microcentrifuge tube by centrifuging at 5000 × g for 10 min. Pellet was resuspended in Buffer ATL (180 µl). After mixing with proteinase K (20 µl), the mixture was

incubated at 56 °C until the cells were completely lysed. Buffer AL (200 µl) and ethanol (200 µl, 96-100%) were then sequentially added. The mixture was transferred to the DNeasy Mini spin column and centrifuged at ≥ 6000 × g for 1 min. The column was then washed by Buffer AW1 (500 µl) and Buffer AW2 (500 µl). Finally, the DNA was eluted from the column by Buffer AE (100 µl).

DNA quantification

The ratio of the readings at 260 nm and 280 nm (A_{260}/A_{280}) provides an estimate of the purity of DNA with respect to contaminants that absorb UV, such as protein. Pure DNA has an A_{260}/A_{280} ratio of 1.8-2.0. DNA concentration was calculated according to the formula below, as an A_{260} value of 1 (with a 1 cm detection path) corresponds to 50 µg DNA per ml water. DNA concentration (µg/ml) = A_{260} × 50 × dilution factor

Gene amplification

The gene encoding *E. coli* FtsH and LpxC was amplified by PCR, using the appropriate forward and reverse oligonucleotide primers designed with the help of online free software Primer 3 (http://frodo.wi.mit.edu/primer3/) (Table 4.1). The forward primer introduced an EcoRI site and the reverse primer introduced an XhoI site downstream from the stop codon. Three extra bases were introduced into the 5' end of each primer as protecting bases to ensure correct digestion of the restriction endonucleases.

Table 4.1 Primers used for plasmid construction.

Primer Name	Sequence
ftsH forward	5'-CCGGAATTCATGGCGAAAAACCTAATAC-3'
lpxC forward	5'-CCGGAATTCATGATCAAACAAAGGACAC-3'
ftsH reverse	5'-CCGCTCGAGTTACTTGTCGCCTAACTGC-3'
lpxC reverse	5'-CCGCTCGAGTTATGCCAGTACAGCTGAAGG- 3'

Vector used for cloning

The vector used in this study was pET-24a (EMD Chemicals, USA), which carry an N-terminal T7·Tag sequence plus an optional C-terminal His·Tag sequence. The map of the vector is shown in Figure 4.1.

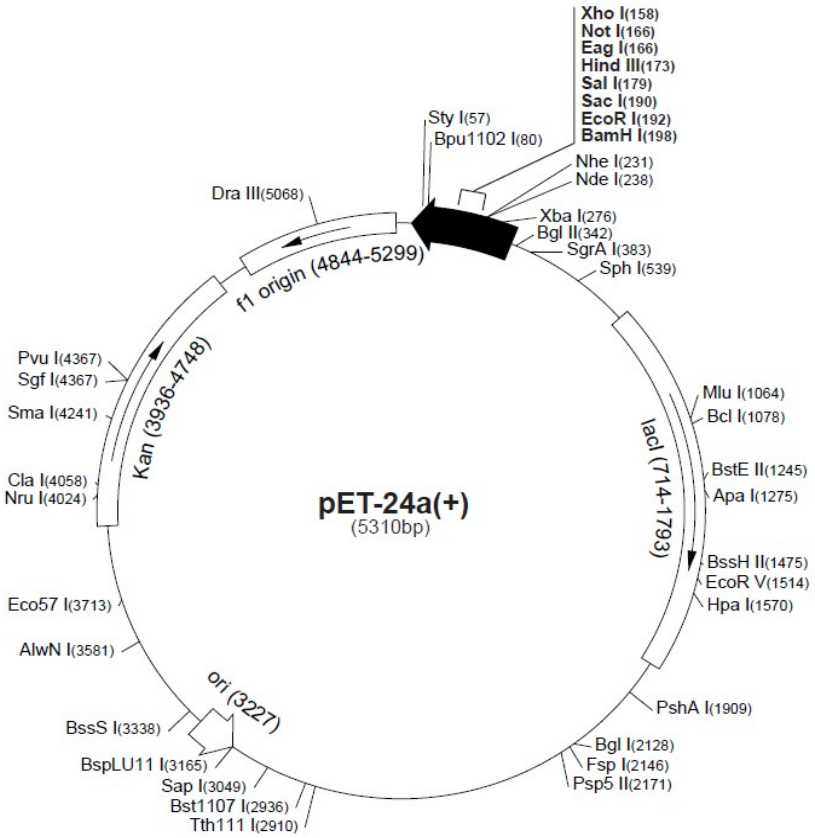

Figure 4.1 Feature map of pET-24a vector. The pET-24a (+) vector carry an N-terminal T7•Tag® sequence plus an optional C-terminal His•Tag® sequence.

PCR purification

The desired DNA fragment was directly purified with QIAquick PCR Purification Kit (QIAGEN, Germany). Briefly, five volumes of Buffer PB were added to one volume of the PCR sample. The mixture was then transferred to a QIAquick spin column and centrifuged at 10,000 rpm for 60 sec. The column was then washed with 0.75 ml of Buffer PE. Finally the DNA was eluted from the column with 30-50 µl Buffer EB.

Endonucleases digestion and CIP treatment

The purified PCR fragments and empty vectors were digested respectively by EcoRI and XhoI (NEW ENGLAND BioLabs Inc., USA). Generally, the purified PCR fragments or vector plasmids (3-5 µg) were digested in an endonuclease mixture (1 × NEB buffer, 5-10 units of endonuclease, and 1 × BSA) at 37 °C for 1-2 hr. Vector DNA was further dephosphorylated with calf intestinal alkaline phosphatase (CIP) (NEW ENGLAND BioLabs Inc., USA) at 37 °C for 30-60 min. This treatment could release the 5' phosphate group of DNA fragments and significantly reduced the rate of self-ligation of vectors in the subsequent ligation reaction.

DNA purification by agarose gel extraction

After digestion, PCR fragments and vectors were extracted by agarose gel electrophoresis and further purified by QIAquick Gel Extraction kit (QIAGEN, Germany). In brief, DNA band slice was excised from the gel. Three volumes of Buffer QG were added to one volume of gel. The mixture was

then incubated at 50 °C for 10 min until the gel was completely dissolved. Then the mixture was mixed with one gel volume of isopropanol and transferred to QIAquick column. After centrifuging, the column was washed with Buffer QG (0.5 ml) and Buffer PE (0.5 ml). Finally, DNA was eluted from the column by Buffer EB (50 µl).

Ligation

Purified PCR fragment and linear vector were ligated with T4 DNA ligase (NEW ENGLAND BioLabs Inc., USA). For each ligation, a 10 µl of reaction mixture was prepared by adding 1 µl of T4 DNA ligase, 1 µl of 10 × T4 DNA ligase buffer, 1µl of vector (50-100 ng) and 7 µl of PCR fragment. The mixture was incubated at room temperature for 1-2 hr.

Preparation of competent E. coli cells

E. coli DH5α stock stain was streaked onto a fresh LB agar plate and incubated at 37 °C overnight. A single clone was picked out from the agar plate and inoculated into 5ml of LB medium and incubated at 37 °C overnight with shaking at 225 rpm. The next day, 1 ml of the amplified bacteria was re-inoculated into fresh 100 ml of LB medium. The culture was incubated at 37 °C with shaking at 225 rpm until OD_{600} of the undiluted culture was between 0.3-0.4, which corresponded to the exponential growth phase. A total of 50 ml of this culture was transferred to 50-ml pre-chilled centrifuge tubes and incubated on ice for 10 min. After centrifuging for 5 min at 4 °C, 5000 rpm, cell pellets were then resuspended in 30 ml of 0.1 M ice-cold $MgCl_2$. After centrifuging again at 4 °C, 5000 rpm for 5 min, the cell

pellets were resuspended in 20 ml 0.1 M ice-cold $CaCl_2$ and incubated on ice for 30 min. After centrifuging once again at 4 °C, 5000 rpm for 5 min, the cell pellets were resuspended in 1.5 ml of solution (0.1 M ice-cold $CaCl_2$ and 15% glycerol). The resulting competent cells could be used immediately or aliquoted into autoclaved fresh tubes and stored at -80 °C.

Transformation

Ligation reaction mixture (10 µl) was added into above competent cells (100 µl). The cells were sequentially incubated on ice for 60 min, at 42 °C for 90 sec, and on ice again for another 90 sec. LB medium without antibiotics (800 µl) was then added into the cell mixture. Cells were recovered by incubating at 37 °C, 225 rpm for 1 hr, and then pelleted by quick spin. Approximately 100 µl of supernatant were left in the tube to resuspend the cell pellet. After that, cell suspension was spread onto a selective LB agar plate. The plate was then incubated at 37 °C for 16-18 hr.

Mini-preparation of plasmids

After overnight incubation, clones on the plate were selected and inoculated into 5 ml LB medium for another overnight incubation. Plasmids were prepared by QIAprep plasmid miniprep kit (QIAGEN, Germany). Briefly, cells from overnight culture were collected by centrifuging at 10,000 rpm for 1 min. Cell pellet was resuspended in Buffer P1 (250 µl, with RNase A). This mixture was first mixed with Buffer P2 (250 µl) and then mixed with Buffer P3 (350 µl). After turning into a homogeneous colorless suspension, the mixture was centrifuged for 10 min at 13,000 rpm. The supernatant was

transferred to the QIAprep spin column. After centrifuging, the column was washed with Buffer PB (0.5 ml) and Buffer PE (0.75 ml). Finally, Buffer EB (50 µl) was added to elute the plasmids.

DNA sequencing and sequence analysis

Plasmids containing genes or promoters were validated by sequencing. Sequences were analyzed and aligned with the software Vector NTI Suite (v.6.0, InfoMax Inc.) according to the manual of the software. After importing the sequences of interest from NCBI Genbank database (http://www.ncbi.nlm.nih.gov/genbank/) into the software, all the restriction enzymes' cutting sites and other sequence elements (including 3'-UTR, 5'-UTR, coding regions, poly A tails and so on) could be viewed under the Analyze function of the software. Once the DNA has been sequenced, the sequencing results can also been imported into the software. By using the Align function of the software, the correction of the cloning can be checked.

4.2.9 Growth Kinetics of Gene-overexpression Strains in Response to Apidaecin IB Challenge

After verifying the DNA sequence, plasmid DNA was transformed into *E. coli* BL21 (DE3) cells. Expression of the two proteins (FtsH and LpxC) is induced by the addition of IPTG (1 mM) for 3 hr. which provides a tightly regulated bacterial expression system. Cell suspensions were then diluted to obtain a concentration of 5×10^5 CFU/ml and incubated without and with $^1/_{10}$ MIC of apidaecin IB. Cell growth was checked by measuring OD_{600} in interval of 1 hr.

4.2.10 Statistical Analysis

Statistical analysis was performed using the same procedure as described in Section 3.2.10 in Chapter 3.

4.3 Results

4.3.1 Membrane Proteins Altered in Response to Apidaecin IB Challenge

To investigate how bacterial membrane proteins changed in response to apidaecin IB challenge, IM and OM proteins were extracted and identified by iTRAQ-coupled 2D LC-MS/MS analysis, respectively. Combining three independent experiments, a total of 75 distinct membrane proteins, including 38 IM proteins, 28 OM proteins, and 9 M proteins (M means whether the protein is found in or associated with the inner or outer cell membrane is unknown), were identified. The Unused ProtScore of those proteins was more than 2 which corresponds to more than 99% confidence. Among them, 5 IM proteins, 1 OM protein and 2 M proteins showed significant changes (p<0.05), and the trend of the changes in 2 hr-apidaecin IB-incubated cells was in accordance with that in 1 hr-apidaecin IB-incubated cells (Table 4.2).

Table 4.2 Membrane proteins of *E. coli* altered in response to apidaecin IB challenge

Accession Number	Protein Name	Unused[a]	Cov[b] (%)	Avg A:C (±S.D.)[c] 1 h	Avg A:C (±S.D.) 2 h	Function	Subcellular Location[d]
P0AAI3	Cell division protease ftsH	18.03	53.26	1.67±0.16	2.23±0.37	Metalloproptease	IM
P31224	Acriflavine resistance protein B	6.54	29.17	0.87±0.02	0.77±0.01	Drug efflux	IM
P09127	Putative uroporphyrinogen-III C-methyltransferase	6	27.23	1.14±0.14	1.44±0.01	Porphyrin biosynthesis	IM
P20966	PTS system fructose-specific EIIBC component	5.8	28.6	0.87±0.04	0.64±0.00	Fructose transport	IM
P15877	Quinoprotein glucose dehydrogenase	3.56	27.39	1.45±0.01	1.53±0.09	Energy conservation	IM
P0A935	Membrane-bound lytic murein transglycosylase A	2.19	23.84	1.12±0.01	1.17±0.07	Murein degradation	OM
P0ADA5	Uncharacterized lipoprotein yajG	9.68	53.13	1.35±0.08	1.66±0.25	Unknown	M
P11557	Protein damX	6	25.23	1.00±0.01	1.27±0.06	Interferes with cell division	M

[a] Unused is Unused ProtScore, a measure of the protein confidence for a detected protein, calculated from the peptide confidence for peptides from spectra that are not already completely "used" by higher scoring winning proteins. A protein with Unused ProtScore of 2.0, which corresponds to 99% confidence, is generally true. [b] The percentage of matching amino acids from identified peptides having confidence greater than 0, divided by the total number of amino acids in the sequence. [c] The ratio of proteins in the apidaecin IB-incubated cells relative to in the control cell. [d] Subcellular location: IM, inner membrane; OM, Outer membrane; M, membrane with whether the protein is found in or associated with the inner or outer cell membrane is not known.

4.3.2 Western Blot Analysis on FtsH and LpxC

Western blot analysis was then performed to validate the change in the level of FtsH identified by LC-MS/MS analysis. Equal amount of cell lysates from apidaecin IB-incubated cells and control cells were tested with antibodies to FtsH respectively. Results shown in Figure 4.2 A indicated that the level of FtsH was increased in both 1 hr and 2 hr-apidaecin-incubated cells, and the increase was greater in 2 hr-apidaecin-incubated cells.

The level of cytoplasmic protein LpxC was also analyzed in both apidaecin IB-incubated cells and control cells. Results showed that no significant changes occurred in the amount of LpxC in cells incubated with apidaecin IB for 1 hr; however, the amount of LpxC markedly decreased in cells incubated with apidaecin IB for 2 hr (Figure 4.2 B).

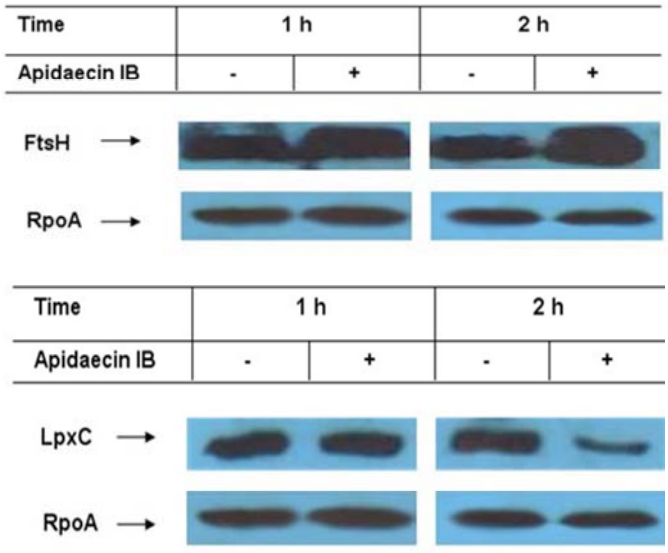

Figure 4.2 Western blot analysis of FtsH (A) and LpxC (B) in *E. coli* incubated with apidaecin IB.

4.3.3 LPS and Phospholipids Analysis

LPS and phospholipids in cell membranes were extracted, and their amounts were analyzed by KDO assay [157] and phosphate assay respectively. Results shown in Figure 4.3 indicated that no significant changes occurred in the amount of LPS and phospholipids in cells incubated with apidaecin IB for 1 hr; however, the amount of LPS and phospholipids was markedly decreased and increased respectively in cells incubated with apidaecin IB for 2 hr.

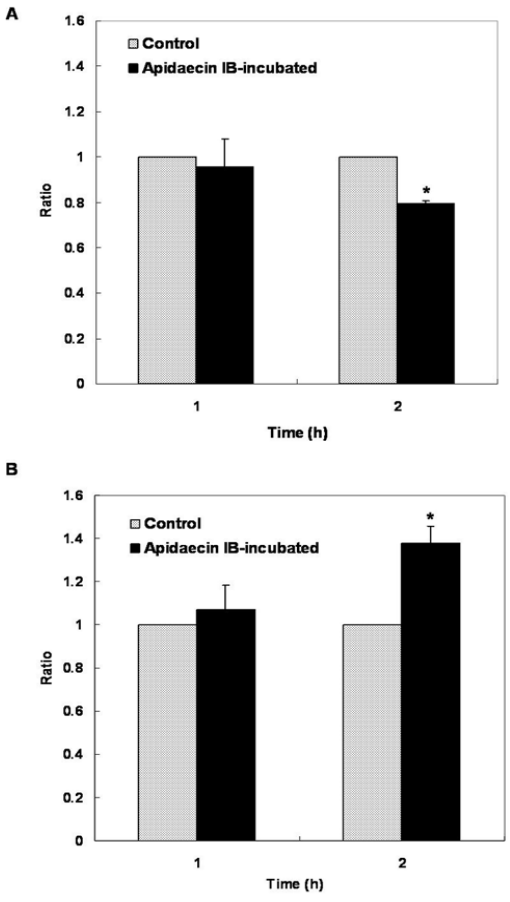

Figure 4.3 Analysis of LPS (A) and phospholipids (B) in *E. coli* incubated with apidaecin IB. LPS and phospholipids were determined by measuring KDO and phosphate respectively. Values for cells without incubation of apidaecin IB were adjusted to 1 and values for those incubated with apidaecin IB were normalized accordingly. Asterisk indicates $p<0.05$.

4.3.4 Growth Kinetics of Gene-overexpression Strains

ftsH or *lpxC* was cloned into a pET-24a vector and expressed in *E. coli* BL21 (DE3) cells. The expression of these two genes was validated by western blot analysis (Figure 4.4). The growth of the cells containing pET-24a, pET-24a/*ftsH* or pET-24a/*lpxC* plasmid was then checked separately. The results shown in Figure 4.5 indicated that overexpression of FtsH enhanced the inhibition effect of apidaecin IB on cells; in contrast, overexpression of LpxC significantly alleviated this effect.

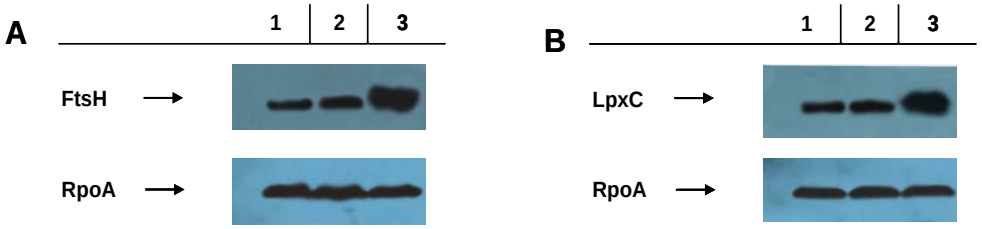

Figure 4.4 Validation the expression of FtsH (A) and LpxC (B) by western blot analysis. Lane 1, mock transformation; lane 2, transformation of empty plasmid; and lane 3, transformation of plasmid that permits controlled expression of FtsH or LpxC.

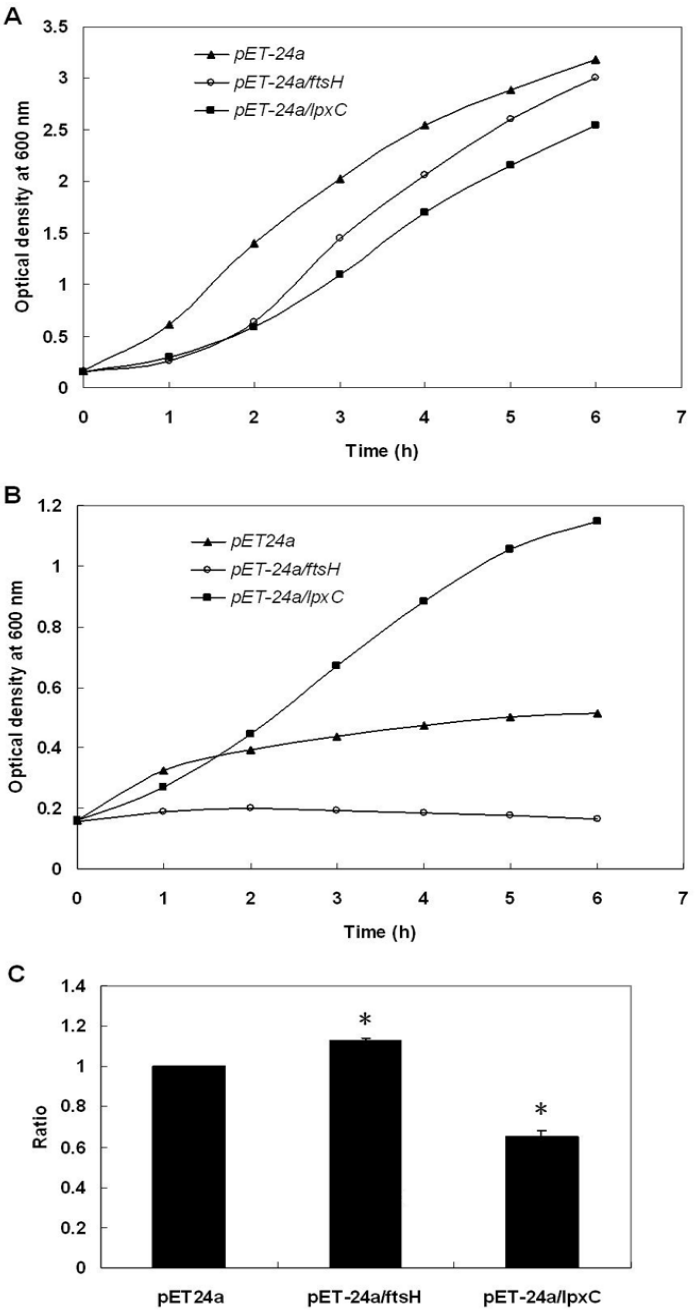

Figure 4.5 Effect of FtsH and LpxC overexpression on the growth of *E. coli* incubated with apidaecin IB. (A) Growth curve of *E. coli* separately harboring pET-24a, pET-24a/*ftsH* and pET-24a/*lpxC* plasmids without apidaecin IB incubation following IPTG induction. (B) Growth curve of *E. coli* separately harboring pET-24a, pET-24a/*ftsH* and pET-24a/*lpxC* plasmids with apidaecin IB incubation following IPTG induction. (C) OD_{600} ratio from 6 hr of cultures. OD_{600} ratio of *E. coli* harboring pET-24a plasmid was adjusted to 1 and those of cells harboring pET-24a/*ftsH* and pET-24a/*lpxC* plasmids were normalized accordingly. Asterisk indicates $p<0.05$.

4.4 Discussion

Membrane proteins are attached to, or associated with the inner or outer bacterial membrane. In order to isolate these proteins, membranes (include both IM and OM) were firstly enriched by ultracentrifuge, proteins of the different membranes were then separately isolated by using two different detergents and analyzed by iTRAQ-coupled 2-D LC–MS/MS. A total of 5 IM proteins, 1 OM protein and 2 M proteins showed differential changes, and the trend of the changes in 2 hr-apidaecin IB-incubated cells was in accordance with that in 1 hr-apidaecin IB-incubated cells (Table 4.2). One of the altered membrane proteins, cell division protease ftsH, captured our attention. The level of FtsH was increased in both 1 hr and 2 hr-apidaecin-incubated cells, with the increase in the latter greater than that in the former (Table 4.3). The change in FtsH was further validated by western blot analysis (Figure 4.2).

Gram-negative bacteria have two membranes—IM and OM. The IM is a phospholipid bilayer, and the OM is an asymmetrical bilayer consisting of phospholipids and LPS in the inner and outer leaflet, respectively. The synthesis of LPS and phospholipids must be properly balanced, which is critical for cell viability. The same reaction precursor (R-3-hydroxymyristoyl-ACP) is used by LpxC for the biosynthesis of the lipid A moiety of LPS (LpxC catalyzes the first committed step) and by (3R)-hydroxymyristoyl-[acyl-carrier-protein] dehydratase (FabZ) for the synthesis of fatty acid (Figure 4.6) ([160-165]. Thus the balance of these enzymes is important to maintain a proper LPS/phospholipids ratio. FtsH is

the sole, ATP-dependent, growth-essential protease of *E. coli* [166]. Its essentiality lies in its function in keeping a proper LpxC/FabZ ratio by degrading LpxC ([167, 168]. The increase in FtsH in this study would probably lead to the change in the cellular level of LpxC. We therefore analyzed LpxC by Western blotting. The results showed no significant changes in the amount of LpxC in cells incubated with apidaecin IB for 1 hr; however, the amount of LpxC was markedly decreased in cells incubated with apidaecin IB for 2 hr (Figure 4.2). We then did LPS and phospholipids analysis. The results showed that the amount of LPS was markedly decreased in cells incubated with apidaecin IB for 2 hr; in contrast, the amount of phospholipids was significantly increased (Figure 4.3).

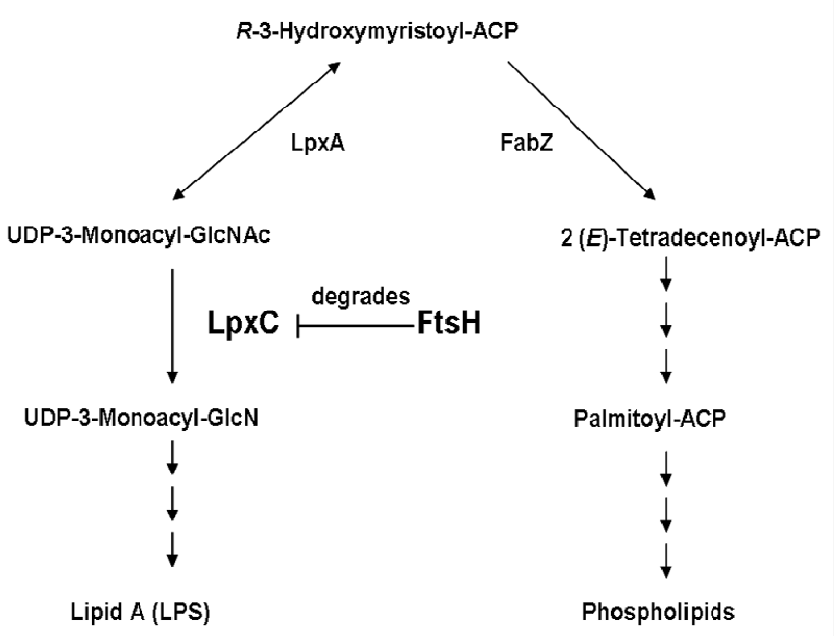

Figure 4.6 Schematic representations of biosynthetic pathways of membrane lipid components. Functions of FtsH in the regulation of biosynthesis of LPS and phospholipids are drawn. ACP, acyl carrier protein; GlcNAc, N-acetylglucosamine; and GlcN, glucosamine.

Moreover, we investigated the characterization of FtsH and LpxC in

response to apidaecin IB challenge by using gene-overexpression strains. *ftsH* or *lpxC* was separately cloned into a pET-24a vector and expressed in *E. coli* BL21 (DE3) cells. Cells containing the pET-24a, pET-24a/*ftsH* or pET-24a/*lpxC* plasmid were then separately cultured in LB-kanamycin medium. After IPTG induction for 3 hr, cell suspensions were diluted to obtain a concentration of 5×10^5 CFUs/ml and then incubated without and with $^1/_{10}$ MIC of apidaecin IB. Cell growth was checked by measuring OD_{600} in interval of 1 hr (Figure 4.7 A, B). The inhibition on the bacteria separately harboring pET-24a, pET-24a/*ftsH* or pET-24a/*lpxC* was obtained by comparing the OD_{600} of the 6 hr cultures. The results showed that overexpression of FtsH enhanced the inhibition effect of apidaecin IB on cells; in contrast, overexpression of LpxC significantly alleviated this effect (Figure 4.7 C). Cellular proteins of the 6 hr cultures were also isolated; the LpxC level in ftsH overexpression cells was further analyzed by western blotting. The results indicated that only with the incubation of apidaecin IB, the overexpression of ftsH can cause the decrease in the cellular level of LpxC (Figure 4.8). Collectively, the data suggested that apidaecin IB acted against *E. coli* by overexpressing FtsH to intensify the degradation of LpxC. As R-3-hydroxymyristoyl-ACP is used by both LpxC for the synthesis of LPS and by FabZ for the synthesis of phospholipids, the over-degradation of LpxC left more R-3-hydroxymyristoyl-ACP to FabZ, and ultimately led to an unbalanced LPS/phospholipids ratio and the loss of membrane lipid homeostasis.

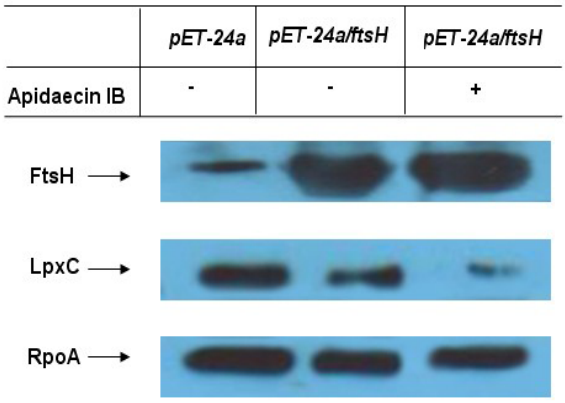

Figure 4.7 Effect of FtsH overexpression on the production of LpxC in *E. coli* incubated with apidaecin IB.

Apidaecins and other short proline-rich ABPs attract particular interest because of their special antibacterial mechanism that is non-membrane-permeabilizing [24]. They can translocate across cell membrane, penetrate into the cytoplasm, and target essential cellular processes to mediate cell death [24]. Previous studies on the antibacterial mechanism of apidaecins and other short proline-rich ABPs identified that they killed bacteria by inhibiting heat shock protein DnaK's two major functions: the ATPase activity and refolding of misfolded proteins [21]. However, it is possible that these peptides inactivate bacteria by other mechanisms. Overproduction of FtsH and the resulting intensified degradation of LpxC in response to apidaecin challenge found in this study could be involved in a new antibacterial mechanism of apidaecins. However, further studies are required to identify the reason of the increase in FtsH and other specific targets of FtsH (i.e. excepting LpxC) to fully understand this new mechanism.

Chapter 5: LC-MS/MS Analysis of Cytoplasmic Protein Profile of *E. coli* in Response to HNP-1 Challenge

(Part of this section was from our paper published in Rapid Commun. Mass Spec. 24(18):2787-90. Permission to use the article in this dissertation was obtained from publisher.)

5.1 Introduction

HNP-1, a 30 amino-acid, β-sheet antibacterial peptide found in human neutrophils [26, 27], is another representative of non-membrane-permeabilizing ABPs. It has activity against bacteria (Gram-positive and Gram-negative) [28], yeast [29, 30] and enveloped viruses [31].

In this chapter, the iTRAQ-coupled LC-MS/MS-based quantitative protein profiling platform established in chapter 3 was utilized to analyze the cytoplasmic protein profile of *E. coli* in response to HNP-1 challenge. Our data indicated that levels of a number of glycolytic enzymes were decreased; in contrast, levels of several proteins were significantly increased, and these proteins were probably involved in a compensatory response to the suppression effect.

5.2 Materials and Methods

5.2.1 Bacterial Strain and Culture

5.2.2 MIC Assay

5.2.3 Growth Kinetics of *E. coli* Incubated with HNP-1

5.2.4 Cytoplasmic Protein Isolation

5.2.5 iTRAQ Labeling

Section 5.2.1 to 5.2.5 was performed using the same procedure as described in Section 3.2.1 to 3.2.5 in Chapter 3.

5.2.6 LC-MS/MS Analysis

5.2.7 Data Analysis

Section 5.2.6 to 5.2.7 was performed using the same procedure as described in Section 4.2.4 to 4.2.5 in Chapter 4.

5.2.8 RNA Extraction and Quantification

Total RNA of *E. coli* cells was isolated using RNeasy Mini kit (QIAGEN, Germany) by following the manufacturer's protocol. Briefly, cell pellet was dissolved in Buffer RTL. After mixing with 1 volume of 70% ethanol, the mixture was transferred to RNeasy mini column and centrifuged. The column was then washed with Buffer Rw1 and Buffer RPE. Finally, RNA was eluted from the colume by RNase-free water. The ratio of the readings at 260 nm and 280 nm (A_{260}/A_{280}) provides an estimate of the purity of RNA

with respect to contaminants that absorb UV, such as protein. Pure RNA has an A_{260}/A_{280} ratio of 1.8-2.0. RNA concentration was calculated according to the formula below, as an A_{260} value of 1 (with a 1 cm detection path) corresponds to 40 µg DNA per ml water. RNA concentration (µg/ml) = A_{260} × 40 × dilution factor.

5.2.9 Real-time RT-PCR

Real-time RT-PCR was performed by utilizing IQ5 multicolor realtime PCR detection system (Bio-Rad Laboratories, Inc., USA) with iScript Onestep RT-PCR kit (Bio-Rad Laboratories, Inc., USA). Primer sequences used were shown in Table 3.1. Reaction mixtures were initially incubated for 10 min at 50 °C and 5 min at 95 °C, followed by 40 cycles of 10 sec at 95 °C and 30 sec at 60 °C. The disassociation analysis was routinely carried out by acquiring fluorescent readings for 1 °C increases from 55 to 95 °C. Microsoft Excel formatted data including amplification analysis, experimental report, melting curve analysis and threshold cycle number were provided automatically by IQ5 optical system software version 2.0 (Bio-Rad Laboratories, Inc., USA). The fold changes were calculated using the following formula: Sample $\Delta Ct = Ct_{sample} - Ct_{rrsD}$; $\Delta\Delta Ct$ = Sample ΔCt-control ΔCt; the fold of sample versus control = $2^{-\Delta\Delta Ct}$.

Table 5.1 Primers used for real-time RT-PCR analysis

Gene	Sense primer sequence (5'-3')	Antisense primer sequence (5'-3')
pfkA	TATTTATGACGGCTATCTGGG	CGCTTCTACAACGGTGCT
gapA	CGG CTA ACC TGA AAT GGG	CGG TAG AGG ACG GGA TGA
eno	CTG TGG AAG CCG AAG T	CCA CCG TTG ATG ATG TT
pgk	GCG AGA AGA AAG ACG ACG	ACC AAC GAT AGC CAC CAT
pykF	ATC GGC AAC AGC GAA ATG	CTG GCA GAG CAA TGG AAA
rrsG	TCAAGGGCACAACCTCCAAGTC	GGTGTAGCGGTGAAATGCGTAG

5.2.10 ATP assay

The cellular ATP level was measured by using a colorimetric assay kit (BioVision, Inc., USA) according to the manufacturer's instructions. Briefly, cells were lysed in ATP assay buffer. After centrifuging at 15,000 × g for 2 min, supernatant was collected and added to a 96-well plate. Then, 50 µl of reaction mixture was added into each well. After 30 min in the dark, the plate was read at 570 nm wavelength on a microplate reader (Benchmark Plus, USA).

5.2.11 Statistical Analysis

Statistical analysis was performed using the same procedure as described in Section 3.2.10 in Chapter 3.

5.3 Results

5.3.1 MIC of HNP-1

MIC of HNP-1 was evaluated by using the same procedure as described in Section 3.2.2. HNP-1 showed obvious antibacterial activity and its MIC was found to be 25 μg/ml, which was slightly lower than that of apidaecin IB.

5.3.2 Growth Kinetics of *E. coli* in Response to HNP-1 Challenge

The growth kinetics of cells was subsequently assayed in the presence of $^{1}/_{10}$ MIC of HNP-1. Compared to no HNP-1 control, $^{1}/_{10}$ MIC of HNP-1 decreased *E. coli* growth starting at 2 hr post-inoculation (Figure 5.1).

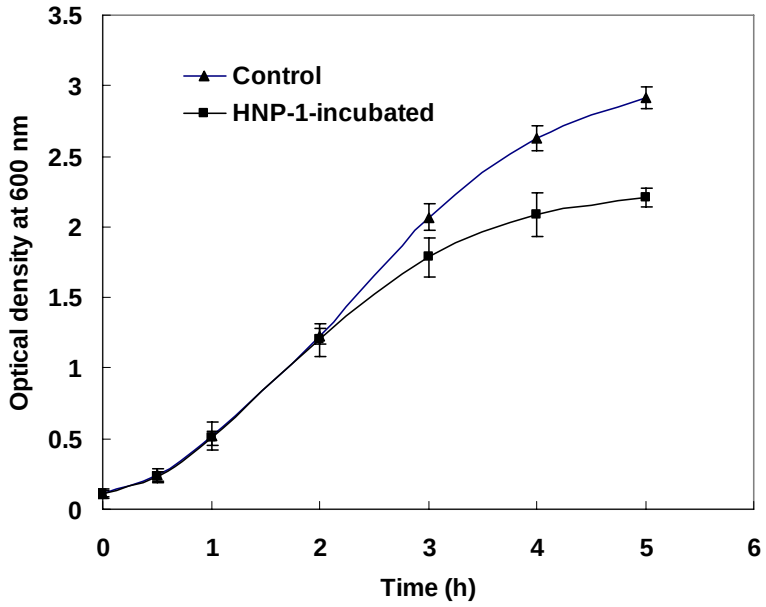

Figure 5.1 Growth kinetics of *E. coli* incubated with $^{1}/_{10}$ MIC HNP-1. Each value represents the mean optical density (OD) readings from two cultures.

5.3.3 Cytoplasmic Proteins Altered in Response to HNP-1 Challenge

To establish the biological difference between HNP-1-incubated cells and control cells, the protein profiles in *E. coli* cells incubated with and without HNP-1 were analyzed. Proteins from cells were collected, lysed, and labeled prior to 2D LC-MS/MS. Combining three independent experiments, a total of 313 and 396 distinct proteins were identified in cells incubated with HNP-1 for 1 hr and 2 hr based on the criterion that the Unused ProtScore of these proteins was more than 2, which corresponds to more than 99% confidence.

Among the identified 313 and 396 distinct proteins, 20 and 35 proteins, respectively, displayed significant changes ($p<0.05$, Table 5.2 and 5.3). These proteins were subsequently categorized into four groups according to their cellular functions: carbohydrate metabolism, defense, amino acids and protein metabolism, and nucleoside metabolism. All information about the 313 and 396 proteins was shown in Appendix 2.

Table 5.2 Altered cytoplasmic proteins of *E. coli* incubated with HNP-1 for 1 hr.

Accession No.	Protein Name	Unused [a]	Cov[b] (%)	Avg. H:C [c] (± SD)
Carbohydrate metabolism				
P0AFG8	Pyruvate dehydrogenase E1 component	51.3	60.7	1.41 ± 0.12
P09373	Formate acetyltransferase 1	36.1	58.4	0.55 ± 0.07
P0A9B2	Glyceraldehyde-3-phosphate dehydrogenase A	29.0	76.7	0.46 ± 0.18
P0A6P9	Enolase	27.4	72.9	0.49 ± 0.20
P0A9Q7	Aldehyde-alcohol dehydrogenase	26.3	50.5	0.53 ± 0.07
P0A799	Phosphoglycerate kinase	21.5	54.5	0.69 ± 0.06
P0AD61	Pyruvate kinase I	16.8	58.1	0.73 ± 0.09
P36683	Aconitate hydratase 2	8.05	34.7	1.14 ± 0.04
P0A796	6-Phosphofructokinase isozyme 1	2	20.3	0.81 ± 0.10
Defense				
P0AE08	Alkyl hydroperoxide reductase subunit C	14.5	59.5	0.71 ± 0.06
P0A862	Thiol peroxidase	14.1	89.3	2.03 ± 0.31
Amino acid and protein metabolism				
P0AC38	Aspartate ammonia-lyase	28.8	63	0.39 ± 0.06
P0A7Z4	DNA-directed RNA polymerase alpha chain	24.5	76.9	1.52 ± 0.18
P0A850	Trigger factor	22.2	72	1.32 ± 0.07
P0A7K2	50S ribosomal protein L7/L12	17.2	81.8	2.29 ± 0.61
P62399	50S ribosomal protein L5	16.5	71.5	1.54 ± 0.24
P02413	50S ribosomal protein L15	12.1	72.9	1.31 ± 0.18
P0A7J7	50S ribosomal protein L11	9.4	57.5	1.66 ± 0.41
P0ADZ4	30S ribosomal protein S15	5.5	82	1.41 ± 0.34
P0A7M6	50S ribosomal protein L29	5.4	79.4	1.42 ± 0.16

[a] Unused is Unused ProtScore, a measure of the protein confidence for a detected protein, calculated from the peptide confidence for peptides from spectra that are not

already completely “used” by higher scoring winning proteins. A protein with Unused ProtScore of 2.0, which corresponds to 99% confidence, is generally true. [b] The percentage of matching amino acids from identified peptides having confidence greater than 0, divided by the total number of amino acids in the sequence. [c] The ratio of proteins in the apidaecin IB-incubated cells relative to in the control cell.

Table 5.3 Altered cytoplasmic proteins of *E. coli* incubated with HNP-1 for 2 hr.

Accession No.	Protein Name	Unused [a]	Cov [b] (%)	avg. H:C [c] (± SD)
Carbohydrate metabolism				
P0AFG8	Pyruvate dehydrogenase E1 component	61.9	70	1.25 ± 0.01
P09373	Formate acetyltransferase 1	62.2	61.2	0.50 ± 0.09
P0A9Q7	Aldehyde-alcohol dehydrogenase	45.2	60.5	0.62 ± 0.14
P0A9B2	Glyceraldehyde-3-phosphate dehydrogenase A	35.6	78.2	0.35 ± 0.11
P0A6P9	Enolase	35.2	75.7	0.45 ± 0.25
P0A799	Phosphoglycerate kinase	30.6	66.7	0.73 ± 0.06
P42632	Keto-acid formate acetyltransferase	26.4	46.1	0.49 ± 0.08
P0A9M8	Phosphate acetyltransferase	26.4	51.5	0.61 ± 0.01
P36683	Aconitate hydratase 2	24.7	42.5	1.81 ± 0.13
P0A6A3	Acetate kinase	24.3	67.5	0.67 ± 0.04
P08200	Isocitrate dehydrogenase	22.0	44.2	1.62 ± 0.15
P0AD61	Pyruvate kinase I	17.4	63.2	0.71 ± 0.07
P0A6T1	Glucose-6-phosphate isomerase	16.0	38.3	0.62 ± 0.07
P0AFG6	Dihydrolipoyllysine-residue succinyltransferase component of 2-oxoglutarate dehydrogenase complex	13.3	45.4	2.09 ± 0.18
P0A858	Triosephosphate isomerase	8.7	49.8	0.47 ± 0.04
P0A796	6-phosphofructokinase isozyme 1	3.54	25.6	0.84 ± 0.03
Defense				
0AE08	Alkyl hydroperoxide reductase subunit C	20.1	75.4	0.44 ± 0.12
P0A862	Thiol peroxidase	13.0	58.9	1.76 ± 0.11
Amino acid and protein metabolism				
P0A6N1	Elongation factor Tu	89.9	85.3	1.21 ± 0.11
P0AC38	Aspartate ammonia-lyase	37.1	65.7	0.31 ± 0.12

Accession No.	Protein Name	Unused [a]	Cov [b] (%)	avg. H:C [c] (± SD)
P0A853	Tryptophanase	26.5	55.4	0.73 ± 0.07
P0A6P1	Elongation factor Ts	24.7	72.8	1.40 ± 0.06
P15288	Aminoacyl-histidine dipeptidase	13.5	43.9	0.50 ± 0.02
P00805	L-asparaginase 2 precursor	10.2	36.2	0.52 ± 0.07
P0A9H3	Lysine decarboxylase, inducible	8.7	29.1	0.28 ± 0.10
P0AG67	30S ribosomal protein S1	52.6	71.5	1.31 ± 0.05
P0A7L0	50S ribosomal protein L1	29.3	85.0	1.35 ± 0.23
P62399	50S ribosomal protein L5	22.4	56.4	2.04 ± 0.48
P60422	50S ribosomal protein L2	21.2	61.5	1.28 ± 0.13
P0A7V3	30S ribosomal protein S3	19.7	54.5	1.43 ± 0.20
P02359	30S ribosomal protein S7	18.3	77.7	1.31 ± 0.10
Nucleoside metabolism				
P0A763	Nucleoside diphosphate kinase	6.2	60.8	2.92 ± 0.28
Others				
P61517	Carbonic anhydrase 2	4.0	17.7	1.42 ± 0.07
P33025	Hypothetical protein yeiN	6.1	29.2	0.37 ± 0.18

[a] Unused is Unused ProtScore, a measure of the protein confidence for a detected protein, calculated from the peptide confidence for peptides from spectra that are not already completely “used” by higher scoring winning proteins. A protein with Unused ProtScore of 2.0, which corresponds to 99% confidence, is generally true. [b] The percentage of matching amino acids from identified peptides having confidence greater than 0, divided by the total number of amino acids in the sequence. [c] The ratio of proteins in the apidaecin IB-incubated cells relative to in the control cell.

5.4 Discussion

HNP-1 is the most active α-defensin. It has activities against bacteria (Gram-positive and Gram-negative), yeast, and enveloped viruses. There is an increasing body of evidence indicating that targeting the essential cellular processes, such as inhibition of nucleic acid synthesis, plays an important role in mediating cell death. Further investigations on different aspects of its mechanisms of action are required.

In this study, the iTRAQ-coupled 2-D LC–MS/MS approach was utilized to analyze the cytoplasmic protein profile of *E. coli* in response to HNP-1 challenge in aim to identify target proteins whose alterations are involved in the antibacterial mechanism of action of this peptide. A total of 313 and 396 distinct proteins were identified in cells incubated with HNP-1 for 1 hr and 2 hr; Among them, 20 and 35 proteins, respectively, displayed significant changes (p<0.05, Table 5.2 and 5.3). A further analysis of these proteins suggested that central metabolism was involved in the response of *E. coli* to HNP-1 challenge. Particularly, levels of a number of enzymes in glycolysis were decreased, including 6-phosphofructokinase isozyme 1 (PfkA), glyceraldehyde-3-phosphate dehydrogenase A (GapA), phosphoglycerate kinase (Pgk), enolase (Eno), and pyruvate kinase I (PykF). Their levels were found to be reduced by 20–60%. The reduction would result in a lower concentration of pyruvate. At the same time, HNP-1

appeared to cause an increase in pyruvate conversion into isocitrate, which was reflected by the increase in the level of pyruvate dehydrogenase (AceE) and aconitate hydratase 2 (AcnB). The disturbance in the metabolism of pyruvate, an important intermediate of respiration, would lower the metabolism rate of cells. This was strengthened by the results of the ATP assay and the growth kinetics assay. The cellular ATP level was significantly decreased in cells incubated with HNP-1 for 2 hr (Figure 5.2) and the growth of *E. coli* culture started to slow down from 2 hr post-inoculation (Figure 5.1).

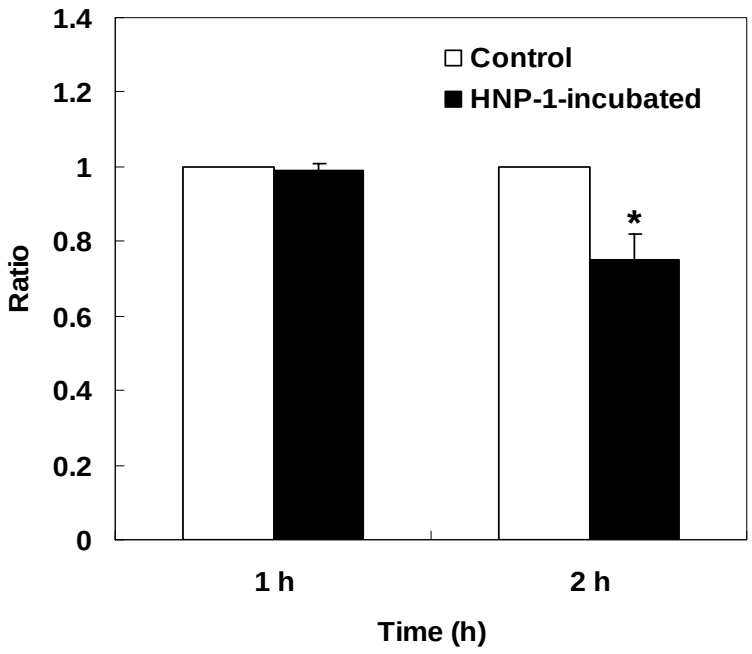

Figure 5.2 ATP level in cells incubated with HNP-1 for 1 hr and 2 hr. Ratios between the HNP-1 incubated and control cells are shown. Asterisks indicate significant difference at $p < 0.05$.

Catabolite repressor/activator (Cra) is a helix-turn-helix DNA-binding protein [169]. It acts as a global regulator of genes encoding enzymes of central carbohydrate metabolism [170]. The unliganded form of Cra binds to the operator regions of target operons, causing either activation or inhibition of transcription. The presence of glucose or other phosphotransferase system sugars produces glycolytic catabolites, such as fructose-1-phosphate, which bind to the Cra protein and cause it to dissociate from the target DNA, resulting in either catabolite repression or catabolite activation. Based on the Regulon DB (http://regulondb.ccg.unam.mx/) database, five of the total nine glycolytic enzymes are known to be under the repressive regulation of the Cra. Interestingly, levels of these five enzymes were all decreased in cells incubated with HNP-1 for both 1hr and 2 hr. The mRNA level of these enzymes was further analyzed. The results shown in Figure 5.3 indicated that the mRNA level of the five enzymes was decreased in cells incubated with HNP-1 for both 1hr and 2 hr, and the trend of the changes was in accordance with that in the protein level. It was thus likely that the transcriptional regulator Cra participated in the cellular response to HNP-1 challenge.

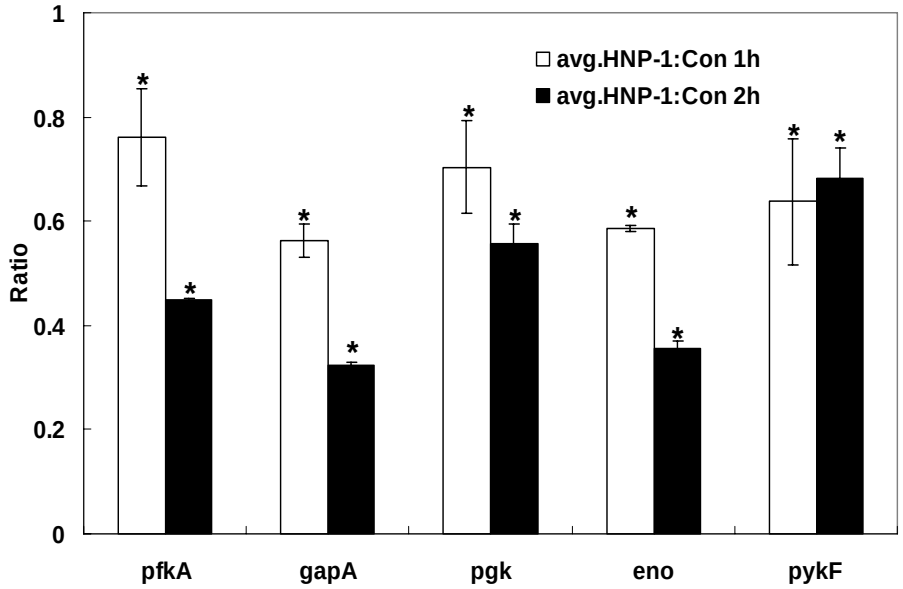

Figure 5.3 mRNA expression analyses of five proteins repressed by transcriptional regulator Cra. pfkA: 6-phosphofructokinase isozyme 1; gapA: glyceraldehyde-3-phosphate dehydrogenase A; pgk: phosphoglycerate kinase; eno: enolase; and pykF: pyruvate kinase. Ratios between the HNP-1 incubated and control cells were shown. Asterisks indicate significant difference at $p < 0.05$.

Further studies are still required on the following two aspects: the role of the Cra protein in the response of *E. coli* cells to the challenge of HNP-1; and those proteins whose levels were changed in response to HNP-1 challenge but playing functions other than regulating carbohydrate metabolism.

Chapter 6: Conclusions and Limitations

6.1 Conclusions

To overcome the continuous growth in the emergence of bacterial resistance to current antibiotics, novel antibacterial drugs are in urgent need. Non-membrane-permeabilizing ABPs, which generally exhibit a broad range of activity, act by specific mechanisms other than direct membrane disrupting, do not easily induce antibacterial-drug resistance, are bacteriocidal as opposed to bacteriostatic, and require a short contact time to induce killing [19-21], are believed as excellent candidates for development as novel antibacterial drugs. Systematic and comprehensive understanding of the mechanism of action of this type of ABPs is thus urgently required. Quantitative protein profiling, which attempts to quantitatively compare changes in the level of proteins between two or more experimental conditions, may aid mechanistic studies of ABPs. However, the platform for such studies has not been established. Confronted by this problem, the aim of this Ph.D. project was to develop a global protein profiling platform to analyze changes in the level of proteins in *E. coli* in response to the challenge of apidaecin IB and HNP-1, two representatives of non-membrane-permeabilizing ABPs, and thus improve the understanding of their mechanisms of action.

The first part of this project, which was reported in Chapter 3 and 4, focused on the development of an iTRAQ-coupled LC-MS/MS platform to investigate changes in the global proteome (cytoplasmic and membrane protein profiles) of *E. coli* in response to apidaecin IB challenge. A number of proteins which take essential roles in cellular protein quality control were found to be significantly changed. Levels of GroES and GroEL, which together form the only essential chaperon system in *E. coli* cytoplasm under all growth conditions, were decreased; in contrast, levels of ATP-dependent proteases ClpX and FtsH, which locate in cytoplasm and IM respectively, were increased. The increase in the proteases was probably involved in a compensatory response to the suppression effect. However, the overproduction of FtsH further intensified the degrading of LpxC, an enzyme catalyzing the first committed step in the biosynthesis of the lipid A moiety of LPS. As the same reaction precursor (R-3-hydroxymyristoyl-ACP) is used by LpxC for the biosynthesis of the lipid A moiety of LPS and by FabZ for the synthesis of fatty acid, the reduction in LpxC led to further unbalanced synthesis of LPS and phospholipids and the loss of membrane lipid homeostasis. These findings suggested a new antibacterial mechanism of apidaecin IB. As most of short-proline-rich ABPs show very similar antibacterial activity, this new antibacterial mechanism may also exists in other short-proline-rich ABPs. Proposed mechanisms of action of apidaecin IB are indicated in Figure 6.1.

The iTRAQ-coupled LC-MS/MS platform for investigation of changes in the global proteome of *E. coli* in response to the challenge of ABPs had been established and the flow diagram is presented in Figure 6.2.

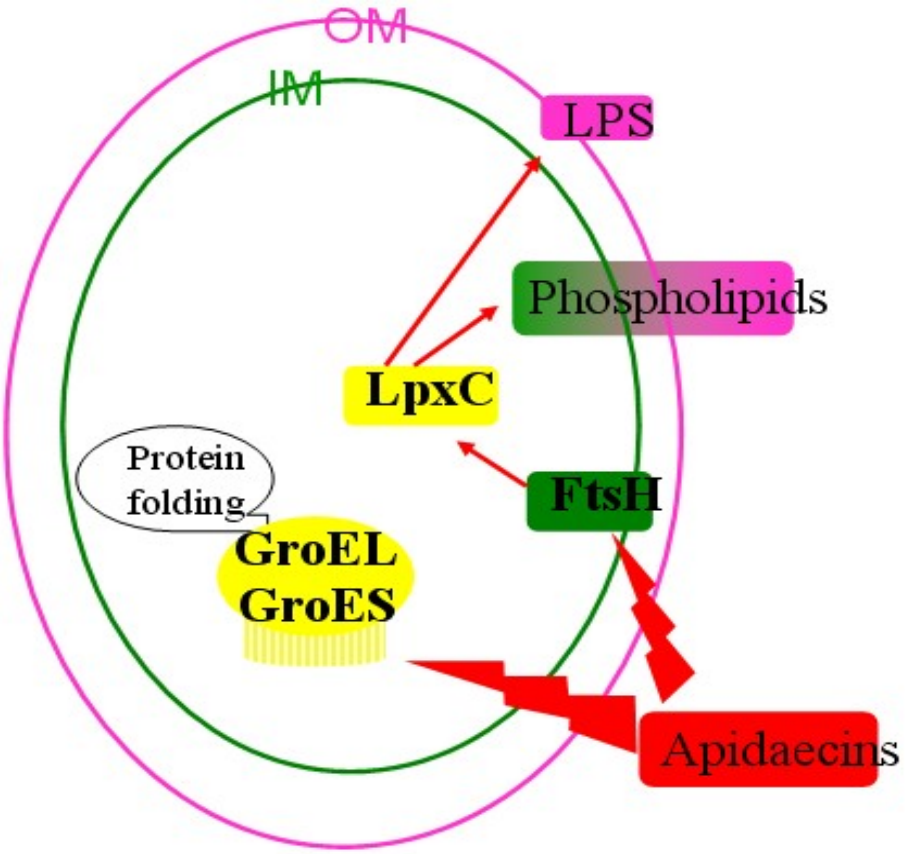

Figure 6.1 Proposed mechanisms of action of apidaecin IB.

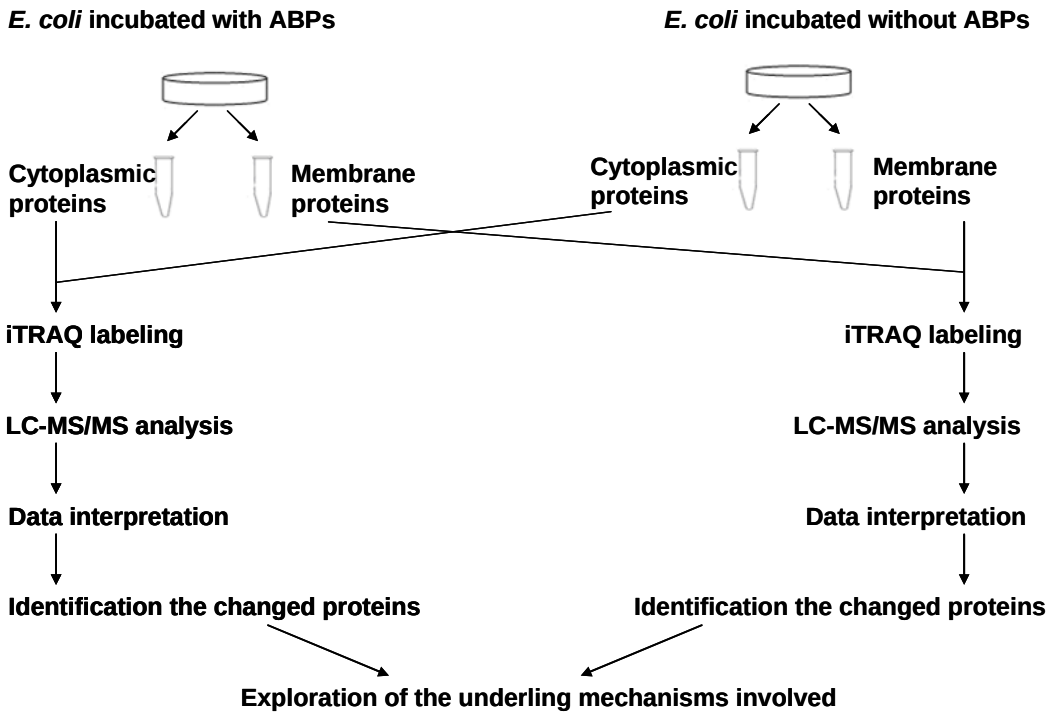

Figure 6.2 Flow diagram of the iTRAQ-coupled LC-MS/MS platform established for investigation of changes in the global proteome of *E. coli* in response to the challenge of ABPs.

Chapter 5 analyzed changes in cytoplasmic proteins of *E. coli* in response to HNP-1 challenge by utilizing the platform established in chapter 3. Levels of a number of enzymes in glycolysis were decreased, including PfkA, GapA, Pgk, Eno and PykF; in contrast, levels of enzymes (AceE and AcnB) which regulate the conversion of pyruvate into isocitrate were increased. In concert with the decreasing in cellular ATP and the slowing down in the growth of *E. coli* culture, central metabolism was suggested to be involved in the *E. coli* response to HNP-1 challenge. In addition, all the five glycolytic enzymes, which were found to be decreased, are known to be under the repressive regulation of the Cra protein. It was thus likely that Cra participated in the cellular response of *E. coli* to HNP-1 challenge.

Proposed mechanisms of action of HNP-1 are indicated in Figure 6.3.

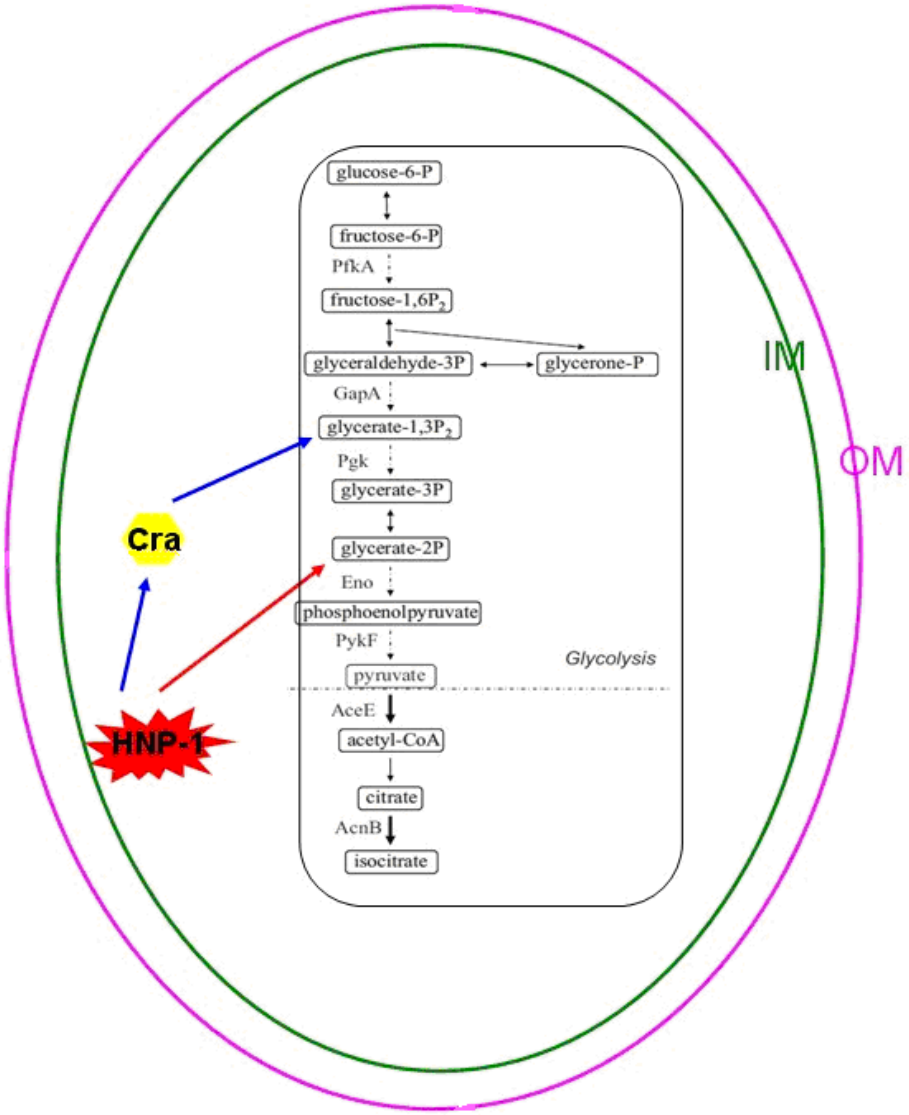

Figure 6.3 Proposed mechanisms of action of HNP-1.

In summary, the results presented in this study provide new insights into the antibacterial mechanism of action of apidaecin IB and HNP-1. Although both of the peptides are membrane-permeabilizing ABPs, the protein profiles of *E. coli* in response to them were quite diverse. This is probably because of the differences of the two peptides in the amino acid

composition and/or structure. This study therefore opens the way for the mechanistic studies of all other non-membrane-permeabilizing ABPs with different amino acid composition and/or structure. The identified altered proteins may be used as novel targets for more effective antibacterial intervention.

6.2 Limitations

The prominent limitation lies in the analysis of membrane protein profile reported in Chapter 4. Membrane proteins are of low abundance and easily masked by predominant cytoplasmic proteins. For this reason, bacterial membranes were enriched by alkaline pH washes and ultracentrifuge separation. However, even after enrichment, a high percentage of proteins (about 20%) identified are still not membrane proteins. Moreover, the transmembrane regions of membrane proteins are either α-helical or β-barrels. The α-helicals are predominantly present in IM; in contrast, the β-barrels are found only in OM. Membrane proteins with these diverse structures cannot be fully isolated by using one single detergent. As a result, after enrichment, IM and OM proteins were separated isolated by using two different detergents. However, even by using two detergents, not all membrane proteins were completely solubilized and the total number of membrane proteins identified was still not high (around 100). Further optimization of membrane protein isolation is still required. Proposed

method is to isolate the protein population from membrane as an unresolved band on a 1D SDS-PAGE gel. IM and OM are separately isolated by Sucrose gradient isolation. Samples are then solubilized in strong detergent and concentrated at the interface of the 4% acrylamide stacking gel and the 20% acrylamide resolving gel. Each membrane protein sample for comparison by quantitative proteomics was then confidently excised as a single band, digested in-gel, and labelled with iTRAQ reagents for quantitative 2D LC-MS/MS. The workflow scheme of this method is shown in Figure 6.4. The results from our repeating experiments showed that quantitative comparison of samples processed by this gel-based method versus a typical in-solution digestion method revealed a good improvement in the total number of membrane proteins identified.

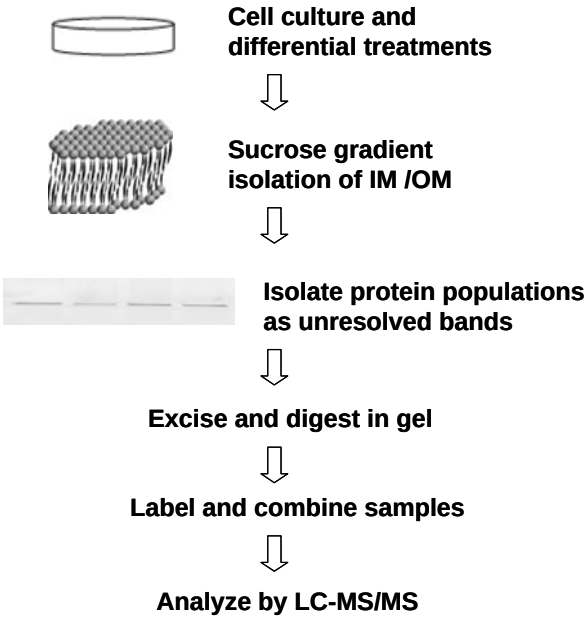

Figure 6.4 Proposed protocol workflow of membrane protein isolation.

Chapter 7: Future Work

7.1 Mechanism Studies on Proteins Identified in Proteomic Analysis

In this study, changes in both cytoplasmic and membrane proteins in *E. coli* in response to apidaecin IB challenge were successfully investigated by utilizing an iTARQ-coupled LC-MS/MS technique. Proteins which play essential roles in cellular protein quality control displayed significant changes, including decreases in GroEL and GroES and an increase in FtsH. The increase in FtsH further intensified the degradation of LpxC and thus led to the loss of membrane lipid homeostasis. Further studies on how apidaecin IB leads to the changes in GroEL, GroES and FtsH, and why the overproduction of FtsH causes the intensified degrading of LpxC are needed.

By utilizing the same platform developed in the analysis of protein profile of *E. coli* in response to apidaecin IB challenge, the cytoplasmic protein profile of *E. coli* in response to HNP-1 challenge was subsequently analyzed. Levels of five essential glycolytic enzymes, which are known to be under the repressive regulation of DNA-binding protein Cra, were decreased. Further studies are required to investigate whether the Cra protein is involved in the response of *E. coli* to the challenge of HNP-1.

This can be achieved by adding glycolytic catabolites, such as fructose-1-phosphate, into the culture medium. Fructose-1-phosphate can bind to the Cra protein and cause it to dissociate from the target DNA, resulting in the release of target DNA from the repressive regulation of the Cra. If the decrease in the five essential glycolytic enzymes is alleviated in HNP-1-incubated cells after adding fructose-1-phosphate, the Cra could be believed to participate in the cellular response to HNP-1 challenge. In addition, analysis of membrane protein profile of *E. coli* in response to HNP-1 challenge is needed to acquire the whole picture of changes in the global protein level and fully explore the underlying mechanisms of action.

7.2 Protein Profile Analysis on Other Pathogenic Bacteria

Bacterial species can be categorized into two large groups, Gram-positive and Gram-negative, based on the chemical and physical properties of their cell walls. Gram-positive bacterium has a thick peptidoglycan layer where the individual peptidoglycan molecules are cross-linked by pentaglycine chains by a DD-transpeptidase enzyme; In contrast, Gram-negative bacterium has a thin peptidoglycan layer, which is much thinner than in Gram-positive bacteria, and the transpeptidase creates a covalent bond directly between peptidoglycan molecules, with no intervening bridge (Figure 7.1). In addition, Gram-negative bacterium has an outer membrane containing LPS in its outer leaflet and phospholipids in the inner leaflet

(Figure 7.1). In this project, only one Gram-negative bacterium, *E. coli,* was used as a control for the mechanistic studies of both apidaecin IB and HNP-1. In order to establish the consistency or universality of the bacteriocidal targets identified or mechanisms proposed, it is necessary to repeat the studies on other Gram-negative bacteria such as *Pseudomonas aeruginosa.* Furthermore, as Gram-positive and Gram-negative bacteria have different structures, the antibacterial mechanism of action on Gram-negative bacteria may be different from that on Gram-positive bacteria, it is thus required to repeat the studies on Gram-positive bacteria, such as *Staphylococcus aureus* and *Enterococcus faecalis,* to thoroughly understand the mechanism of action of these two ABPs.

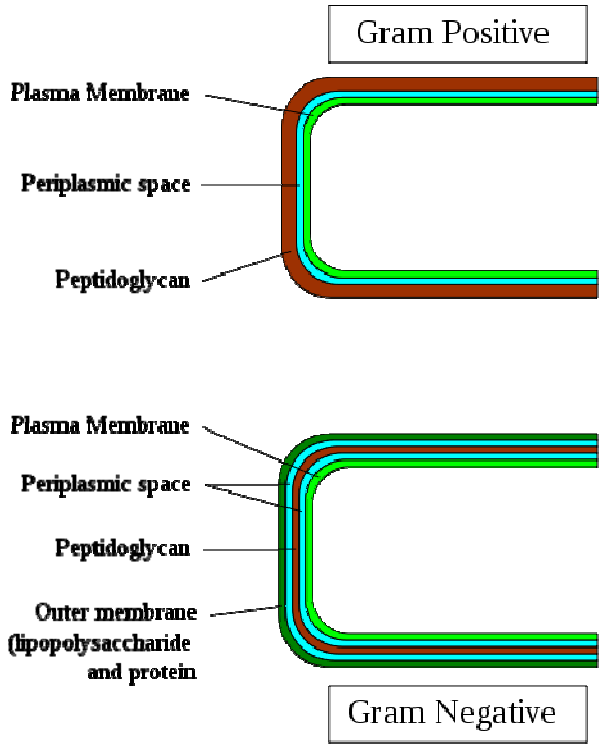

Figure 7.1 Gram-positive and -negative cell wall structures.

7.3 Protein Profile Analysis on Other Non-Membrane-Permeabilizing ABPs

In this study, the same platform was applied to study the cytoplasmic protein profile of *E. coli* in response to the challenge of either HNP-1 or apidaecin IB. Although both of the peptides are non-membrane-permeabilizing ABPs, the protein profiles of *E coli* in response to them were quite diverse. This is probably because of the differences of the two peptides in the amino acid composition and/or structure. The platform can thus be expanded into the analysis of protein profile of *E. coli* in response to other representatives of non-membrane-permeabilizing ABPs with different amino acid composition and/or structure, and further improve the understanding of their antibacterial mechanism of action. The proteomic response reference compendium established on all the representative non-membrane-permeabilizing ABPs can be used to rapidly formulate a hypothesis on the target area or mechanism of the newly identified or structurally modified ABPs by means of pattern matching. For example, if the protein profile of *E. coli* in response to the challenge of a newly identified antibacterial peptide matches that in response to apidaecin IB attack, such as decreases in GroEL and GroES and an increase in FtsH, this newly identified peptide probably has the same mechanism of action

as apidaecin IB. Moreover, the specific altered proteins in response to different representative non-membrane-permeabilizing ABPs can be used as novel targets for more effective antibacterial intervention.

References

[1] Sassetti, C. M., Rubin, E. J., The open book of infectious diseases. *Nat Med* 2007, *13*, 279-280.

[2] Barlow, M., What antimicrobial resistance has taught us about horizontal gene transfer. *Methods Mol Biol* 2009, *532*, 397-411.

[3] Goossens, H., Ferech, M., Vander Stichele, R., Elseviers, M., Outpatient antibiotic use in Europe and association with resistance: a cross-national database study. *Lancet* 2005, *365*, 579-587.

[4] Klevens, R. M., Morrison, M. A., Nadle, J., Petit, S.*, et al.*, Invasive Methicillin-Resistant Staphylococcus aureus Infections in the United States. *JAMA: The Journal of the American Medical Association* 2007, *298*, 1763-1771.

[5] Hancock, R. E., Lehrer, R., Cationic peptides: a new source of antibiotics. *Trends Biotechnol* 1998, *16*, 82-88.

[6] Brogden, K. A., Antimicrobial peptides: Pore formers or metabolic inhibitors in bacteria? *Nature Reviews Microbiology* 2005, *3*, 238-250.

[7] Hancock, R. E., Scott, M. G., The role of antimicrobial peptides in animal defenses. *Proc Natl Acad Sci U S A* 2000, *97*, 8856-8861.

[8] Zasloff, M., Magainins, a class of antimicrobial peptides from Xenopus skin: isolation, characterization of two active forms, and partial cDNA sequence of a precursor. *Proc Natl Acad Sci U S A* 1987, *84*, 5449-5453.

[9] Nakamura, T., Furunaka, H., Miyata, T., Tokunaga, F.*, et al.*, Tachyplesin, a class of antimicrobial peptide from the hemocytes of the horseshoe crab (Tachypleus tridentatus). Isolation and chemical structure. *J Biol Chem* 1988, *263*, 16709-16713.

[10] Selsted, M. E., Novotny, M. J., Morris, W. L., Tang, Y. Q.*, et al.*, Indolicidin, a novel bactericidal tridecapeptide amide from neutrophils. *J Biol Chem* 1992, *267*, 4292-4295.

[11] Iwanaga, S., Muta, T., Shigenaga, T., Seki, N.*, et al.*, Structure-function relationships of tachyplesins and their analogues. *Ciba Found Symp* 1994, *186*, 160-174; discussion 174-165.

[12] Ahmad, I., Perkins, W. R., Lupan, D. M., Selsted, M. E., Janoff, A. S., Liposomal entrapment of the neutrophil-derived peptide indolicidin endows it with in vivo antifungal activity. *Biochim Biophys Acta* 1995, *1237*, 109-114.

[13] Morvan, A., Iwanaga, S., Comps, M., Bachere, E., In Vitro Activity of the Limulus Antimicrobial Peptide Tachyplesin I on Marine Bivalve Pathogens. *J Invertebr Pathol* 1997, *69*, 177-182.

[14] Aley, S. B., Zimmerman, M., Hetsko, M., Selsted, M. E., Gillin, F. D., Killing of Giardia lamblia by cryptdins and cationic neutrophil peptides. *Infect Immun* 1994, *62*, 5397-5403.

[15] Aboudy, Y., Mendelson, E., Shalit, I., Bessalle, R., Fridkin, M., Activity of two synthetic amphiphilic peptides and magainin-2 against herpes simplex virus types 1 and 2. *Int J Pept Protein Res* 1994, *43*, 573-582.

[16] Murakami, T., Niwa, M., Tokunaga, F., Miyata, T., Iwanaga, S., Direct virus inactivation of tachyplesin I and its isopeptides from horseshoe crab hemocytes. *Chemotherapy* 1991, *37*, 327-334.

[17] Robinson, W. E., Jr., McDougall, B., Tran, D., Selsted, M. E., Anti-HIV-1 activity of indolicidin, an antimicrobial peptide from neutrophils. *J Leukoc Biol* 1998, *63*, 94-100.

[18] Jenssen, H., Hamill, P., Hancock, R. E., Peptide antimicrobial agents. *Clin Microbiol Rev* 2006, *19*, 491-511.

[19] Marr, A. K., Gooderham, W. J., Hancock, R. E., Antibacterial peptides for therapeutic use: obstacles and realistic outlook. *Curr Opin Pharmacol* 2006, *6*, 468-472.

[20] Otvos, L., The short proline-rich antibacterial peptide family. *Cellular and Molecular Life Sciences* 2002, *59*, 1138-1150.

[21] Otvos, L., Jr., O, I., Rogers, M. E., Consolvo, P. J.*, et al.*, Interaction between heat shock proteins and antimicrobial peptides. *Biochemistry* 2000, *39*, 14150-14159.

[22] Otvos, L., Jr., The short proline-rich antibacterial peptide family. *Cell Mol Life Sci* 2002, *59*, 1138-1150.

[23] Casteels, P., Ampe, C., Jacobs, F., Vaeck, M., Tempst, P., Apidaecins: antibacterial peptides from honeybees. *EMBO J* 1989, *8*, 2387-2391.

[24] Li, W. F., Ma, G. X., Zhou, X. X., Apidaecin-type peptides: biodiversity, structure-function relationships and mode of action. *Peptides* 2006, *27*, 2350-2359.

[25] Casteels, P., Tempst, P., Apidaecin-Type Peptide Antibiotics Function through a Nonporeforming Mechanism Involving Stereospecificity. *Biochemical and Biophysical Research Communications* 1994, *199*, 339-345.

[26] Selsted, M. E., Ouellette, A. J., Mammalian defensins in the antimicrobial immune response. *Nat Immunol* 2005, *6*, 551-557.

[27] Ganz, T., Biosynthesis of defensins and other antimicrobial peptides. *Ciba Found Symp* 1994, *186*, 62-71; discussion 71-66.

[28] Lehrer, R. I., Lichtenstein, A. K., Ganz, T., Defensins: antimicrobial and cytotoxic peptides of mammalian cells. *Annu Rev Immunol* 1993, *11*, 105-128.

[29] Lehrer, R. I., Ganz, T., Szklarek, D., Selsted, M. E., Modulation of the in vitro candidacidal activity of human neutrophil defensins by target cell metabolism and divalent cations. *J Clin Invest* 1988, *81*, 1829-1835.

[30] Ganz, T., Selsted, M. E., Szklarek, D., Harwig, S. S.*, et al.*, Defensins. Natural peptide antibiotics of human neutrophils. *J Clin Invest* 1985, *76*, 1427-1435.

[31] Daher, K. A., Selsted, M. E., Lehrer, R. I., Direct inactivation of viruses by human granulocyte defensins. *J Virol* 1986, *60*, 1068-1074.

[32] Lehrer, R. I., Barton, A., Daher, K. A., Harwig, S. S.*, et al.*, Interaction of human defensins with Escherichia coli. Mechanism of bactericidal activity. *J Clin Invest* 1989, *84*, 553-561.

[33] Anderson, N. G., Anderson, N. L., Twenty years of two-dimensional electrophoresis: past, present and future. *Electrophoresis* 1996, *17*, 443-453.

[34] Wasinger, V. C., Cordwell, S. J., Cerpa-Poljak, A., Yan, J. X.*, et al.*, Progress with gene-product mapping of the Mollicutes: Mycoplasma genitalium. *Electrophoresis* 1995, *16*, 1090-1094.

[35] Wilkins, M. R., Sanchez, J. C., Gooley, A. A., Appel, R. D.*, et al.*, Progress with proteome projects: why all proteins expressed by a genome should be identified and how to do it. *Biotechnol Genet Eng Rev* 1996, *13*, 19-50.

[36] Ali-Khan, N., Zuo, X., Speicher, D. W., Overview of proteome analysis. *Curr Protoc Protein Sci* 2003, *Chapter 22*, Unit 22 21.

[37] Bowdish, D. M., Davidson, D. J., Hancock, R. E., A re-evaluation of the role of host defence peptides in mammalian immunity. *Curr Protein Pept Sci* 2005, *6*, 35-51.

[38] Scott, M. G., Hancock, R. E. W., Cationic Antimicrobial Peptides and Their Multifunctional Role in the Immune System. 2000, *20*, 24.

[39] Yang, D., Biragyn, A., Hoover, D. M., Lubkowski, J., Oppenheim, J. J., Multiple roles of antimicrobial defensins, cathelicidins, and eosinophil-derived neurotoxin in host defense. *Annu Rev Immunol* 2004, *22*, 181-215.

[40] Zanetti, M., Cathelicidins, multifunctional peptides of the innate immunity. *Journal of Leukocyte Biology* 2004, *75*, 39-48.

[41] Castro, M. S., Cilli, E. M., Fontes, W., Combinatorial synthesis and directed evolution applied to the production of alpha-helix forming antimicrobial peptides analogues. *Current Protein & Peptide Science* 2006, *7*, 473-478.

[42] Boman, H. G., Peptide antibiotics and their role in innate immunity. *Annu. Rev. Immunol.* 1995, *13*, 61-92.

[43] Hancock, R. E., Peptide antibiotics. *Lancet* 1997, *349*, 418-422.

[44] Reddy, K. V. R., Yedery, R. D., Aranha, C., Antimicrobial peptides: premises and promises. *International journal of antimicrobial agents* 2004, *24*, 536-547.

[45] Powers, J. P., Hancock, R. E., The relationship between peptide structure and antibacterial activity. *Peptides* 2003, *24*, 1681-1691.

[46] Giangaspero, A., Sandri, L., Tossi, A., Amphipathic alpha helical antimicrobial peptides. *Eur J Biochem* 2001, *268*, 5589-5600.

[47] Gennaro, R., Zanetti, M., Structural features and biological activities of the cathelicidin-derived antimicrobial peptides. *Biopolymers* 2000, *55*, 31-49.

[48] Kawano, K., Yoneya, T., Miyata, T., Yoshikawa, K.*, et al.*, Antimicrobial peptide, tachyplesin I, isolated from hemocytes of the horseshoe crab (Tachypleus tridentatus). NMR determination of the beta-sheet structure. *J Biol Chem* 1990, *265*, 15365-15367.

[49] Yeaman, M. R., Yount, N. Y., Mechanisms of antimicrobial peptide action and resistance. *Pharmacol Rev* 2003, *55*, 27-55.

[50] Matsuzaki, K., Why and how are peptide-lipid interactions utilized for self-defense? Magainins and tachyplesins as archetypes. *Biochim. Biophys. Acta-Biomembr.* 1999, *1462*, 1-10.

[51] Tossi, A., Sandri, L., Giangaspero, A., Amphipathic, alpha-helical antimicrobial peptides. *Biopolymers* 2000, *55*, 4-30.

[52] Zasloff, M., Antimicrobial peptides of multicellular organisms. *Nature* 2002, *415*, 389-395.

[53] Matsuzaki, K., Control of cell selectivity of antimicrobial peptides. *Biochim Biophys Acta* 2009, *1788*, 1687-1692.

[54] Brogden, K. A., Antimicrobial peptides: pore formers or metabolic inhibitors in bacteria? *Nat Rev Microbiol* 2005, *3*, 238-250.

[55] Hancock, R. E., Rozek, A., Role of membranes in the activities of antimicrobial cationic peptides. *FEMS Microbiol Lett* 2002, *206*, 143-149.

[56] Hallock, K. J., Lee, D. K., Ramamoorthy, A., MSI-78, an analogue of the magainin antimicrobial peptides, disrupts lipid bilayer structure via positive curvature strain. *Biophys. J.* 2003, *84*, 3052-3060.

[57] Wildman, K. A. H., Lee, D. K., Ramamoorthy, A., Mechanism of lipid bilayer disruption by the human antimicrobial peptide, LL-37. *Biochemistry* 2003, *42*, 6545-6558.

[58] Matsuzaki, K., Murase, O., Fujii, N., Miyajima, K., An antimicrobial peptide, magainin 2, induced rapid flip-flop of phospholipids coupled with pore formation and peptide translocation. *Biochemistry* 1996, *35*, 11361-11368.

[59] Yang, L., Harroun, T. A., Weiss, T. M., Ding, L., Huang, H. W., Barrel-stave model or toroidal model? A case study on melittin pores. *Biophys. J.* 2001, *81*, 1475-1485.

[60] Ehrenstein, G., Lecar, H., Electrically gated ionic channels in lipid bilayers. *Q. Rev. Biophys.* 1977, *10*, 1-34.

[61] He, K., Ludtke, S. J., Worcester, D. L., Huang, H. W., Neutron scattering in the plane of membranes: Structure of alamethicin pores. *Biophys. J.* 1996, *70*, 2659-2666.

[62] Spaar, A., Munster, C., Salditt, T., Conformation of peptides in lipid membranes studied by X-ray grazing incidence scattering. *Biophys. J.* 2004, *87*, 396-407.

[63] Zhang, L. J., Rozek, A., Hancock, R. E. W., Interaction of cationic antimicrobial peptides with model membranes. *Journal of Biological Chemistry* 2001, *276*, 35714-35722.

[64] Pouny, Y., Rapaport, D., Mor, A., Nicolas, P., Shai, Y., Interaction of

antimicrobial dermaseptin and its fluorescently labeled analogs with phospholipid-membranes. *Biochemistry* 1992, *31*, 12416-12423.

[65] Yamaguchi, S., Huster, D., Waring, A., Lehrer, R. I.*, et al.*, Orientation and dynamics of an antimicrobial peptide in the lipid bilayer by solid-state NMR spectroscopy. *Biophys. J.* 2001, *81*, 2203-2214.

[66] Oren, Z., Shai, Y., Mode of action of linear amphipathic alpha-helical antimicrobial peptides. *Biopolymers* 1998, *47*, 451-463.

[67] Park, C. B., Yi, K. S., Matsuzaki, K., Kim, M. S., Kim, S. C., Structure-activity analysis of buforin II, a histone H2A-derived antimicrobial peptide: the proline hinge is responsible for the cell-penetrating ability of buforin II. *Proc Natl Acad Sci U S A* 2000, *97*, 8245-8250.

[68] Patrzykat, A., Friedrich, C. L., Zhang, L., Mendoza, V., Hancock, R. E., Sublethal concentrations of pleurocidin-derived antimicrobial peptides inhibit macromolecular synthesis in Escherichia coli. *Antimicrob Agents Chemother* 2002, *46*, 605-614.

[69] Subbalakshmi, C., Sitaram, N., Mechanism of antimicrobial action of indolicidin. *FEMS Microbiol Lett* 1998, *160*, 91-96.

[70] Boman, H. G., Agerberth, B., Boman, A., Mechanisms of action on Escherichia coli of cecropin P1 and PR-39, two antibacterial peptides from pig intestine. *Infect Immun* 1993, *61*, 2978-2984.

[71] Friedrich, C. L., Rozek, A., Patrzykat, A., Hancock, R. E. W., Structure and Mechanism of Action of an Indolicidin Peptide Derivative with Improved Activity against Gram-positive Bacteria. *Journal of Biological Chemistry* 2001, *276*, 24015-24022.

[72] Kragol, G., Lovas, S., Varadi, G., Condie, B. A.*, et al.*, The antibacterial peptide pyrrhocoricin inhibits the ATPase actions of DnaK and prevents chaperone-assisted protein folding. *Biochemistry* 2001, *40*, 3016-3026.

[73] Otvos, L., O, I., Rogers, M. E., Consolvo, P. J.*, et al.*, Interaction between heat shock proteins and antimicrobial peptides. *Biochemistry* 2000, *39*, 14150-14159.

[74] Brotz, H., Bierbaum, G., Reynolds, P. E., Sahl, H. G., The lantibiotic mersacidin inhibits peptidoglycan biosynthesis at the level of transglycosylation. *Eur J Biochem* 1997, *246*, 193-199.

[75] Brumfitt, W., Salton, M. R. J., Hamilton-Miller, J. M. T., Nisin, alone and combined with peptidoglycan-modulating antibiotics: activity against methicillin-resistant Staphylococcus aureus and vancomycin-resistant enterococci. *Journal of Antimicrobial Chemotherapy* 2002, *50*, 731-734.

[76] Kruszewska, D., Sahl, H. G., Bierbaum, G., Pag, U.*, et al.*, Mersacidin eradicates methicillin-resistant Staphylococcus aureus (MRSA) in a mouse rhinitis model. *J Antimicrob Chemother* 2004, *54*, 648-653.

[77] Gennaro, R., Zanetti, M., Benincasa, M., Podda, E., Miani, M., Pro-rich antimicrobial peptides from animals: structure, biological functions and mechanism of action. *Curr Pharm Des* 2002, *8*, 763-778.

[78] Markossian, K. A., Zamyatnin, A. A., Kurganov, B. I., Antibacterial proline-rich oligopeptides and their target proteins. *Biochemistry (Mosc)* 2004, *69*, 1082-1091.

[79] Kay, B. K., Williamson, M. P., Sudol, P., The importance of being proline: the interaction of proline-rich motifs in signaling proteins with their cognate domains. *Faseb Journal* 2000, *14*, 231-241.

[80] Oren, Z., Hong, J., Shai, Y., A repertoire of novel antibacterial diastereomeric peptides with selective cytolytic activity. *Journal of Biological Chemistry* 1997, *272*, 14643-14649.

[81] Casteels, P., Ampe, C., Jacobs, F., Vaeck, M., Tempst, P., Apidaecins - Antibacterial Peptides from Honeybees. *Embo Journal* 1989, *8*, 2387-2391.

[82] Castle, M., Nazarian, A., Yi, S. S., Tempst, P., Lethal Effects of Apidaecin on Escherichia coliInvolve Sequential Molecular Interactions with Diverse Targets. *Journal of Biological Chemistry* 1999, *274*, 32555-32564.

[83] Zhou, X. X., Li, W. F., Pan, Y. J., Functional and structural characterization of apidaecin and its N-terminal and C-terminal fragments.

Journal of Peptide Science 2008, *14*, 697-707.

[84] Chesnokova, L. S., Slepenkov, S. V., Witt, S. N., The insect antimicrobial peptide, L-pyrrhocoricin, binds to and stimulates the ATPase activity of both wild-type and lidless DnaK. *Febs Letters* 2004, *565*, 65-69.

[85] Ganz, T., Defensins: antimicrobial peptides of innate immunity. *Nat Rev Immunol* 2003, *3*, 710-720.

[86] Lehrer, R. I., Primate defensins. *Nat Rev Microbiol* 2004, *2*, 727-738.

[87] Washburn, M. P., Wolters, D., Yates, J. R., 3rd, Large-scale analysis of the yeast proteome by multidimensional protein identification technology. *Nat Biotechnol* 2001, *19*, 242-247.

[88] Auerbach, D., Thaminy, S., Hottiger, M. O., Stagljar, I., The post-genomic era of interactive proteomics: facts and perspectives. *Proteomics* 2002, *2*, 611-623.

[89] McCormack, A. L., Schieltz, D. M., Goode, B., Yang, S.*, et al.*, Direct analysis and identification of proteins in mixtures by LC/MS/MS and database searching at the low-femtomole level. *Anal Chem* 1997, *69*, 767-776.

[90] Link, A. J., Eng, J., Schieltz, D. M., Carmack, E.*, et al.*, Direct analysis of protein complexes using mass spectrometry. *Nat Biotechnol* 1999, *17*, 676-682.

[91] Motoyama, A., Yates, J. R., 3rd, Multidimensional LC separations in shotgun proteomics. *Anal Chem* 2008, *80*, 7187-7193.

[92] Fenn, J. B., Mann, M., Meng, C. K., Wong, S. F., Whitehouse, C. M., Electrospray ionization for mass spectrometry of large biomolecules. *Science* 1989, *246*, 64-71.

[93] Hillenkamp, F., Karas, M., Mass spectrometry of peptides and proteins by matrix-assisted ultraviolet laser desorption/ionization. *Methods Enzymol* 1990, *193*, 280-295.

[94] Iribarne, J. V., Thomson, B. A., On the evaporation of small ions from charged droplets. *The Journal of Chemical Physics* 1976, *64*, 2287-2294.

[95] Nguyen, S., Fenn, J. B., Gas-phase ions of solute species from charged droplets of solutions. *Proceedings of the National Academy of Sciences* 2007, *104*, 1111-1117.

[96] Wilm, M., Shevchenko, A., Houthaeve, T., Breit, S.*, et al.*, Femtomole sequencing of proteins from polyacrylamide gels by nano-electrospray mass spectrometry. *Nature* 1996, *379*, 466-469.

[97] Strittmatter, E. F., Ferguson, P. L., Tang, K., Smith, R. D., Proteome analyses using accurate mass and elution time peptide tags with capillary LC time-of-flight mass spectrometry. *J Am Soc Mass Spectrom* 2003, *14*, 980-991.

[98] Roepstorff, P., Fohlman, J., Proposal for a common nomenclature for sequence ions in mass spectra of peptides. *Biomed Mass Spectrom* 1984, *11*, 601.

[99] Johnson, R. S., Martin, S. A., Biemann, K., Collision-induced fragmentation of (M + H)+ ions of peptides. Side chain specific sequence ions. *International Journal of Mass Spectrometry and Ion Processes* 1988, *86*, 137-154.

[100] Ross, P. L., Huang, Y. N., Marchese, J. N., Williamson, B.*, et al.*, Multiplexed protein quantitation in Saccharomyces cerevisiae using amine-reactive isobaric tagging reagents. *Mol Cell Proteomics* 2004, *3*, 1154-1169.

[101] Shiio, Y., Aebersold, R., Quantitative proteome analysis using isotope-coded affinity tags and mass spectrometry. *Nat. Protocols* 2006, *1*, 139-145.

[102] Yao, X., Freas, A., Ramirez, J., Demirev, P. A., Fenselau, C., Proteolytic 18O labeling for comparative proteomics: model studies with two serotypes of adenovirus. *Anal Chem* 2001, *73*, 2836-2842.

[103] Ong, S. E., Blagoev, B., Kratchmarova, I., Kristensen, D. B.*, et al.*, Stable isotope labeling by amino acids in cell culture, SILAC, as a simple

and accurate approach to expression proteomics. *Mol Cell Proteomics* 2002, *1*, 376-386.

[104] Zeng, D., Li, S., Improved CILAT reagents for quantitative proteomics. *Bioorg Med Chem Lett* 2009, *19*, 2059-2061.

[105] Haqqani, A. S., Kelly, J. F., Stanimirovic, D. B., Quantitative protein profiling by mass spectrometry using isotope-coded affinity tags. *Methods Mol Biol* 2008, *439*, 225-240.

[106] Zhang, R., Sioma, C. S., Thompson, R. A., Xiong, L., Regnier, F. E., Controlling deuterium isotope effects in comparative proteomics. *Anal Chem* 2002, *74*, 3662-3669.

[107] Zhang, R., Sioma, C. S., Wang, S., Regnier, F. E., Fractionation of isotopically labeled peptides in quantitative proteomics. *Anal Chem* 2001, *73*, 5142-5149.

[108] Borisov, O. V., Goshe, M. B., Conrads, T. P., Rakov, V. S.*, et al.*, Low-energy collision-induced dissociation fragmentation analysis of cysteinyl-modified peptides. *Anal Chem* 2002, *74*, 2284-2292.

[109] Yu, L. R., Conrads, T. P., Uo, T., Issaq, H. J.*, et al.*, Evaluation of the acid-cleavable isotope-coded affinity tag reagents: application to camptothecin-treated cortical neurons. *J Proteome Res* 2004, *3*, 469-477.

[110] Mirgorodskaya, O. A., Kozmin, Y. P., Titov, M. I., Korner, R.*, et al.*, Quantitation of peptides and proteins by matrix-assisted laser desorption/ionization mass spectrometry using (18)O-labeled internal standards. *Rapid Commun Mass Spectrom* 2000, *14*, 1226-1232.

[111] Stewart, II, Thomson, T., Figeys, D., 18O labeling: a tool for proteomics. *Rapid Commun Mass Spectrom* 2001, *15*, 2456-2465.

[112] Reynolds, K. J., Yao, X., Fenselau, C., Proteolytic 18O labeling for comparative proteomics: evaluation of endoprotease Glu-C as the catalytic agent. *J Proteome Res* 2002, *1*, 27-33.

[113] Reynolds, K. J., Fenselau, C., Quantitative protein analysis using

proteolytic [18O]water labeling. *Curr Protoc Protein Sci* 2004, *Chapter 23*, Unit 23 24.

[114] Julka, S., Regnier, F., Quantification in proteomics through stable isotope coding: a review. *J Proteome Res* 2004, *3*, 350-363.

[115] Choe, L., D'Ascenzo, M., Relkin, N. R., Pappin, D.*, et al.*, 8-plex quantitation of changes in cerebrospinal fluid protein expression in subjects undergoing intravenous immunoglobulin treatment for Alzheimer's disease. *Proteomics* 2007, *7*, 3651-3660.

[116] Pierce, A., Unwin, R. D., Evans, C. A., Griffiths, S.*, et al.*, Eight-channel iTRAQ enables comparison of the activity of six leukemogenic tyrosine kinases. *Mol Cell Proteomics* 2008, *7*, 853-863.

[117] Phanstiel, D., Unwin, R., McAlister, G. C., Coon, J. J., Peptide quantification using 8-plex isobaric tags and electron transfer dissociation tandem mass spectrometry. *Anal Chem* 2009, *81*, 1693-1698.

[118] Unwin, R. D., Quantification of proteins by iTRAQ. *Methods Mol Biol*, *658*, 205-215.

[119] Boehm, A., Putz, S., Altenhofer, D., Sickmann, A., Falk, M., Precise protein quantification based on peptide quantification using iTRAQTM. *BMC Bioinformatics* 2007, *8*, 214.

[120] D'Ascenzo, M., Choe, L., Lee, K. H., iTRAQPak: an R based analysis and visualization package for 8-plex isobaric protein expression data. *Brief Funct Genomic Proteomic* 2008, *7*, 127-135.

[121] Hundertmark, C., Fischer, R., Reinl, T., May, S.*, et al.*, MS-specific noise model reveals the potential of iTRAQ in quantitative proteomics. *Bioinformatics* 2009, *25*, 1004-1011.

[122] Lacerda, C. M., Xin, L., Rogers, I., Reardon, K. F., Analysis of iTRAQ data using Mascot and Peaks quantification algorithms. *Brief Funct Genomic Proteomic* 2008, *7*, 119-126.

[123] Laderas, T., Bystrom, C., McMillen, D., Fan, G., McWeeney, S.,

TandTRAQ: an open-source tool for integrated protein identification and quantitation. *Bioinformatics* 2007, *23*, 3394-3396.

[124] Lin, W. T., Hung, W. N., Yian, Y. H., Wu, K. P.*, et al.*, Multi-Q: a fully automated tool for multiplexed protein quantitation. *J Proteome Res* 2006, *5*, 2328-2338.

[125] Shadforth, I., Dunkley, T., Lilley, K., Bessant, C., i-Tracker: For quantitative proteomics using iTRAQTM. *BMC Genomics* 2005, *6*, 145.

[126] Yu, C.-Y., Tsui, Y.-H., Yian, Y.-H., Sung, T.-Y., Hsu, W.-L., The Multi-Q web server for multiplexed protein quantitation. *Nucleic Acids Research* 2007, *35*, W707-W712.

[127] Hill, E. G., Schwacke, J. H., Comte-Walters, S., Slate, E. H.*, et al.*, A statistical model for iTRAQ data analysis. *J Proteome Res* 2008, *7*, 3091-3101.

[128] Bantscheff, M., Boesche, M., Eberhard, D., Matthieson, T.*, et al.*, Robust and sensitive iTRAQ quantification on an LTQ Orbitrap mass spectrometer. *Mol Cell Proteomics* 2008, *7*, 1702-1713.

[129] Griffin, T. J., Xie, H., Bandhakavi, S., Popko, J.*, et al.*, iTRAQ reagent-based quantitative proteomic analysis on a linear ion trap mass spectrometer. *J Proteome Res* 2007, *6*, 4200-4209.

[130] Guo, T., Gan, C. S., Zhang, H., Zhu, Y.*, et al.*, Hybridization of Pulsed-Q Dissociation and Collision-Activated Dissociation in Linear Ion Trap Mass Spectrometer for iTRAQ Quantitation. *J. Proteome Res.* 2008, *7*, 4831-4840.

[131] DeSouza, L. V., Taylor, A. M., Li, W., Minkoff, M. S.*, et al.*, Multiple reaction monitoring of mTRAQ-labeled peptides enables absolute quantification of endogenous levels of a potential cancer marker in cancerous and normal endometrial tissues. *J Proteome Res* 2008, *7*, 3525-3534.

[132] Oda, Y., Huang, K., Cross, F. R., Cowburn, D., Chait, B. T., Accurate quantitation of protein expression and site-specific phosphorylation. *Proc Natl Acad Sci U S A* 1999, *96*, 6591-6596.

[133] Conrads, T. P., Alving, K., Veenstra, T. D., Belov, M. E.*, et al.*, Quantitative analysis of bacterial and mammalian proteomes using a combination of cysteine affinity tags and 15N-metabolic labeling. *Anal Chem* 2001, *73*, 2132-2139.

[134] Washburn, M. P., Koller, A., Oshiro, G., Ulaszek, R. R.*, et al.*, Protein pathway and complex clustering of correlated mRNA and protein expression analyses in Saccharomyces cerevisiae. *Proceedings of the National Academy of Sciences* 2003, *100*, 3107-3112.

[135] Bindschedler, L. V., Palmblad, M., Cramer, R., Hydroponic isotope labelling of entire plants (HILEP) for quantitative plant proteomics; an oxidative stress case study. *Phytochemistry* 2008, *69*, 1962-1972.

[136] Pan, C., Gnad, F., Olsen, J. V., Mann, M., Quantitative phosphoproteome analysis of a mouse liver cell line reveals specificity of phosphatase inhibitors. *Proteomics* 2008, *8*, 4534-4546.

[137] Molina, H., Parmigiani, G., Pandey, A., Assessing reproducibility of a protein dynamics study using in vivo labeling and liquid chromatography tandem mass spectrometry. *Anal Chem* 2005, *77*, 2739-2744.

[138] Molina, H., Yang, Y., Ruch, T., Kim, J. W.*, et al.*, Temporal profiling of the adipocyte proteome during differentiation using a five-plex SILAC based strategy. *J Proteome Res* 2009, *8*, 48-58.

[139] Cox, J., Matic, I., Hilger, M., Nagaraj, N.*, et al.*, A practical guide to the MaxQuant computational platform for SILAC-based quantitative proteomics. *Nat. Protocols* 2009, *4*, 698-705.

[140] Rigbolt, K. T., Blagoev, B., Proteome-wide quantitation by SILAC. *Methods Mol Biol*, *658*, 187-204.

[141] Ong, S. E., Kratchmarova, I., Mann, M., Properties of 13C-substituted arginine in stable isotope labeling by amino acids in cell culture (SILAC). *J Proteome Res* 2003, *2*, 173-181.

[142] Bendall, S. C., Hughes, C., Stewart, M. H., Doble, B.*, et al.*, Prevention of Amino Acid Conversion in SILAC Experiments with Embryonic Stem Cells. *Molecular & Cellular Proteomics* 2008, *7*,

1587-1597.

[143] Wiegand, I., Hilpert, K., Hancock, R. E. W., Agar and broth dilution methods to determine the minimal inhibitory concentration (MIC) of antimicrobial substances. *Nature Protocols* 2008, *3*, 163-175.

[144] Niu, D., Sui, J., Zhang, J., Feng, H., Chen, W. N., iTRAQ-coupled 2-D LC-MS/MS analysis of protein profile associated with HBV-modulated DNA methylation. *Proteomics* 2009, *9*, 3856-3868.

[145] Ellis, R. J., Hemmingsen, S. M., Molecular chaperones - proteins essential for the biogenesis of some macromolecular structures. *Trends Biochem.Sci.* 1989, *14*, 339-342.

[146] Hartl, F. U., Molecular chaperones in cellular protein folding. *Nature* 1996, *381*, 571-580.

[147] Wickner, S., Maurizi, M. R., Gottesman, S., Posttranslational quality control: Folding, refolding, and degrading proteins. *Science* 1999, *286*, 1888-1893.

[148] Houry, W. A., Chaperone-assisted protein folding in the cell cytoplasm. *Curr. Protein Pept. Sci.* 2001, *2*, 227-244.

[149] Fayet, O., Ziegelhoffer, T., Georgopoulos, C., The GroES and GroEL heat-shock gene-products of Escherichia-coli are essential for bacterial-growth at all temperatures. *J. Bacteriol.* 1989, *171*, 1379-1385.

[150] Ewalt, K. L., Hendrick, J. P., Houry, W. A., Hartl, F. U., In vivo observation of polypeptide flux through the bacterial chaperonin system. *Cell* 1997, *90*, 491-500.

[151] Houry, W. A., Frishman, D., Eckerskorn, C., Lottspeich, F., Hartl, F. U., Identification of in vivo substrates of the chaperonin GroEL. *Nature* 1999, *402*, 147-154.

[152] Kerner, M. J., Naylor, D. J., Ishihama, Y., Maier, T.*, et al.*, Proteome-wide Analysis of Chaperonin-Dependent Protein Folding in Escherichia coli. *Cell* 2005, *122*, 209-220.

[153] Sui, J., Zhang, J., Tan, T. L., Ching, C. B., Chen, W. N., Comparative proteomics analysis of vascular smooth muscle cells incubated with S- and R-enantiomers of atenolol using iTRAQ-coupled two-dimensional LC-MS/MS. *Mol Cell Proteomics* 2008, *7*, 1007-1018.

[154] Sui, J., Tan, T. L., Zhang, J., Ching, C. B., Chen, W. N., iTRAQ-coupled 2D LC-MS/MS analysis on protein profile in vascular smooth muscle cells incubated with S- and R-enantiomers of propranolol: possible role of metabolic enzymes involved in cellular anabolism and antioxidant activity. *J Proteome Res* 2007, *6*, 1643-1651.

[155] Zhang, J., Niu, D., Sui, J., Ching, C. B., Chen, W. N., Protein profile in hepatitis B virus replicating rat primary hepatocytes and HepG2 cells by iTRAQ-coupled 2-D LC-MS/MS analysis: Insights on liver angiogenesis. *Proteomics* 2009, *9*, 2836-2845.

[156] Zhang, J., Sui, J., Ching, C. B., Chen, W. N., Protein profile in neuroblastoma cells incubated with S- and R-enantiomers of ibuprofen by iTRAQ-coupled 2-D LC-MS/MS analysis: possible action of induced proteins on Alzheimer's disease. *Proteomics* 2008, *8*, 1595-1607.

[157] Karkhanis, Y. D., Zeltner, J. Y., Jackson, J. J., Carlo, D. J., A new and improved microassay to determine 2-keto-3-deoxyoctonate in lipopolysaccharide of Gram-negative bacteria. *Anal Biochem* 1978, *85*, 595-601.

[158] Kloser, A., Laird, M., Deng, M., Misra, R., Modulations in lipid A and phospholipid biosynthesis pathways influence outer membrane protein assembly in Escherichia coli K-12. *Mol Microbiol* 1998, *27*, 1003-1008.

[159] Chen, P. S., Toribara, T. Y., Warner, H., Microdetermination of phosphorus. *Anal. Chem.* 1956, *28*, 1756-1758.

[160] Anderson, M. S., Raetz, C. R. H., Biosynthesis of lipid-a precursors in Escherichia-coli - a cytoplasmic acyltransferase that converts UDP-n-acetylglucosamine to UDP-3-0-(r-3-hydroxymyristoyl)-n-acetylglucosamine. *Journal of Biological Chemistry* 1987, *262*, 5159-5169.

[161] Anderson, M. S., Robertson, A. D., Macher, I., Raetz, C. R. H.,

Biosynthesis of lipid-a in Escherichia-coli - identification of UDP-3-o-[(r)-3-hydroxymyristoyl]-alpha-d-glucosamine as a precursor of UDP-n,2,o-3-bis[(r)-3-hydroxymyristoyl]-alpha-d-glucosamine. *Biochemistry* 1988, *27*, 1908-1917.

[162] Anderson, M. S., Bull, H. G., Galloway, S. M., Kelly, T. M.*, et al.*, UDP-n-acetylglucosamine acyltransferase of Escherichia-coli - the 1st step of endotoxin biosynthesis is thermodynamically unfavorable. *Journal of Biological Chemistry* 1993, *268*, 19858-19865.

[163] Anderson, M. S., Bulawa, C. E., Raetz, C. R. H., The biosynthesis of gram-negative endotoxin - formation of lipid a precursors from UDP-glcnac in extracts of Escherichia-coli. *Journal of Biological Chemistry* 1985, *260*, 5536-5541.

[164] Heath, R. J., Rock, C. O., Roles of the FabA and FabZ beta-hydroxyacyl-acyl carrier protein dehydratases in Escherichia coli fatty acid biosynthesis. *Journal of Biological Chemistry* 1996, *271*, 27795-27801.

[165] Mohan, S., Kelly, T. M., Eveland, S. S., Raetz, C. R. H., Anderson, M. S., an Escherichia-coli gene (fabz) encoding (3r)-hydroxymyristoyl acyl carrier protein dehydrase - relation to fabA and suppression of mutations in lipid a biosynthesis. *Journal of Biological Chemistry* 1994, *269*, 32896-32903.

[166] Tomoyasu, T., Gamer, J., Bukau, B., Kanemori, M.*, et al.*, Escherichia-coli FtsH is a membrane-bound, ATP-dependent protease which degrades the heat-shock transcription factor sigma(32). *Embo J.* 1995, *14*, 2551-2560.

[167] Ogura, T., Inoue, K., Tatsuta, T., Suzaki, T.*, et al.*, Balanced biosynthesis of major membrane components through regulated degradation of the committed enzyme of lipid A biosynthesis by the AAA protease FtsH (HflB) in Escherichia coli. *Mol Microbiol* 1999, *31*, 833-844.

[168] Fuhrer, F., Muller, A., Baumann, H., Langklotz, S.*, et al.*, Sequence and length recognition of the C-terminal turnover element of LpxC, the membrane-bound FtsH a soluble substrate of protease. *J. Mol. Biol.* 2007, *372*, 485-496.

[169] Saier, M. H., Ramseier, T. M., The catabolite repressor/activator (Cra) protein of enteric bacteria. *J. Bacteriol.* 1996, *178*, 3411-3417.

[170] Ramseier, T. M., Cra and the control of carbon flux via metabolic pathways. *Research in Microbiology* 1996, *147*, 489-493.

Appendix

Appendix 1: Cytoplasmic proteins identified in *E. coli* incubated with apidaecin IB

Appendix 2: Cytoplasmic proteins identified in *E. coli* incubated with HNP-1

Appendix 1

Group	Distinct Peptides	% AA Coverage	Avg A:C 1 h	Avg A:C 2 h	Database Accession	Protein Name
1	32	59	1.03	1.03	P0A6M8	Elongation factor G OS=Escherichia coli (strain K12) GN=fusA PE=1 SV=2
2	34	45	0.97	0.99	P0AFG8	Pyruvate dehydrogenase E1 component OS=Escherichia coli (strain K12) GN=aceE PE=1 S
3	34	34	0.92	1.24	P0A8T7	DNA-directed RNA polymerase subunit beta' OS=Escherichia coli (strain K12) GN=rpoC P
4	23	79	1.04	0.86	P0CE48	Elongation factor Tu 2 OS=Escherichia coli (strain K12) GN=tufB PE=1 SV=1
5	25	59	0.7	0.62	P0A6F5	60 kDa chaperonin OS=Escherichia coli (strain K12) GN=groL PE=1 SV=2
6	31	32	0.95	0.82	P0A8V2	DNA-directed RNA polymerase subunit beta OS=Escherichia coli (strain K12) GN=rpoB P
7	22	37	0.86	0.48	P09373	Formate acetyltransferase 1 OS=Escherichia coli (strain K12) GN=pflB PE=1 SV=2
8	23	56	1.13	0.98	P0A850	Trigger factor OS=Escherichia coli (strain K12) GN=tig PE=1 SV=1
9	20	62	1.12	0.78	P0ABB4	ATP synthase subunit beta OS=Escherichia coli (strain K12) GN=atpD PE=1 SV=2
10	22	38	0.98	1.04	P06959	Dihydrolipoyllysine-residue acetyltransferase component of pyruvate dehydrogenase comp
11	21	42	0.8	1.16	P0A6Y8	Chaperone protein dnaK OS=Escherichia coli (strain K12) GN=dnaK PE=1 SV=2
12	19	37	0.97	1	P0AG67	30S ribosomal protein S1 OS=Escherichia coli (strain K12) GN=rpsA PE=1 SV=1
13	15	54	0.94	0.65	P0A6P9	Enolase OS=Escherichia coli (strain K12) GN=eno PE=1 SV=2
14	15	30	0.85	0.85	P0A9M8	Phosphate acetyltransferase OS=Escherichia coli (strain K12) GN=pta PE=1 SV=2
15	15	77	1.1	1.02	P0A7V0	30S ribosomal protein S2 OS=Escherichia coli (strain K12) GN=rpsB PE=1 SV=2
16	16	59	1.08	0.98	P60422	50S ribosomal protein L2 OS=Escherichia coli (strain K12) GN=rplB PE=1 SV=2
17	16	40	1.1	0.88	P0ABB0	ATP synthase subunit alpha OS=Escherichia coli (strain K12) GN=atpA PE=1 SV=1
18	14	54	0.92	0.92	P0A6P1	Elongation factor Ts OS=Escherichia coli (strain K12) GN=tsf PE=1 SV=2
19	14	65	1	1.3	P0A7L0	50S ribosomal protein L1 OS=Escherichia coli (strain K12) GN=rplA PE=1 SV=2
20	13	41	0.85	0.49	P0A9B2	Glyceraldehyde-3-phosphate dehydrogenase A OS=Escherichia coli (strain K12) GN=gapA
21	14	22	1.08	0.64	P23538	Phosphoenolpyruvate synthase OS=Escherichia coli (strain K12) GN=ppsA PE=1 SV=5
22	15	35	0.83	0.49	P0AC38	Aspartate ammonia-lyase OS=Escherichia coli (strain K12) GN=aspA PE=1 SV=1
23	16	25	1.18	0.8	P36683	Aconitate hydratase 2 OS=Escherichia coli (strain K12) GN=acnB PE=1 SV=3
24	13	40	1.16	0.68	P0A9P0	Dihydrolipoyl dehydrogenase OS=Escherichia coli (strain K12) GN=lpdA PE=1 SV=2
25	12	61	1.34	1.42	P62399	50S ribosomal protein L5 OS=Escherichia coli (strain K12) GN=rplE PE=1 SV=2
26	13	40	1.03	1.12	P00350	6-phosphogluconate dehydrogenase, decarboxylating OS=Escherichia coli (strain K12) GN
27	12	60	0.97	0.89	P0A7V3	30S ribosomal protein S3 OS=Escherichia coli (strain K12) GN=rpsC PE=1 SV=2
28	13	37	1.1	0.68	P08200	Isocitrate dehydrogenase [NADP] OS=Escherichia coli (strain K12) GN=icd PE=1 SV=1

						Isocitrate dehydrogenase [NADP] OS=Escherichia coli (strain K12) GN=icd PE=1 SV=1
29	13	62	0.86	0.6	P61889	Malate dehydrogenase OS=Escherichia coli (strain K12) GN=mdh PE=1 SV=1
30	10	55	1.12	1.1	P02359	30S ribosomal protein S7 OS=Escherichia coli (strain K12) GN=rpsG PE=1 SV=3
31	12	51	1.04	1.21	P60438	50S ribosomal protein L3 OS=Escherichia coli (strain K12) GN=rplC PE=1 SV=1
32	11	30	0.89	0.94	P0A7D4	Adenylosuccinate synthetase OS=Escherichia coli (strain K12) GN=purA PE=1 SV=2
33	12	22	1	0.99	P05055	Polyribonucleotide nucleotidyltransferase OS=Escherichia coli (strain K12) GN=pnp PE=1
34	11	50	1	0.96	P0A7V8	30S ribosomal protein S4 OS=Escherichia coli (strain K12) GN=rpsD PE=1 SV=2
35	11	47	0.91	0.85	P0A870	Transaldolase B OS=Escherichia coli (strain K12) GN=talB PE=1 SV=2
36	10	85	1.07	113.02	P0A7K2	50S ribosomal protein L7/L12 OS=Escherichia coli (strain K12) GN=rplL PE=1 SV=2
37	12	34	0.86	0.88	P0AD61	Pyruvate kinase I OS=Escherichia coli (strain K12) GN=pykF PE=1 SV=1
38	11	28	0.91	1.22	P0A910	Outer membrane protein A OS=Escherichia coli (strain K12) GN=ompA PE=1 SV=1
39	13	20	1.35	0.87	P0A705	Translation initiation factor IF-2 OS=Escherichia coli (strain K12) GN=infB PE=1 SV=1
40	11	77	1.08	0.97	P0A7R1	50S ribosomal protein L9 OS=Escherichia coli (strain K12) GN=rplI PE=1 SV=1
41	9	50	1.11	1.14	P0AG55	50S ribosomal protein L6 OS=Escherichia coli (strain K12) GN=rplF PE=1 SV=2
42	11	42	0.93	0.92	P0A6A3	Acetate kinase OS=Escherichia coli (strain K12) GN=ackA PE=1 SV=1
43	11	20	1.27	1.07	P0A7E5	CTP synthase OS=Escherichia coli (strain K12) GN=pyrG PE=1 SV=2
44	9	49	1.35	1.12	P60723	50S ribosomal protein L4 OS=Escherichia coli (strain K12) GN=rplD PE=1 SV=1
45	10	18	0.87	0.73	P63284	Chaperone protein clpB OS=Escherichia coli (strain K12) GN=clpB PE=1 SV=1
46	10	36	0.86	0.57	P0A799	Phosphoglycerate kinase OS=Escherichia coli (strain K12) GN=pgk PE=1 SV=2
47	10	38	0.99	1.01	P0A7Z4	DNA-directed RNA polymerase subunit alpha OS=Escherichia coli (strain K12) GN=rpoA
48	8	55	1.09	0.9	P0A7W1	30S ribosomal protein S5 OS=Escherichia coli (strain K12) GN=rpsE PE=1 SV=2
49	10	23	0.98	0.95	P17169	Glucosamine--fructose-6-phosphate aminotransferase [isomerizing] OS=Escherichia coli (
50	11	28	0.81	0.67	P0A6F3	Glycerol kinase OS=Escherichia coli (strain K12) GN=glpK PE=1 SV=2
51	9	60	2.12	1.02	P0ACF8	DNA-binding protein H-NS OS=Escherichia coli (strain K12) GN=hns PE=1 SV=2
52	9	13	1.14	0.62	P0AFG3	2-oxoglutarate dehydrogenase E1 component OS=Escherichia coli (strain K12) GN=sucA
53	9	66	0.99	0.29	P68066	Autonomous glycyl radical cofactor OS=Escherichia coli (strain K12) GN=grcA PE=1 SV=
54	8	67	1.18	1.15	P61175	50S ribosomal protein L22 OS=Escherichia coli (strain K12) GN=rplV PE=1 SV=1
55	11	33	0.88	0.63	P0A825	Serine hydroxymethyltransferase OS=Escherichia coli (strain K12) GN=glyA PE=1 SV=1
56	8	50	1.19	1.07	P0AE08	Alkyl hydroperoxide reductase subunit C OS=Escherichia coli (strain K12) GN=ahpC PE=
57	7	59	1.37	1.34	P0A7S9	30S ribosomal protein S13 OS=Escherichia coli (strain K12) GN=rpsM PE=1 SV=2
58	7	24	0.97	0.84	P0AG30	Transcription termination factor rho OS=Escherichia coli (strain K12) GN=rho PE=1 SV=1
59	7	16	1.13	1.62	P0A9P6	Cold-shock DEAD box protein A OS=Escherichia coli (strain K12) GN=deaD PE=1 SV=2
60	8	57	1.11	1.17	P0A7W7	30S ribosomal protein S8 OS=Escherichia coli (strain K12) GN=rpsH PE=1 SV=2
61	8	21	0.75	0.76	P16659	Prolyl-tRNA synthetase OS=Escherichia coli (strain K12) GN=proS PE=1 SV=4

						Prolyl-tRNA synthetase OS=Escherichia coli (strain K12) GN=proS PE=1 SV=4
62	8	49	1.02	0.98	P0ADY7	50S ribosomal protein L16 OS=Escherichia coli (strain K12) GN=rplP PE=1 SV=1
63	7	19	1.38	0.79	P04949	Flagellin OS=Escherichia coli (strain K12) GN=fliC PE=1 SV=2
64	7	59	0.95	1.1	P0A7K6	50S ribosomal protein L19 OS=Escherichia coli (strain K12) GN=rplS PE=1 SV=2
65	7	54	1.01	1.01	P02413	50S ribosomal protein L15 OS=Escherichia coli (strain K12) GN=rplO PE=1 SV=1
66	6	43	1.11	1.48	P0A7J7	50S ribosomal protein L11 OS=Escherichia coli (strain K12) GN=rplK PE=1 SV=2
67	7	58	1.15	1.38	P0AA10	50S ribosomal protein L13 OS=Escherichia coli (strain K12) GN=rplM PE=1 SV=1
68	8	24	1.23	1.07	P0AFF6	Transcription elongation protein nusA OS=Escherichia coli (strain K12) GN=nusA PE=1 S
69	6	50	1.12	1.33	P0A7J3	50S ribosomal protein L10 OS=Escherichia coli (strain K12) GN=rplJ PE=1 SV=2
70	6	21	0.82	0.79	P0A953	3-oxoacyl-[acyl-carrier-protein] synthase 1 OS=Escherichia coli (strain K12) GN=fabB PE=
71	6	42	1.11	1.38	P0A7X3	30S ribosomal protein S9 OS=Escherichia coli (strain K12) GN=rpsI PE=1 SV=2
72	6	60	0.98	0.91	P02358	30S ribosomal protein S6 OS=Escherichia coli (strain K12) GN=rpsF PE=1 SV=1
73	7	14	0.89	0.56	P27302	Transketolase 1 OS=Escherichia coli (strain K12) GN=tktA PE=1 SV=5
74	6	15	0.7	0.62	P13029	Catalase-peroxidase OS=Escherichia coli (strain K12) GN=katG PE=1 SV=2
75	6	65	0.83	0.73	P0ACF0	DNA-binding protein HU-alpha OS=Escherichia coli (strain K12) GN=hupA PE=1 SV=1
76	7	29	0.79	0.56	P0A717	Ribose-phosphate pyrophosphokinase OS=Escherichia coli (strain K12) GN=prs PE=1 SV
77	8	19	0.94	1.16	P0A8M0	Asparaginyl-tRNA synthetase OS=Escherichia coli (strain K12) GN=asnS PE=1 SV=2
78	6	20	1.61	1.21	P0A836	Succinyl-CoA ligase [ADP-forming] subunit beta OS=Escherichia coli (strain K12) GN=suc
79	7	10	0.82	0.83	P07118	Valyl-tRNA synthetase OS=Escherichia coli (strain K12) GN=valS PE=1 SV=2
80	6	62	1.21	1.06	P0A7R5	30S ribosomal protein S10 OS=Escherichia coli (strain K12) GN=rpsJ PE=1 SV=1
81	6	20	0.88	0.58	P21599	Pyruvate kinase II OS=Escherichia coli (strain K12) GN=pykA PE=1 SV=3
82	6	29	1.11	1.26	P0ABD5	Acetyl-coenzyme A carboxylase carboxyl transferase subunit alpha OS=Escherichia coli (
83	6	33	1.07	1.07	P0AEK2	3-oxoacyl-[acyl-carrier-protein] reductase OS=Escherichia coli (strain K12) GN=fabG PE=
84	6	42	1	0.88	P0A8F0	Uracil phosphoribosyltransferase OS=Escherichia coli (strain K12) GN=upp PE=1 SV=1
85	6	60	0.78	0.59	P0AF93	UPF0076 protein yjgF OS=Escherichia coli (strain K12) GN=yjgF PE=1 SV=2
86	7	22	0.9	0.94	P0A8L1	Seryl-tRNA synthetase OS=Escherichia coli (strain K12) GN=serS PE=1 SV=1
87	6	33	0.84	0.9	P0AEK4	Enoyl-[acyl-carrier-protein] reductase [NADH] OS=Escherichia coli (strain K12) GN=fabI P
88	6	28	0.84	0.7	P45523	FKBP-type peptidyl-prolyl cis-trans isomerase fkpA OS=Escherichia coli (strain K12) GN=
89	7	10	1.22	1.14	P07813	Leucyl-tRNA synthetase OS=Escherichia coli (strain K12) GN=leuS PE=1 SV=2
90	6	13	1.36	1.37	P00961	Glycyl-tRNA synthetase beta subunit OS=Escherichia coli (strain K12) GN=glyS PE=1 SV
91	5	32	0.91	0.82	P0A9P4	Thioredoxin reductase OS=Escherichia coli (strain K12) GN=trxB PE=1 SV=2
92	6	41	0.84	0.79	P0A805	Ribosome-recycling factor OS=Escherichia coli (strain K12) GN=frr PE=1 SV=1
93	5	23	1.27	1.98	P0ADG7	Inosine-5'-monophosphate dehydrogenase OS=Escherichia coli (strain K12) GN=guaB PE
94	7	18	0.96	0.8	P04805	Glutamyl-tRNA synthetase OS=Escherichia coli (strain K12) GN=gltX PE=1 SV=1

						Glutamyl-tRNA synthetase OS=Escherichia coli (strain K12) GN=gltX PE=1 SV=1
95	7	12	1.01	1.19	P21889	Aspartyl-tRNA synthetase OS=Escherichia coli (strain K12) GN=aspS PE=1 SV=1
96	5	50	0.73	0.73	P69783	Glucose-specific phosphotransferase enzyme IIA component OS=Escherichia coli (strain
97	6	12	0.9	0.76	P07395	Phenylalanyl-tRNA synthetase beta chain OS=Escherichia coli (strain K12) GN=pheT PE=
98	6	13	0.87	1.26	P0A9M0	ATP-dependent protease La OS=Escherichia coli (strain K12) GN=lon PE=1 SV=1
99	6	50	0.98	0.97	P0ADY3	50S ribosomal protein L14 OS=Escherichia coli (strain K12) GN=rplN PE=1 SV=1
100	6	10	0.82	0.75	P0A8N3	Lysyl-tRNA synthetase OS=Escherichia coli (strain K12) GN=lysS PE=1 SV=2
101	7	32	1.02	0.66	P0AGE9	Succinyl-CoA ligase [ADP-forming] subunit alpha OS=Escherichia coli (strain K12) GN=su
102	6	15	0.97	0.92	P32132	GTP-binding protein typA/BipA OS=Escherichia coli (strain K12) GN=typA PE=1 SV=2
103	5	22	0.94	0.52	P0AB71	Fructose-bisphosphate aldolase class 2 OS=Escherichia coli (strain K12) GN=fbaA PE=1
104	7	12	0.87	0.73	P0AC41	Succinate dehydrogenase flavoprotein subunit OS=Escherichia coli (strain K12) GN=sdhA
105	4	40	1.03	1.19	P0ACF4	DNA-binding protein HU-beta OS=Escherichia coli (strain K12) GN=hupB PE=1 SV=1
106	5	30	0.75	0.83	P0ACA3	Stringent starvation protein A OS=Escherichia coli (strain K12) GN=sspA PE=1 SV=2
107	6	11	1.02	0.71	P0A6Z3	Chaperone protein htpG OS=Escherichia coli (strain K12) GN=htpG PE=1 SV=1
108	6	7	1.02	0.86	P21513	Ribonuclease E OS=Escherichia coli (strain K12) GN=rne PE=1 SV=6
109	5	38	1.09	1.26	P0A9L3	FKBP-type 22 kDa peptidyl-prolyl cis-trans isomerase OS=Escherichia coli (strain K12) G
110	5	19	1.1	1.34	P0A817	S-adenosylmethionine synthetase OS=Escherichia coli (strain K12) GN=metK PE=1 SV=
111	5	24	0.86	0.83	P62707	2,3-bisphosphoglycerate-dependent phosphoglycerate mutase OS=Escherichia coli (strain
112	5	42	0.84	0.69	P0A912	Peptidoglycan-associated lipoprotein OS=Escherichia coli (strain K12) GN=pal PE=1 SV=
113	4	33	1.08	1.03	P0A7R9	30S ribosomal protein S11 OS=Escherichia coli (strain K12) GN=rpsK PE=1 SV=2
114	5	52	1.04	0.83	P0A7T3	30S ribosomal protein S16 OS=Escherichia coli (strain K12) GN=rpsP PE=1 SV=1
115	5	40	1.04	2.69	P0AG59	30S ribosomal protein S14 OS=Escherichia coli (strain K12) GN=rpsN PE=1 SV=2
116	5	52	0.83	0.68	P0AA25	Thioredoxin-1 OS=Escherichia coli (strain K12) GN=trxA PE=1 SV=2
117	4	16	0.95	0.47	P0AEX9	Maltose-binding periplasmic protein OS=Escherichia coli (strain K12) GN=malE PE=1 SV
118	6	9	0.83	1.1	P00956	Isoleucyl-tRNA synthetase OS=Escherichia coli (strain K12) GN=ileS PE=1 SV=5
119	3	10	0.88	0.5	P0A9C5	Glutamine synthetase OS=Escherichia coli (strain K12) GN=glnA PE=1 SV=2
120	5	67	0.76	1.75	P0A800	DNA-directed RNA polymerase subunit omega OS=Escherichia coli (strain K12) GN=rpoZ
121	4	48	1.05	1.39	P0A7T7	30S ribosomal protein S18 OS=Escherichia coli (strain K12) GN=rpsR PE=1 SV=2
122	5	24	0.8	0.79	P69441	Adenylate kinase OS=Escherichia coli (strain K12) GN=adk PE=1 SV=1
123	4	58	1.63	1.1	P0A7M6	50S ribosomal protein L29 OS=Escherichia coli (strain K12) GN=rpmC PE=1 SV=1
124	5	18	0.86	1.1	P0A9A6	Cell division protein ftsZ OS=Escherichia coli (strain K12) GN=ftsZ PE=1 SV=1
125	5	41	0.96	0.77	P0C018	50S ribosomal protein L18 OS=Escherichia coli (strain K12) GN=rplR PE=1 SV=1
126	6	8	0.96	0.83	P00957	Alanyl-tRNA synthetase OS=Escherichia coli (strain K12) GN=alaS PE=1 SV=2
127	4	32	1.06	0.98	P0AG44	50S ribosomal protein L17 OS=Escherichia coli (strain K12) GN=rplQ PE=1 SV=1

						50S ribosomal protein L17 OS=Escherichia coli (strain K12) GN=rplQ PE=1 SV=1
128	5	12	1	1.21	P0A9W3	Uncharacterized ABC transporter ATP-binding protein yjjK OS=Escherichia coli (strain K1
129	3	20	0.96	1.06	P0A6L4	N-acetylneuraminate lyase OS=Escherichia coli (strain K12) GN=nanA PE=1 SV=2
130	4	37	1.13	0.91	P60624	50S ribosomal protein L24 OS=Escherichia coli (strain K12) GN=rplX PE=1 SV=2
131	5	13	0.92	1.06	P0ABH7	Citrate synthase OS=Escherichia coli (strain K12) GN=gltA PE=1 SV=1
132	4	40	0.81	1.15	P0ADZ0	50S ribosomal protein L23 OS=Escherichia coli (strain K12) GN=rplW PE=1 SV=1
133	5	11	0.66	0.54	P0A6H5	ATP-dependent hsl protease ATP-binding subunit hslU OS=Escherichia coli (strain K12) G
134	4	37	1.5	0.64	P61714	6,7-dimethyl-8-ribityllumazine synthase OS=Escherichia coli (strain K12) GN=ribH PE=1 S
135	4	15	0.5	0.29	P00805	L-asparaginase 2 OS=Escherichia coli (strain K12) GN=ansB PE=1 SV=2
136	4	16	1.21	2.22	P0ABA6	ATP synthase gamma chain OS=Escherichia coli (strain K12) GN=atpG PE=1 SV=1
137	4	54	1.12	2.33	P0A9X9	Cold shock protein cspA OS=Escherichia coli (strain K12) GN=cspA PE=1 SV=2
138	6	19	1.07	0.98	P33232	L-lactate dehydrogenase [cytochrome] OS=Escherichia coli (strain K12) GN=lldD PE=1 S
139	6	16	0.81	1.05	P24182	Biotin carboxylase OS=Escherichia coli (strain K12) GN=accC PE=1 SV=2
140	5	13	0.99	1.45	P0A6B7	Cysteine desulfurase OS=Escherichia coli (strain K12) GN=iscS PE=1 SV=1
141	5	32	0.94	0.81	P0A707	Translation initiation factor IF-3 OS=Escherichia coli (strain K12) GN=infC PE=1 SV=1
142	4	26	0.7	0.5	P0A715	2-dehydro-3-deoxyphosphooctonate aldolase OS=Escherichia coli (strain K12) GN=kdsA
143	4	15	1.2	1.33	P0A6H1	ATP-dependent Clp protease ATP-binding subunit clpX OS=Escherichia coli (strain K12) G
144	4	23	0.77	0.74	P0AAI9	Malonyl CoA-acyl carrier protein transacylase OS=Escherichia coli (strain K12) GN=fabD
145	4	17	0.66	0.94	P0A9X4	Rod shape-determining protein mreB OS=Escherichia coli (strain K12) GN=mreB PE=1 S
146	4	17	0.76	3.04	P76177	Protein ydgH OS=Escherichia coli (strain K12) GN=ydgH PE=1 SV=1
147	3	9	1.25	0.96	P04079	GMP synthase [glutamine-hydrolyzing] OS=Escherichia coli (strain K12) GN=guaA PE=1
148	5	16	0.78	0.84	P23893	Glutamate-1-semialdehyde 2,1-aminomutase OS=Escherichia coli (strain K12) GN=hemL
149	4	18	0.79	0.8	P0A9D8	2,3,4,5-tetrahydropyridine-2,6-dicarboxylate N-succinyltransferase OS=Escherichia coli (s
150	3	22	1.19	1.07	P0A7L3	50S ribosomal protein L20 OS=Escherichia coli (strain K12) GN=rplT PE=1 SV=2
151	4	39	0.93	1.32	P0A7M2	50S ribosomal protein L28 OS=Escherichia coli (strain K12) GN=rpmB PE=1 SV=2
152	3	8	0.93	0.38	P22259	Phosphoenolpyruvate carboxykinase [ATP] OS=Escherichia coli (strain K12) GN=pckA PI
153	4	34	0.67	1.19	P0A862	Thiol peroxidase OS=Escherichia coli (strain K12) GN=tpx PE=1 SV=2
154	4	10	0.73	0.83	P08839	Phosphoenolpyruvate-protein phosphotransferase OS=Escherichia coli (strain K12) GN=pt
155	5	7	1.02	0.91	P0A8M3	Threonyl-tRNA synthetase OS=Escherichia coli (strain K12) GN=thrS PE=1 SV=1
156	5	9	1.12	3.71	P00452	Ribonucleoside-diphosphate reductase 1 subunit alpha OS=Escherichia coli (strain K12) G
157	4	20	0.83	0.64	P0ACJ8	Catabolite gene activator OS=Escherichia coli (strain K12) GN=crp PE=1 SV=1
158	5	27	1.22	0.76	P0A9Q5	Acetyl-coenzyme A carboxylase carboxyl transferase subunit beta OS=Escherichia coli (s
159	4	38	1.11	0.92	P68919	50S ribosomal protein L25 OS=Escherichia coli (strain K12) GN=rplY PE=1 SV=1
160	4	36	1.03	1.04	P0A7U3	30S ribosomal protein S19 OS=Escherichia coli (strain K12) GN=rpsS PE=1 SV=2

						30S ribosomal protein S15 OS=Escherichia coli (strain K12) GN=rpsO PE=1 SV=2
161	4	6	1.81	0.67	P0A9Q7	Aldehyde-alcohol dehydrogenase OS=Escherichia coli (strain K12) GN=adhE PE=1 SV=2
162	4	8	1.06	1.22	P00579	RNA polymerase sigma factor rpoD OS=Escherichia coli (strain K12) GN=rpoD PE=1 SV=
163	3	17	0.87	1.03	P0A9K9	FKBP-type peptidyl-prolyl cis-trans isomerase slyD OS=Escherichia coli (strain K12) GN=
164	4	27	2.29	2.14	P23836	Transcriptional regulatory protein phoP OS=Escherichia coli (strain K12) GN=phoP PE=1
165	3	14	0.95	0.56	P0AAI5	3-oxoacyl-[acyl-carrier-protein] synthase 2 OS=Escherichia coli (strain K12) GN=fabF PE=
166	4	10	0.5	0.91	P60785	GTP-binding protein lepA OS=Escherichia coli (strain K12) GN=lepA PE=1 SV=1
167	3	39	0.85	1.03	P68679	30S ribosomal protein S21 OS=Escherichia coli (strain K12) GN=rpsU PE=1 SV=2
168	4	9	1.4	0.46	P21170	Biosynthetic arginine decarboxylase OS=Escherichia coli (strain K12) GN=speA PE=1 SV
169	3	18	0.59	0.56	P28635	D-methionine-binding lipoprotein metQ OS=Escherichia coli (strain K12) GN=metQ PE=1
170	4	13	1.08	0.96	P00962	Glutaminyl-tRNA synthetase OS=Escherichia coli (strain K12) GN=glnS PE=1 SV=3
171	4	19	0.91	1.17	P0ADG4	Inositol-1-monophosphatase OS=Escherichia coli (strain K12) GN=suhB PE=1 SV=1
172	4	18	0.94	1.12	P02925	D-ribose-binding periplasmic protein OS=Escherichia coli (strain K12) GN=rbsB PE=1 SV=
173	4	15	1.03	0.78	P0ABU2	GTP-dependent nucleic acid-binding protein engD OS=Escherichia coli (strain K12) GN=e
174	3	9	1.12	0.72	P76658	Bifunctional protein hldE OS=Escherichia coli (strain K12) GN=hldE PE=1 SV=1
175	3	34	1.04	1.28	P0A7U7	30S ribosomal protein S20 OS=Escherichia coli (strain K12) GN=rpsT PE=1 SV=2
176	4	32	1.72	0.6	P0ABT2	DNA protection during starvation protein OS=Escherichia coli (strain K12) GN=dps PE=1 S
177	4	9	0.8	0.67	P0ABJ9	Cytochrome d ubiquinol oxidase subunit 1 OS=Escherichia coli (strain K12) GN=cydA PE
178	4	8	0.95	0.68	P0A6T1	Glucose-6-phosphate isomerase OS=Escherichia coli (strain K12) GN=pgi PE=1 SV=1
179	3	8	0.63	0.41	P0AFG6	Dihydrolipoyllysine-residue succinyltransferase component of 2-oxoglutarate dehydrogenas
180	3	43	0.92	0.65	P0A8J4	UPF0250 protein ybeD OS=Escherichia coli (strain K12) GN=ybeD PE=1 SV=1
181	3	18	0.91	1.4	P0A6R0	3-oxoacyl-[acyl-carrier-protein] synthase 3 OS=Escherichia coli (strain K12) GN=fabH PE=
182	4	50	0.8	0.61	P0A6F9	10 kDa chaperonin OS=Escherichia coli (strain K12) GN=groS PE=1 SV=1
183	3	33	0.7	0.57	P0A6A8	Acyl carrier protein OS=Escherichia coli (strain K12) GN=acpP PE=1 SV=2
184	4	34	0.85	0.89	P0AGD3	Superoxide dismutase [Fe] OS=Escherichia coli (strain K12) GN=sodB PE=1 SV=2
185	3	8	0.84	2.07	P0ABI8	Ubiquinol oxidase subunit 1 OS=Escherichia coli (strain K12) GN=cyoB PE=1 SV=1
186	3	49	1	0.84	P0ADZ4	30S ribosomal protein S15 OS=Escherichia coli (strain K12) GN=rpsO PE=1 SV=2
187	3	42	1.23	1.04	P69776	Major outer membrane lipoprotein OS=Escherichia coli (strain K12) GN=lpp PE=1 SV=1
188	3	22	0.95	0.63	P0AEU7	Chaperone protein skp OS=Escherichia coli (strain K12) GN=skp PE=1 SV=1
189	3	6	1.92	0.44	P33195	Glycine dehydrogenase [decarboxylating] OS=Escherichia coli (strain K12) GN=gcvP PE=
190	4	12	1.67	0.67	P31120	Phosphoglucosamine mutase OS=Escherichia coli (strain K12) GN=glmM PE=1 SV=3
191	3	12	0.89	0.6	P0AB77	2-amino-3-ketobutyrate coenzyme A ligase OS=Escherichia coli (strain K12) GN=kbl PE=
192	4	8	0.91	0.37	P00363	Fumarate reductase flavoprotein subunit OS=Escherichia coli (strain K12) GN=frdA PE=1
193	4	20	0.91	0.91	P0A6L2	Dihydrodipicolinate synthase OS=Escherichia coli (strain K12) GN=dapA PE=1 SV=1

						Dihydrodipicolinate synthase OS=Escherichia coli (strain K12) GN=dapA PE=1 SV=1
194	2	10	1.25	0.68	P36672	PTS system trehalose-specific EIIBC component OS=Escherichia coli (strain K12) GN=tre
195	3	31	0.94	1.33	P0A7M9	50S ribosomal protein L31 OS=Escherichia coli (strain K12) GN=rpmE PE=1 SV=1
196	3	27	1.06	1.15	P0AG48	50S ribosomal protein L21 OS=Escherichia coli (strain K12) GN=rplU PE=1 SV=1
197	3	5	0.72	1.41	P10408	Protein translocase subunit secA OS=Escherichia coli (strain K12) GN=secA PE=1 SV=2
198	3	30	0.82	0.76	P0ACG1	DNA-binding protein stpA OS=Escherichia coli (strain K12) GN=stpA PE=3 SV=1
199	3	6	1.02	0.75	P0AG90	Protein-export membrane protein secD OS=Escherichia coli (strain K12) GN=secD PE=3
200	3	8	0.88	1.4	P21507	ATP-dependent RNA helicase srmB OS=Escherichia coli (strain K12) GN=srmB PE=1 SV
201	4	14	0.75	0.43	P09147	UDP-glucose 4-epimerase OS=Escherichia coli (strain K12) GN=galE PE=1 SV=1
202	2	17	0.77	4.62	P0ABJ1	Ubiquinol oxidase subunit 2 OS=Escherichia coli (strain K12) GN=cyoA PE=1 SV=1
203	3	13	0.42	0.43	P0A858	Triosephosphate isomerase OS=Escherichia coli (strain K12) GN=tpiA PE=1 SV=1
204	3	14	0.8	0.63	P09372	Protein grpE OS=Escherichia coli (strain K12) GN=grpE PE=1 SV=1
205	3	13	0.86	0.81	P0ABP8	Purine nucleoside phosphorylase deoD-type OS=Escherichia coli (strain K12) GN=deoD P
206	3	6	0.7	1.06	P39396	Inner membrane protein yjiY OS=Escherichia coli (strain K12) GN=yjiY PE=1 SV=2
207	2	11	0.62	0.69	P00954	Tryptophanyl-tRNA synthetase OS=Escherichia coli (strain K12) GN=trpS PE=1 SV=3
208	2	21	1.31	0.39	P0A998	Ferritin-1 OS=Escherichia coli (strain K12) GN=ftnA PE=1 SV=1
209	3	13	0.44	0.66	P69797	PTS system mannose-specific EIIAB component OS=Escherichia coli (strain K12) GN=m
210	3	10	0.72	0.89	P0A7G6	Protein recA OS=Escherichia coli (strain K12) GN=recA PE=1 SV=2
211	3	40	0.77	0.8	P0A972	Cold shock-like protein cspE OS=Escherichia coli (strain K12) GN=cspE PE=1 SV=2
212	3	5	0.71	0.84	P0ADY1	Peptidyl-prolyl cis-trans isomerase D OS=Escherichia coli (strain K12) GN=ppiD PE=1 SV
213	3	48	0.75	1.38	P0AG99	Protein-export membrane protein secG OS=Escherichia coli (strain K12) GN=secG PE=1
214	3	17	0.94	1.34	P0AFG0	Transcription antitermination protein nusG OS=Escherichia coli (strain K12) GN=nusG PE
215	3	40	0.79	0.52	P0A9Y6	Cold shock-like protein cspC OS=Escherichia coli (strain K12) GN=cspC PE=1 SV=2
216	3	11	0.7	0.61	P0AEI1	(Dimethylallyl)adenosine tRNA methylthiotransferase miaB OS=Escherichia coli (strain K1
217	2	8	0.65	0.62	P00509	Aspartate aminotransferase OS=Escherichia coli (strain K12) GN=aspC PE=1 SV=1
218	2	5	0.64	1.05	P0AES6	DNA gyrase subunit B OS=Escherichia coli (strain K12) GN=gyrB PE=1 SV=2
219	3	6	0.98	0.86	P30850	Exoribonuclease 2 OS=Escherichia coli (strain K12) GN=rnb PE=1 SV=3
220	2	10	1.3	0.81	P42641	GTPase obgE/cgtA OS=Escherichia coli (strain K12) GN=obgE PE=1 SV=1
221	3	38	0.72	1.9	P0A7S3	30S ribosomal protein S12 OS=Escherichia coli (strain K12) GN=rpsL PE=1 SV=2
222	2	13	1.22	0.48	P0AFM2	Glycine betaine-binding periplasmic protein OS=Escherichia coli (strain K12) GN=proX PE
223	3	10	1.03	0.42	P35340	Alkyl hydroperoxide reductase subunit F OS=Escherichia coli (strain K12) GN=ahpF PE=
224	3	27	1.25	0.69	P0A7L8	50S ribosomal protein L27 OS=Escherichia coli (strain K12) GN=rpmA PE=1 SV=2
225	3	7	1.09	1.53	P0AGD7	Signal recognition particle protein OS=Escherichia coli (strain K12) GN=ffh PE=1 SV=1
226	2	11	0.83	0.4	P0AEE5	D-galactose-binding periplasmic protein OS=Escherichia coli (strain K12) GN=mglB PE=1

						D-galactose-binding periplasmic protein OS=Escherichia coli (strain K12) GN=mglB PE=1
227	3	6	1.47	0.69	P24175	Phosphomannomutase OS=Escherichia coli (strain K12) GN=manB PE=3 SV=1
228	2	4	2.84	1.06	P0AES4	DNA gyrase subunit A OS=Escherichia coli (strain K12) GN=gyrA PE=1 SV=1
229	3	16	0.95	0.77	P63224	Phosphoheptose isomerase OS=Escherichia coli (strain K12) GN=gmhA PE=1 SV=1
230	2	9	0.31	0.94	P07650	Thymidine phosphorylase OS=Escherichia coli (strain K12) GN=deoA PE=1 SV=3
231	2	18	0.59	1.3	P37665	Inner membrane lipoprotein yiaD OS=Escherichia coli (strain K12) GN=yiaD PE=1 SV=2
232	2	11	0.68	0.38	P0AC47	Fumarate reductase iron-sulfur subunit OS=Escherichia coli (strain K12) GN=frdB PE=1 S
233	3	21	1.71	0.78	P0A6D7	Shikimate kinase 1 OS=Escherichia coli (strain K12) GN=aroK PE=1 SV=2
234	2	7	0.39	1.41	P0AGJ5	Uncharacterized tRNA/rRNA methyltransferase yfiF OS=Escherichia coli (strain K12) GN=
235	2	4	0.57	3.26	P33599	NADH-quinone oxidoreductase subunit C/D OS=Escherichia coli (strain K12) GN=nuoC P
236	2	9	0.46	0.42	P0AEZ3	Septum site-determining protein minD OS=Escherichia coli (strain K12) GN=minD PE=1 S
237	3	4	0.84	1.65	P04825	Aminopeptidase N OS=Escherichia coli (strain K12) GN=pepN PE=1 SV=2
238	3	19	0.64	1.25	P0A6Q3	3-hydroxydecanoyl-[acyl-carrier-protein] dehydratase OS=Escherichia coli (strain K12) GN
239	3	7	1.68	0.96	P26616	NAD-dependent malic enzyme OS=Escherichia coli (strain K12) GN=sfcA PE=3 SV=4
240	3	4	1.08	0.7	P0A940	Outer membrane protein assembly factor yaeT OS=Escherichia coli (strain K12) GN=yaeT
241	3	23	1.08	2.85	P0ABA0	ATP synthase subunit b OS=Escherichia coli (strain K12) GN=atpF PE=1 SV=1
242	2	6	1.07	1.69	P21888	Cysteinyl-tRNA synthetase OS=Escherichia coli (strain K12) GN=cysS PE=1 SV=2
243	3	49	0.95	1.02	P0A7N9	50S ribosomal protein L33 OS=Escherichia coli (strain K12) GN=rpmG PE=1 SV=2
244	2	33	0.94	1.06	P0AG51	50S ribosomal protein L30 OS=Escherichia coli (strain K12) GN=rpmD PE=1 SV=2
245	2	6	0.76	0.95	P0AGJ9	Tyrosyl-tRNA synthetase OS=Escherichia coli (strain K12) GN=tyrS PE=1 SV=2
246	2	19	0.58	0.48	P61949	Flavodoxin-1 OS=Escherichia coli (strain K12) GN=fldA PE=1 SV=2
247	2	16	0.85	1.03	P0AG63	30S ribosomal protein S17 OS=Escherichia coli (strain K12) GN=rpsQ PE=1 SV=2
248	2	8	0.75	0.66	P0AB24	UPF0409 protein ycdO OS=Escherichia coli (strain K12) GN=ycdO PE=1 SV=1
249	2	15	0.55	0.52	P0A955	KHG/KDPG aldolase OS=Escherichia coli (strain K12) GN=eda PE=1 SV=1
250	2	11	1.58	1.07	P00960	Glycyl-tRNA synthetase alpha subunit OS=Escherichia coli (strain K12) GN=glyQ PE=1 S
251	3	22	0.85	0.88	P0A6W5	Transcription elongation factor greA OS=Escherichia coli (strain K12) GN=greA PE=1 SV=
252	3	13	1	9.46	P60716	Lipoyl synthase OS=Escherichia coli (strain K12) GN=lipA PE=1 SV=1
253	2	22	0.82	0.55	P0AG86	Protein-export protein secB OS=Escherichia coli (strain K12) GN=secB PE=1 SV=1
254	2	13	1.02	0.81	P0AGE0	Single-stranded DNA-binding protein OS=Escherichia coli (strain K12) GN=ssb PE=1 SV=
255	2	5	0.72	3	P00393	NADH dehydrogenase OS=Escherichia coli (strain K12) GN=ndh PE=1 SV=2
256	2	13	7.4	4.69	P14176	Glycine betaine/L-proline transport system permease protein proW OS=Escherichia coli (s
257	2	25	0.69	0.41	P0ADW3	Putative cytochrome d ubiquinol oxidase subunit 3 OS=Escherichia coli (strain K12) GN=y
258	2	10	0.84	0.75	P0A9C3	Aldose 1-epimerase OS=Escherichia coli (strain K12) GN=galM PE=1 SV=1
259	2	7	1.1	0.69	P77774	Lipoprotein yfgL OS=Escherichia coli (strain K12) GN=yfgL PE=1 SV=1

						Lipoprotein yigL OS=Escherichia coli (strain K12) GN=yigL PE=1 SV=1
260	2	12	0.56	0.62	P0A7Z0	Ribose-5-phosphate isomerase A OS=Escherichia coli (strain K12) GN=rpiA PE=1 SV=1
261	2	10	0.99	0.48	P07014	Succinate dehydrogenase iron-sulfur subunit OS=Escherichia coli (strain K12) GN=sdhB P
262	2	8	1.28	1.47	P0A8A0	UPF0082 protein yebC OS=Escherichia coli (strain K12) GN=yebC PE=1 SV=1
263	2	5	2.86	1.25	P75838	UPF0142 protein ycaO OS=Escherichia coli (strain K12) GN=ycaO PE=3 SV=2
264	2	8	1.11	0.71	P0A749	UDP-N-acetylglucosamine 1-carboxyvinyltransferase OS=Escherichia coli (strain K12) GN
265	2	5	1.95	5	P25888	ATP-dependent RNA helicase rhlE OS=Escherichia coli (strain K12) GN=rhlE PE=1 SV=3
266	2	28	0.96	1.13	P0A7P5	50S ribosomal protein L34 OS=Escherichia coli (strain K12) GN=rpmH PE=1 SV=1
267	2	5	0.72	1.72	P60906	Histidyl-tRNA synthetase OS=Escherichia coli (strain K12) GN=hisS PE=1 SV=2
268	2	4	0.92	0.49	P0AC33	Fumarate hydratase class I, aerobic OS=Escherichia coli (strain K12) GN=fumA PE=1 SV
269	2	9	1.35	0.42	P15034	Xaa-Pro aminopeptidase OS=Escherichia coli (strain K12) GN=pepP PE=1 SV=2
270	2	7	0.78	0.95	P0AGA2	Preprotein translocase subunit secY OS=Escherichia coli (strain K12) GN=secY PE=1 SV
271	2	12	1.03	1.1	P0A9A9	Ferric uptake regulation protein OS=Escherichia coli (strain K12) GN=fur PE=1 SV=1
272	2	14	0.83	0.56	P0ACR9	Transcriptional repressor mprA OS=Escherichia coli (strain K12) GN=mprA PE=2 SV=1
273	1	9	0.74	0.63	P0A6G7	ATP-dependent Clp protease proteolytic subunit OS=Escherichia coli (strain K12) GN=clp
274	2	17	1.08	1.47	P0AG27	Uncharacterized protein yibN OS=Escherichia coli (strain K12) GN=yibN PE=1 SV=1
275	2	32	1.26	0.74	P0AF36	Cell division protein zapB OS=Escherichia coli (strain K12) GN=zapB PE=1 SV=1
276	1	4	0.88	0.73	P36938	Phosphoglucomutase OS=Escherichia coli (strain K12) GN=pgm PE=1 SV=1
277	2	4	4.81	0.73	P00582	DNA polymerase I OS=Escherichia coli (strain K12) GN=polA PE=1 SV=1
278	2	11	1	0.24	P12281	Molybdopterin molybdenumtransferase OS=Escherichia coli (strain K12) GN=moeA PE=1
279	2	14	0.19	2.05	P0ABF6	Cytidine deaminase OS=Escherichia coli (strain K12) GN=cdd PE=1 SV=1
280	2	35	0.56	0.77	P77695	Protein gnsB OS=Escherichia coli (strain K12) GN=gnsB PE=3 SV=2
281	1	10	0.27	0.19	P0AEQ6	Glutamine transport system permease protein glnP OS=Escherichia coli (strain K12) GN=
282	2	8	0.71	1	P0AFK9	Spermidine/putrescine-binding periplasmic protein OS=Escherichia coli (strain K12) GN=p
283	2	8	1.27	2.37	P0AE06	Acriflavine resistance protein A OS=Escherichia coli (strain K12) GN=acrA PE=1 SV=1
284	2	12	0.75	0.64	P60955	Prolipoprotein diacylglyceryl transferase OS=Escherichia coli (strain K12) GN=lgt PE=1 S
285	1	10	1.01	0.74	P69503	Adenine phosphoribosyltransferase OS=Escherichia coli (strain K12) GN=apt PE=1 SV=1
286	2	7	0.7	1.95	P08312	Phenylalanyl-tRNA synthetase alpha chain OS=Escherichia coli (strain K12) GN=pheS PE
287	2	6	0.64	1.24	P0A927	Nucleoside-specific channel-forming protein tsx OS=Escherichia coli (strain K12) GN=tsx
288	1	12	1.22	1.09	P0AE52	Putative peroxiredoxin bcp OS=Escherichia coli (strain K12) GN=bcp PE=1 SV=1
289	2	4	0.75	0.83	P28904	Trehalose-6-phosphate hydrolase OS=Escherichia coli (strain K12) GN=treC PE=3 SV=3
290	2	10	1.31	1.02	P0A9E5	Fumarate and nitrate reduction regulatory protein OS=Escherichia coli (strain K12) GN=fn
291	2	3	1.05	0.99	P77804	Protein ydgA OS=Escherichia coli (strain K12) GN=ydgA PE=1 SV=1
292	2	8	0.75	0.49	P0A9S5	Glycerol dehydrogenase OS=Escherichia coli (strain K12) GN=gldA PE=1 SV=1

						Glycerol dehydrogenase OS=Escherichia coli (strain K12) GN=gldA PE=1 SV=1
293	1	5	0.47	0.28	P39173	Putative glucose-6-phosphate 1-epimerase OS=Escherichia coli (strain K12) GN=yeaD PE
294	2	19	0.7	0.95	P0A6X7	Integration host factor subunit alpha OS=Escherichia coli (strain K12) GN=ihfA PE=1 SV=
295	2	4	0.55	1.56	P0A6P5	GTP-binding protein engA OS=Escherichia coli (strain K12) GN=engA PE=3 SV=1
296	2	4	0.45	0.79	P13035	Aerobic glycerol-3-phosphate dehydrogenase OS=Escherichia coli (strain K12) GN=glpD P
297	2	11	0.95	1.26	P63020	Fe/S biogenesis protein nfuA OS=Escherichia coli (strain K12) GN=nfuA PE=1 SV=1
298	1	11	1.12	1.04	P0A763	Nucleoside diphosphate kinase OS=Escherichia coli (strain K12) GN=ndk PE=1 SV=2
299	1	6	1.1	0.23	P68187	Maltose/maltodextrin import ATP-binding protein malK OS=Escherichia coli (strain K12) G
300	1	6	1.22	1.91	P0AA47	Inner membrane transport protein yeeF OS=Escherichia coli (strain K12) GN=yeeF PE=1
301	1	11	0.56	0.5	P0AFK6	Spermidine/putrescine transport system permease protein potC OS=Escherichia coli (stra
302	1	18	0.69	1.23	P0AD10	Uncharacterized protein yecJ OS=Escherichia coli (strain K12) GN=yecJ PE=4 SV=1
303	2	5	0.54	1.07	P0A855	Protein tolB OS=Escherichia coli (strain K12) GN=tolB PE=1 SV=1
304	2	11	0.67	0.83	P0A9M5	Xanthine phosphoribosyltransferase OS=Escherichia coli (strain K12) GN=gpt PE=1 SV=1
305	1	6	0.74	0.85	P0A6N4	Elongation factor P OS=Escherichia coli (strain K12) GN=efp PE=1 SV=2
306	1	4	0.57	0.45	P37095	Peptidase B OS=Escherichia coli (strain K12) GN=pepB PE=1 SV=2
307	2	21	1.11	0.58	P0A6Y1	Integration host factor subunit beta OS=Escherichia coli (strain K12) GN=ihfB PE=1 SV=1
308	2	3	1.24	0.69	P0A7A7	Glycerol-3-phosphate acyltransferase OS=Escherichia coli (strain K12) GN=plsB PE=1 SV
309	2	11	0.63	0.66	P0AF12	5'-methylthioadenosine/S-adenosylhomocysteine nucleosidase OS=Escherichia coli (strai
310	1	5	2.19	0.66	P0C0V0	Protease do OS=Escherichia coli (strain K12) GN=degP PE=1 SV=1
311	2	3	0.86	1.26	P0AAD6	Serine transporter OS=Escherichia coli (strain K12) GN=sdaC PE=1 SV=1
312	2	10	1.23	0.8	P0ADA5	Uncharacterized lipoprotein yajG OS=Escherichia coli (strain K12) GN=yajG PE=4 SV=1
313	1	5	1.62	0.35	P04425	Glutathione synthetase OS=Escherichia coli (strain K12) GN=gshB PE=1 SV=1
314	1	13	1.07	0.89	P0A7G2	Ribosome-binding factor A OS=Escherichia coli (strain K12) GN=rbfA PE=1 SV=2
315	2	4	1.4	0.68	P31979	NADH-quinone oxidoreductase subunit F OS=Escherichia coli (strain K12) GN=nuoF PE=
316	1	7	0.77	0.41	P22524	Chromosome partition protein mukE OS=Escherichia coli (strain K12) GN=mukE PE=1 SV
317	1	10	1.63	0.34	P0A8E7	UPF0234 protein yajQ OS=Escherichia coli (strain K12) GN=yajQ PE=1 SV=2
318	1	5	1.73	10.76	P60752	Lipid A export ATP-binding/permease protein msbA OS=Escherichia coli (strain K12) GN=
319	2	20	0.5	2.12	P68699	ATP synthase subunit c OS=Escherichia coli (strain K12) GN=atpE PE=1 SV=1
320	1	36	0.82	1.39	P0AD24	UPF0352 protein yejL OS=Escherichia coli (strain K12) GN=yejL PE=1 SV=1
321	1	5	1.08	1.26	P0ABD8	Biotin carboxyl carrier protein of acetyl-CoA carboxylase OS=Escherichia coli (strain K12)
322	2	15	1.62	1.31	P0ADK0	Uncharacterized protein yiaF OS=Escherichia coli (strain K12) GN=yiaF PE=4 SV=2
323	2	3	1.47	0.75	P11875	Arginyl-tRNA synthetase OS=Escherichia coli (strain K12) GN=argS PE=1 SV=1
324	1	2	0.93	0.76	P09323	PTS system N-acetylglucosamine-specific EIICBA component OS=Escherichia coli (strain
325	2	16	1.07	0.8	P61316	Outer-membrane lipoprotein carrier protein OS=Escherichia coli (strain K12) GN=lolA PE=

						Outer membrane lipoprotein carrier protein OS=Escherichia coli (strain K12) GN=lolA PE
326	1	13	0.54	0.99	P0ABQ4	Dihydrofolate reductase OS=Escherichia coli (strain K12) GN=folA PE=1 SV=1
327	1	8	0	6.06	P0AAX8	Uncharacterized protein ybiS OS=Escherichia coli (strain K12) GN=ybiS PE=1 SV=1
328	1	3	1.06	0.4	P0AAI3	Cell division protease ftsH OS=Escherichia coli (strain K12) GN=ftsH PE=1 SV=1
329	1	13	1.43	0.79	P0A742	Large-conductance mechanosensitive channel OS=Escherichia coli (strain K12) GN=mscl
330	2	6	0.83	0.58	P69924	Ribonucleoside-diphosphate reductase 1 subunit beta OS=Escherichia coli (strain K12) GI
331	1	8	0.34	0.6	P0AC02	UPF0169 lipoprotein yfiO OS=Escherichia coli (strain K12) GN=yfiO PE=1 SV=1
332	2	9	0.38	0.43	P67910	ADP-L-glycero-D-manno-heptose-6-epimerase OS=Escherichia coli (strain K12) GN=hldD
333	1	9	2.57	0.55	P0AFZ3	Stringent starvation protein B OS=Escherichia coli (strain K12) GN=sspB PE=1 SV=1
334	1	13	0.51	1.02	P0AGK8	HTH-type transcriptional regulator iscR OS=Escherichia coli (strain K12) GN=iscR PE=1 S
335	1	14	1.43	2.91	P0AFY8	Protein seqA OS=Escherichia coli (strain K12) GN=seqA PE=1 SV=1
336	1	11	0.91	0.81	P39177	Universal stress protein G OS=Escherichia coli (strain K12) GN=uspG PE=1 SV=2
337	1	4	0	2.55	P07001	NAD(P) transhydrogenase subunit alpha OS=Escherichia coli (strain K12) GN=pntA PE=1
338	1	20	2.67	3.1	P0A7Q1	50S ribosomal protein L35 OS=Escherichia coli (strain K12) GN=rpmI PE=1 SV=2
339	1	4	0.62	0.5	P26646	Putative quinone oxidoreductase yhdH OS=Escherichia coli (strain K12) GN=yhdH PE=1 S
340	1	2	0.2	0.54	P0A853	Tryptophanase OS=Escherichia coli (strain K12) GN=tnaA PE=1 SV=1
341	1	11	0.69	0.72	P0AC69	Glutaredoxin-4 OS=Escherichia coli (strain K12) GN=grxD PE=1 SV=1
342	1	8	0.59	0.17	P0A8D0	Transcriptional repressor nrdR OS=Escherichia coli (strain K12) GN=nrdR PE=1 SV=1
343	1	4	1.05	0.72	P76116	Uncharacterized protein yncE OS=Escherichia coli (strain K12) GN=yncE PE=1 SV=1
344	1	6	0.52	1.1	P0ADV7	Probable phospholipid-binding protein mlaC OS=Escherichia coli (strain K12) GN=mlaC P
345	1	9	0.8	0.82	P64604	Probable phospholipid ABC transporter-binding protein mlaD OS=Escherichia coli (strain K
346	1	3	1.16	1.15	P02930	Outer membrane protein tolC OS=Escherichia coli (strain K12) GN=tolC PE=1 SV=3
347	1	5	0.72	0.72	P24203	Uncharacterized GTP-binding protein yjiA OS=Escherichia coli (strain K12) GN=yjiA PE=1
348	1	2	0.69	0	P33602	NADH-quinone oxidoreductase subunit G OS=Escherichia coli (strain K12) GN=nuoG PE=
349	1	2	0.66	0.43	P00490	Maltodextrin phosphorylase OS=Escherichia coli (strain K12) GN=malP PE=1 SV=7
350	1	18	0	0.23	P0AFW4	Regulator of nucleoside diphosphate kinase OS=Escherichia coli (strain K12) GN=rnk PE=
351	1	2	0.61	0.7	P76558	NADP-dependent malic enzyme OS=Escherichia coli (strain K12) GN=maeB PE=1 SV=1
352	1	2	1.84	1.6	P0A7I4	Peptide chain release factor 3 OS=Escherichia coli (strain K12) GN=prfC PE=1 SV=2
353	1	8	2	0	P76506	Probable phospholipid-binding lipoprotein mlaA OS=Escherichia coli (strain K12) GN=mlaA
354	1	8	1.42	0.93	P0AGF2	Uncharacterized sufE-like protein ygdK OS=Escherichia coli (strain K12) GN=ygdK PE=1
355	2	6	0.84	0.87	P69786	PTS system glucose-specific EIICB component OS=Escherichia coli (strain K12) GN=pts
356	1	14	0.61	1.23	P0ACE7	HIT-like protein hinT OS=Escherichia coli (strain K12) GN=hinT PE=1 SV=1
357	1	8	0.87	0.73	P0ADZ7	UPF0092 membrane protein yajC OS=Escherichia coli (strain K12) GN=yajC PE=1 SV=1
358	1	3	0.97	1.22	P10384	Long-chain fatty acid transport protein OS=Escherichia coli (strain K12) GN=fadL PE=1 S

						Long chain fatty acid transport protein OS=Escherichia coli (strain K12) GN=fadL PE=1 S
359	2	3	0.41	0.53	P32176	Formate dehydrogenase-O major subunit OS=Escherichia coli (strain K12) GN=fdoG PE=
360	1	5	1.79	1.02	P07913	L-threonine 3-dehydrogenase OS=Escherichia coli (strain K12) GN=tdh PE=1 SV=1
361	1	4	2.24	0.49	P0AGF6	Threonine dehydratase catabolic OS=Escherichia coli (strain K12) GN=tdcB PE=1 SV=1
362	1	2	1.53	0.38	P07363	Chemotaxis protein cheA OS=Escherichia coli (strain K12) GN=cheA PE=1 SV=3
363	1	12	0.7	1.32	P0AEG4	Thiol:disulfide interchange protein dsbA OS=Escherichia coli (strain K12) GN=dsbA PE=1
364	1	8	0.9	0.68	P0AAA1	Inner membrane protein yagU OS=Escherichia coli (strain K12) GN=yagU PE=1 SV=1
365	2	3	0.76	1.16	P15288	Aminoacyl-histidine dipeptidase OS=Escherichia coli (strain K12) GN=pepD PE=1 SV=3
366	1	8	5.26	0.49	P75915	Uncharacterized protein ycdY OS=Escherichia coli (strain K12) GN=ycdY PE=3 SV=1
367	1	6	2.15	3.7	P0AB98	ATP synthase subunit a OS=Escherichia coli (strain K12) GN=atpB PE=1 SV=1
368	1	5	0.94	0.15	P0A8Y5	Phosphatase yidA OS=Escherichia coli (strain K12) GN=yidA PE=1 SV=1
369	1	13	0.69	0.55	P0AD33	UPF0381 protein yfcZ OS=Escherichia coli (strain K12) GN=yfcZ PE=3 SV=1
370	1	7	0.72	0.57	P76290	tRNA (cmo5U34)-methyltransferase OS=Escherichia coli (strain K12) GN=cmoA PE=1 SV
371	1	5	0.64	2.13	P08390	USG-1 protein OS=Escherichia coli (strain K12) GN=usg PE=1 SV=1
372	1	3	0.46	0.97	P0AFK0	Protein pmbA OS=Escherichia coli (strain K12) GN=pmbA PE=1 SV=1
373	1	8	0	0.2	P63417	Uncharacterized N-acetyltransferase yhbS OS=Escherichia coli (strain K12) GN=yhbS PE
374	1	3	1.69	1.3	P07012	Peptide chain release factor 2 OS=Escherichia coli (strain K12) GN=prfB PE=1 SV=3
375	1	2	1	0.73	P16095	L-serine dehydratase 1 OS=Escherichia coli (strain K12) GN=sdaA PE=1 SV=3
376	1	2	0.59	0.54	P77398	Bifunctional polymyxin resistance protein arnA OS=Escherichia coli (strain K12) GN=arnA
377	1	5	0.92	0.58	P39199	Uncharacterized adenine-specific methylase yfcB OS=Escherichia coli (strain K12) GN=yf
378	1	18	0.59	1.08	P0AC62	Glutaredoxin-3 OS=Escherichia coli (strain K12) GN=grxC PE=1 SV=2
379	1	5	2.39	0.24	P0AA16	Transcriptional regulatory protein ompR OS=Escherichia coli (strain K12) GN=ompR PE=1
380	1	11	1.04	0.94	P37903	Universal stress protein F OS=Escherichia coli (strain K12) GN=uspF PE=1 SV=2
381	1	6	0.79	0.65	P0AEQ3	Glutamine-binding periplasmic protein OS=Escherichia coli (strain K12) GN=glnH PE=1 S
382	1	9	0.51	0.54	P0A9L8	Pyrroline-5-carboxylate reductase OS=Escherichia coli (strain K12) GN=proC PE=1 SV=1
383	1	10	0.78	0.3	P69411	Protein rcsF OS=Escherichia coli (strain K12) GN=rcsF PE=4 SV=1
384	1	0	1.79	2.32	P24230	ATP-dependent DNA helicase recG OS=Escherichia coli (strain K12) GN=recG PE=1 SV=
385	1	6	0.77	0.97	P0AG07	Ribulose-phosphate 3-epimerase OS=Escherichia coli (strain K12) GN=rpe PE=1 SV=1
386	1	4	0.9	0.95	P36979	Ribosomal RNA large subunit methyltransferase N OS=Escherichia coli (strain K12) GN=r
387	1	3	0.89	0.93	P09127	Putative uroporphyrinogen-III C-methyltransferase OS=Escherichia coli (strain K12) GN=he
388	1	6	1.88	0.92	P12758	Uridine phosphorylase OS=Escherichia coli (strain K12) GN=udp PE=1 SV=3
389	1	7	1.65	0	P64596	Uncharacterized protein yraP OS=Escherichia coli (strain K12) GN=yraP PE=4 SV=1
390	1	6	0.4	1.53	P37440	Oxidoreductase ucpA OS=Escherichia coli (strain K12) GN=ucpA PE=1 SV=3
391	1	7	1.14	0.52	P0A722	Acyl-[acyl-carrier-protein]--UDP-N-acetylglucosamine O-acyltransferase OS=Escherichia c

Appendix 2-1

N	Unused	%Cov	Avg. H:C 1h	Accession	Name
1	62.6	85.3	1.01	P0A6N1|EFTU_ECOLI	Elongation factor Tu (EF-Tu) (P-43) - Escherichia coli
2	57.6	74.4	0.98	P0A6M8|EFG_ECOLI	Elongation factor G (EF-G) - Escherichia coli
3	51.3	60.7	1.41	P0AFG8|ODP1_ECOLI	Pyruvate dehydrogenase E1 component (EC 1.2.4.1) - Escherichia coli
4	43.1	75.2	1.02	P0AG67|RS1_ECOLI	30S ribosomal protein S1 - Escherichia coli
5	39.6	67.2	1.01	P0A6Y8|DNAK_ECOLI	Chaperone protein dnaK (Heat shock protein 70) (Heat shock 70 kDa protein) (HSP7
6	36.2	41.9	1.02	P0A8T7|RPOC_ECOLI	DNA-directed RNA polymerase beta' chain (EC 2.7.7.6) (RNAP beta' subunit) (Transc
7	36.1	58.4	0.55	P09373|PFLB_ECOLI	Formate acetyltransferase 1 (EC 2.3.1.54) (Pyruvate formate-lyase 1) - Escherichia c
8	32.6	65.3	0.96	P0A6F5|CH60_ECOLI	60 kDa chaperonin (Protein Cpn60) (groEL protein) - Escherichia coli
9	30	72.6	0.99	P0A7L0|RL1_ECOLI	50S ribosomal protein L1 - Escherichia coli
10	29	76.7	0.46	P0A9B2|G3P1_ECOLI	Glyceraldehyde-3-phosphate dehydrogenase A (EC 1.2.1.12) (GAPDH-A) - Escherich
11	28.8	63	0.39	P0AC38|ASPA_ECOLI	Aspartate ammonia-lyase (EC 4.3.1.1) (Aspartase) - Escherichia coli
12	27.4	72.9	0.49	P0A6P9|ENO_ECOLI	Enolase (EC 4.2.1.11) (2-phosphoglycerate dehydratase) (2-phospho-D-glycerate hy
13	26.3	50.5	0.53	P0A9Q7|ADHE_ECOLI	Aldehyde-alcohol dehydrogenase [Includes: Alcohol dehydrogenase (EC 1.1.1.1) (AD
14	25.3	74.3	0.99	P0A7V0|RS2_ECOLI	30S ribosomal protein S2 - Escherichia coli
15	24.8	52.5	0.99	P0A9M8|PTA_ECOLI	Phosphate acetyltransferase (EC 2.3.1.8) (Phosphotransacetylase) - Escherichia coli
16	24.5	76.9	1.52	P0A7Z4|RPOA_ECOLI	DNA-directed RNA polymerase alpha chain (EC 2.7.7.6) (RNAP alpha subunit) (Tran
17	22.9	41.7	1.02	P0A8V2|RPOB_ECOLI	DNA-directed RNA polymerase beta chain (EC 2.7.7.6) (RNAP beta subunit) (Transc
18	22.2	72	1.32	P0A850|TIG_ECOLI	Trigger factor (TF) - Escherichia coli
19	22.1	83.2	0.94	P0A6A3|ACKA_ECOLI	Acetate kinase (EC 2.7.2.1) (Acetokinase) - Escherichia coli
20	21.7	61.1	0.93	P00350|6PGD_ECOLI	6-phosphogluconate dehydrogenase, decarboxylating (EC 1.1.1.44) - Escherichia col
21	21.5	54.5	0.69	P0A799|PGK_ECOLI	Phosphoglycerate kinase (EC 2.7.2.3) - Escherichia coli
22	20.9	83.2	0.97	P60422|RL2_ECOLI	50S ribosomal protein L2 - Escherichia coli
23	17.6	68.9	1.03	P0A6P1|EFTS_ECOLI	Elongation factor Ts (EF-Ts) - Escherichia coli
24	17.2	81.8	2.29	P0A7K2|RL7_ECOLI	50S ribosomal protein L7/L12 (L8) - Escherichia coli
25	16.8	61.5	1.06	P02358|RS6_ECOLI	30S ribosomal protein S6 [Contains: 30S ribosomal protein S6, fully modified isoform;
26	16.8	58.1	0.73	P0AD61|KPYK1_ECOLI	Pyruvate kinase I (EC 2.7.1.40) (PK-1) - Escherichia coli
27	16.5	71.5	1.54	P62399|RL5_ECOLI	50S ribosomal protein L5 - Escherichia coli
28	16.3	57.8	1.01	P0A9P0|DLDH_ECOLI	Dihydrolipoyl dehydrogenase (EC 1.8.1.4) (E3 component of pyruvate and 2-oxoglut

29	16.1	81.9	1.06	P0A7R1|RL9_ECOLI	50S ribosomal protein L9 - Escherichia coli
30	16	53.2	0.95	P0A7D4|PURA_ECOLI	Adenylosuccinate synthetase (EC 6.3.4.4) (IMP--aspartate ligase) (AdSS) (AMPSase
31	15.8	79	0.99	P0A7W1|RS5_ECOLI	30S ribosomal protein S5 - Escherichia coli
32	15.6	42.9	1.04	P0ABB0|ATPA_ECOLI	ATP synthase subunit alpha (EC 3.6.3.14) (ATPase subunit alpha) (ATP synthase F1
33	15.2	60.5	1.05	P0AG55|RL6_ECOLI	50S ribosomal protein L6 - Escherichia coli
34	15.2	60.1	0.98	P0A7V3|RS3_ECOLI	30S ribosomal protein S3 - Escherichia coli
35	14.9	63.1	1.01	P02359|RS7_ECOLI	30S ribosomal protein S7 - Escherichia coli
36	14.7	72.5	1.04	P06959|ODP2_ECOLI	Dihydrolipoyllysine-residue acetyltransferase component of pyruvate dehydrogenase
37	14.5	38.4	1.02	P0AFF6|NUSA_ECOLI	Transcription elongation protein nusA (N utilization substance protein A) (L factor) - E
38	14.5	59.9	0.71	P0AE08|AHPC_ECOLI	Alkyl hydroperoxide reductase subunit C (EC 1.11.1.15) (Peroxiredoxin) (Thioredoxin
39	14.2	69.5	0.98	P0A7S9|RS13_ECOLI	30S ribosomal protein S13 - Escherichia coli
40	14.1	89.3	2.03	P0A862|TPX_ECOLI	Thiol peroxidase (EC 1.11.1.-) (Scavengase P20) - Escherichia coli
41	14.1	34.6	0.92	P15288|PEPD_ECOLI	Aminoacyl-histidine dipeptidase (EC 3.4.13.3) (Xaa-His dipeptidase) (X-His dipeptida
42	13.8	53	0.93	P17169|GLMS_ECOLI	Glucosamine--fructose-6-phosphate aminotransferase [isomerizing] (EC 2.6.1.16) (He
43	13.7	63.1	1.02	P0A7V8|RS4_ECOLI	30S ribosomal protein S4 - Escherichia coli
44	13.5	54.6	0.97	P0A7W7|RS8_ECOLI	30S ribosomal protein S8 - Escherichia coli
45	13.3	48.7	1.03	P0ABB4|ATPB_ECOLI	ATP synthase subunit beta (EC 3.6.3.14) (ATPase subunit beta) (ATP synthase F1 s
46	13.1	45.5	1.02	P0A9P6|DEAD_ECOLI	Cold-shock DEAD box protein A (EC 3.6.1.-) (ATP-dependent RNA helicase deaD) -
47	13.1	80.9	1.00	P60438|RL3_ECOLI	50S ribosomal protein L3 - Escherichia coli
48	12.2	72.2	0.93	P0A7A9|IPYR_ECOLI	Inorganic pyrophosphatase (EC 3.6.1.1) (Pyrophosphate phospho-hydrolase) (PPase
49	12.1	72.9	1.31	P02413|RL15_ECOLI	50S ribosomal protein L15 - Escherichia coli
50	12.1	69.1	0.92	P0AB71|ALF_ECOLI	Fructose-bisphosphate aldolase class 2 (EC 4.1.2.13) (Fructose-bisphosphate aldola
51	11.6	73.2	1.03	P0AA10|RL13_ECOLI	50S ribosomal protein L13 - Escherichia coli
52	11.1	61.7	1.06	P60723|RL4_ECOLI	50S ribosomal protein L4 - Escherichia coli
53	11	71.8	0.95	P61175|RL22_ECOLI	50S ribosomal protein L22 - Escherichia coli
54	11	52.1	0.99	P16659|SYP_ECOLI	Prolyl-tRNA synthetase (EC 6.1.1.15) (Proline--tRNA ligase) (ProRS) (Global RNA sy
55	10.8	32.6	0.99	P0AGD3|SODF_ECOLI	Superoxide dismutase [Fe] (EC 1.15.1.1) - Escherichia coli
56	10.7	49.1	0.93	P0A7J3|RL10_ECOLI	50S ribosomal protein L10 (50S ribosomal protein L8) - Escherichia coli
57	10.6	45.2	0.94	P0ABP8|DEOD_ECOLI	Purine nucleoside phosphorylase deoD-type (EC 2.4.2.1) (PNP) (Inosine phosphoryla
58	10.4	48.6	1.09	P0A870|TALB_ECOLI	Transaldolase B (EC 2.2.1.2) - Escherichia coli
59	10.4	63.9	0.90	P69783|PTGA_ECOLI	Glucose-specific phosphotransferase enzyme IIA component (EC 2.7.1.-) (PTS syste
60	10.4	48.8	0.97	P0A910|OMPA_ECOLI	Outer membrane protein A precursor (Outer membrane protein II*) - Escherichia coli

61	10.2	62.1	1.03	P0A7R5|RS10_ECOLI	30S ribosomal protein S10 - Escherichia coli
62	10.2	48.7	0.95	P0A825|GLYA_ECOLI	Serine hydroxymethyltransferase (EC 2.1.2.1) (Serine methylase) (SHMT) - Escherich
63	10	47.8	0.99	P0ADY7|RL16_ECOLI	50S ribosomal protein L16 - Escherichia coli
64	9.8	66.7	1.05	P0A7R9|RS11_ECOLI	30S ribosomal protein S11 - Escherichia coli
65	9.7	78.8	0.98	P60624|RL24_ECOLI	50S ribosomal protein L24 - Escherichia coli
66	9.6	46.2	1.02	P0A705|IF2_ECOLI	Translation initiation factor IF-2 - Escherichia coli
67	9.4	50	1.01	P0A7U3|RS19_ECOLI	30S ribosomal protein S19 - Escherichia coli
68	9.4	57.7	1.66	P0A7J7|RL11_ECOLI	50S ribosomal protein L11 - Escherichia coli
69	8.7	34.7	0.96	P05055|PNP_ECOLI	Polyribonucleotide nucleotidyltransferase (EC 2.7.7.8) (Polynucleotide phosphorylase
70	8.7	84.6	1.00	P0ABA0|ATPF_ECOLI	ATP synthase B chain (EC 3.6.3.14) - Escherichia coli
71	8.5	63.4	0.94	P0ADY3|RL14_ECOLI	50S ribosomal protein L14 - Escherichia coli
72	8.3	85.4	1.06	P0A7T3|RS16_ECOLI	30S ribosomal protein S16 - Escherichia coli
73	8.2	53.7	1.05	P45523|FKBA_ECOLI	FKBP-type peptidyl-prolyl cis-trans isomerase fkpA precursor (EC 5.2.1.8) (PPIase) (I
74	8.2	78.9	0.96	P0ACF0|DBHA_ECOLI	DNA-binding protein HU-alpha (NS2) (HU-2) - Escherichia coli
75	8.1	51.8	1.06	P0ACF8|HNS_ECOLI	DNA-binding protein H-NS (Histone-like protein HLP-II) (Protein H1) (Protein B1) - Es
76	8.1	56.1	0.91	P61889|MDH_ECOLI	Malate dehydrogenase (EC 1.1.1.37) - Escherichia coli
77	8.1	34.7	1.14	P36683|ACON2_ECOLI	Aconitate hydratase 2 (EC 4.2.1.3) (Citrate hydro-lyase 2) (Aconitase 2) - Escherichia
78	8	46.3	1.00	P0A8N3|SYK1_ECOLI	Lysyl-tRNA synthetase (EC 6.1.1.6) (Lysine--tRNA ligase) (LysRS) - Escherichia coli
79	8	37.9	0.98	P0A7S3|RS12_ECOLI	30S ribosomal protein S12 - Escherichia coli
80	8	27.6	0.98	P22259|PPCK_ECOLI	Phosphoenolpyruvate carboxykinase [ATP] (EC 4.1.1.49) (PEP carboxykinase) (Phos
81	8	38.5	1.02	P0A817|METK_ECOLI	S-adenosylmethionine synthetase (EC 2.5.1.6) (Methionine adenosyltransferase) (Ad
82	8	22.2	1.06	P32132|TYPA_ECOLI	GTP-binding protein typA/BipA (Tyrosine phosphorylated protein A) - Escherichia coli
83	8	36.6	1.02	P0AEK4|FABI_ECOLI	Enoyl-[acyl-carrier-protein] reductase [NADH] (EC 1.3.1.9) (NADH-dependent enoyl-A
84	7.7	28.8	0.94	P0A6T1|G6PI_ECOLI	Glucose-6-phosphate isomerase (EC 5.3.1.9) (GPI) (Phosphoglucose isomerase) (PG
85	7.2	55	0.97	P0AA25|THIO_ECOLI	Thioredoxin 1 (TRX1) (TRX) - Escherichia coli
86	7.2	41.1	0.93	P35340|AHPF_ECOLI	Alkyl hydroperoxide reductase subunit F (EC 1.6.4.-) (Alkyl hydroperoxide reductase
87	7.1	53.9	0.96	P0A7K6|RL19_ECOLI	50S ribosomal protein L19 - Escherichia coli
88	7	73.2	1.01	P0AG44|RL17_ECOLI	50S ribosomal protein L17 - Escherichia coli
89	6.9	73.2	1.01	P0A6F9|CH10_ECOLI	10 kDa chaperonin (Protein Cpn10) (groES protein) - Escherichia coli
90	6.6	31.4	1.00	P0A6Z3|HTPG_ECOLI	Chaperone protein htpG (Heat shock protein htpG) (High temperature protein G) (Hea
91	6.5	78.3	0.96	P0A9Y6|CSPC_ECOLI	Cold shock-like protein cspC (CSP-C) - Escherichia coli
92	6.3	68.1	0.98	P0A972|CSPE_ECOLI	Cold shock-like protein cspE (CSP-E) - Escherichia coli

93	6	25.9	1.06	P04805|SYE_ECOLI	Glutamyl-tRNA synthetase (EC 6.1.1.17) (Glutamate--tRNA ligase) (GluRS) - Escheri
94	6	27	0.98	P07395|SYFB_ECOLI	Phenylalanyl-tRNA synthetase beta chain (EC 6.1.1.20) (Phenylalanine--tRNA ligase
95	6	47	0.97	P0A717|KPRS_ECOLI	Ribose-phosphate pyrophosphokinase (EC 2.7.6.1) (RPPK) (Phosphoribosyl pyropho
96	6	37.8	0.86	P68066|GRCA_ECOLI	Autonomous glycyl radical cofactor - Escherichia coli
97	6	41.5	0.88	P27302|TKT1_ECOLI	Transketolase 1 (EC 2.2.1.1) (TK 1) - Escherichia coli
98	6	19.7	1.00	P00957|SYA_ECOLI	Alanyl-tRNA synthetase (EC 6.1.1.7) (Alanine--tRNA ligase) (AlaRS) - Escherichia co
99	6	45	1.00	P0AAI5|FABF_ECOLI	3-oxoacyl-[acyl-carrier-protein] synthase 2 (EC 2.3.1.41) (3-oxoacyl-[acyl-carrier-prote
100	6	20.7	1.05	P08200|IDH_ECOLI	Isocitrate dehydrogenase [NADP] (EC 1.1.1.42) (Oxalosuccinate decarboxylase) (IDH
101	6	53.8	0.99	P69776|LPP_ECOLI	Major outer membrane lipoprotein precursor (Murein-lipoprotein) - Escherichia coli
102	6	28.4	0.99	P61949|FLAV_ECOLI	Flavodoxin-1 - Escherichia coli
103	6	18.1	1.07	P09424|MTLD_ECOLI	Mannitol-1-phosphate 5-dehydrogenase (EC 1.1.1.17) - Escherichia coli
104	5.8	35.4	0.95	P00956|SYI_ECOLI	Isoleucyl-tRNA synthetase (EC 6.1.1.5) (Isoleucine--tRNA ligase) (IleRS) - Escherichi
105	5.6	69.2	1.03	P0A763|NDK_ECOLI	Nucleoside diphosphate kinase (EC 2.7.4.6) (NDK) (NDP kinase) (Nucleoside-2-P kir
106	5.5	82	1.41	P0ADZ4|RS15_ECOLI	30S ribosomal protein S15 - Escherichia coli
107	5.4	81.5	0.96	P0A7X3|RS9_ECOLI	30S ribosomal protein S9 - Escherichia coli
108	5.4	79.4	1.42	P0A7M6|RL29_ECOLI	50S ribosomal protein L29 - Escherichia coli
109	5.4	29.7	0.87	P0A6K6|DEOB_ECOLI	Phosphopentomutase (EC 5.4.2.7) (Phosphodeoxyribomutase) - Escherichia coli
110	5.3	56.2	1.04	P0A9D8|DAPD_ECOLI	2,3,4,5-tetrahydropyridine-2,6-dicarboxylate N-succinyltransferase (EC 2.3.1.117) (Te
111	5.2	69.2	1.05	P61714|RISB_ECOLI	6,7-dimethyl-8-ribityllumazine synthase (EC 2.5.1.9) (DMRL synthase) (Lumazine syr
112	5.2	56.4	1.03	P0C018|RL18_ECOLI	50S ribosomal protein L18 - Escherichia coli
113	5.2	67.8	1.02	P69441|KAD_ECOLI	Adenylate kinase (EC 2.7.4.3) (ATP-AMP transphosphorylase) (AK) - Escherichia col
114	5.2	30.8	1.00	P0A6Y5|HSLO_ECOLI	33 kDa chaperonin (Heat shock protein 33) (HSP33) - Escherichia coli
115	5.1	27.5	1.03	P0A6B7|ISCS_ECOLI	Cysteine desulfurase (EC 2.8.1.7) (Thil transpersulfidase) (NifS protein homolog) - Es
116	5	51.5	1.07	P0AG48|RL21_ECOLI	50S ribosomal protein L21 - Escherichia coli
117	5	27.7	0.89	P0AES4|GYRA_ECOLI	DNA gyrase subunit A (EC 5.99.1.3) - Escherichia coli
118	4.9	89.7	1.06	P0A7M2|RL28_ECOLI	50S ribosomal protein L28 - Escherichia coli
119	4.8	53.4	0.94	P0A7L3|RL20_ECOLI	50S ribosomal protein L20 - Escherichia coli
120	4.8	58.6	0.87	P0A7U7|RS20_ECOLI	30S ribosomal protein S20 - Escherichia coli
121	4.8	37.8	1.02	P23869|PPIB_ECOLI	Peptidyl-prolyl cis-trans isomerase B (EC 5.2.1.8) (PPIase B) (Rotamase B) - Escheri
122	4.7	37.9	0.98	P0AAI9|FABD_ECOLI	Malonyl CoA-acyl carrier protein transacylase (EC 2.3.1.39) (MCT) - Escherichia coli
123	4.7	39.4	0.87	P0A9A6|FTSZ_ECOLI	Cell division protein ftsZ - Escherichia coli
124	4.7	42.5	0.89	P0A6L0|DEOC_ECOLI	Deoxyribose-phosphate aldolase (EC 4.1.2.4) (Phosphodeoxyriboaldolase) (Deoxyrib

125	4.7	40.5	0.89	P36938|PGM_ECOLI	Phosphoglucomutase (EC 5.4.2.2) (Glucose phosphomutase) (PGM) - Escherichia co
126	4.7	44.8	1.01	P0ACA3|SSPA_ECOLI	Stringent starvation protein A - Escherichia coli
127	4.5	32.5	0.98	P13029|CATA_ECOLI	Peroxidase/catalase HPI (EC 1.11.1.6) (Catalase-peroxidase) (Hydroperoxidase I) - E
128	4.5	35	1.04	P00363|FRDA_ECOLI	Fumarate reductase flavoprotein subunit (EC 1.3.99.1) - Escherichia coli
129	4.4	41.6	1.00	P62707|GPMA_ECOLI	2,3-bisphosphoglycerate-dependent phosphoglycerate mutase (EC 5.4.2.1) (Phospho
130	4.4	30.8	1.03	P07813|SYL_ECOLI	Leucyl-tRNA synthetase (EC 6.1.1.4) (Leucine--tRNA ligase) (LeuRS) - Escherichia c
131	4.4	61.4	0.91	P0A9X9|CSPA_ECOLI	Cold shock protein cspA (CSP-A) (7.4 kDa cold shock protein) (CS7.4) - Escherichia
132	4.4	25	1.06	P60240|RAPA_ECOLI	RNA polymerase-associated protein rapA (EC 3.6.1.-) (ATP-dependent helicase hepA
133	4.4	28.8	0.97	P37689|GPMI_ECOLI	2,3-bisphosphoglycerate-independent phosphoglycerate mutase (EC 5.4.2.1) (Phosp
134	4.3	45.5	0.95	P0A9P4|TRXB_ECOLI	Thioredoxin reductase (EC 1.8.1.9) (TRXR) - Escherichia coli
135	4.3	31.2	0.98	P0A8M3|SYT_ECOLI	Threonyl-tRNA synthetase (EC 6.1.1.3) (Threonine--tRNA ligase) (ThrRS) - Escherich
136	4.2	45.1	0.86	P0A858|TPIS_ECOLI	Triosephosphate isomerase (EC 5.3.1.1) (TIM) (Triose-phosphate isomerase) - Esche
137	4.2	21.5	1.06	P0AGE9|SUCD_ECOLI	Succinyl-CoA ligase [ADP-forming] subunit alpha (EC 6.2.1.5) (Succinyl-CoA synthet
138	4.2	53.1	1.01	P0AF36|YIIU_ECOLI	Hypothetical protein yiiU - Escherichia coli
139	4.1	42.2	0.94	P63224|GMHA_ECOLI	Phosphoheptose isomerase (EC 5.3.1.-) (Sedoheptulose 7-phosphate isomerase) - E
140	4.1	37.7	0.95	P24175|MANB_ECOLI	Phosphomannomutase (EC 5.4.2.8) (PMM) - Escherichia coli
141	4.1	27.2	1.00	P21170|SPEA_ECOLI	Biosynthetic arginine decarboxylase (EC 4.1.1.19) (ADC) - Escherichia coli
142	4.1	74.5	1.06	P0AG99|SECG_ECOLI	Protein-export membrane protein secG (Preprotein translocase band 1 subunit) (P12)
143	4.1	25.8	0.92	P0A8L1|SYS_ECOLI	Seryl-tRNA synthetase (EC 6.1.1.11) (Serine--tRNA ligase) (SerRS) - Escherichia col
144	4	64.3	1.06	P0A7M9|RL31_ECOLI	50S ribosomal protein L31 - Escherichia coli
145	4	11.9	1.07	P0ABI8|CYOB_ECOLI	Ubiquinol oxidase subunit 1 (EC 1.10.3.-) (Ubiquinol oxidase polypeptide I) (Cytochro
146	4	24.1	0.90	P12758|UDP_ECOLI	Uridine phosphorylase (EC 2.4.2.3) (UrdPase) (UPase) - Escherichia coli
147	4	25.3	0.91	P76558|MAO2_ECOLI	NADP-dependent malic enzyme (EC 1.1.1.40) (NADP-ME) - Escherichia coli
148	4	29.1	0.96	P42632|TDCE_ECOLI	Keto-acid formate acetyltransferase (EC 2.3.1.-) (Keto-acid formate-lyase) - Escherich
149	4	21.2	1.02	P00579|RPOD_ECOLI	RNA polymerase sigma factor rpoD (Sigma-70) - Escherichia coli
150	4	21.7	1.08	P04079|GUAA_ECOLI	GMP synthase [glutamine-hydrolyzing] (EC 6.3.5.2) (Glutamine amidotransferase) (G
151	4	13.5	0.89	P10408|SECA_ECOLI	Preprotein translocase secA subunit - Escherichia coli
152	4	44.5	1.07	P0ABD5|ACCA_ECOLI	Acetyl-coenzyme A carboxylase carboxyl transferase subunit alpha (EC 6.4.1.2) (Ace
153	4	41.3	1.06	P0A8F0|UPP_ECOLI	Uracil phosphoribosyltransferase (EC 2.4.2.9) (UMP pyrophosphorylase) (UPRTase)
154	4	35.1	0.94	P0A836|SUCC_ECOLI	Succinyl-CoA synthetase beta chain (EC 6.2.1.5) (SCS-beta) - Escherichia coli
155	4	20.1	1.00	P36672|PTTBC_ECOLI	PTS system trehalose-specific EIIBC component (EIIBC-Tre) (EII-Tre) [Includes: Treh
156	4	20.4	1.12	P21888|SYC_ECOLI	Cysteinyl-tRNA synthetase (EC 6.1.1.16) (Cysteine--tRNA ligase) (CysRS) - Escherich

157	4	29.1	0.97	P14176|PROW_ECOLI	Glycine betaine/L-proline transport system permease protein proW - Escherichia coli
158	4	23.5	1.00	P0AAD6|SDAC_ECOLI	Serine transporter - Escherichia coli
159	4	27.3	1.06	P61517|CAN_ECOLI	Carbonic anhydrase 2 (EC 4.2.1.1) - Escherichia coli
160	4	19.4	0.97	P0AEX9|MALE_ECOLI	Maltose-binding periplasmic protein precursor (Maltodextrin-binding protein) (MMBP)
161	4	17.3	1.00	P0ABH7|CISY_ECOLI	Citrate synthase (EC 2.3.3.1) - Escherichia coli
162	4	20.4	0.95	P09147|GALE_ECOLI	UDP-glucose 4-epimerase (EC 5.1.3.2) (Galactowaldenase) (UDP-galactose 4-epime
163	4	40.9	1.08	P45578|LUXS_ECOLI	S-ribosylhomocysteine lyase (EC 4.4.1.21) (Autoinducer-2 production protein luxS) (A
164	4	39.1	1.04	P0ABD8|BCCP_ECOLI	Biotin carboxyl carrier protein of acetyl-CoA carboxylase (BCCP) - Escherichia coli
165	4	69.4	0.92	P0AA04|PTHP_ECOLI	Phosphocarrier protein HPr (Histidine-containing protein) - Escherichia coli
166	4	26.8	1.08	P68679|RS21_ECOLI	30S ribosomal protein S21 - Escherichia coli
167	4	66	1.03	P0AGK4|YHBY_ECOLI	UPF0044 protein yhbY - Escherichia coli
168	4	41.7	1.04	P0AG63|RS17_ECOLI	30S ribosomal protein S17 - Escherichia coli
169	4	30.9	1.04	P0A7N9|RL33_ECOLI	50S ribosomal protein L33 - Escherichia coli
170	4	26.1	1.06	P0A6N4|EFP_ECOLI	Elongation factor P (EF-P) - Escherichia coli
171	4	22.6	0.99	P0AG86|SECB_ECOLI	Protein-export protein secB - Escherichia coli
172	4	7.9	1.09	P0A953|FABB_ECOLI	3-oxoacyl-[acyl-carrier-protein] synthase 1 (EC 2.3.1.41) (3-oxoacyl-[acyl-carrier-prote
173	4	29.3	0.96	P0A7T7|RS18_ECOLI	30S ribosomal protein S18 - Escherichia coli
174	4	8.6	0.97	P09148|GAL7_ECOLI	Galactose-1-phosphate uridylyltransferase (EC 2.7.7.12) (Gal-1-P uridylyltransferase)
175	4	42.9	1.04	P0AGJ9|SYY_ECOLI	Tyrosyl-tRNA synthetase (EC 6.1.1.1) (Tyrosine--tRNA ligase) (TyrRS) - Escherichia
176	3.7	34	1.04	P68919|RL25_ECOLI	50S ribosomal protein L25 - Escherichia coli
177	3.7	12.2		P0ABN5|DCUA_ECOLI	Anaerobic C4-dicarboxylate transporter dcuA - Escherichia coli
178	3.6	34	1.02	P0A9X4|MREB_ECOLI	Rod shape-determining protein mreB - Escherichia coli
179	3.6	36.6	0.96	P0AG59|RS14_ECOLI	30S ribosomal protein S14 - Escherichia coli
180	3.5	34.6	1.07	P0A8A0|YEBC_ECOLI	UPF0082 protein yebC - Escherichia coli
181	3.5	40.2	1.00	P33232|LLDD_ECOLI	L-lactate dehydrogenase [cytochrome] (EC 1.1.2.3) - Escherichia coli
182	3.5	24.1	1.02	P38521|YGGL_ECOLI	Hypothetical protein yggL - Escherichia coli
183	3.5	22	1.09	P0ADZ0|RL23_ECOLI	50S ribosomal protein L23 - Escherichia coli
184	3.5	24.2	0.98	P00452|RIR1_ECOLI	Ribonucleoside-diphosphate reductase 1 subunit alpha (EC 1.17.4.1) (Ribonucleoside
185	3.4	34.5	0.92	P0A998|FTNA_ECOLI	Ferritin-1 (EC 1.16.3.1) - Escherichia coli
186	3.4	23.1	1.06	P21889|SYD_ECOLI	Aspartyl-tRNA synthetase (EC 6.1.1.12) (Aspartate--tRNA ligase) (AspRS) - Escheric
187	3.3	35.9	0.88	P0A853|TNAA_ECOLI	Tryptophanase (EC 4.1.99.1) (L-tryptophan indole-lyase) (TNase) - Escherichia coli
188	3.3	64.4	0.93	P0ACF4|DBHB_ECOLI	DNA-binding protein HU-beta (NS1) (HU-1) - Escherichia coli

189	3.3	28.9	1.05	P0AFD1|NUOE_ECOLI	NADH-quinone oxidoreductase chain E (EC 1.6.99.5) (NADH dehydrogenase I, chain
190	3.3	47	1.07	P0A805|RRF_ECOLI	Ribosome recycling factor (Ribosome-releasing factor) (RRF) - Escherichia coli
191	3.2	20.7	1.08	P68767|AMPA_ECOLI	Cytosol aminopeptidase (EC 3.4.11.1) (Leucine aminopeptidase) (LAP) (Leucyl amino
192	3.2	17.4	1.01	P0ADG7|IMDH_ECOLI	Inosine-5'-monophosphate dehydrogenase (EC 1.1.1.205) (IMP dehydrogenase) (IMP
193	3.1	29.4	1.00	P0AG30|RHO_ECOLI	Transcription termination factor rho (EC 3.6.1.-) (ATP-dependent helicase rho) - Esch
194	3.1	50.4	1.04	P0AD49|RAIA_ECOLI	Ribosome-associated inhibitor A (Protein Y) (SpotY) (pY) - Escherichia coli
195	3.1	50.5	1.08	P0A9L3|FKBB_ECOLI	FKBP-type 22 kDa peptidyl-prolyl cis-trans isomerase (EC 5.2.1.8) (PPIase) (Rotama
196	3.1	43.7	1.08	P21507|SRMB_ECOLI	ATP-dependent RNA helicase srmB (EC 3.6.1.-) - Escherichia coli
197	3.1	23.4	1.06	P06992|KSGA_ECOLI	Dimethyladenosine transferase (EC 2.1.1.-) (S-adenosylmethionine-6-N', N'-adenosyl
198	2.9	41	1.02	P0A6A8|ACP_ECOLI	Acyl carrier protein (ACP) (Cytosolic-activating factor) (CAF) (Fatty acid synthase acy
199	2.9	46.7	0.97	P0AEK2|FABG_ECOLI	3-oxoacyl-[acyl-carrier-protein] reductase (EC 1.1.1.100) (3-ketoacyl-acyl carrier prote
200	2.8	16.2	0.88	P28904|TREC_ECOLI	Trehalose-6-phosphate hydrolase (EC 3.2.1.93) (Alpha,alpha-phosphotrehalase) - Es
201	2.8	20.4	1.03	P33602|NUOG_ECOLI	NADH-quinone oxidoreductase chain G (EC 1.6.99.5) (NADH dehydrogenase I, chain
202	2.8	29.9	0.88	P0A6F3|GLPK_ECOLI	Glycerol kinase (EC 2.7.1.30) (ATP:glycerol 3-phosphotransferase) (Glycerokinase) (
203	2.8	30	1.09	P11875|SYR_ECOLI	Arginyl-tRNA synthetase (EC 6.1.1.19) (Arginine--tRNA ligase) (ArgRS) - Escherichia
204	2.7	43.9	0.98	P00960|SYGA_ECOLI	Glycyl-tRNA synthetase alpha chain (EC 6.1.1.14) (Glycine--tRNA ligase alpha chain)
205	2.7	6.9	0.93	P69786|PTGCB_ECOLI	PTS system glucose-specific EIICB component (EIICB-Glc) (EII-Glc) [Includes: Glucc
206	2.7	19.9	1.08	P0AEG6|DSBC_ECOLI	Thiol:disulfide interchange protein dsbC precursor - Escherichia coli
207	2.7	30.7	0.90	P0A6D3|AROA_ECOLI	3-phosphoshikimate 1-carboxyvinyltransferase (EC 2.5.1.19) (5-enolpyruvylshikimate
208	2.6	27.1	0.97	P0A715|KDSA_ECOLI	2-dehydro-3-deoxyphosphooctonate aldolase (EC 2.5.1.55) (Phospho-2-dehydro-3-d
209	2.6	31.6	1.06	P0A9M5|XGPT_ECOLI	Xanthine phosphoribosyltransferase (EC 2.4.2.22) (Xanthine-guanine phosphoribosyl
210	2.3	13.8	1.04	P0AFG0|NUSG_ECOLI	Transcription antitermination protein nusG - Escherichia coli
211	2.2	16.9	1.00	P77395|YBBN_ECOLI	Protein ybbN - Escherichia coli
212	2.2	36.8	0.95	P0AGA2|SECY_ECOLI	Preprotein translocase secY subunit - Escherichia coli
213	2.2	20.7	0.89	P0AFJ1|PHNA_ECOLI	Protein phnA - Escherichia coli
214	2.2	28	0.95	P04825|AMPN_ECOLI	Aminopeptidase N (EC 3.4.11.2) (Alpha-aminoacylpeptide hydrolase) - Escherichia c
215	2.2	41.8	1.02	P0A6W5|GREA_ECOLI	Transcription elongation factor greA (Transcript cleavage factor greA) - Escherichia c
216	2.2	21.2	1.09	P0A7L8|RL27_ECOLI	50S ribosomal protein L27 - Escherichia coli
217	2.1	29.6	1.07	P00448|SODM_ECOLI	Superoxide dismutase [Mn] (EC 1.15.1.1) (MnSOD) - Escherichia coli
218	2.1	28.8	1.07	P0AG51|RL30_ECOLI	50S ribosomal protein L30 - Escherichia coli
219	2.1	34.4	0.99	P00490|PHSM_ECOLI	Maltodextrin phosphorylase (EC 2.4.1.1) - Escherichia coli
220	2.1	29.4	1.09	P0A9W3|YJJK_ECOLI	ABC transporter ATP-binding protein yjjK - Escherichia coli

221	2.1	34.3	0.93	P0ABZ6|SURA_ECOLI	Chaperone surA precursor (Peptidyl-prolyl cis-trans isomerase surA) (EC 5.2.1.8) (PF
222	2	29.4	0.94	P0A6Z1|HSCA_ECOLI	Chaperone protein hscA (Hsc66) - Escherichia coli
223	2	56.7	0.97	P0A707|IF3_ECOLI	Translation initiation factor IF-3 [Contains: IF-3L; IF-3S] - Escherichia coli
224	2	35.9	1.03	P0AGF6|THD2_ECOLI	Threonine dehydratase catabolic (EC 4.3.1.19) (Threonine deaminase) - Escherichia
225	2	27.1	0.97	P21599|KPYK2_ECOLI	Pyruvate kinase II (EC 2.7.1.40) (PK-2) - Escherichia coli
226	2	39.4	0.96	P0A9N4|PFLA_ECOLI	Pyruvate formate-lyase 1-activating enzyme (EC 1.97.1.4) (PFL-activating enzyme) (I
227	2	27.8	0.95	P00954|SYW_ECOLI	Tryptophanyl-tRNA synthetase (EC 6.1.1.2) (Tryptophan--tRNA ligase) (TrpRS) - Esc
228	2	31	0.93	P31120|GLMM_ECOLI	Phosphoglucosamine mutase (EC 5.4.2.10) - Escherichia coli
229	2	26.2	0.94	P0ABP3|DCUC_ECOLI	Anaerobic C4-dicarboxylate transporter dcuC - Escherichia coli
230	2	9.9	1.05	P23893|GSA_ECOLI	Glutamate-1-semialdehyde 2,1-aminomutase (EC 5.4.3.8) (GSA) (Glutamate-1-semia
231	2	13.5	1.03	P0A905|SLYB_ECOLI	Outer membrane lipoprotein slyB precursor - Escherichia coli
232	2	22.6	1.07	P0AG90|SECD_ECOLI	Protein-export membrane protein secD - Escherichia coli
233	2	25	1.02	P00959|SYM_ECOLI	Methionyl-tRNA synthetase (EC 6.1.1.10) (Methionine--tRNA ligase) (MetRS) - Esche
234	2	30.8	0.91	P63284|CLPB_ECOLI	Chaperone clpB (Heat-shock protein F84.1) - Escherichia coli
235	2	28.7	0.87	P0A9M0|LON_ECOLI	ATP-dependent protease La (EC 3.4.21.53) - Escherichia coli
236	2	25	0.98	P00864|CAPP_ECOLI	Phosphoenolpyruvate carboxylase (EC 4.1.1.31) (PEPCase) (PEPC) - Escherichia co
237	2	22.4	0.91	P21499|RNR_ECOLI	Ribonuclease R (EC 3.1.-.-) (RNase R) (Protein vacB) - Escherichia coli
238	2	29.9	1.04	P60785|LEPA_ECOLI	GTP-binding protein lepA - Escherichia coli
239	2	25	1.00	P39396|YJIY_ECOLI	Inner membrane protein yjiY - Escherichia coli
240	2	38.8	1.04	P21165|PEPQ_ECOLI	Xaa-Pro dipeptidase (EC 3.4.13.9) (X-Pro dipeptidase) (Proline dipeptidase) (Prolidas
241	2	15.9	1.02	P07118|SYV_ECOLI	Valyl-tRNA synthetase (EC 6.1.1.9) (Valine--tRNA ligase) (ValRS) - Escherichia coli
242	2	23.9	1.00	P43672|UUP_ECOLI	ABC transporter ATP-binding protein uup - Escherichia coli
243	2	22.4	0.93	P33363|BGLX_ECOLI	Periplasmic beta-glucosidase precursor (EC 3.2.1.21) (Gentiobiase) (Cellobiase) (Bet
244	2	32.8	1.05	P25888|RHLE_ECOLI	Putative ATP-dependent RNA helicase rhlE (EC 3.6.1.-) - Escherichia coli
245	2	34.2	1.03	P0AB77|KBL_ECOLI	2-amino-3-ketobutyrate coenzyme A ligase (EC 2.3.1.29) (AKB ligase) (Glycine acety
246	2	57.4	1.04	P0A8E7|YAJQ_ECOLI	UPF0234 protein yajQ - Escherichia coli
247	2	39.9	0.99	P0ADR8|YGDH_ECOLI	Hypothetical protein ygdH - Escherichia coli
248	2	59.6	0.87	P0ACY1|YDJA_ECOLI	Protein ydjA - Escherichia coli
249	2	16.5	0.85	P08201|NIRB_ECOLI	Nitrite reductase [NAD(P)H] large subunit (EC 1.7.1.4) - Escherichia coli
250	2	43.6	0.94	P07012|RF2_ECOLI	Peptide chain release factor 2 (RF-2) - Escherichia coli
251	2	23.1	0.94	P60716|LIPA_ECOLI	Lipoyl synthase (EC 2.8.1.-) (Lipoic acid synthase) (Lipoate synthase) (Lipoyl-acyl-ca
252	2	31.7	0.91	P0AFF2|NUPC_ECOLI	Nucleoside permease nupC (Nucleoside-transport system protein nupC) - Escherichi

253	2	15.8	1.01	P0AEI1|YLEA_ECOLI	UPF0004 protein yleA - Escherichia coli
254	2	78	1.04	P0A8B5|YBAB_ECOLI	UPF0133 protein ybaB - Escherichia coli
255	2	34	1.04	P75949|NAGZ_ECOLI	Beta-hexosaminidase (EC 3.2.1.52) (N-acetyl-beta-glucosaminidase) (Beta-N-acetylh
256	2	16.9	0.93	P75867|LONH_ECOLI	Putative protease La homolog (EC 3.4.21.-) - Escherichia coli
257	2	46.9	0.89	P69805|PTND_ECOLI	Mannose permease IID component (PTS system mannose-specific EIID component)
258	2	60.7	0.94	P0AGE0|SSB_ECOLI	Single-stranded DNA-binding protein (SSB) (Helix-destabilizing protein) - Escherichia
259	2	36.6	0.96	P0AEU7|SKP_ECOLI	Chaperone protein skp precursor (Seventeen kilodalton protein) (Histone-like protein
260	2	29.3	0.93	P0AEG4|DSBA_ECOLI	Thiol:disulfide interchange protein dsbA precursor - Escherichia coli
261	2	27.1	0.96	P0AAD8|TDCC_ECOLI	Threonine/serine transporter - Escherichia coli
262	2	19.7	1.02	P0A8J8|RHLB_ECOLI	ATP-dependent RNA helicase rhlB (EC 3.6.1.-) - Escherichia coli
263	2	26.1	1.08	P69811|PTFAH_ECOLI	Multiphosphoryl transfer protein (MTP) (Phosphotransferase FPr protein) (Pseudo-HF
264	2	24	1.08	P33025|YEIN_ECOLI	Hypothetical protein yeiN - Escherichia coli
265	2	26.2		P0AC13|DHPS_ECOLI	Dihydropteroate synthase (EC 2.5.1.15) (DHPS) (Dihydropteroate pyrophosphorylase
266	2	22.8	0.95	P0ABT2|DPS_ECOLI	DNA protection during starvation protein (EC 1.16.-.-) - Escherichia coli
267	2	45.3		P0A738|MOAC_ECOLI	Molybdenum cofactor biosynthesis protein C - Escherichia coli
268	2	29.7	0.89	P0A6T5|GCH1_ECOLI	GTP cyclohydrolase I (EC 3.5.4.16) (GTP-CH-I) - Escherichia coli
269	2	11.3	1.03	P08312|SYFA_ECOLI	Phenylalanyl-tRNA synthetase alpha chain (EC 6.1.1.20) (Phenylalanine--tRNA ligase
270	2	46.6	1.07	P63020|GNTY_ECOLI	Protein gntY - Escherichia coli
271	2	13.3	0.93	P37773|MPL_ECOLI	UDP-N-acetylmuramate:L-alanyl-gamma-D-glutamyl-meso-diaminopimelate ligase (E
272	2	21.6	0.94	P30177|YBIB_ECOLI	Hypothetical protein ybiB - Escherichia coli
273	2	26	1.04	P0AER0|GLPF_ECOLI	Glycerol uptake facilitator protein (Aquaglyceroporin) - Escherichia coli
274	2	45.9	1.04	P0AD59|IVY_ECOLI	Inhibitor of vertebrate lysozyme precursor - Escherichia coli
275	2	11.4	0.91	P0ACC7|GLMU_ECOLI	Bifunctional protein glmU [Includes: UDP-N-acetylglucosamine pyrophosphorylase (E
276	2	57.8	1.01	P0AC62|GLRX3_ECOLI	Glutaredoxin-3 (Grx3) - Escherichia coli
277	2	15	0.90	P0AAJ5|FDOH_ECOLI	Formate dehydrogenase-O, iron-sulfur subunit (Formate dehydrogenase-O subunit be
277	0	18.7		P0AAJ3|FDNH_ECOLI	Formate dehydrogenase, nitrate-inducible, iron-sulfur subunit (Formate dehydrogenas
278	2	24.1	0.98	P0A9Z1|GLNB_ECOLI	Nitrogen regulatory protein P-II 1 - Escherichia coli
279	2	18.8	0.94	P0A9S5|GLDA_ECOLI	Glycerol dehydrogenase (EC 1.1.1.6) (GLDH) - Escherichia coli
280	2	37.9	0.87	P0A9L8|P5CR_ECOLI	Pyrroline-5-carboxylate reductase (EC 1.5.1.2) (P5CR) (P5C reductase) - Escherichia
281	2	21.6	1.01	P0A7F6|SPED_ECOLI	S-adenosylmethionine decarboxylase proenzyme (EC 4.1.1.50) (AdoMetDC) (SamDC
282	2	20.3	0.81	P0A796|K6PF1_ECOLI	6-phosphofructokinase isozyme 1 (EC 2.7.1.11) (6-phosphofructokinase isozyme I) (F
283	2	21.8	0.90	P09372|GRPE_ECOLI	Protein grpE (HSP-70 cofactor) (Heat shock protein B25.3) (HSP24) - Escherichia col

284	2	17.1	0.95	P08244|PYRF_ECOLI	Orotidine 5'-phosphate decarboxylase (EC 4.1.1.23) (OMP decarboxylase) (OMPDCa
285	2	25.6	1.01	P07014|DHSB_ECOLI	Succinate dehydrogenase iron-sulfur protein (EC 1.3.99.1) - Escherichia coli
286	2	16.2	0.96	P02925|RBSB_ECOLI	D-ribose-binding periplasmic protein precursor - Escherichia coli
287	2	17.3	0.85	P60844|AQPZ_ECOLI	Aquaporin Z (Bacterial nodulin-like intrinsic protein) - Escherichia coli
288	2	9.4	1.03	P0AFQ7|YCFH_ECOLI	Putative deoxyribonuclease ycfH (EC 3.1.21.-) - Escherichia coli
289	2	23.5		P0AF40|YIJD_ECOLI	Inner membrane protein yijD - Escherichia coli
290	2	16	0.95	P0AD33|YFCZ_ECOLI	UPF0381 protein yfcZ - Escherichia coli
291	2	13.7	0.95	P0ABK2|CYDB_ECOLI	Cytochrome d ubiquinol oxidase subunit 2 (EC 1.10.3.-) (Cytochrome d ubiquinol oxic
292	2	26.6	1.09	P0A6G7|CLPP_ECOLI	ATP-dependent Clp protease proteolytic subunit precursor (EC 3.4.21.92) (Endopepti
293	2	13.8	1.07	P62617|ISPF_ECOLI	2-C-methyl-D-erythritol 2,4-cyclodiphosphate synthase (EC 4.6.1.12) (MECPS) (MEC
294	2	8.3	1.06	P37666|TKRA_ECOLI	2-ketogluconate reductase (EC 1.1.1.215) (2KR) (2-ketoaldonate reductase) - Escher
295	2	7	0.93	P0AFM2|PROX_ECOLI	Glycine betaine-binding periplasmic protein precursor - Escherichia coli
296	2	16	0.95	P0ACV8|YMJA_ECOLI	Hypothetical protein ymjA - Escherichia coli
297	2	10.5	1.05	P0ACC3|YADR_ECOLI	Hypothetical protein yadR - Escherichia coli
298	2	11.3	1.08	P0AC69|YDHD_ECOLI	Probable monothiol glutaredoxin ydhD - Escherichia coli
299	2	17.5	1.04	P0A7N4|RL32_ECOLI	50S ribosomal protein L32 - Escherichia coli
300	2	7.6	1.04	P0A722|LPXA_ECOLI	Acyl-[acyl-carrier-protein]--UDP-N-acetylglucosamine O-acyltransferase (EC 2.3.1.12
301	2	7.5	1.03	P0AA39|RLUC_ECOLI	Ribosomal large subunit pseudouridine synthase C (EC 5.4.99.-) (rRNA-uridine isome
302	2	36.2	0.94	P00805|ASPG2_ECOLI	L-asparaginase 2 precursor (EC 3.5.1.1) (L-asparaginase II) (L-asparagine amidohyd
303	2	25.1	1.03	P0A6H5|HSLU_ECOLI	ATP-dependent hsl protease ATP-binding subunit hslU (Heat shock protein hslU) - Es
304	2	17.2	0.87	P20966|PTFBC_ECOLI	PTS system fructose-specific EIIBC component (EIIBC-Fru) [Includes: Fructose-spec
305	2	48.1	1.03	P0A7E9|PYRH_ECOLI	Uridylate kinase (EC 2.7.4.-) (UK) (Uridine monophosphate kinase) (UMP kinase) - Es
306	2	35.1	1.01	P0ABS1|DKSA_ECOLI	DnaK suppressor protein - Escherichia coli
307	2	12.8	1.03	P0A6I0|KCY_ECOLI	Cytidylate kinase (EC 2.7.4.14) (CK) (Cytidine monophosphate kinase) (CMP kinase)
308	2	25.2	0.98	P24182|ACCC_ECOLI	Biotin carboxylase (EC 6.3.4.14) (Acetyl-CoA carboxylase subunit A) (EC 6.4.1.2) (AC
309	2	23.1	1.08	P69924|RIR2_ECOLI	Ribonucleoside-diphosphate reductase 1 subunit beta (EC 1.17.4.1) (Ribonucleotide
310	2	21.1	0.92	P0AF08|MRP_ECOLI	Protein mrp - Escherichia coli
311	2	59.4	1.00	P0AF93|YJGF_ECOLI	UPF0076 protein yjgF - Escherichia coli
312	2	42.8	0.93	P0ABQ4|DYR_ECOLI	Dihydrofolate reductase (EC 1.5.1.3) - Escherichia coli
313	2	27.5	1.07	P0A832|SSRP_ECOLI	SsrA-binding protein (Small protein B) - Escherichia coli

Appendix 2-2

N	Unused	%Cov	Avg. H:C 2h	Accession	Name
1	89.9	85.3	1.21	P0A6N1|EFTU_ECOLI	Elongation factor Tu (EF-Tu) (P-43) - Escherichia coli
2	62.2	61.2	0.50	P09373|PFLB_ECOLI	Formate acetyltransferase 1 (EC 2.3.1.54) (Pyruvate formate-lyase 1) - E
3	62.1	69.3	1.03	P0A6M8|EFG_ECOLI	Elongation factor G (EF-G) - Escherichia coli
4	61.9	70.0	1.25	P0AFG8|ODP1_ECOLI	Pyruvate dehydrogenase E1 component (EC 1.2.4.1) - Escherichia coli
5	52.6	71.5	1.31	P0AG67|RS1_ECOLI	30S ribosomal protein S1 - Escherichia coli
6	46.2	74.8	0.98	P0A6F5|CH60_ECOLI	60 kDa chaperonin (Protein Cpn60) (groEL protein) - Escherichia coli
7	45.9	45.6	1.09	P0A8T7|RPOC_ECOLI	DNA-directed RNA polymerase beta' chain (EC 2.7.7.6) (RNAP beta' sub
8	45.8	64.1	0.97	P0A6Y8|DNAK_ECOLI	Chaperone protein dnaK (Heat shock protein 70) (Heat shock 70 kDa prc
9	45.2	60.5	0.62	P0A9Q7|ADHE_ECOLI	Aldehyde-alcohol dehydrogenase [Includes: Alcohol dehydrogenase (EC
10	44.8	48.1	1.02	P0A8V2|RPOB_ECOLI	DNA-directed RNA polymerase beta chain (EC 2.7.7.6) (RNAP beta subu
11	37.3	78.1	1.08	P06959|ODP2_ECOLI	Dihydrolipoyllysine-residue acetyltransferase component of pyruvate deh
12	37.1	65.7	0.91	P0AC38|ASPA_ECOLI	Aspartate ammonia-lyase (EC 4.3.1.1) (Aspartase) - Escherichia coli
13	35.6	78.2	0.35	P0A9B2|G3P1_ECOLI	Glyceraldehyde-3-phosphate dehydrogenase A (EC 1.2.1.12) (GAPDH-A
14	35.2	75.7	0.45	P0A6P9|ENO_ECOLI	Enolase (EC 4.2.1.11) (2-phosphoglycerate dehydratase) (2-phospho-D-g
15	32.4	58.2	1.06	P0A9P0|DLDH_ECOLI	Dihydrolipoyl dehydrogenase (EC 1.8.1.4) (E3 component of pyruvate an
16	30.6	66.7	0.73	P0A799|PGK_ECOLI	Phosphoglycerate kinase (EC 2.7.2.3) - Escherichia coli
17	29.4	68.1	1.07	P0A7Z4|RPOA_ECOLI	DNA-directed RNA polymerase alpha chain (EC 2.7.7.6) (RNAP alpha su
18	29.3	85.0	1.35	P0A7L0|RL1_ECOLI	50S ribosomal protein L1 - Escherichia coli
19	27.4	66.4	1.04	P0A850|TIG_ECOLI	Trigger factor (TF) - Escherichia coli
20	26.5	55.4	0.73	P0A853|TNAA_ECOLI	Tryptophanase (EC 4.1.99.1) (L-tryptophan indole-lyase) (TNase) - Esch
21	26.4	46.1	0.49	P42632|TDCE_ECOLI	Keto-acid formate acetyltransferase (EC 2.3.1.-) (Keto-acid formate-lyase
22	26.4	51.5	0.61	P0A9M8|PTA_ECOLI	Phosphate acetyltransferase (EC 2.3.1.8) (Phosphotransacetylase) - Esc
23	26.0	60.6	1.04	P0A7D4|PURA_ECOLI	Adenylosuccinate synthetase (EC 6.3.4.4) (IMP--aspartate ligase) (AdSS
24	25.7	54.1	1.01	P0ABB4|ATPB_ECOLI	ATP synthase subunit beta (EC 3.6.3.14) (ATPase subunit beta) (ATP sy
25	24.7	42.5	1.81	P36683|ACON2_ECOLI	Aconitate hydratase 2 (EC 4.2.1.3) (Citrate hydro-lyase 2) (Aconitase 2) -
26	24.7	83.8	1.04	P0A7V0|RS2_ECOLI	30S ribosomal protein S2 - Escherichia coli
27	24.7	72.8	1.40	P0A6P1|EFTS_ECOLI	Elongation factor Ts (EF-Ts) - Escherichia coli
28	24.3	67.5	0.67	P0A6A3|ACKA_ECOLI	Acetate kinase (EC 2.7.2.1) (Acetokinase) - Escherichia coli

29	23.7	62.6	1.00	P00350|6PGD_ECOLI	6-phosphogluconate dehydrogenase, decarboxylating (EC 1.1.1.44) - Es
30	22.8	70.1	1.03	P0A7W1|RS5_ECOLI	30S ribosomal protein S5 - Escherichia coli
31	22.6	39.7	0.90	P0A6Z3|HTPG_ECOLI	Chaperone protein htpG (Heat shock protein htpG) (High temperature pr
32	22.4	56.4	2.04	P62399|RL5_ECOLI	50S ribosomal protein L5 - Escherichia coli
33	22.2	59.6	1.04	P61889|MDH_ECOLI	Malate dehydrogenase (EC 1.1.1.37) - Escherichia coli
34	22.0	42.0	1.00	P0AG30|RHO_ECOLI	Transcription termination factor rho (EC 3.6.1.-) (ATP-dependent helicase
35	22.0	44.2	1.62	P08200|IDH_ECOLI	Isocitrate dehydrogenase [NADP] (EC 1.1.1.42) (Oxalosuccinate decarbo
36	21.2	61.5	1.28	P60422|RL2_ECOLI	50S ribosomal protein L2 - Escherichia coli
37	20.1	75.4	0.44	P0AE08|AHPC_ECOLI	Alkyl hydroperoxide reductase subunit C (EC 1.11.1.15) (Peroxiredoxin) (
38	19.7	54.5	1.43	P0A7V3|RS3_ECOLI	30S ribosomal protein S3 - Escherichia coli
39	19.4	90.9	1.05	P0A7K2|RL7_ECOLI	50S ribosomal protein L7/L12 (L8) - Escherichia coli
40	18.6	41.0	1.01	P13029|CATA_ECOLI	Peroxidase/catalase HPI (EC 1.11.1.6) (Catalase-peroxidase) (Hydroper
41	18.5	38.4	1.01	P0ABB0|ATPA_ECOLI	ATP synthase subunit alpha (EC 3.6.3.14) (ATPase subunit alpha) (ATP
42	18.3	77.7	1.31	P02359|RS7_ECOLI	30S ribosomal protein S7 - Escherichia coli
43	17.5	32.7	0.94	P0A8N5|SYK2_ECOLI	Lysyl-tRNA synthetase, heat inducible (EC 6.1.1.6) (Lysine--tRNA ligase)
44	17.4	63.2	0.71	P0AD61|KPYK1_ECOLI	Pyruvate kinase I (EC 2.7.1.40) (PK-1) - Escherichia coli
45	17.3	79.8	0.97	P0AGD3|SODF_ECOLI	Superoxide dismutase [Fe] (EC 1.15.1.1) - Escherichia coli
46	17.1	86.6	1.03	P0A7R1|RL9_ECOLI	50S ribosomal protein L9 - Escherichia coli
47	17.0	41.6	0.98	P0A8L1|SYS_ECOLI	Seryl-tRNA synthetase (EC 6.1.1.11) (Serine--tRNA ligase) (SerRS) - Es
48	16.7	46.3	1.02	P0AFF6|NUSA_ECOLI	Transcription elongation protein nusA (N utilization substance protein A) (
49	16.2	41.9	0.88	P22259|PPCK_ECOLI	Phosphoenolpyruvate carboxykinase [ATP] (EC 4.1.1.49) (PEP carboxyk
50	16.2	48.2	0.89	P63284|CLPB_ECOLI	Chaperone clpB (Heat-shock protein F84.1) - Escherichia coli
51	16.1	40.8	1.09	P05055|PNP_ECOLI	Polyribonucleotide nucleotidyltransferase (EC 2.7.7.8) (Polynucleotide ph
52	16.1	40.2	1.03	P17169|GLMS_ECOLI	Glucosamine--fructose-6-phosphate aminotransferase [isomerizing] (EC
53	16.0	38.3	0.62	P0A6T1|G6PI_ECOLI	Glucose-6-phosphate isomerase (EC 5.3.1.9) (GPI) (Phosphoglucose isc
54	15.7	63.0	1.00	P02358|RS6_ECOLI	30S ribosomal protein S6 [Contains: 30S ribosomal protein S6, fully modi
55	15.2	42.2	0.89	P0AGF6|THD2_ECOLI	Threonine dehydratase catabolic (EC 4.3.1.19) (Threonine deaminase) -
56	14.2	54.6	0.92	P0AB71|ALF_ECOLI	Fructose-bisphosphate aldolase class 2 (EC 4.1.2.13) (Fructose-bisphos
57	14.1	37.1	1.02	P04079|GUAA_ECOLI	GMP synthase [glutamine-hydrolyzing] (EC 6.3.5.2) (Glutamine amidotra
58	14.0	34.1	0.90	P27302|TKT1_ECOLI	Transketolase 1 (EC 2.2.1.1) (TK 1) - Escherichia coli
59	14.0	47.3	1.07	P0AEK4|FABI_ECOLI	Enoyl-[acyl-carrier-protein] reductase [NADH] (EC 1.3.1.9) (NADH-depen
60	13.7	62.1	1.02	P0AG55|RL6_ECOLI	50S ribosomal protein L6 - Escherichia coli

61	13.6	51.9	1.07	P0A7V8|RS4_ECOLI	30S ribosomal protein S4 - Escherichia coli
62	13.5	43.9	0.50	P15288|PEPD_ECOLI	Aminoacyl-histidine dipeptidase (EC 3.4.13.3) (Xaa-His dipeptidase) (X-H
63	13.3	34.6	1.00	P00957|SYA_ECOLI	Alanyl-tRNA synthetase (EC 6.1.1.7) (Alanine--tRNA ligase) (AlaRS) - Es
64	13.3	45.4	2.09	P0AFG6|ODO2_ECOLI	Dihydrolipoyllysine-residue succinyltransferase component of 2-oxoglutar
65	13.1	86.6	0.95	P68066|GRCA_ECOLI	Autonomous glycyl radical cofactor - Escherichia coli
66	13.0	58.9	1.76	P0A862|TPX_ECOLI	Thiol peroxidase (EC 1.11.1.-) (Scavengase P20) - Escherichia coli
67	12.9	76.4	1.06	P61175|RL22_ECOLI	50S ribosomal protein L22 - Escherichia coli
68	12.7	41.4	0.90	P14407|FUMB_ECOLI	Fumarate hydratase class I, anaerobic (EC 4.2.1.2) (Fumarase) - Escher
69	12.6	50.0	1.06	P0A7U3|RS19_ECOLI	30S ribosomal protein S19 - Escherichia coli
70	12.5	56.8	0.98	P69783|PTGA_ECOLI	Glucose-specific phosphotransferase enzyme IIA component (EC 2.7.1.-)
71	12.5	28.2	1.03	P07118|SYV_ECOLI	Valyl-tRNA synthetase (EC 6.1.1.9) (Valine--tRNA ligase) (ValRS) - Esch
72	12.4	51.4	1.01	P16659|SYP_ECOLI	Prolyl-tRNA synthetase (EC 6.1.1.15) (Proline--tRNA ligase) (ProRS) (Gl
73	12.3	43.6	1.01	P62707|GPMA_ECOLI	2,3-bisphosphoglycerate-dependent phosphoglycerate mutase (EC 5.4.2
74	12.2	37.8	0.92	P0A817|METK_ECOLI	S-adenosylmethionine synthetase (EC 2.5.1.6) (Methionine adenosyltran
75	12.1	90.0	0.98	P0ACF0|DBHA_ECOLI	DNA-binding protein HU-alpha (NS2) (HU-2) - Escherichia coli
76	12.0	61.8	1.02	P02413|RL15_ECOLI	50S ribosomal protein L15 - Escherichia coli
77	12.0	58.5	1.02	P0A7S9|RS13_ECOLI	30S ribosomal protein S13 - Escherichia coli
78	12.0	74.3	1.01	P0ADY7|RL16_ECOLI	50S ribosomal protein L16 - Escherichia coli
79	12.0	47.3	0.99	P0A7J3|RL10_ECOLI	50S ribosomal protein L10 (50S ribosomal protein L8) - Escherichia coli
80	12.0	27.9	0.99	P0A9M0|LON_ECOLI	ATP-dependent protease La (EC 3.4.21.53) - Escherichia coli
81	11.9	69.7	1.05	P60723|RL4_ECOLI	50S ribosomal protein L4 - Escherichia coli
82	11.7	31.9	1.04	P00961|SYGB_ECOLI	Glycyl-tRNA synthetase beta chain (EC 6.1.1.14) (Glycine--tRNA ligase b
83	11.7	35.6	0.91	P21599|KPYK2_ECOLI	Pyruvate kinase II (EC 2.7.1.40) (PK-2) - Escherichia coli
84	11.5	45.2	0.88	P0AEX9|MALE_ECOLI	Maltose-binding periplasmic protein precursor (Maltodextrin-binding prote
85	11.3	42.6	1.02	P0A9A6|FTSZ_ECOLI	Cell division protein ftsZ - Escherichia coli
86	11.1	44.3	1.04	P0A7K6|RL19_ECOLI	50S ribosomal protein L19 - Escherichia coli
87	11.1	36.7	0.98	P0A953|FABB_ECOLI	3-oxoacyl-[acyl-carrier-protein] synthase 1 (EC 2.3.1.41) (3-oxoacyl-[acyl-
88	11.0	60.8	1.08	P60438|RL3_ECOLI	50S ribosomal protein L3 - Escherichia coli
89	10.9	69.7	1.06	P0AA10|RL13_ECOLI	50S ribosomal protein L13 - Escherichia coli
90	10.9	41.0	0.96	P0A910|OMPA_ECOLI	Outer membrane protein A precursor (Outer membrane protein II*) - Esch
91	10.4	39.0	0.70	P35340|AHPF_ECOLI	Alkyl hydroperoxide reductase subunit F (EC 1.6.4.-) (Alkyl hydroperoxide
92	10.2	31.1	1.04	P0A6F3|GLPK_ECOLI	Glycerol kinase (EC 2.7.1.30) (ATP:glycerol 3-phosphotransferase) (Glyc

93	10.2	36.2	0.52	P00805|ASPG2_ECOLI	L-asparaginase 2 precursor (EC 3.5.1.1) (L-asparaginase II) (L-asparagir
94	10.1	38.5	1.01	P0AES4|GYRA_ECOLI	DNA gyrase subunit A (EC 5.99.1.3) - Escherichia coli
95	10.0	24.7	0.88	P37689|GPMI_ECOLI	2,3-bisphosphoglycerate-independent phosphoglycerate mutase (EC 5.4
96	10.0	40.1	0.86	P0A6L4|NANA_ECOLI	N-acetylneuraminate lyase (EC 4.1.3.3) (N-acetylneuraminic acid aldolas
97	10.0	51.9	0.96	P0ACA3|SSPA_ECOLI	Stringent starvation protein A - Escherichia coli
98	10.0	28.8	1.00	P0AFM2|PROX_ECOLI	Glycine betaine-binding periplasmic protein precursor - Escherichia coli
99	10.0	31.9	1.04	P07395|SYFB_ECOLI	Phenylalanyl-tRNA synthetase beta chain (EC 6.1.1.20) (Phenylalanine--
100	9.7	33.5	1.04	P23538|PPSA_ECOLI	Phosphoenolpyruvate synthase (EC 2.7.9.2) (Pyruvate, water dikinase) (I
101	9.7	38.8	1.00	P0A870|TALB_ECOLI	Transaldolase B (EC 2.2.1.2) - Escherichia coli
102	9.6	44.2	1.09	P60624|RL24_ECOLI	50S ribosomal protein L24 - Escherichia coli
103	9.5	17.9	0.91	P0A6K6|DEOB_ECOLI	Phosphopentomutase (EC 5.4.2.7) (Phosphodeoxyribomutase) - Escheri
104	9.4	47.9	1.05	P0A7J7|RL11_ECOLI	50S ribosomal protein L11 - Escherichia coli
105	9.3	38.7	0.92	P0A9D8|DAPD_ECOLI	2,3,4,5-tetrahydropyridine-2,6-dicarboxylate N-succinyltransferase (EC 2.
106	9.1	35.2	0.87	P09147|GALE_ECOLI	UDP-glucose 4-epimerase (EC 5.1.3.2) (Galactowaldenase) (UDP-galact
107	9.1	65.4	1.02	P0A7W7|RS8_ECOLI	30S ribosomal protein S8 - Escherichia coli
108	9.0	54.7	1.01	P0ACF8|HNS_ECOLI	DNA-binding protein H-NS (Histone-like protein HLP-II) (Protein H1) (Pro
109	8.9	55.3	1.02	P0A7R5|RS10_ECOLI	30S ribosomal protein S10 - Escherichia coli
110	8.9	63.0	0.93	P45523|FKBA_ECOLI	FKBP-type peptidyl-prolyl cis-trans isomerase fkpA precursor (EC 5.2.1.8
111	8.7	49.8	0.47	P0A858|TPIS_ECOLI	Triosephosphate isomerase (EC 5.3.1.1) (TIM) (Triose-phosphate isomer
112	8.7	29.1	0.28	P0A9H3|LDCI_ECOLI	Lysine decarboxylase, inducible (EC 4.1.1.18) (LDC) - Escherichia coli
113	8.5	22.5	1.05	P21889|SYD_ECOLI	Aspartyl-tRNA synthetase (EC 6.1.1.12) (Aspartate--tRNA ligase) (AspRS
114	8.4	57.3	1.01	P0A7T3|RS16_ECOLI	30S ribosomal protein S16 - Escherichia coli
115	8.4	33.1	0.87	P0ABP8|DEOD_ECOLI	Purine nucleoside phosphorylase deoD-type (EC 2.4.2.1) (PNP) (Inosine
116	8.2	74.8	1.08	P0AG44|RL17_ECOLI	50S ribosomal protein L17 - Escherichia coli
117	8.1	31.7	1.00	P23869|PPIB_ECOLI	Peptidyl-prolyl cis-trans isomerase B (EC 5.2.1.8) (PPIase B) (Rotamase
118	8.1	65.0	1.01	P0A707|IF3_ECOLI	Translation initiation factor IF-3 [Contains: IF-3L; IF-3S] - Escherichia coli
119	8.1	27.8	0.97	P08312|SYFA_ECOLI	Phenylalanyl-tRNA synthetase alpha chain (EC 6.1.1.20) (Phenylalanine-
120	8.1	55.0	0.93	P0AA25|THIO_ECOLI	Thioredoxin 1 (TRX1) (TRX) - Escherichia coli
121	8.1	63.1	1.01	P0A7X3|RS9_ECOLI	30S ribosomal protein S9 - Escherichia coli
122	8.1	78.3	0.95	P0A9Y6|CSPC_ECOLI	Cold shock-like protein cspC (CSP-C) - Escherichia coli
123	8.1	32.7	1.01	P04805|SYE_ECOLI	Glutamyl-tRNA synthetase (EC 6.1.1.17) (Glutamate--tRNA ligase) (GluR
124	8.0	44.9	1.00	P0A805|RRF_ECOLI	Ribosome recycling factor (Ribosome-releasing factor) (RRF) - Escherich

125	8.0	37.4	1.00	P0AGE9|SUCD_ECOLI	Succinyl-CoA ligase [ADP-forming] subunit alpha (EC 6.2.1.5) (Succinyl-(
126	8.0	50.0	0.86	P0AF93|YJGF_ECOLI	UPF0076 protein yjgF - Escherichia coli
127	8.0	52.8	0.93	P0ADY3|RL14_ECOLI	50S ribosomal protein L14 - Escherichia coli
128	8.0	32.8	0.89	P0AC47|FRDB_ECOLI	Fumarate reductase iron-sulfur protein (EC 1.3.99.1) - Escherichia coli
129	8.0	23.7	0.89	P09394|GLPQ_ECOLI	Glycerophosphoryl diester phosphodiesterase precursor (EC 3.1.4.46) (G
130	8.0	41.9	0.98	P0A7S3|RS12_ECOLI	30S ribosomal protein S12 - Escherichia coli
131	7.9	18.0	0.93	P0A9S5|GLDA_ECOLI	Glycerol dehydrogenase (EC 1.1.1.6) (GLDH) - Escherichia coli
132	7.7	27.9	0.94	P28904|TREC_ECOLI	Trehalose-6-phosphate hydrolase (EC 3.2.1.93) (Alpha,alpha-phosphotre
133	7.7	50.0	1.08	P0A993|F16P_ECOLI	Fructose-1,6-bisphosphatase (EC 3.1.3.11) (D-fructose-1,6-bisphosphate
134	7.7	30.2	0.87	P0A8M3|SYT_ECOLI	Threonyl-tRNA synthetase (EC 6.1.1.3) (Threonine--tRNA ligase) (ThrRS
135	7.5	78.3	1.07	P0A972|CSPE_ECOLI	Cold shock-like protein cspE (CSP-E) - Escherichia coli
136	7.5	59.6	0.93	P0A8M6|YEEX_ECOLI	UPF0265 protein yeeX - Escherichia coli
137	7.4	32.2	1.06	P0A705|IF2_ECOLI	Translation initiation factor IF-2 - Escherichia coli
138	7.4	22.6	1.06	P21170|SPEA_ECOLI	Biosynthetic arginine decarboxylase (EC 4.1.1.19) (ADC) - Escherichia c(
139	7.4	79.3	1.08	P0A7U7|RS20_ECOLI	30S ribosomal protein S20 - Escherichia coli
140	7.4	61.1	0.90	P0ACF4|DBHB_ECOLI	DNA-binding protein HU-beta (NS1) (HU-1) - Escherichia coli
141	7.3	56.2	1.00	P0A717|KPRS_ECOLI	Ribose-phosphate pyrophosphokinase (EC 2.7.6.1) (RPPK) (Phosphorib(
142	7.3	74.6	1.09	P0A7M6|RL29_ECOLI	50S ribosomal protein L29 - Escherichia coli
143	7.2	42.6	1.02	P0AEK2|FABG_ECOLI	3-oxoacyl-[acyl-carrier-protein] reductase (EC 1.1.1.100) (3-ketoacyl-acyl
144	7.2	51.2	1.07	P0ADG7|IMDH_ECOLI	Inosine-5'-monophosphate dehydrogenase (EC 1.1.1.205) (IMP dehydrog
145	7.2	28.1	1.05	P0AFG3|ODO1_ECOLI	2-oxoglutarate dehydrogenase E1 component (EC 1.2.4.2) (Alpha-ketogl
146	7.2	24.5	1.03	P0A9C5|GLNA_ECOLI	Glutamine synthetase (EC 6.3.1.2) (Glutamate--ammonia ligase) - Esche
147	7.1	42.0	1.03	P0ABD5|ACCA_ECOLI	Acetyl-coenzyme A carboxylase carboxyl transferase subunit alpha (EC 6
148	7.1	47.3	0.99	P0A998|FTNA_ECOLI	Ferritin-1 (EC 1.16.3.1) - Escherichia coli
149	7.0	55.8	1.01	P0A7R9|RS11_ECOLI	30S ribosomal protein S11 - Escherichia coli
150	7.0	32.2	1.01	P69441|KAD_ECOLI	Adenylate kinase (EC 2.7.4.3) (ATP-AMP transphosphorylase) (AK) - Esc
151	7.0	64.9	0.99	P0ACG1|STPA_ECOLI	DNA-binding protein stpA (H-NS homolog stpA) - Escherichia coli
152	6.9	37.2	1.07	P36672|PTTBC_ECOLI	PTS system trehalose-specific EIIBC component (EIIBC-Tre) (EII-Tre) [In
153	6.9	38.5	0.92	P63224|GMHA_ECOLI	Phosphoheptose isomerase (EC 5.3.1.-) (Sedoheptulose 7-phosphate isc
154	6.9	47.9	1.08	P0A836|SUCC_ECOLI	Succinyl-CoA synthetase beta chain (EC 6.2.1.5) (SCS-beta) - Escherich
155	6.9	34.4	0.87	P12758|UDP_ECOLI	Uridine phosphorylase (EC 2.4.2.3) (UrdPase) (UPase) - Escherichia coli
156	6.8	28.4	0.97	P0AG86|SECB_ECOLI	Protein-export protein secB - Escherichia coli

157	6.8	16.3	1.03	P00363|FRDA_ECOLI	Fumarate reductase flavoprotein subunit (EC 1.3.99.1) - Escherichia coli
158	6.8	25.2	1.01	P21513|RNE_ECOLI	Ribonuclease E (EC 3.1.4.-) (RNase E) - Escherichia coli
159	6.6	42.0	0.98	P0A825|GLYA_ECOLI	Serine hydroxymethyltransferase (EC 2.1.2.1) (Serine methylase) (SHMT
160	6.5	45.2	0.96	P36938|PGM_ECOLI	Phosphoglucomutase (EC 5.4.2.2) (Glucose phosphomutase) (PGM) - Es
161	6.4	36.9	1.06	P31979|NUOF_ECOLI	NADH-quinone oxidoreductase chain F (EC 1.6.99.5) (NADH dehydroger
162	6.4	31.7	0.98	P0ABT2|DPS_ECOLI	DNA protection during starvation protein (EC 1.16.-.-) - Escherichia coli
163	6.2	45.6	1.04	P0AEQ3|GLNH_ECOLI	Glutamine-binding periplasmic protein precursor (GlnBP) - Escherichia co
164	6.2	25.2	1.03	P0A9P4|TRXB_ECOLI	Thioredoxin reductase (EC 1.8.1.9) (TRXR) - Escherichia coli
165	6.2	60.8	2.92	P0A763|NDK_ECOLI	Nucleoside diphosphate kinase (EC 2.7.4.6) (NDK) (NDP kinase) (Nucleo
166	6.1	29.2	0.37	P33025|YEIN_ECOLI	Hypothetical protein yeiN - Escherichia coli
167	6.0	17.2	1.00	P0A7E5|PYRG_ECOLI	CTP synthase (EC 6.3.4.2) (UTP--ammonia ligase) (CTP synthetase) - E
168	6.0	28.4	1.03	P0A794|PDXJ_ECOLI	Pyridoxal phosphate biosynthetic protein pdxJ (PNP synthase) - Escheric
169	6.0	30.6	0.89	P0A715|KDSA_ECOLI	2-dehydro-3-deoxyphosphooctonate aldolase (EC 2.5.1.55) (Phospho-2-d
170	6.0	34.0	1.01	P33602|NUOG_ECOLI	NADH-quinone oxidoreductase chain G (EC 1.6.99.5) (NADH dehydroge
171	6.0	31.6	1.04	P10408|SECA_ECOLI	Preprotein translocase secA subunit - Escherichia coli
172	6.0	16.2	0.89	P33195|GCSP_ECOLI	Glycine dehydrogenase [decarboxylating] (EC 1.4.4.2) (Glycine decarbox
173	6.0	21.2	0.99	P00579|RPOD_ECOLI	RNA polymerase sigma factor rpoD (Sigma-70) - Escherichia coli
174	6.0	32.8	1.07	P0ABU2|ENGD_ECOLI	GTP-dependent nucleic acid-binding protein engD - Escherichia coli
175	6.0	29.0	1.00	P0ABH7|CISY_ECOLI	Citrate synthase (EC 2.3.3.1) - Escherichia coli
176	6.0	32.2	1.06	P0A8F0|UPP_ECOLI	Uracil phosphoribosyltransferase (EC 2.4.2.9) (UMP pyrophosphorylase)
177	6.0	42.7	1.05	P45578|LUXS_ECOLI	S-ribosylhomocysteine lyase (EC 4.4.1.21) (Autoinducer-2 production pro
178	6.0	19.9	0.91	P11868|TDCD_ECOLI	Propionate kinase (EC 2.7.2.15) - Escherichia coli
179	6.0	50.4	0.99	P0AD49|RAIA_ECOLI	Ribosome-associated inhibitor A (Protein Y) (SpotY) (pY) - Escherichia co
180	6.0	34.3	0.99	P0A8E7|YAJQ_ECOLI	UPF0234 protein yajQ - Escherichia coli
181	6.0	33.3	0.96	P0A6A8|ACP_ECOLI	Acyl carrier protein (ACP) (Cytosolic-activating factor) (CAF) (Fatty acid s
182	6.0	41.0	0.91	P61714|RISB_ECOLI	6,7-dimethyl-8-ribityllumazine synthase (EC 2.5.1.9) (DMRL synthase) (L
183	6.0	13.4	1.04	P21888|SYC_ECOLI	Cysteinyl-tRNA synthetase (EC 6.1.1.16) (Cysteine--tRNA ligase) (CysRS
184	6.0	17.1	1.01	P0ACJ8|CRP_ECOLI	Catabolite gene activator (cAMP receptor protein) (cAMP-regulatory prote
185	6.0	30.7	1.04	P0AAI9|FABD_ECOLI	Malonyl CoA-acyl carrier protein transacylase (EC 2.3.1.39) (MCT) - Escl
186	6.0	29.1	1.07	P0A9L3|FKBB_ECOLI	FKBP-type 22 kDa peptidyl-prolyl cis-trans isomerase (EC 5.2.1.8) (PPIas
187	6.0	62.9	0.95	P0A6F9|CH10_ECOLI	10 kDa chaperonin (Protein Cpn10) (groES protein) - Escherichia coli
188	5.9	57.9	0.94	P0A6B7|ISCS_ECOLI	Cysteine desulfurase (EC 2.8.1.7) (Thil transpersulfidase) (NifS protein h

189	5.7	46.6	0.95	P0A7L3|RL20_ECOLI	50S ribosomal protein L20 - Escherichia coli
190	5.7	19.7	1.04	P33599|NUOCD_ECOLI	NADH-quinone oxidoreductase chain C/D (EC 1.6.99.5) (NADH dehydro
191	5.7	27.8	1.04	P77395|YBBN_ECOLI	Protein ybbN - Escherichia coli
192	5.5	17.7	1.00	P00962|SYQ_ECOLI	Glutaminyl-tRNA synthetase (EC 6.1.1.18) (Glutamine--tRNA ligase) (Glr
193	5.4	40.0	1.03	P0A7T7|RS18_ECOLI	30S ribosomal protein S18 - Escherichia coli
194	5.4	34.1	0.99	P0AES6|GYRB_ECOLI	DNA gyrase subunit B (EC 5.99.1.3) - Escherichia coli
195	5.4	31.9	0.99	P0ABU0|MENB_ECOLI	Naphthoate synthase (EC 4.1.3.36) (Dihydroxynaphthoic acid synthetase
196	5.4	29.5	1.02	P0A6Y5|HSLO_ECOLI	33 kDa chaperonin (Heat shock protein 33) (HSP33) - Escherichia coli
197	5.3	20.8	0.98	P0AGJ9|SYY_ECOLI	Tyrosyl-tRNA synthetase (EC 6.1.1.1) (Tyrosine--tRNA ligase) (TyrRS) -
198	5.2	35.2	0.94	P0A7A9|IPYR_ECOLI	Inorganic pyrophosphatase (EC 3.6.1.1) (Pyrophosphate phospho-hydrol
199	5.2	22.3	0.92	P77318|YDEN_ECOLI	Putative sulfatase ydeN precursor (EC 3.1.6.-) - Escherichia coli
200	5.1	33.1	0.90	P00509|AAT_ECOLI	Aspartate aminotransferase (EC 2.6.1.1) (Transaminase A) (ASPAT) - Es
201	5.0	21.1	1.08	P00959|SYM_ECOLI	Methionyl-tRNA synthetase (EC 6.1.1.10) (Methionine--tRNA ligase) (Me
202	5.0	30.2	1.05	P0AFK9|POTD_ECOLI	Spermidine/putrescine-binding periplasmic protein precursor (SPBP) - Es
203	4.9	41.8	1.08	P0AAC0|USPE_ECOLI	Universal stress protein E - Escherichia coli
204	4.9	39.6	1.08	P60906|SYH_ECOLI	Histidyl-tRNA synthetase (EC 6.1.1.21) (Histidine--tRNA ligase) (HisRS) -
205	4.8	21.1	1.05	P0A9W3|YJJK_ECOLI	ABC transporter ATP-binding protein yjjK - Escherichia coli
206	4.8	24.8	0.93	P0AEU7|SKP_ECOLI	Chaperone protein skp precursor (Seventeen kilodalton protein) (Histone
207	4.6	24.5	0.94	P27248|GCST_ECOLI	Aminomethyltransferase (EC 2.1.2.10) (Glycine cleavage system T protei
208	4.6	58.1	0.90	P0AGL2|TDCF_ECOLI	Protein tdcF - Escherichia coli
209	4.6	43.5	1.04	P45577|PROQ_ECOLI	ProP effector - Escherichia coli
210	4.6	28.8	0.98	P0AE52|BCP_ECOLI	Putative peroxiredoxin bcp (EC 1.11.1.15) (Thioredoxin reductase) (Bacte
211	4.4	36.0	0.99	P00864|CAPP_ECOLI	Phosphoenolpyruvate carboxylase (EC 4.1.1.31) (PEPCase) (PEPC) - Es
212	4.3	46.8	1.06	P68919|RL25_ECOLI	50S ribosomal protein L25 - Escherichia coli
213	4.3	25.6	0.94	P08839|PT1_ECOLI	Phosphoenolpyruvate-protein phosphotransferase (EC 2.7.3.9) (Phospho
214	4.2	67.1	1.03	P0A7M9|RL31_ECOLI	50S ribosomal protein L31 - Escherichia coli
215	4.2	25.3	0.87	P77718|THII_ECOLI	Thiamine biosynthesis protein thiI - Escherichia coli
216	4.2	30.5	1.03	P0AAI5|FABF_ECOLI	3-oxoacyl-[acyl-carrier-protein] synthase 2 (EC 2.3.1.41) (3-oxoacyl-[acyl-
217	4.1	26.5	0.91	P37095|PEPB_ECOLI	Peptidase B (EC 3.4.11.23) (Aminopeptidase B) - Escherichia coli
218	4.1	12.9	0.97	P76558|MAO2_ECOLI	NADP-dependent malic enzyme (EC 1.1.1.40) (NADP-ME) - Escherichia
219	4.0	22.8	1.04	P26616|MAO1_ECOLI	NAD-dependent malic enzyme (EC 1.1.1.38) (NAD-ME) - Escherichia col
220	4.0	32.9	0.97	P21507|SRMB_ECOLI	ATP-dependent RNA helicase srmB (EC 3.6.1.-) - Escherichia coli

221	4.0	31.8	0.92	P76536|YFEX_ECOLI	Hypothetical protein yfeX - Escherichia coli
222	4.0	30.7	0.94	P0A8N3|SYK1_ECOLI	Lysyl-tRNA synthetase (EC 6.1.1.6) (Lysine--tRNA ligase) (LysRS) - Escl
223	4.0	33.4	1.08	P0A9X4|MREB_ECOLI	Rod shape-determining protein mreB - Escherichia coli
224	4.0	43.6	1.01	P0AFY8|SEQA_ECOLI	Protein seqA - Escherichia coli
225	4.0	17.7	1.42	P61517|CAN_ECOLI	Carbonic anhydrase 2 (EC 4.2.1.1) - Escherichia coli
226	4.0	15.8	1.01	P24182|ACCC_ECOLI	Biotin carboxylase (EC 6.3.4.14) (Acetyl-CoA carboxylase subunit A) (EC
227	4.0	48.8	1.01	P0AG63|RS17_ECOLI	30S ribosomal protein S17 - Escherichia coli
228	4.0	18.3	0.89	P0AAD8|TDCC_ECOLI	Threonine/serine transporter - Escherichia coli
229	4.0	23.1	1.02	P32176|FDOG_ECOLI	Formate dehydrogenase-O, major subunit (EC 1.2.1.2) (Formate dehydrc
230	4.0	25.0	0.94	P30850|RNB_ECOLI	Exoribonuclease 2 (EC 3.1.13.1) (Exoribonuclease II) (Ribonuclease II) (I
231	4.0	26.6	0.95	P68767|AMPA_ECOLI	Cytosol aminopeptidase (EC 3.4.11.1) (Leucine aminopeptidase) (LAP) (
232	4.0	21.6	0.94	P32132|TYPA_ECOLI	GTP-binding protein typA/BipA (Tyrosine phosphorylated protein A) - Esc
233	4.0	14.9	1.03	P00956|SYI_ECOLI	Isoleucyl-tRNA synthetase (EC 6.1.1.5) (Isoleucine--tRNA ligase) (IleRS)
234	4.0	71.1	0.96	P39177|USPG_ECOLI	Universal stress protein G - Escherichia coli
235	4.0	38.7	1.01	P0ABA6|ATPG_ECOLI	ATP synthase gamma chain (EC 3.6.3.14) (ATP synthase F1 sector gam
236	4.0	25.8	1.09	P07012|RF2_ECOLI	Peptide chain release factor 2 (RF-2) - Escherichia coli
237	4.0	65.4	0.96	P0AF36|YIIU_ECOLI	Hypothetical protein yiiU - Escherichia coli
238	4.0	51.9	1.08	P0ABA0|ATPF_ECOLI	ATP synthase B chain (EC 3.6.3.14) - Escherichia coli
239	4.0	9.0	0.89	P76658|HLDE_ECOLI	Bifunctional protein hldE [Includes: D-beta-D-heptose 7-phosphate kinase
240	4.0	47.9	1.08	P0A6Y1|IHFB_ECOLI	Integration host factor subunit beta (IHF-beta) - Escherichia coli
241	4.0	19.4	0.92	P0A6T3|GAL1_ECOLI	Galactokinase (EC 2.7.1.6) (Galactose kinase) - Escherichia coli
242	4.0	26.4	0.95	P09372|GRPE_ECOLI	Protein grpE (HSP-70 cofactor) (Heat shock protein B25.3) (HSP24) - Es
243	4.0	22.0	0.90	P02925|RBSB_ECOLI	D-ribose-binding periplasmic protein precursor - Escherichia coli
244	4.0	39.8	1.06	P63020|GNTY_ECOLI	Protein gntY - Escherichia coli
245	4.0	31.6	1.06	P0C018|RL18_ECOLI	50S ribosomal protein L18 - Escherichia coli
246	4.0	37.3	1.09	P0AG99|SECG_ECOLI	Protein-export membrane protein secG (Preprotein translocase band 1 su
247	4.0	21.8	1.02	P0ABD8|BCCP_ECOLI	Biotin carboxyl carrier protein of acetyl-CoA carboxylase (BCCP) - Esche
248	4.0	45.9	0.93	P0AA04|PTHP_ECOLI	Phosphocarrier protein HPr (Histidine-containing protein) - Escherichia co
249	4.0	30.9	0.92	P0A7N9|RL33_ECOLI	50S ribosomal protein L33 - Escherichia coli
250	4.0	5.6	1.00	P69924|RIR2_ECOLI	Ribonucleoside-diphosphate reductase 1 subunit beta (EC 1.17.4.1) (Rib
251	4.0	33.3	1.07	P69222|IF1_ECOLI	Translation initiation factor IF-1 - Escherichia coli
252	4.0	27.7	0.86	P0AD33|YFCZ_ECOLI	UPF0381 protein yfcZ - Escherichia coli

253	4.0	25.5	0.92	P0A9K9|SLYD_ECOLI	FKBP-type peptidyl-prolyl cis-trans isomerase slyD (EC 5.2.1.8) (PPIase)
254	4.0	21.6	1.06	P0A7E3|PYRE_ECOLI	Orotate phosphoribosyltransferase (EC 2.4.2.10) (OPRT) (OPRTase) - E
255	3.9	27.5	0.93	P00954|SYW_ECOLI	Tryptophanyl-tRNA synthetase (EC 6.1.1.2) (Tryptophan--tRNA ligase) (T
256	3.7	25.2	1.01	P10121|FTSY_ECOLI	Cell division protein ftsY - Escherichia coli
257	3.7	73.2	0.97	P68679|RS21_ECOLI	30S ribosomal protein S21 - Escherichia coli
258	3.7	36.3	0.90	P0AD59|IVY_ECOLI	Inhibitor of vertebrate lysozyme precursor - Escherichia coli
259	3.7	33.3	1.06	P0A7M2|RL28_ECOLI	50S ribosomal protein L28 - Escherichia coli
260	3.6	56.2	0.91	P0ADP9|YIHD_ECOLI	Protein yihD - Escherichia coli
261	3.5	25.6	0.84	P0A796|K6PF1_ECOLI	6-phosphofructokinase isozyme 1 (EC 2.7.1.11) (6-phosphofructokinase
262	3.5	42.9	1.02	P0A9Q1|ARCA_ECOLI	Aerobic respiration control protein arcA (Dye resistance protein) - Escher
263	3.3	36.2	0.97	P0A6N4|EFP_ECOLI	Elongation factor P (EF-P) - Escherichia coli
264	3.3	45.9	1.05	P0A7L8|RL27_ECOLI	50S ribosomal protein L27 - Escherichia coli
265	3.3	24.1	1.09	P0A6W5|GREA_ECOLI	Transcription elongation factor greA (Transcript cleavage factor greA) - E
266	3.3	11.6	1.01	P0AFG0|NUSG_ECOLI	Transcription antitermination protein nusG - Escherichia coli
267	3.3	37.9	0.97	P0AG48|RL21_ECOLI	50S ribosomal protein L21 - Escherichia coli
268	3.2	73.0	1.08	P0ADZ4|RS15_ECOLI	30S ribosomal protein S15 - Escherichia coli
269	3.2	13.9	1.02	P76341|YEDX_ECOLI	Transthyretin-like protein precursor - Escherichia coli
270	3.1	19.7	0.93	P00490|PHSM_ECOLI	Maltodextrin phosphorylase (EC 2.4.1.1) - Escherichia coli
271	3.0	62.5	0.93	P0AED0|USPA_ECOLI	Universal stress protein A - Escherichia coli
272	2.9	16.6	0.90	P0AGD7|SRP54_ECOLI	Signal recognition particle protein (Fifty-four homolog) (p48) - Escherichia
273	2.7	18.9	0.91	P0AEP3|GALU_ECOLI	UTP--glucose-1-phosphate uridylyltransferase (EC 2.7.7.9) (UDP-glucose
274	2.7	18.0	0.87	P0ACE0|MBHM_ECOLI	Hydrogenase-2 large chain precursor (EC 1.12.99.6) (NiFe hydrogenase)
275	2.7	42.0	1.00	P0ADZ0|RL23_ECOLI	50S ribosomal protein L23 - Escherichia coli
276	2.7	41.6	0.97	P0AG59|RS14_ECOLI	30S ribosomal protein S14 - Escherichia coli
277	2.7	55.2	1.04	P0A8J4|YBED_ECOLI	UPF0250 protein ybeD - Escherichia coli
278	2.5	16.2	1.02	P07813|SYL_ECOLI	Leucyl-tRNA synthetase (EC 6.1.1.4) (Leucine--tRNA ligase) (LeuRS) - E
279	2.5	25.1	0.91	P27298|OPDA_ECOLI	Oligopeptidase A (EC 3.4.24.70) - Escherichia coli
280	2.4	34.3	1.09	P33232|LLDD_ECOLI	L-lactate dehydrogenase [cytochrome] (EC 1.1.2.3) - Escherichia coli
281	2.2	21.7	1.04	P0AC69|YDHD_ECOLI	Probable monothiol glutaredoxin ydhD - Escherichia coli
282	2.2	17.3	1.07	P60240|RAPA_ECOLI	RNA polymerase-associated protein rapA (EC 3.6.1.-) (ATP-dependent h
283	2.2	26.6	1.09	P0A9Q5|ACCD_ECOLI	Acetyl-coenzyme A carboxylase carboxyl transferase subunit beta (EC 6.
284	2.1	17.3	0.95	P0A927|TSX_ECOLI	Nucleoside-specific channel-forming protein tsx precursor - Escherichia c

285	2.1	40.4	0.93	P23857|PSPE_ECOLI	Phage shock protein E precursor - Escherichia coli
286	2.0	21.1	1.04	P43672|UUP_ECOLI	ABC transporter ATP-binding protein uup - Escherichia coli
287	2.0	43.2	0.89	P0A7C6|PEPE_ECOLI	Peptidase E (EC 3.4.13.21) (Alpha-aspartyl dipeptidase) (Asp-specific dip
288	2.0	15.8	0.92	P09148|GAL7_ECOLI	Galactose-1-phosphate uridylyltransferase (EC 2.7.7.12) (Gal-1-P uridyly
289	2.0	34.7	0.92	P0A9P6|DEAD_ECOLI	Cold-shock DEAD box protein A (EC 3.6.1.-) (ATP-dependent RNA helica
290	2.0	67.9	0.98	P22255|CYSQ_ECOLI	Protein cysQ - Escherichia coli
291	2.0	28.8	0.96	P0AG51|RL30_ECOLI	50S ribosomal protein L30 - Escherichia coli
292	2.0	16.5	0.86	P0A6H5|HSLU_ECOLI	ATP-dependent hsl protease ATP-binding subunit hslU (Heat shock prote
293	2.0	16.2	0.88	P0AFJ1|PHNA_ECOLI	Protein phnA - Escherichia coli
294	2.0	12.5	1.07	P0A7I4|RF3_ECOLI	Peptide chain release factor 3 (RF-3) - Escherichia coli
295	2.0	16.0	0.90	P21165|PEPQ_ECOLI	Xaa-Pro dipeptidase (EC 3.4.13.9) (X-Pro dipeptidase) (Proline dipeptida
296	2.0	18.5	1.01	P0AG82|PSTS_ECOLI	Phosphate-binding periplasmic protein precursor (PBP) - Escherichia coli
297	2.0	17.8	0.88	P0ABZ6|SURA_ECOLI	Chaperone surA precursor (Peptidyl-prolyl cis-trans isomerase surA) (EC
298	2.0	16.8	0.93	P0AEG4|DSBA_ECOLI	Thiol:disulfide interchange protein dsbA precursor - Escherichia coli
299	2.0	26.5	1.07	P0AC33|FUMA_ECOLI	Fumarate hydratase class I, aerobic (EC 4.2.1.2) (Fumarase) - Escherich
300	2.0	31.3	0.95	P46837|YHGF_ECOLI	Protein yhgF - Escherichia coli
301	2.0	21.4	0.94	P52647|NIFJ_ECOLI	Probable pyruvate-flavodoxin oxidoreductase (EC 1.2.7.-) - Escherichia c
302	2.0	29.5	0.97	P0AEI1|YLEA_ECOLI	UPF0004 protein yleA - Escherichia coli
303	2.0	45.4	0.95	P25888|RHLE_ECOLI	Putative ATP-dependent RNA helicase rhlE (EC 3.6.1.-) - Escherichia col
304	2.0	13.2	1.04	P15254|PUR4_ECOLI	Phosphoribosylformylglycinamidine synthase (EC 6.3.5.3) (FGAM syntha
305	2.0	33.0	0.90	P0A9C0|GLPA_ECOLI	Anaerobic glycerol-3-phosphate dehydrogenase subunit A (EC 1.1.99.5)
306	2.0	22.1	1.02	P00452|RIR1_ECOLI	Ribonucleoside-diphosphate reductase 1 subunit alpha (EC 1.17.4.1) (Ri
307	2.0	26.7	1.01	P21499|RNR_ECOLI	Ribonuclease R (EC 3.1.-.-) (RNase R) (Protein vacB) - Escherichia coli
308	2.0	39.3	1.07	P31120|GLMM_ECOLI	Phosphoglucosamine mutase (EC 5.4.2.10) - Escherichia coli
309	2.0	20.9	1.02	P0A6Z1|HSCA_ECOLI	Chaperone protein hscA (Hsc66) - Escherichia coli
310	2.0	18.5	1.04	P75864|YCBY_ECOLI	UPF0020/UPF0064 protein ycbY - Escherichia coli
311	2.0	38.7	0.91	P29745|PEPT_ECOLI	Peptidase T (EC 3.4.11.4) (Tripeptide aminopeptidase) (Aminotripeptidas
312	2.0	25.1	1.02	P0AC53|G6PD_ECOLI	Glucose-6-phosphate 1-dehydrogenase (EC 1.1.1.49) (G6PD) - Escheric
313	2.0	69.5	1.08	P0A955|ALKH_ECOLI	KHG/KDPG aldolase [Includes: 4-hydroxy-2-oxoglutarate aldolase (EC 4.
314	2.0	48.6	1.02	P0A6L2|DAPA_ECOLI	Dihydrodipicolinate synthase (EC 4.2.1.52) (DHDPS) - Escherichia coli
315	2.0	22.3	0.98	P69741|MBHT_ECOLI	Hydrogenase-2 small chain precursor (EC 1.12.99.6) (NiFe hydrogenase
316	2.0	20.4	1.01	P36928|YEGD_ECOLI	Hypothetical chaperone protein yegD - Escherichia coli

317	2.0	28.6	0.95	P0A7G6|RECA_ECOLI	Protein recA (Recombinase A) - Escherichia coli
318	2.0	48.5	1.02	P0A7D1|PTH_ECOLI	Peptidyl-tRNA hydrolase (EC 3.1.1.29) (PTH) - Escherichia coli
319	2.0	25.8	0.92	P42630|TDCG_ECOLI	L-serine dehydratase tdcG (EC 4.3.1.17) (L-serine deaminase) (SDH) - E
320	2.0	32.4	0.92	P37666|TKRA_ECOLI	2-ketogluconate reductase (EC 1.1.1.215) (2KR) (2-ketoaldonate reducta
321	2.0	34.5	0.89	P08660|AK3_ECOLI	Lysine-sensitive aspartokinase 3 (EC 2.7.2.4) (Lysine-sensitive aspartoki
322	2.0	40.3	1.91	P61949|FLAV_ECOLI	Flavodoxin-1 - Escherichia coli
323	2.0	19.9	1.00	P0AE06|ACRA_ECOLI	Acriflavine resistance protein A precursor - Escherichia coli
324	2.0	21.9	1.03	P0ABQ0|COABC_ECOLI	Coenzyme A biosynthesis bifunctional protein coaBC (DNA/pantothenate
325	2.0	25.3	1.08	P06715|GSHR_ECOLI	Glutathione reductase (EC 1.8.1.7) (GR) (GRase) - Escherichia coli
326	2.0	11.3	0.94	Q46829|BGLA_ECOLI	6-phospho-beta-glucosidase bglA (EC 3.2.1.86) - Escherichia coli
327	2.0	5.6	0.96	Q03961|KPSD1_ECOLI	Polysialic acid transport protein kpsD precursor - Escherichia coli
327	0.0	5.6		P42213|KPSD5_ECOLI	Polysialic acid transport protein kpsD precursor - Escherichia coli
328	2.0	29.3	1.03	P77247|YNIC_ECOLI	Phosphatase yniC (EC 3.1.3.-) - Escherichia coli
329	2.0	7.6	1.08	P33363|BGLX_ECOLI	Periplasmic beta-glucosidase precursor (EC 3.2.1.21) (Gentiobiase) (Cel
330	2.0	25.4	0.86	P25397|TEHB_ECOLI	Tellurite resistance protein tehB - Escherichia coli
331	2.0	30.9	0.88	P22564|RIHC_ECOLI	Nonspecific ribonucleoside hydrolase rihC (EC 3.2.-.-) (Purine/pyrimidine
332	2.0	11.9	0.98	P22106|ASNB_ECOLI	Asparagine synthetase B [glutamine-hydrolyzing] (EC 6.3.5.4) - Escherich
333	2.0	18.9	1.02	P0ACC7|GLMU_ECOLI	Bifunctional protein glmU [Includes: UDP-N-acetylglucosamine pyrophos
334	2.0	5.5	0.94	P0ABH9|CLPA_ECOLI	ATP-dependent Clp protease ATP-binding subunit clpA - Escherichia coli
335	2.0	21.3	0.94	P0A988|DPO3B_ECOLI	DNA polymerase III subunit beta (EC 2.7.7.7) - Escherichia coli
336	2.0	58.2	0.95	P0A800|RPOZ_ECOLI	DNA-directed RNA polymerase omega chain (EC 2.7.7.6) (RNAP omega
337	2.0	43.5	0.87	P0A738|MOAC_ECOLI	Molybdenum cofactor biosynthesis protein C - Escherichia coli
338	2.0	30.0	1.02	P0A6R0|FABH_ECOLI	3-oxoacyl-[acyl-carrier-protein] synthase 3 (EC 2.3.1.41) (3-oxoacyl-[acyl
339	2.0	35.7	0.93	P0A6G7|CLPP_ECOLI	ATP-dependent Clp protease proteolytic subunit precursor (EC 3.4.21.92
340	2.0	10.1	0.95	P0A6D3|AROA_ECOLI	3-phosphoshikimate 1-carboxyvinyltransferase (EC 2.5.1.19) (5-enolpyru
341	2.0	19.0	1.01	P04425|GSHB_ECOLI	Glutathione synthetase (EC 6.3.2.3) (Glutathione synthase) (GSH synthe
342	2.0	15.3	1.02	P76177|YDGH_ECOLI	Protein ydgH precursor - Escherichia coli
343	2.0	13.7	0.97	P68187|MALK_ECOLI	Maltose/maltodextrin import ATP-binding protein malK (EC 3.6.3.19) - Es
344	2.0	14.5	0.98	P67910|HLDD_ECOLI	ADP-L-glycero-D-manno-heptose-6-epimerase (EC 5.1.3.20) (ADP-L-gly
345	2.0	61.9	0.90	P0AGK4|YHBY_ECOLI	UPF0044 protein yhbY - Escherichia coli
346	2.0	11.2	0.91	P0AF12|MTNN_ECOLI	MTA/SAH nucleosidase (EC 3.2.2.9) (P46) (5'-methylthioadenosine nucle
347	2.0	12.2	0.97	P0AE01|YFHQ_ECOLI	Hypothetical tRNA/rRNA methyltransferase yfhQ (EC 2.1.1.-) - Escherich

348	2.0	20.7	1.03	P0ABU5|ELBB_ECOLI	Enhancing lycopene biosynthesis protein 2 (Sigma cross-reacting protein
349	2.0	11.8	1.04	P0AB77|KBL_ECOLI	2-amino-3-ketobutyrate coenzyme A ligase (EC 2.3.1.29) (AKB ligase) (G
350	2.0	27.0	0.92	P0AB46|YMGD_ECOLI	Hypothetical protein ymgD precursor - Escherichia coli
351	2.0	5.1	1.04	P0AAD6|SDAC_ECOLI	Serine transporter - Escherichia coli
352	2.0	18.1	0.92	P0A6L0|DEOC_ECOLI	Deoxyribose-phosphate aldolase (EC 4.1.2.4) (Phosphodeoxyriboaldolas
353	2.0	6.2	1.01	P09323|PTW3C_ECOLI	PTS system N-acetylglucosamine-specific EIICBA component (EIICBA-N
354	2.0	17.7	0.99	P07004|PROA_ECOLI	Gamma-glutamyl phosphate reductase (EC 1.2.1.41) (GPR) (Glutamate-
355	2.0	10.1	0.90	P69805|PTND_ECOLI	Mannose permease IID component (PTS system mannose-specific EIID
356	2.0	23.8	1.10	P64581|YQJD_ECOLI	Hypothetical protein yqjD - Escherichia coli
357	2.0	21.6	0.91	P63417|YHBS_ECOLI	Hypothetical acetyltransferase yhbS (EC 2.3.1.-) - Escherichia coli
358	2.0	9.7	1.09	P39396|YJIY_ECOLI	Inner membrane protein yjiY - Escherichia coli
359	2.0	6.9		P39286|ENGC_ECOLI	Probable GTPase engC precursor (EC 3.6.1.-) - Escherichia coli
360	2.0	33.3	1.04	P37903|USPF_ECOLI	Universal stress protein F - Escherichia coli
361	2.0	5.9	1.05	P36767|RDGC_ECOLI	Recombination-associated protein rdgC - Escherichia coli
362	2.0	7.8	1.02	P28248|DCD_ECOLI	Deoxycytidine triphosphate deaminase (EC 3.5.4.13) (dCTP deaminase)
363	2.0	4.8	0.98	P24169|DCOS_ECOLI	Ornithine decarboxylase, inducible (EC 4.1.1.17) - Escherichia coli
364	2.0	26.5	1.00	P23827|ECOT_ECOLI	Ecotin precursor - Escherichia coli
365	2.0	27.7	0.96	P0AFU8|RISA_ECOLI	Riboflavin synthase alpha chain (EC 2.5.1.9) - Escherichia coli
366	2.0	50.7	1.00	P0ADW3|YHCB_ECOLI	Putative cytochrome d ubiquinol oxidase subunit III (EC 1.10.3.-) (Cytoch
367	2.0	8.1	0.93	P0ADS6|YGGE_ECOLI	Hypothetical protein yggE - Escherichia coli
368	2.0	11.4	1.01	P0ACR9|MPRA_ECOLI	Transcriptional repressor mprA (Protein emrR) - Escherichia coli
369	2.0	59.5	0.94	P0A968|CSPD_ECOLI	Cold shock-like protein cspD (CSP-D) - Escherichia coli
370	2.0	14.5	1.02	P0A6I0|KCY_ECOLI	Cytidylate kinase (EC 2.7.4.14) (CK) (Cytidine monophosphate kinase) (C
371	2.0	10.4	1.08	P09158|SPEE_ECOLI	Spermidine synthase (EC 2.5.1.16) (Putrescine aminopropyltransferase)
372	2.0	8.0	0.87	P07014|DHSB_ECOLI	Succinate dehydrogenase iron-sulfur protein (EC 1.3.99.1) - Escherichia
373	2.0	6.7	0.91	P65556|YFCD_ECOLI	Putative Nudix hydrolase yfcD (EC 3.6.-.-) - Escherichia coli
374	2.0	5.8	0.94	P39199|YFCB_ECOLI	Hypothetical adenine-specific methylase yfcB (EC 2.1.1.72) - Escherichia
375	2.0	12.1	0.87	P0AEM0|FKBX_ECOLI	FKBP-type 16 kDa peptidyl-prolyl cis-trans isomerase (EC 5.2.1.8) (PPIa
376	2.0	12.3	0.97	P0AEB7|YOAB_ECOLI	UPF0076 protein yoaB - Escherichia coli
377	2.0	30.1	1.05	P0AC62|GLRX3_ECOLI	Glutaredoxin-3 (Grx3) - Escherichia coli
378	2.0	7.0	0.92	P0A9D2|GST_ECOLI	Glutathione S-transferase (EC 2.5.1.18) - Escherichia coli
379	2.0	8.7	1.07	P0A912|PAL_ECOLI	Peptidoglycan-associated lipoprotein precursor - Escherichia coli

380	2.0	17.4	0.80	P0A7P5|RL34_ECOLI	50S ribosomal protein L34 - Escherichia coli
381	2.0	17.8	0.94	P0A6T9|GCSH_ECOLI	Glycine cleavage system H protein - Escherichia coli
382	2.0	20.9	1.03	P0A6E6|ATPE_ECOLI	ATP synthase epsilon chain (EC 3.6.3.14) (ATP synthase F1 sector epsil
383	2.0	31.1	0.99	P0ACE7|YCFF_ECOLI	HIT-like protein ycfF - Escherichia coli
384	2.0	25.9	1.07	P52061|HAM1_ECOLI	HAM1 protein homolog - Escherichia coli
385	2.0	18.1	1.09	P0AD10|YECJ_ECOLI	Hypothetical protein yecJ - Escherichia coli
386	2.0	19.4	1.09	P0AC41|DHSA_ECOLI	Succinate dehydrogenase flavoprotein subunit (EC 1.3.99.1) - Escherichi
387	2.0	16.8	0.89	P04825|AMPN_ECOLI	Aminopeptidase N (EC 3.4.11.2) (Alpha-aminoacylpeptide hydrolase) - E
388	2.0	28.3	0.91	P07658|FDHF_ECOLI	Formate dehydrogenase H (EC 1.2.1.2) (Formate-hydrogen-lyase-linked,
389	2.0	20.1	1.00	P0AAA1|YAGU_ECOLI	Inner membrane protein yagU - Escherichia coli
390	2.0	34.4	0.87	P23830|PSS_ECOLI	CDP-diacylglycerol--serine O-phosphatidyltransferase (EC 2.7.8.8) (Phos
391	2.0	8.8	0.97	P0A722|LPXA_ECOLI	Acyl-[acyl-carrier-protein]--UDP-N-acetylglucosamine O-acyltransferase (
392	2.0	29.5	0.87	P0A6W9|GSH1_ECOLI	Glutamate--cysteine ligase (EC 6.3.2.2) (Gamma-glutamylcysteine synth
393	2.0	18.6	0.95	P23843|OPPA_ECOLI	Periplasmic oligopeptide-binding protein precursor - Escherichia coli
394	2.0	21.6	0.89	P0A884|TYSY_ECOLI	Thymidylate synthase (EC 2.1.1.45) (TS) (TSase) - Escherichia coli
395	2.0	22.4	0.91	P69503|APT_ECOLI	Adenine phosphoribosyltransferase (EC 2.4.2.7) (APRT) - Escherichia co
396	2.0	16.8	0.98	P0A9C3|GALM_ECOLI	Aldose 1-epimerase (EC 5.1.3.3) (Mutarotase) - Escherichia coli